Immunology of persistent viral infection

Inauguraldissertation
zur
Erlangung der Würde eines Doktors der Philosophie
vorgelegt der
Philosophisch-Naturwissenschaftlichen Fakultät
der Universität Basel

von
Mirela Dimitrova

Basel, 2023

Genehmigt von der Philosophisch-Naturwissenschaftlichen Fakultät der Universität Basel

auf Antrag von

Erstbetreuer: Prof. Daniel Pinschewer
Zweitbetreuer: Prof. Urs Jenal
Externer Experte: Prof. Doron Merkler

Basel, den 22. Juni 2021

Prof. Marcel Mayor
Dekan

Table of Contents

List of Abbreviations

Ab(s)	antibody (antibodies)
ADCC	Antibody-dependent cellular cytotoxicity
AID	Activation-induced cytidine deaminase
APC(s)	Antigen presenting cell(s)
ASC(s)	Antibody secreting cell(s)
BACH	BTB and CNC homology
BAFF	B-cell activating factor
BCL6	B cell lymphoma protein 6
BCR	B cell receptor
BLIMP-1	B lymphocyte-induced maturation protein 1
bnAb(s)	broadly neutralizing antibody (antibodies)
CD	cluster of differentiation
CSR	Class switch recombination
CTL	Cytotoxic T lymphocytes
CXCL	chemokine (C-X-C motif) ligand
CXCR	chemokine (C-X-C motif) receptor
EBI2	Epstein-Barr virus-induced G-protein coupled receptor 2
Env	Envelope protein
eOD-GT	engineered outer domain-germline targeting
FcRL	Fc receptor-like
FDCs	follicular dendric cells
GC	Germinal center
GP-1	glycoprotein-1
GPC	glycoprotein complex
HBV	Hepatitis B virus
HCV	Hepatitis C virus
HIV	Human immunodeficiency virus
IFN	interferon
Ig	immunoglobulin
IGR	intergenic region
IL	interleukin
IRF4	interferon regulatory factor (4)
LCMV	lymphocytic choriomeningitis
LLPC	long-lived plasma cells
LN	lymph nodes
MBC(s)	Memory B cell(s)
MG	minigenome
MHC	major histocompatibility complex
MZ	marginal zone
nAb(s)	neutralizing antibodies
NP	nucleoprotein
ORF	open reading frame
PAX5	paired box protein
PB	plasma blast
PC	plasma cell
PD-1	programmed cells death protein-1
PPs	Peyer's patches
Prdm1	PR domain 1 (gene encoding Blimp-1)
RM	resting memory
RNP	ribonucleoprotein
S1P	sphingosine-1-phosphate
S1PR	sphingosine-1-phosphate receptor
SHM	somatic hypermutation
Siglec	sialic acid-binding immunoglobulin-type lectins

SIV	simian immunodeficiency virus
SLPC	short-lived plasma cells
SSP	stable signal peptide
TLM	tissue-like memory
TNF	tumor necrosis factor
UTR	untranslated region
XBP-1	X-box binding protein

General introduction

Lymphocytic choriomeningitis virus (LCMV)

We use lymphocytic choriomeningitis virus (LCMV) throughout this thesis as a murine model of chronic viral infection. LCMV belongs to the Arenaviridae family of viruses. They are two groups of Arenaviruses, based on genetic and geographical characteristics. The Old World group includes LCMV and Lassa virus, while the New World comprise Junin, Machupo and Guanarito viruses in South America and Whitewater Arroyo in North America [1-4]. The natural host of Arenaviruses are mainly rodents. In the case of LCMV, the reservoir is established in mice via neonatal/transplacental transmission (from mother to offspring) leading to lifelong asymptomatic infection. LCMV can be transmitted by feces, urine and saliva in adult mice but it does not normally lead to chronic disease. LCMV can be also transmitted to humans trough fresh urine/feces/body fluids or nesting material from rodents or by accidental exposure in the lab. Clinical manifestations are usually mild, flu-like, but can also include meningitis requiring a hospitalization [5]. Other Arenaviruses such as Lassa, Junin, Guanarito can be much more pathogenic, causing severe hemorrhagic fever and death [6].

LCMV was discovered in 1930 and has been used since then as a tool to understand basic principles in immunology and virology. Famously, LCMV contributed to the Nobel prize in 1996, shared between Peter Doherty and Rolf Zinkernagel "for their discoveries concerning the specificity of the cell mediated immune response" [7, 8].

Arenaviruses virions range between 40-300nm in diameter, are spherical or pleomorphic in shape and are enveloped. The name "arenavirus" comes from the Latin word for "sand" due to the appearance of the viral particles under electron microscope (EM) [9]. The genome of the mammalian arenavirus consists of two single-stranded ambisense RNA molecules, namely the large (L) and small (S) segments, and purified RNA from virion alone is not infectious. Importantly, both the 5' and 3' of each segment has noncoding untranslated regions (UTRs) containing conserved complementary sequence of 19-30 nucleotides on each side [10]. It is predicted that these termini form a panhandle structure through base pairing [11, 12]. The 3'UTR of each segment contains a promoter directing RNA replication and gene transcription [13, 14].

Each arenavirus segment encodes two proteins in two separate ORFs of opposite polarities, also called ambisense coding strategy [15, 16]. The L segment which is around 7'200 nt long encodes the viral RNA-dependent RNA polymerase and a zinc-binding matrix protein, also designated as Z [17]. The small segment (~3'500nt) encodes a nucleoprotein (NP) and a precursor for the envelope glycoprotein (GPC) which is posttranslationally cleaved [18-20]. Between the ORFs of each segment there are intergenic noncoding region (IGR) which form stem-loop (hairpin) structures [15, 21]. The IGR has an important function in termination of transcription, which is structure-dependent, and virus assembly and/or budding [22-25].

The mRNAs of mammalian arenaviruses are capped and not polyadenylated [22, 26, 27] with the 5' ends containing several nontemplated bases [22, 28, 29]. The mechanism of transcription initiation is similar to the cap-snatching mechanism which involves cleavages of the caps and the bases associated with them by endonuclease activity linked to the viral L polymerase [30]. Importantly, the cap leader is used as a primer to initiate transcription of the arenavirus genome [30].

A major structural protein of mammalian arenaviruses is the NP which is associated with viral RNA in a bead-like structure. NP interacts efficiently with the RNA-dependent RNA polymerase (L protein), the trans-acting viral factors indispensable for viral RNA replication and transcription [31] [32]. Similar to other RNA-dependent RNA polymerases, the L of mammarenaviruses carries both process of transcription and replication [28, 33-36]. The matrix Z protein contains a RING motif binding zinc and it is the main component driving virus budding [14, 17, 37, 38]. It also blocks RNA synthesis in a dose-dependent manner [39-44]. The two envelope glycoproteins, GP1 and GP2, are posttranslationally cleaved from GPC. Together with a stable signal peptide (SSP) which is cleaved off during GPC synthesis form the spike of the virion [20, 45, 46] and mediate attachment [47] and fusion with the membranes of their target cells [48-51]. Importantly, GP protein and its outer globular domain (GP-1) is the only target for arising neutralizing antibodies during infection [52].

Infection involves attachment of the arenavirus to host cell-surface receptor followed by endocytosis mediated internalization [53-56]. Late endosomes release the ribonucleoprotein (RNP) complex consisting of NP, L and viral genomic RNA into the cytoplasm via pH-dependent fusion and RNP then directs both RNA genome replication and transcription [57]. During the process of replication, the L pol generates uncapped antigenomic and genomic RNAs which contain one single nontemplated G at the 5' end [28, 29, 58]. It is possible that the initiation of replication actually involved slippage mechanism of the L in the next RNA [34]. Transcription of GPC and Z mRNAs occurs only after a full round of viral replication during which the antigenomes of both S and L are

produced. The polyprotein GPC is synthesized in the ER where it is extensively glycosylated, forms oligomers and is proteolytically cleaved by (SKI-1/S1P) [59]. SSP plays a role in the proteolytic processing of GPC and trafficking of the protein from ER to cell surface [60]. Finally, the virion budding occurs in the plasma membrane of the infected cells by which provides the viral envelope for the newly released virions [14, 38, 61-65].
We and others described a reverse genetic technique to recover LCMV only from cDNA [66, 67]. Simply transfecting permissive cells with purified RNA of negative-strand viruses like LCMV does not lead to infectious cycle, due mainly to the inability of these RNAs to serve as mRNA. To this end, the viral RNA segments must be complemented with minimal viral-transacting factors in order to initiate genomic replication and transcription. The first breakthrough was the design of minigenome system (MG) which allowed studies of viral cis- and trans-acting factors and the initiation of transcription, replication and formation of infectious particles. [25, 32, 68-70]. Other arenaviruses like Lassa virus (LASV) also have an established reverse genetic rescue systems [71], [72]. Finally, in 2006 recovery of infectious LCMV entirely from plasmid was achieved. The basics are that the two viral genomes, S and L, are given as polymerase I-driven plasmids. The trans-acting elements, NP and L proteins, are introduced on separate sets of plasmids, these ones designed as polymerase-II-driven. Transfection of all the four plasmids using lipofectamine provides the viral genome and the necessary trans-acting elements which ensures the production of a full infectious LCMV particles. Recovery of LCMV entirely from plasmid DNA makes it easier to generate recombinant viruses, carrying variety of mutations that we can design according to our purposes.

Adaptive immune responses to viral infections: T cells

Adoptive immune responses are main players in containing viral pathogens with both T and B cells having their important role. Certain viruses, such as influenza viruses [73] or coronaviruses [74], can cause short duration (or acute) infection while other pathogen, like HIV and HCV, cause prolonged (or chronic) illness [75], [76]. Acute infections are either quickly resolved or the patient rapidly succumbs to death, whereas chronic infection can linger for years or may never be cleared by the host, as it is the case with HIV. Persistent pathogens usually lead to fatal outcome many years after infection. While HIV-1 is usually obligatory chronic due to its retroviral nature [77, 78], other pathogens such as HBV or HCV, or murine LCMV, can lead to either life-long (chronic) persistence or protracted but self-limiting infection. There are many biological factors from both pathogen and host side which can influence the course of the infection. One key determinant is the adaptive immune system of the host, as shown with the previously mentioned prototypic infection model with LCMV. In the murine experimental model of LCMV, the strain and dose of LCMV, as well as the MHC class I haplotype of the mouse define the outcome of LCMV infection in mice [79]. If the C57BL/6 mouse (H-2b) is infected with LCMV strain Armstrong or low dose WE the outcome is an acute infection with a typical rapid onset of the disease or asymptomatic progression and low viremia titers, resolved within days. Contrary to that, infection with clone 13 LCMV or Docile LCMV results in persisting viremia, detectable in certain organs and tissues months after exposure [80, 81]. One can appreciate the viral factors of persistence when comparing virus clearance of Clone 13 and Armstrong which differ in L1079 mutation in Cl13 polymerase, resulting in increased chronicity and exhaustion of virus-specific T-cell response [82].
Cytotoxic CD8+ T cells (CTLs) have been shown to play a major role in the clearance of LCMV infection [83-88], although noticeable differences were described for adaptive CTL responses to either acute or chronic LCMV. Acute infection leads to activated CD8+ T cells, followed by clonal expansion in response to antigen stimulation [89]. Upon activation CD8+ CTLs differentiate into effector cells expressing inflammatory and cytotoxic molecules such as IFN-γ, TNF-α, perforin and granzyme B thus mediating direct killing of infected cells [90]. Following the expansion and effector stages, CD8+ contract by undergoing apoptosis and differentiating in memory T cells [91, 92]. The anti-viral memory T cells are the essential line of defense due to their quick re-expansion and effector function upon re-challenge with the original pathogen as summarized in [93]. Chronic infections push the differentiation of CTLs in a different direction. Upon infection, the CTLs clonally expand, similar to acute infection with LCMV, but many get clonally deleted [94]. The remaining CTLs lose effector functions over time, developing a functionally impaired state referred to as “exhaustion” [95] [81]. Exhaustion can be summarized as a reduced ability to kill infected cells, impaired proliferation in response to cognate antigen and altered production of cytokines such as IL-2, IFN-γ and TNF-α. The viral factor, determining persistence, is the single-point mutation in the polymerase, increasing the intracellular viral load in plasmacytoid dendritic cells, thus outpacing the antiviral immune response to the host [82]. Chronic infection, therefore, leads to progressive impairment and loss of antiviral CTLs which favors the persistence of LCMV [81, 96-98].

CD8+ T cells are sufficient to control acute LCMV even in the absence of CD4+ helper T cells [99-101]. CD4+ T cells are essential, however, in the clearance of chronic infection [102]. Without CD4+ T helper cells compartment, CTLs are depleted during an ongoing chronic infection [102, 103]. Interestingly, CD4+ can also undergo functional changes, similar or "exhaustion" due to continuous antigenic exposure rather than an early event in the ongoing infection [104, 105]. Despite this, CD4+ are capable of providing help to both CD8+ T cells and B cells during chronic infection. An example of this role is the production of IL-21 by CD4+ which improves the functionality of CD8+ T cells and play a pivotal role in the antiviral control [106-108].

Adaptive immune responses to viral infections: B cells

In addition to T cells, a critical role in clearance of chronic LCMV infection play B cells. Initiation of humoral response starts with the encounter of a specific B cell with its cognate antigen which takes place in lymphoid tissues such as spleen, lymph nodes (LNs) and Peyer's patches (PPs). Lymphoid organs have a filtration capacity, allowing to capture and present foreign antigens to the B cells. Second, the lymphoid tissues have specialized endothelial cells which mediate binding to lymphocytes and their compartmentalization forming lymphoid follicles [109, 110]. Follicular dendritic cells (FDC) are embedded in the follicles, which are stromal cells, specialized in capturing and presenting antigens for long periods [111-115]. B cells migrate to follicles upon sensing chemokine CXCL13, ligand for CXCR5, which is produced by the FDCs and other stromal cells [116, 117]. Within the follicle, B cells slowly scan for surface-displayed antigens presented by macrophages and FDCs [118]. Stromal cells in the lymphoid organs secrete BAFF, an essential B cell survival factor [119]. In order to get to the outer parts of the follicle where they can interact with helper T cells, B cells sense a second factor, the oxysterol 7a, 25-HC, which is also produced by stromal cells and act via receptor EBI2 [120, 121]. If antigen is not encountered by the B cells, the cells exit lymphoid tissue in response to sphingosine-1-phosphate (S1P) sensed via its receptor S1PR1 [122]. After egressing from spleen or LNs, B cells exit in blood or lymphatic vessels, and travel to another lymphoid tissue to repeat the process of surveillance for foreign antigen. If no activation occurs, the B cells die and are replaced by new bone marrow B cell emigrants [123]. If engagement of the B cell receptor (BCR) with cognate antigen occurs, B cells migrate to the T-B cell border where they interact with cognate CD4+ T cells leading to reciprocal activation as B cells exert their antigen-presenting cells (APCs) properties [124-127]. When CD4+ T cells recognize the peptide bound to the MHCII on B cells they upregulate CD40L [128] and cytokines, such as interleukin-4 (IL-4) and IL-6 that in turn induce the activation of B cells [129-131]. This mechanism ensures a very precise "turn on" of the adaptive immune system against pathogens and B-T cell interactions are known to be reciprocally regulated since B cells are needed for CD4+ T cell activation and vice versa [132, 133].

Upon activation, B cells are migrating to the follicle border to the T cell zone and starting to expand, following various differentiation routes [134]. The first one is differentiating into short-lived plasmablasts (PBs) which are antibody-secreting cells (ASCs) [135, 136]. These extrafollicular responses usually produce IgM ASCs which are not mutated via somatic hypermutation (SHM) and are mostly from low-affinity. In the meantime, B cells and T cells continue to interact at the T-B border and start to form a geminal center (GC) upon migration back into follicle, as part of the T cell-dependent antibody response. The GCs are structures, described first by Flemming in 1884, where lymphoid cells undergo mitosis or expand [137-139]. The mechanisms of this decision-making are poorly understood, but it is suggested that the affinity of interaction between the BCR for the antigen, the amount of engagement between antigen and receptor and the co-stimulatory molecules availability from T cells may all play a role [140-146]. In the GCs, B cells undergo somatic hypermutation (SHM) and class-switch recombination (CSR) increasing the affinity and quality of the antibody response, respectively. The enzyme activation-induced cytidine deaminase (AID) acts in both processes of SHM and CSR [147, 148]. CSR is the process of switching the antibody class from IgM, which is the "default" class, to IgA, IgG or IgE. During CSR, activation induced deaminase (AID) enzyme in combination with CSR co-factors basically excises all constant regions except the only left to be expressed under its promoter. SHM is causing accumulation of mutations in the BCR's variable regions in the immunoglobulin genes, ultimately leading to a B cell clone with a high affinity for its cognate antigen via competition for help from CD4+ cells [149-151]. This process is called affinity maturation. The GCs reaction eventually leads to the formation of high-affinity, isotype switched B cells which can further differentiate into plasma cells (PCs) or memory B cells (MBCs) [152]. Typical GC reactions last a few weeks followed by dissolution of the structure but can persist in chronic infections [153-155]. The outcome of this prolonged GC in response to persistent antigen is the production of affinity matured antibodies [155], [156-160]. Plasma cells are the antibody-secreting cells which are defined by reduction of surface immunoglobulin (Ig), CD138 expression and a proliferation halt [161]. PCs exit GCs and home in peripheral tissue, lymph nodes and

spleen. They can be either short-lived (SLPCs) or long-lived (LLPCs) but both types secrete antibodies [162]. The latter find a specific niche in the bone marrow and can reside there for at least as long as memory B cells (MBCs) [163], which are the alternative outcome of the GC reaction. They are characterized by slow or absent division, express surface Ig and do not secrete antibodies. MBCs can produce rapid and robust respond to secondary challenge with previously encountered pathogen [164-171]. The mechanisms leading to the end-differentiation of B cells into LLPCs or MBCs is not fully understood but it could be influenced by cytokines (IL-5), CD40-CD40L interaction, by BCR affinity or by temporal control of the GC reaction [152, 172, 173].
Virus-specific antibodies (Abs) are essential to reduce viral load thus supporting CTLs' effector functions [174-177]. In chronic LCMV infection the emergence of neutralizing antibodies (nAbs) correlate with virus clearance [155, 177]. Despite great redundancy of the human immune system, many of the currently used vaccines work via inducing nAbs in serum or mucosa and thus blocking infection. Therefore, nAbs are the most widely-accepted correlate for protection by vaccination [178] and many vaccine strategies aim at inducing protective antibody responses. For HIV infections, the induction of bnAbs is considered the "holy grail" in vaccine design as reviewed in [179-182]. nAbs have been shown to protect also against other infections, such as in the murine HCV and SHIV models [183-191]. The induction of nAbs in chronic infection, however, represents a major challenge. Whereas acute infection which require around 2 weeks to induce neutralizing titer, nAbs against persistent pathogens occur only after prolonged periods of protracted viremia [192-194]. This delay is influenced by several factors such extensive glycosylation of surface viral envelope [195, 196], viral escape mutants from nAbs [177, 195, 197-199] and recently described early decimation of B cells at the onset of chronic viral infection [200].
Induction of nAbs by vaccination against HIV and HCV were unsuccessful which can be partially explained by the correlation of protracted viral burden and the emergence of nAbs [155, 201]. Non-neutralizing antibodies, on the other hand, appear early in LCMV [193] and in HIV [202]. HIV and were shown to exert an antiviral function via antibody-dependent cellular cytotoxicity (ADCC) and Fc-mediated inhibition [203-209]. Promising new strategies for bnAbs induction are now development, namely combining B cell engineering and vaccination [210].

Transcriptional regulation of B cell differentiation

There are several master regulators of B cells differentiation: paired box protein 5 (PAX5) [211], B-cell lymphoma 6 (BCL-6) [212, 213], interferon regulatory factor 4 (IRF4) [214-216], B lymphocyte-induced maturation protein-1 (BLIMP1) [217-219], X-box binding protein 1 (XBP1) [220, 221] and BTB and CNC homology 2 (BACH2) [222]. In short, the B cell lineage is regulated by BCL6 and PAX5, whereas IRF4, BLIMP1 and XBP1 have a repressive function on B cell-associated genes and activate the plasma cell differentiation program. Upon initiation of the PC program, BCL6 and PAX5 are repressed on the account of IRF4, BLIMP1 and XBP1.
PAX5 binds DNA as a bipartite paired domain and can function as repressor or activator of transcription [223, 224]. It is now well established that PAX5 controls gene transcription by inducing transcription factor (TF) complexes, involved in chromatin remodeling, histone modification and basic transcription at target genes, thus suppressing inappropriate genes and activating B-cell-lineage genes. Thus, it restricts non-committed progenitor cells to the B cell pathway, regulates the cellular functions, induces V_H-DJ_H recombination, facilitates pre-B cell receptor signaling and guiding these pre-B cells to their full commitment in the B cells lineage [225].
BACH2 belongs to the BACH family of transcription factors and, together with MAF proteins binds to MAF-recognition elements and represses immunoglobulin heavy chain 3' enhancer. It is expressed in early B cells and shut-down in plasma cells [226].
BCL6 was first described as proto-oncogene in B cell lymphoma [227] and consequently recognized as a transcriptional repressor, containing six zinc-fingers and BTB domain [228]. It has been shown that BCL6 upregulation in pre-germinal center B cells contributed to the sustained interaction between pre-GC B cells and their Tfh cells and the B cell entry into GC clusters [229]. BCL6 is, therefore, a master regulator of the GC reactions.
Blimp-1 is five-zinc-finger domain which represses the promoter for interferon-I (IFN-I) [230]. It has a consensus recognition site similar to the one of interferon-regulatory factors 1 and 2 (IRF1 and IRF2). Quantitative changes in Blimp-1 define plasma cells ontogeny with highest expression in LLPCs [217]. Using DNA microarrays, it has been shown that Blimp-1 represses genes encoding TFs that regulate signaling by the BCR, as well as blocking expression of AID, Ku70 and STAT6 which leads to the inhibition of Ig class switching [231-235]. Moreover, XBP1, downstream of Blimp-1 increases protein synthesis in plasma cells thus supporting Ab secretion [220]. Blimp-1 is necessary for the B cell differentiation into immunoglobulin secreting plasma cells, as shown with

prdm1$^{flox/flox}$CD19^{Cre} mice (*prdm1* is the gene encoding Blimp-1) which do not develop PCs nor secreting antibodies [236].
Interferon-regulatory factor 4 (IRF-4) can heterodimerize with different partners to either activate or repress transcription of the target gene [237] [238]. One of the many functions of IRF4 is control of plasma cell differentiation and class-switch recombination [239]. By using conditional deletion of *Irf4* in GC B cells, it was shown that IRF4 is necessary for post-germinal center plasma cells, as well as for the differentiation to plasma cells from memory B cells. Both Blimp-1 and IRF4 were necessary for plasma cell differentiation and both acted upstream of XBP-1.

Perturbations of B cells in chronic viral infections

T cell responses to chronic viral infection has been extensively studied as T cell "exhaustion" was thought to be the main mechanism for the failure of immune responses against chronic viral infections. Indeed, in the field of cancer research, reversal of T cell exhaustion via inhibition of PD-1: PD-L2 pathway proved to be effective for treatment of some cancers, as summarized in [240]. The discovery deserved a Nobel prize in 2018, awarded to James P. Allison and Tasuku Honjo "for their discovery of cancer therapy by inhibition of negative immune regulation". This approach, however, was not that successful in chronic viral diseases. In recent years, the specific role of B cells in antiviral responses was studies in more detail. B cell alterations were also identified with persistent-prone pathogens, for both, whether T cell-dependent or -independent reactions [241-256].
B cell dysfunction is now regarded as a main pathological feature of HIV infections, affecting memory B cell compartments, GC B cells and marginal zone (MZ) B cells with both HIV-specific and non-specific populations affected. Some B cell populations, such as MZ B cells and GC B cells are decreased at the expense of increased plasma cells in HIV (humans) and SIV (macaques). In contrast to healthy humans where the resting memory B cells (RM) represent the majority of the memory B cell population with expression of surface markers CD21 and CD27, in HIV patients the majority of memory B cells are abnormal. These B cells isolated from HIV patients are CD21^{lo}CD27^{-}, called tissue-like memory B cells (TLM) and CD21^{lo}CD27^{+} activated memory B cells (AM) [242]. HCV chronic infection also resulted in "exhausted" peripheral B cell phenotype CD21^{-}CD27^{-} [257]. TLMs also express Fc receptor-like protein 4 (FCRL4) and sialic acid-binding Ig-like lectin 6 (Siglec-6), both putative inhibitory receptors [258]. Hypergammaglobulinemia has been shown to consist of mainly HIV-unspecific antibody clones, whereas dysregulated memory B cells in HIV patients were enriched for HIV-specific clones. These perturbations in the B cell compartment of chronically infected individuals are thought to play a major role in increased frequency of autoimmune diseases and poor vaccine response in HIV patients.
HCV, HBV chronic infections [254, 256, 259, 260], Plasmodium [261-264], Schistosoma [265, 266], Mycobacterium tuberculosis [267, 268] have all been related to the induction of abnormal B cell responses. This points towards a general mechanism of immune subversion by persistent-prone pathogens.

B cell competition and immunodominance

B cell responses to complex antigens has been identified as a major hurdle in vaccine design. Major factors play B cell precursor frequencies, B cell receptor affinity for its cognate antigen, antigen avidity and T cell help, as summarized in this recent review [269]. It has been shown that GC reaction have three main outputs: death by apoptosis [270], memory B cells (MBCs) [271-274] and plasma cells [275](both long-lived and short-lived). The decision making for each GC B cells is still debated, but there is evidence that affinity of the BCR to antigen plays a role. It is thought that high-affinity GC B cells form the long-lived plasma cells (LLPC) whereas low-affinity clones differentiate into B memory cells. It has been shown that apoptosis of very low-affinity B cells in GC guides the selection of B cells clones in GCs [276].
Many of the fate-decision studies on B cells have been performed using haptens [277-279] which are valuable approaches but mostly fail to model the B cell response to more complex antigens such as HIV Env trimer. There is increasing evidence that immunodominance of B cells specific non-neutralizing epitopes is a great obstacle for HIV vaccine design [280-282]. Immunodominance is a naturally occurring process, in which particular B and T cell clones are selected in GC reaction at the expense of other cell pathogen-specific clones, thus limiting the breadth of the immune response. The fact that some immunodominant B cell clones are off-target is of major importance for future vaccination strategies and may be correlated with the specific B cell precursor frequency, affinity and valency of the epitope.
Precursor frequencies of B cells have been studied in detail in the context of HIV infection with a focus of broadly neutralizing antibodies like the VRC01 class bnAbs, developing in some HIV+ patients [283-286]. It was shown

recently that precursor B cells for VRC01-class bnAbs exist in the majority of human population but are relatively rare with frequencies around 1 in 300'000 [287-290]. Moreover, these studies indicate that high-affinity VRC01 precursor B cells were even less common in human naïve repertoire, around 1 in 10^6 B cells. Therefore, it was possible to assume, therefore, that small precursor numbers of a given B cell clone may dictate its immunodominance. A breakthrough was made using knock-in B cells expressing germline-reverted form of the VRC01-class of BCR [291], VRC01^{gHL}, and engineered outer domain germline-targeting (eOD-GT) immunogens for HIV Env. This protein antigen is known to induce specifically germline VRC01-class bnAbs [289]. The authors showed that the precursor frequency of epitope-specific B cells was critical for successful competition of this B cell clone during germinal reaction upon immunization. It could result in a 1000-fold change in the ability to induce an antigen-specific response. Importantly, when the precursor number was close to human physiological range for VRC01-class antibodies, affinity to the antigen became main factor [291, 292]. The importance of precursor numbers have been shown using human knock-in for IgHV1-69 to study influenza responses, demonstrating that antibody responses are dependent on B cell precursor numbers in the naïve repertoire [293]. Another important factor for establishing protective immunity is the maturation of specific antibodies from germline to neutralizing affinity. Immunization studies using eOD-GT immunogens identified that VRC01-class bnAbs lack measurable binding to HIV Env when converted to germline sequence [160]. This suggested that multiple rounds of affinity maturation in the GC were needed for bnAbs to arise from their precursors [294]. Alternatively, it was proposed that a few unlikely mutations, rather than large mutational load leaded to successful production of bnAbs in HIV [156-159]. Precursor numbers of epitope-specific B cells should be taken into account in vaccinology studies because they play a major role in the success (or failure) of humoral immunity.

Antigen affinity was determined as one of the key parameters in fate-decision of B cells upon immunization. One study showed that in T cell-dependent responses with limiting numbers of high- and low-affinity B cells mixed in wild-type recipient mice identified that only high-affinity B cells accumulated in GCs [144]. When tested in T cell-independent responses, antigen affinity played a role but to a lesser extend [295]. Low-affinity B cells have been described in multiple studies, suggesting that they have a capacity to get activated by low-affinity antigens [141, 296-298]. In these studies, however, precursor number frequency was not tested alongside affinity, meaning that key information about competition was lacking. It seemed that re-entering GCs upon booster immunization was also dependent on high-affinity memory B cells [299], consistent with priming of the immune response [290].

The relationship between affinity and precursor frequency in determining the fate of B cells have been investigated in this elegant study [291]. In short, when the epitope-specific B cell precursor frequency was high, there was a representation of both high- and low-affinity B cells in GC. When the precursor numbers were reduced to physiological levels in the 1 in 10^6 range, there was a strong preference for the high-affinity naïve B cells in GC. A separate study using N332-supersite on HIV Env trimer germline targeting showed that designing high-affinity antigens could elicit expansion of bnAbs precursor B cells, despite rare precursor frequencies for the latter [300]. Experiments utilizing authentic naïve VRC01-class B cells showed that both precursor frequency and affinity influenced responses to HIV immunogen, underlying the importance of germline targeting approach to vaccine design against HIV [301].

Immune subversion mechanisms of pathogens

Mutational escape from antibodies and T cells is a common feature of chronic pathogens such as HIV and LCMV in mice [302-308] [309], [192, 310-318]. In LCMV infection, antibody escape mutants are usually observed in the absence of CTLs [176]. Additional escape, from the CTL epitopes of the nucleoprotein and the glycoprotein has been also described and is thought to contribute to viral persistence. It is similar for HIV where both antibody escape variants, bnAb escape variants and CTL escape variants have been described in HIV-infected patients. This is one of the most controversial observations in antibody evolution during chronic HIV: despite the need for chronicity for antibody breadth to evolve, this also give a chance of each viral variant to escape the newly-evolved antibodies [194, 314, 319].

Other factors, apart from mutational, escape have been described to negatively impact humoral responses during chronic infections. These include extensive glycosylation preventing neutralization, huge CTL response, polyclonal B cell activation and high antigen load [195, 196, 320-324].

Several studies suggested that CTLs mediate the destruction of the lymphoid structure, consequently affecting GC organization and effective interaction between lymphocytes [325-327] [328]. It is still debated whether CTL direct killing of B cells is also involved in the delay of humoral response [329-331]. Hypergammaglobulinemia is

a well-known part of the clinical picture for HIV patients and it has been described for HCV and LCMV in mice [243, 259, 260, 332-334]. It is suggested that hypergammaglobulinemia is one of the pathological skewing of B cells responses which lead to failure to control the virus due to polyclonal B cell activation. Activation of polyclonal B cells and overproduction of antibodies could be at the expense of other B cell compartments. Finally, the antigen load as a sole parameter is not so clear and it seems to be a point of controversy. High antigen load in LCMV had been reported to lead to terminal differentiation of antiviral B cells into short-lived IgM-producing ACSs [324]. On the other hand, mice with impaired CTL responses (TAP) developed high nAbs over time [177, 320]. Our group showed as well that chronic infection results in productive GC reaction and eventual development of neutralizing titer against LCMV, supporting the fact that one of the requirements for developing HIV broadly neutralizing antibodies (bnAbs) is infection time [155, 201].

Aims of the thesis

The aim of this study was to investigate the immune responses to chronic viral infections. Our main focus was the longitudinal response of monoclonal antiviral B cells (KL25) in the context of chronic viral infection with lymphocytic choriomeningitis virus (LCMV).

Selective deletion of high-affinity B cells in the late phase of chronic viral infection

Mirela Dimitrova[1], Marianna Florova[1], Kerstin Narr[1], Yusuf I. Ertuna[1] and Daniel D. Pinschewer[1]*

Affiliations
[1] University of Basel, Department of Biomedicine-Haus Petersplatz, Division of Experimental Virology, 4009 Basel, Switzerland

*Corresponding author:
Daniel D. Pinschewer, M.D.
Department of Biomedicine-Haus Petersplatz, Division of Experimental Virology, 4009 Basel, Switzerland
E-Mail: daniel.pinschewer@unibas.ch
Phone: +41 79 543 39 70

Abstract

Perturbed B cell responses and late formation of neutralizing antibodies are hallmarks of chronic infections but the mechanisms underlying the dysfunctional humoral responses remain poorly defined. We used adoptive transfer of monoclonal anti-viral B cells (KL25) in the context of chronic lymphocytic choriomeningitis virus (LCMV) infection in mice and we observed late clonal deletion of the KL25 cells. This process was governed by the binding affinity of the KL25 B cell receptor (BCR) to its target, the viral glycoprotein (GP), and the persistence of the antigen. We found that the loss of the KL25 B cells was independent of IFN-I inflammation, and it was the result of terminal differentiation into short-lived antibody secreting cells (ASCs). In a striking difference to antiviral T cells, long-term viremia did not result in a significantly altered transcriptional program in the LCMV- specific B cells compartment. The late deletion of high-affinity B cells in chronic infection may explain the delayed neutralizing antibody response to persistent pathogens. Strategies to counter B cell clonal deletion should help us improve humoral immunity against chronic infectious diseases.

One-sentence summary

High-affinity antiviral B cells are deleted in late phase of chronic LCMV infection due to their terminal differentiation into short-lived antibody secreting cells.

Introduction

Chronic systemic viral infections such as HIV (a), Hepatitis B virus (HBV) (b), and Hepatitis C virus (HCV) (c) infect millions of people around the world, thus representing a major medical and humanitarian challenge (WHO a,b,c- accessed March 2021). The main postulate is that the host organism fails to clear the pathogen due to the outpacing of the adaptive immune system by the pathogen, more specifically of the $CD8^+$ cytotoxic T cells [82, 94, 95, 335-338]. In such infections, antiviral T cell responses can undergo "exhaustion", which encompasses their deletion or their functional alteration, associated with upregulation of inhibitory receptors, such as PD-1 [339-343]. In contrast, B cell responses to chronic viral challenge have been studied less extensively and are less well understood. Data from HBV and HIV infected individuals indicate that their B cell compartment can undergo phenotypic alterations such as accumulation of atypical memory B cells [250, 344-347] with upregulation of inhibitory receptors such as FcRL4 and PD-1. Accordingly, HBV-specific B cells from chronically infected individuals produce limited amounts of antibodies in culture and exhibit defective antibody-secreting cells (ASCs) differentiation upon ex-vivo stimulation, both of which can be alleviated with anti-PD-1 blockade [344, 348]. Moreover, immunosuppression in HIV patients comprises humoral arm of the adaptive immune defense as evident in impaired in antibody responses to vaccination [349] and a decreased life span of memory B cells [350].

Chronic infection of mice with lymphocytic choriomeningitis virus has long served as model to study host-pathogen interactions in persistent viral infections. Similar to HIV, LCMV infection suppresses antibody response to third-party antigens [82]. Moreover, at the onset of chronic viral infection, antiviral B cells are deleted in a type I interferon- (IFN-I-) dependent manner, termed decimation [200, 351, 352]. Non-canonical features of humoral immune defense to protracted or chronic viremia comprise also the clonal dominance of low affinity B cell clones in murine salmonellosis and their mostly extrafollicular hypermutation [353]. The dominance of IgM memory B cell recall responses to Plasmodium parasites and the importance of multimeric IgM antibodies in restricting parasite invasion in erythrocytes represent additional examples [354, 355].

These recent findings demonstrate the limitations in our understanding of B cell responses to chronic infections, which in critical parameters can differ from B cell responses to protein immunization. Here, we performed adoptive transfer experiments with monoclonal virus-neutralizing B cells to investigate their differentiation in chronic persistent LCMV infection. We found that high-affinity but not low-affinity B cells were clonally deleted owing to the cells' biased differentiation into short-lived antibody-secreting cells (ASCs). This clonal dominance pattern was reversed in the context of acute infection or vaccination and was independent of IFN-I-driven inflammation, thus offering a mechanism for the delayed formation of high-affinity virus-neutralizing antibodies in chronic infections such as HIV and HCV.

Materials and Methods

Cells

BHK-21 cells (ECC) were cultured in Dulbecco's Modified Eagle's Medium High Glucose (DMEM) with 4500mg/L glucose (Gibco), L-glutamine, sodium bicarbonate (Sigma Aldrich), supplemented with 10% heat-inactivated foetal bovine/calf serum (FBS or FCS, Sigma), 10mM HEPES (Gibco), 1mM sodium pyruvate (Gibco), 1X tryptase phosphate broth (TPB)(Sigma). BHK-23, a producer cell line expressing WE glycoprotein, was cultured in complete BHK21 supplemented with Puromycin (200µg/ml stock concentration, Thermofisher). 3T3 cells were cultured in DMEM medium supplemented with 10% FBS and Penicillin/Streptomycin (10'000 U/ml penicillin and 20mg/l streptomycin, stock concentrations, Gibco). Suspension cells 293F suspension cells were cultured with 293 expression media (Gibco). MDCK cell line was maintained in minimum essential media (MEM) and 10% FCS. All cell lines were routinely Mycoplasma tested.

Plasmids

The pol I/II- driven rescue system has been previously described [66]. For the rescues of LCM viruses and New World Arenaviruses (Pichinde and Candid#1) used in this study we used their respective pC-L and pC-NP [66, 356]. The recombinant viruses are described in detail in Table 1.

Viruses

Clone 13 LCM virus was [80] derived from LCMV Armstrong, isolated from infected monkeys [357] by Charles Armstrong in 1934. WE strain was isolated in 1935 by Scott and McNair [358]. Aggressive and docile LCM viruses were cloned from blood of an adult mouse, infected at birth with LCMV UBC (University of British Columbia isolate) [359], [360]. Pichinde was first described in 1971 [361] with PICV natural vaccine vectors also described before [362, 363]. The Argentine hemorrhagic fever was described in 1953 and the first vaccination study was done in 1998 [364]. The viruses were always propagated either BHK-21 or suspension cells 293F by infecting with M.O.I. (multiplicity of infection) 0.01. The supernatant was harvested and titers were determined by plaque forming assay. Mice were infected with various doses and routes, described in figure legends and results for each individual experiment.

Virus name	Glycoprotein	Viral backbone	pCs (L and NP)	KL25 KD(M)
rCl13/WE	GP-WE	LCMV Clone 13	LCMV	5.04E-09
rCl13/N119D	GP-WE (N119D)	LCMV Clone 13	LCMV	1.60E-07
rCl13/N119S	GP-WE (N119S)	LCMV Clone 13	LCMV	< detection
rDOC/N119D	GP-DOC (N119D)	LCMV Docile	LCMV	Not measured*
rAGG/N119D	GP-DOC (N119D)	LCMV Aggressive	LCMV	Not measured*
rArm/WE	GP-WE	LCMV Armstrong	LCMV	5.04E-09
rArm/N119S	GP-WE (N119S)	LCMV Armstrong	LCMV	< detection
rPICV/WE	GP-WE	Pichinde	PIC	5.04E-09
rPICV/N119S	GP-WE (N119S)	Pichinde	PIC	< detection
rCAND/WE	GP-WE	Junin	CAND	5.04E-09
rCAND/N119S	GP-WE	Junin	CAND	< detection

Table 1. Recombinant viruses and their genetic description. Virus name is the name used throughout this work to describe the corresponding recombinant arenavirus. Glycoproteins and their single point mutations are described. Viral backbone refers to which is the large (L) segment used to rescue the recombinant virus. pCs are the transacting elements used in the pol/II-driven rescues of the viruses. KL25 KD(M) refers to the surface plasmon resonance study, performed by Dr. Remy and published in her thesis. For these KD values KL25 was used as a Fab analyte.

Transfection of cells and rescue of recombinant viruses

We seeded BHK-21 or BHK-23 cells at $5X10^5$ cells/well in a 6-well plate format in BHK-21 or BHK-23 medium. The next day, the cells were transfected with plasmid DNA using lipofectamine/OptiMEM (Invitrogen, 3µl/µg of DNA) according to manufacturer's instructions. For rescue of all the two-segmented viruses, the trans-acting factors NP and L were supplied form pol-II-driven plasmids at 0.8µg/rescue of pC-NP and 1.4µg/rescue of pC-L. They were co-transfected with 1ug/rescue from each of the two pol-I-driven Arenavirus segments, segment S and segment L. Plasmid GFP-expressing minigenome (MG) was included in each rescue experiment to assess the success of transfection based on the GFP expression. 48 hours after transfection, we transferred the supernatant and cells into T-75 flasks. 72 hours later, the supernatant was collected, centrifuged to remove cell debris and stored at -80°C. The viruses were further passaged on either BHK-21 or suspension cells 293F (Invitrogen) and titrated on 3T3 cells.

The reverse engineering and rescue of LCMV clone 13 (Cl13) and Armstrong (Arm), expressing WE and variants thereof, expressing either N119D or N11S mutations [176] has been described before [66, 195, 365]. DOCILE (DOC) and Agrressive (Aggr), expressing N119D mutation were also designed and rescued in a similar fashion as previously described [366] and stocks were grown on MDCK cells. The generation of the New World Arenavirus Pichinde and the live-attenuated Candid #1 was achieved by using engineering and rescue systems as before [356]. Mutations of the WE GP were introduced by site-directed mutagenesis (SDM) to introduce the single point mutation in the glycoprotein, encoded in PolI-S-segment of the corresponding virus.

Virus stocks were produced on BHK-21 or 293F suspension cells (Invitrogen). Viral titers and viremia from mouse blood samples were determined by focus forming assays on 3T3 cells (ATCC)[367].

Focus forming assay (FFA)

FFA for determination of LCMV titers was described before [367]. For determination of viral titers in general, 3T3 cells were seeded at $0.5X10^5$ cells/well and mixed with 3-fold dilutions of viruses, starting neat, in MEM with 2% FBS in a 96-well format. For determination of blood viral titers, $1X10^5$ cells per well were mixed with 200µl neat virus or 10-fold diluted virus in medium in a 24-well plate.

The plates were incubated at 37°C, 5% humidity for 2-3 hours until the 3T3 cells attached and Methylcellulose medium (2% Methylcellulose in supplemented DMEM) was added (80µl for the 96-well plate and 200µl for the 24-well plate) to ensure the virus spreads only through neighboring cells and not through the supernatant. After 48 hours, the plates were flicked off and fixed with 4% paraformaldehyde (PFA) for 15-30 min. This and all following protocol steps were performed at room temperature and the volumes added to the plates were either 100 µl/well for 96-well plates or 200µl/well for the 24-well plates. Next, cells were permeabilised with Triton-X (BSS with 1%Triton-X-100, Merck Millipore) for 20 min and blocked for 15 min with PBS with 5% FCS. For detection of LCMV an anti-LCMV NP at 1:30 (human VL4) was used and for Pichinde and Candid, anti-Pichinde-NP (1:200) and anti-Candid (1:400) were used, respectively. The antibodies were diluted with PBS/2.5% FCS and incubated for 1 hour. The plates were flicked off and washed in tap water and the secondary HRP-goat-anti-rat-IgG was added at 1:100 dilution in PBS/2.5% FCS and incubated for 1 hour. Again, the plates were washed and the color reaction (0.5g/l DAB (Thermofisher), 0.5 g/l Ammonium Nickel (II) Sulfate (Sigma) in PBS with 0.015% H_2O_2) was added. The reaction was stopped after 15 min by washing with tap water. Stained plaques were counted either manually (when background was high) or using C.T.L. counter (ImmunoSpot ®) using BioSpot® software. Final titers were calculated according to the dilution.

Mice and animal experimentation

KL25HL B cells express the LCMV-neutralizing KL25 antibody as a B cell receptor (BCR). The VDJ of the KL25 is a knock-in in the immunoglobulin heavy chain locus, replacing all DQ52 and JH elements with V_HDJ_H of the KL25 in embryonic stem cells [368]. The light chain of KL25HL is a newly generated transgenic line (BasL36) (Narr *et al.* , manuscript in preparation) or knock-in line (HkiL) (Florova *et al.* , manuscript in preparation). The light chain VJ knock-in was achieved via homologous recombination to replace J1-J5 J elements of the IgL locus with the KL25 VJ using CRISPR/Cas9 system. The HkiL was on a RAG2 knock- out background [369].

KL25L (carrying only the LC as a transgene) mice served as recipients to avoid anti-idiotypic rejection [155, 200] throughout this project and were always referred to as wild-type (wt) recipient mice. Throughout Figure 3, they are labelled as wt since they are compared to *Ifnar-/-* XTgL mice which are simply referred to as *Ifnar-/-* recipients. *Ifnar-/-* mice were described before [370] and were crossed to KL25L mice.

Blimp-1-GFP KL25 reporter mouse was generated as a cross between heterozygous Blimp-1-GFP reporter [217] and KL25 BasL36 mouse. Due to technical reasons, we have kept the Blimp-1-GFP KL25 reporter as a chimeric mouse on C57BL/6 background. The chimeric animals were generated by adoptive transfer of bone marrow and

splenocyte from donor Blimp-1-GFP KL25 reporter mouse into CD45.2 lethally irradiated recipients one day after irradiation.
All mice were on a C57BL/6 background and were kept under specific-pathogen-free (SPF) conditions for colony maintenance and experiments. Breeding was conducted at the University of Zurich and at the University of Basel. Experiments were performed at the University of Basel in accordance with the Swiss law for animal protection and with authorization by the Cantonal Veterinary Office Basel-Stadt.

Isolation of cells and cell transfer
For transfer of purified KL25 B cells, we used a magnetic-activated cell sorting (EasySep™ Mouse B cell Isolation Kit, StemCell. Purity (>95%) was confirmed by three separate FACS experiments (data not shown). After isolation the KL25 B cells were washed with BSS and counted using hemacytometer at 40X magnification under the microscope. The cells were step-wise diluted to the appropriate concentration for adoptive transfer and transferred in a 5ml polystyrene (FACS) tubes, always taking into account that engraftment was 5% as shown in Supplementary Figure 2. The adoptive transfer was performed via tail vein i.v. injection after inducing peripheral vasodilation by warming. If the injection was not 100% successful, the results were scrutinized when analysed and suspected failed engraftment samples were excluded from further analysis.

Flow cytometry
Organs were collected in RPMI-1640/5% FCS, adjusted to mouse osmolarity. Single cell suspensions were obtained by digesting the isolated spleens with collagenase D (Roche) and DNase (Sigma-Aldrich) in mouse osmolarity adjusted medium [371]. Staining of spleen samples was performed in PBS containing 2% FCS, 5mM ethylenediaminetetraacetic acid (EDTA) and 0.05% sodium azide (staining buffer). For staining of splenocytes, antibodies (clones) against the following antigens were used: CD45.1 (A20), CD45.2 (104), B220 (RA3-6B2), CD19 (1D3), CD138 (281-2), GL7 (GL7), CD38 (90), CD22 (OX-97), TACI (ebioBF10-3), IRF4 (3E4) from eBioscience™ and Bcl6 (K11-91) from BDBiosciences. The Zombie UV™ Fixable viability kit (BioLegend) was used to exclude dead cells as described in the manufacturer's protocol.
For intracellular staining of transcription factors, the cell suspensions were treated with FoxP3 transcription factor staining buffer from eBioscience™ following the provider's instructions.
Stained cells were measured on a BD LSRFortessa™ (BD Biosciences) flow cytometer and data were analysed using FlowJo software (FlowJo LLC, version 10.5.3).

Fluorescent-activated cell sorting (FACS)
Spleens were collected as described before and stained in a similar fashion but using Na Azide-free buffer with mouse osmolarity. Samples were sorted unfixed in TRI reagent and immediately snap frozen on dry ice.

Next generation RNA sequencing and bioinformatic data analyses
Bulk RNA sequencing: CD45.1^{+}CD19+GL7+ B cells were sorted directly in TRI Reagent (Sigma-Aldrich) using a FACSAria II (BectonDickinson). RNA was extracted with Direct-zol RNA MicroPrep Kit (Zymo Research) in a plasmid-free laminar flow cabinet. The RNA concentrations were measured with eukaryote total RNA pico with concentrations ranging from 10pg/µl. Library preparation was performed using TruSeq kit (Illumina) and were quality checked. Samples were pooled to equal molarity and sequenced with NextSeq500 (Kit V2) (Illumina) and the results were 37-66 million reads/sample.
Reads were aligned to the mouse genome and data was analyzed in sciCORE using limma_voom gene mapping method with quality weights [372, 373]. Cut-off for significant difference in gene expression between experimental groups was set at log2 (fold change) >2.

Enzyme-linked immunosorbent assay (ELISA)
LCMV GP-1-specific antibodies in serum were measured by enzyme-linked immunosorbent assay (ELISA) using a recombinant fusion protein consisting of the outer globular GP-1 domain of the LCMV-WE glycoprotein fused to the human IgG constant domain (GP1-Fc) [374]. To perform ELISAs, 96-well flat bottom high-binding plates were coated with 50µl/well anti-human Fc-specific antibody (Jackson ImmunoResearch Europe Ltd, UK) diluted in coating buffer (15 mM Na_2CO_3 35mM $NaHCO_3$ dissolved in ddH_20, pH: 9.6) and incubated overnight at 4°C. The following day, the coating solution was removed and the plate was incubated with 200µl/well blocking buffer (5% milk powder PBS-Tween-20 (5%) (PBS-T) (Merk, Germany) at RT for 2 hours. The blocking buffer was removed and the WEGP was diluted in blocking buffer and added to the plates (50µl/well), followed by incubation at RT for 1 hour. Plates were washed 3X with PBS-T. Mouse sera were serially diluted (1:3) with a first

dilution 1:10 for samples where high antibody titers were expected. 50µl of the samples/well were transferred to coated and blocked plates, followed 1 hours of incubation at RT. Then the plates were washed 3X with PBS-T. HRP-conjugated anti-IgG antibody (Jackson) was diluted in blocking buffer and was added to the plates for detection of bound serum antibodies (50µl/well). The plates were washed 3X with PBS-T and once with PBS. The color reaction solution was prepared by mixing 2.8 ml 0.1 M citric acid (Sigma Aldrich), 2.2 ml of 0.2 M Na_2HPO_4 (Sigma Aldrich), 5ml of ddH_20, 10µl H_20_2 and 10mg ABTS (2,2'-Azino-bis (3-ethylbenzothiazoline-6-sulfonic acid) diammonium salt, Sigma Aldrich). It was added to the wells at 50µl/well and 15 minutes later absorbance was measured on a monochromator (Safire II™, Tecan Group Ltd, Switzerland). KL25 IgG1 (BioCell) control antibody (at 100ug/ml starting concentration) was used to quantify the precise amounts of KL25 antibody per ml of blood.

Data and statistical analysis

In order to compare a single parameter between two experimental groups, we have performed unpaired two-tailed Student`s t -test. For comparison of a single parameter across multiple groups one-way ANOVA or multiple unpaired two-tailed Student`s t -tests were used as indicated in each figure legend. For comparison of multiple parameters across multiple groups two-way ANOVA with multiple comparisons test was used (simple effect within row option). Details about statistics are given in figure legends. Statistical tests were performed using Prism 8 for MacOS (version 8.1.1 (224)). ELISA titers were calculated using Gen5™ (BioTek™) software. FlowJo software (FlowJo LLC, version 10.5.3) was used for the analysis of the flow cytometry data.

Results

High-affinity B cells are deleted in chronic viral infection

We used LCMV, a prototypic mouse virus [79, 357, 375], to model chronic virus infection in this study. Recipient mice were infected with high dose (approx. 10^6 pfu/mouse) LCMV Cl13 (Fig 1A), engineered to express WE glycoprotein (rCl13/WE), as described before [66]. A week later (day 0) we adoptively transferred titrated numbers of KL25 B cells into infected recipients, resulting in an engraftment of approximately 10, 100 or 1000 cells per spleen. Engraftment was calculated by analyzing KL25 cell numbers one day after transfer in uninfected recipients and it was estimated to be in the range of 3-5% (Fig. S2), in line with previous reports [291, 292]. The engrafted KL25 cells have a BCR which binds with very high neutralizing affinity to WE glycoprotein and KL25 Abs are capable of neutralizing LCMV carrying WE GP [176]. Four weeks later, the KL25 B cells were detected in the experimental groups where 10^3 and 100 cells were engrafted (Fig 1B and C) while the 10 engrafted KL25 cells were under detection limit as in recipient mice with no adoptive transfer (AdTF). Moreover, the cell numbers at week 4 from the 10^3 cells group were an average of 10-folds higher than recovered from the 100 cells group (Fig 1C), reflecting the difference the initial number of engrafted cells. Intriguingly, however, the latter group's KL25 cells exceeded the technical background by >>10-fold. Hence, a proportionally expanded population of KL25 B cells in the 10 cells recipient group should have been readily detected (projected to be 1-2X103 cells/spleen which is readily detectable above technical background). The lack KL25 progeny population raised the possibility that the 10 engrafted KL25 did not expand at all and were lost after adoptive transfer. Contrary to this hypothesis, the KL25 cell-derived antibody was detected in the serum of recipient mice one week after transfer, indicating that some of the engrafted 10 cells survived, expanded and part of their progeny differentiated into ASCs (Figure 1D). Four out of five mice from the 10 engrafted cells group exhibited KL25 antibody was above the detection limit of the ELISA assay (0.05µg/ml) and above the no AdTF control group. The control group (no AdTF) did not produce GP1-specific antibodies over technical background, indicating that GP-1-specific antibody responses of the KL25 recipients originated from the transferred cells. The phenotype of the surviving KL25 cells in the 100 and 1000 cells transfer groups was predominantly of a germinal center (GC) phenotype ($CD38^-GL7^+$) (Figure 1B). Viremia was detectable throughout the 4 weeks of the experiment in the mouse group with 10 engrafted KL25 cells, although it was somewhat suppressed at weeks 2 and 3, supposedly due to the secreted high-affinity antibody from the transferred KL25 cells. This limited amount of the antibody was apparently not sufficient to completely suppress the virus as evident from the viremia at week 4 in this experimental group. In contrast, the 100 and 1000 KL25 engrafted cells produced copious amounts of antibody (Figure D), resulting in early complete clearance of rCl13/WE virus from blood (Figure E).

We next sought to investigate the fate of the disappearing 10 engrafted KL25 B cells. We performed LCMV infection and adoptively transferred 10 or 100 KL25 B cells as before (Figure 2A). 100 KL25 B cells expanded during week 2 and were maintained until week 3, whereas 10 engrafted KL25 B cells peaked at week 2 but were not found at week 3 anymore (Figure 1B and enumeration in C). By week 2 the 100 KL25 cells engraftment group has cleared the virus from blood, while most animals in the 10 engrafted cells group were viremic throughout week 3 (Figure 2D). Anti-GP1 responses in serum peaked at week 2 in both KL25 recipient groups but at week 3 only the group of mice with 100 engrafted cells still had a detectable antibody titer (Figure 2E).

The differentiation of the KL25 B cells differed fundamentally between the 100 and the 10 cells groups. At week 2, the cells in both groups had expanded similarly (Figure 2B and 2C), however the KL25 cell progeny in the 100 cells group consisted almost entirely of $CD19^+CD138^-$ B cells, while the 10-cell transfer yielded mainly $CD19^-$ $CD138^+$ ASCs or $CD19^-CD138^-$ pre-plasmablast B cells, suggesting they were mainly a population of cells consisting of or committed to become ASCs (Figure 2F and 2G).

Together, these observations indicated that a physiological precursor numbers of 10 high-affinity antiviral B cells [291] expanded vigorously upon adoptive transfer into viremic hosts but were eventually deleted as the chronic infection progressed. In contrast, higher numbers (:::100) of such cells secreted sufficient amounts of KL25 antibody to clear the infection within a few days after engraftment, and avoided the aforementioned deletion.

Chronic viral infection causes limited transcriptional changes in the antiviral KL25 B cells

Chronic viral infection promotes unique differentiation programs in CD4 and CD8 T cells [376] [377], but the impact of persistent infection on antigen-specific B cells remains to be further investigated. The aforementioned sets of results had raised the possibility that persisting viral antigen per se could profoundly influence the fate of antiviral B cells. The early elimination of rCl13/WE by as few as 100 engrafted KL25 cells had, however, prevented us from formally differentiating the impact of chronic antigenic exposure from transferred cell number effects. To overcome these limitations, we engineered LCMV viruses, which were based on the Docile

and Aggressive variants of LCMV-WE, resulting in chronic and acute infection, respectively (Figure 3A) [359, 378]. Differential persistence of Docile and Aggressive is due to mutations in their large (L) genome segment [379]. Accordingly, we used viruses carrying either a Docile (DOC) or an Aggressive (AGG) L segment together with the same Docile small (S) segment. The latter was engineered to contain a single point mutation N119D in the GP gene, reducing KL25 affinity to below a critical threshold [176], thus enabling the viral persistence throughout the experiment even when confronted with a strong KL25 B cells response. We infected mice with either DOC/N119D or AGG/N119D and engrafted 100 KL25 B cells after one week (Figure 3B). DOC/N119D resulted in chronic viremia, while AGG/N119D remained below detection limit, as expected (Figure 3C). 4 weeks after adoptive transfer the KL25 B cells were detectable in all recipients (Figure 3D and percentage in Figure 3E). Irrespective of considerable of intra-group variation (Figure 3E) chronic viremia had not resulted in the deletion of the engrafted KL25 cells on day 25 (4 weeks). This finding prompted us to investigate potential transcriptional alterations resulting from chronic antigen exposure. A genome-wide transcription expression analysis of the KL25 B cells at week 4 showed that only very few genes were differentially regulated in cells emerging from acute as compared to chronic infection (Figure 3F). Accordingly, a principal component analysis (PCA) failed to show a clear clustering of KL25 B cells to either one or the other infection setting (Figure 3G). The top three differentially expressed genes upregulated in the chronic infection group were Ifi27l2a, Ifi27 and Usp18. All three are interferon-stimulated genes (ISGs) and Usp18 has been identified as a key regulator of interferon signaling in the context of LCMV infection [380-385]. These observations are in line with sustained type I interferon effect that last well into the chronic phase of LCMV [386]. At the same time, the absence of marked transcriptomic differences between B cells emerging from chronic and acute LCMV infection, and their long-term survival in the chronic infection rendered it unlikely that persistent antigenic stimulation alone was sufficient to account for the deletion of B cells described in previous paragraph and in Figure 1 and Figure 2.

BCR affinity rather than interferon-driven inflammation account for late KL25 B cell deletion

Our group and others have reported on the phenomenon of type I interferon (IFN-) driven deletion of KL25 cells at the onset of chronic LCMV infection [200, 352] herein referred to as “early decimation”. Hence, we sought to investigate to which extent interferon signaling may contribute to the phenotype of late deletion as described in Figure 1. Early IFN-I-driven deletion of KL25 cells occurs in a B cell-extrinsic fashion, supposedly by an IFN-I induced inflammatory milieu [200, 331]. Accordingly, it is prevented when hemopoietic cells other than B cells lack the type I interferon receptor (IFNAR), but not when B cells are IFNAR-deficient. Thus, we compared wild-type (wt) and interferon receptor deficient (*Ifnar-/-)* mice [370] as recipients in our experiments, to test whether late deletion relied on similar pathways as early decimation. As an alternative hypothesis to late IFN-I-driven deletion we considered that KL25 cells persisted when engrafted in chronically DOC/N119D-viremic mice but were deleted when exposed to persistent rCl13/WE (Compare Figures 1 and 3). This observation raised the possibility that antigenic affinity contributed to late B cell deletion in persistent viral infection. To this end, we used either *ifnar-/-* or wt mice as recipients and infected them with either rCl13/WE or with a variant thereof named rCl13/N119S (Figure 4A and Table 1). rCl13/N119S was engineered to carry a GP point mutation resulting in even lower KL25 affinity than the N119D variant when measured by Surface Plasmon Resonance, see Table 1 [176]. Three weeks after engraftment of KL25 cells, the progeny of these cells was largely deleted in both rCl13/WE infected *ifnar-/-* and wt recipient, suggesting IFN-I-driven inflammation did not have a major contribution to late deletion (Figure 4B and C). In contrast, both types of recipients sustained the expansion of KL25 B cells when infected with the low-affinity rCl13/N119S variant virus (Figures 4B and C). These findings pinpointed a major role of BCR affinity in late deletion.

To further scrutinize the role of inflammation we used congenitally infected LCMV carriers, which have been used for almost a century as a model for tolerant persistent infections with only very low-level IFN-I-driven inflammation [174], [387]. We infected pups within 24 hours of their birth (Figure 4D) and when the mice reached adult age, we engrafted 250, 100 or 10 KL25 cells per recipient. Four weeks later, the KL25 cells had expanded and were detectable in all groups except in the rCl13/WE-infected mice with only 10 engrafted cells (Figures 4E and F). In this group only one out of three mice retained a detectable population of KL25 B cells. Analogous experiments were conducted with rCl13/N119S carrier mice (Figures 4E and F). In these latter animals adoptively transferred KL25 cells were consistently detected at week four, even when only 10 cells were engrafted, further supporting the concept that high-affinity B cells may be subject to late deletion when engrafted at physiologically low numbers. Virus persisted in all animals, irrespective of its GP (WE or WE-N119S mutant), and independently of the number of KL25 cells engrafted. Viremia was detectable in all carrier mice, as expected (Figure 4G).

Together, these data suggest that the observed late deletion of KL25 B cells in chronic viral infection occurs independently of IFN-I-driven inflammation but is chiefly governed by BCR affinity.

B cell receptor affinity governs late deletion of antiviral B cells in chronic infection

Next, we sought to elucidate in more detail how BCR affinity impacts the late deletion of KL25 B cells. We infected adult recipient mice with either rCl13/WE, rCl13/N119D or rCl13/N119S (Figure 5A), and six days later we engrafted 10 KL25 cells per recipient and analyzed the cells' progeny 4 weeks later (Figure 5B). Infection with Cl13/N119D or Cl13/N119S resulted in the maintenance of a KL25 B cell population while the recipients infected with rCl13/WE were virtually devoid of KL25 cells, as expected (Fig 5C and D). The surviving cells were all B cells ($B220^{+}CD138^{-}$) rather than ASCs (Figure 5E). Intriguingly, the initial expansion of KL25 B cells after the first week was largely independent of the BCR's affinity for the viral GP (Figures 5G and H), with affinity-dependent deletion only evident by the end of week 3 (Figure 5G and H).

These data corroborate that the affinity of interaction between antiviral B cells and their cognate antigen is the key determinant of late B cell deletion in chronic viral infection.

KL25 cells of all affinities are maintained in a self-limited acute viral infection

These findings of an inverse relationship between BCR affinity and B cell clonal maintenance (compare Figures 1 and 5) were counterintuitive and suggested that chronic infection promoted B cells clones of low to intermediate affinities. Such a putative affinity hierarchy in chronic infection, therefore, challenged the concept of clonal selection and subsequent evolution of the B cell response, which poses that B cell clones of higher affinity - generally resulting from affinity maturation - are selected to dominate the immune response as it progresses [388-392]. Hence, we tested whether the classical hierarchy applied also to KL25 B cells when responding to acute infection or to live-replicating viral vaccines. We infected recipients with a low dose of 200 plaque forming units (PFU) of either rCl13/WE, rCl13/N119D or rCl13/N119S, resulting in an acute self-limited infection, and engrafted 10 KL25 B cells 1 week later (Figure 6A). Indeed, the number of KL25 B cells recovered at week 1 reflected the affinity hierarchy: the highest affinity virus (rCl13/WE) resulted in the largest expansion of the cells, the intermediate affinity virus (rCl13/N119D) caused lower but detectable expansion and the lowest affinity virus (Cl13/N119S) only weakly expanded the B cells or not at all (Fig 6B and 6C). At week 4, however, these differences evened out, and all groups of recipients exhibited a similarly sized population of transferred KL25 cells, irrespective of the affinity of the KL25 BCR for the viral envelope GP (Figures 6B and C).

Next, we infected animals with WE-GP- or WE-GP-N119S-expressing viruses based on the less invasive Armstrong (Arm) strain of LCMV [82] (Table 1). Three weeks after engraftment all recipients exhibited a clear KL25 B cell population which was of comparable size, irrespective of the affinity for the viral antigen (Figure 6D and E).

Finally, in an attempt to test the KL25 B cell responses to prototypic live-attenuated viral vaccines we engineered Pichinde virus (PICV-) and Junin Candid#1 (CAND-)-based viruses, expressing WE-GP or WE-GP_N119S as their envelope protein [356] (Table 1). Pichinde is a very widely studied and highly immunogenic Clade A New World arenavirus that replicates poorly in mice [393]. Candid#1 is a live-attenuated vaccine used for prevention of disease by the Clade B arenavirus Junin, the causative agent of Argentine hemorrhagic fever [394]. One week after infection with either one of these viruses we engrafted 100 KL25 cells per recipients and analyzed population expansion and maintenance four weeks later. Corroborating and extending the trend observed with acute LCMV infection, rPICV/WE and rCAND/WE resulted in a more robust expansion and maintenance of the KL25 B cells 4 weeks after engraftment than their respective WE-GP_N119S low-affinity counterparts (Figure 6F and G).

Taken together, these data showed that the commonly held concept of affinity-driven selection and dominance of B cell clones applies also to KL25 B cells responding to acute infection or vaccination, whereas that chronic infection perturbs this hierarchy by causing late deletion of high-affinity clones.

High-affinity B cells responding to chronic infection undergo terminal ASC differentiation

We were interested in the differentiation pathway KL25 B cells undergo in chronic rCl13/WE infection, leading to their deletion. We infected mice with rCl13/WE or rCl13/N119S and engrafted either 100 or 10 KL25-Blimp-1 reporter B cells on day 6 [217] (Figure 6A). One week later we analyzed the differentiation of the transferred cells. All KL25-Blimp-1 reporter cells expanded to a detectable extent (Fig. 6B), with 100 engrafted KL25-Blimp- 1 cells yielding more progeny than the 10 cells, as expected. This difference was, however, more pronounced in the context of high-affinity rCl13/WE than with rCl13/N119S, and the group of mice receiving 10 engrafted cells expanded comparably, regardless of the infecting virus (Fig 6B and C). rCl13/WE infection resulted in a significantly higher proportion of KL25-Blimp-1 ASCs progeny and higher absolute KL25-Blimp-1 ASCs counts per spleen than in animals undergoing rCl13/N119S infection. Conversely, the majority of KL25-Blimp-1 cells

progeny in the latter group were B cells, and their absolute number exceeded those in rCl13/WE-infected recipients. These data suggested there was a skewing of the high-affinity B cells to terminal ASC differentiation in chronic infection, which was prevented by lowering the affinity of interaction between the B cells and their cognate viral antigen.

To further assess ASCs differentiation of KL25-Blimp-1 B cells we made use of an the engineered reporter allele Blimp-1^{gfp} [217], reporting Blimp-1, a master transcription factor determining ASC differentiation, as a green fluorescence. Blimp-1 and TACI are both essential for ACS differentiation [395] [396-398] and were expressed in a higher proportion of KL25 cells responding to high-affinity antigen (WE) than in a setting of low-affinity infection (N119S) (Figure 6D). In line with this observation, CD22, a BCR inhibitory receptor downregulated during ASCs differentiation, was significantly lower in KL25 B cells responding to rCl13/WE than in the low-affinity rCl13/N119S setting (Figures 6D and E).

To further investigate the impact of BCR affinity on transcriptional regulation of B cells we determined intracellular levels of the transcription factors (TFs) IRF4, known to be required for plasma cells differentiation [239], and of BCL6, the GC B cells' master transcription factor [229, 399, 400]. Most KL25-Blimp-1 cells responding to high-affinity rCl13/WE expressed IRF4, whereas rCl13/N119S yielded balanced population of IRF^{+} and $IRF4^{-}$ KL25 B cell progeny. The proportion of cells expressing BCL6 was rather modest in general, but was clearly augmented in B cells responding to low-affinity antigen, as opposed to a virtual absence of such cells in high affinity infection (Figures 6F and G).

Together, these data show that chronic infection promotes terminal ASCs differentiation of high affinity B cells, which may culminate in the cells' clonal deletion.

Discussion

HIV and HCV in human are associated with dysregulation in B cells responses, hypergammaglobulinemia and delayed development of neutralizing antibodies nAbs [250, 345-347, 349, 401, 402] [193, 320, 321, 403-406]. We observed clonal deletion of physiological-like precursor numbers [291, 292, 407] of high-affinity antiviral B cells in the chronic phase of the LCMV infection which may explain the late development of neutralizing antibodies against LCMV [175, 193, 320]. We hypothesize, therefore, that that clonal selection of the highest-affinity B cell clone against invading pathogen may be perturbed in a chronic infection. This may represent a novel immune subversion mechanism exploited by the chronic pathogen and may explain why is the mammalian immune system failing to clear persistent-prone pathogens.

Previous studies described early IFN-mediated decimation of LCMV-specific B cells as a partial reason for late production of neutralizing antibody in chronic viral infection with LCMV [200, 351, 352]. The decimation could be reversed by blocking IFN-I signaling, deplete myeloid cells or by blocking IL-10 and TNF-α [200, 352]. The observations reported here are fundamentally different in what the underlying mechanisms and key parameters are concerned. We perform AdTF 6 days after infection when initial IFN-I levels have already declined as shown before by Fallet et al, 2016 [200]. KL25 B cells are also deleted in the late phase of infection in *ifnar-/-* recipients, indicating extrinsic IFN-I signaling does not play a role in the late deletion observed in the current study. Moreover, the majority of WE carriers failed to maintain KL25 B cells when only 10 cells were engrafted, rendering IFN-I-driven inflammation an unlikely cause of late deletion of high-affinity B cells, while the same are apparently essential for early decimation. Early decimation is affinity-independent as shown by infection with the N121K and N119D mutants, which are low-affinity GP variants but still lead to early B cell decimation. Together, these data show that both early decimation [200] and late deletion of B cells result from skewed proliferation of the KL25 cells into short-lived ASCs. The mechanisms and biological parameters governing these two phenomena are, however, fundamentally different from each other.

After decimation in the first phase of infection, the B cell repertoire can be replenished by bone marrow B cell emigrants and ongoing GC reactions [324, 408]. Indeed, there is increasing evidence that chronic infection results in a particularly productive GC reaction, leading to the formation of nAbs in both LCMV and HIV-1 [155, 201]. In LCMV infection, the neutralizing titer seems to evolve after viremia drops, suggesting that the B cell clones carrying high-affinity BCRs can only reach critical clonal dominance after viral loads are suppressed [155]. Importantly though, the reciprocal relationship of the two phenomena poses a perfect chicken-and-egg problem, where the causality between arising nAb responses and viral control (or escape) could be linked in a different way. It is a commonly held opinion that arising nAb force the virus to escape. Alternatively, and our data suggest so, virus control may be due to the combined action of the other immune defense mechanisms such as non-neutralizing antibodies [175] [176] and CD8+ T cells, whereby the first would force the virus to acquire antibody escape mutations. Only once antigenic loads of the non-mutated viral protein fall below critical threshold would nAbs-producing B cells specific for the original virus variant be able to expand and form nAbs. Fallet *et al.* (2020) [155] showed that chronic LCMV infection promotes more robust GC reactions resulting in higher nAbs titers than acute infection. nAbs responses do not, however, overlap timewise with high-level viremia unless the dominant viral quasispecies exhibit escape mutations.

An unexpected discovery in our study was the minute differences in gene expression profile between B cells emerging from chronic and acute viral infection, as evident in a lack of group clustering in PCA and only a few clearly differentially regulated genes. This contrasts with Staupe *et al.* (2020) reporting differential gene expression between LCMV-specific B cells in acute and chronic LCMV infection [409]. The main difference, however, Staupe *et al*. detected on day 15 in GC B cells, an effect largely lost by day 45. These studies did not, however, take into account that LCMV Clone 13 infection is commonly cleared by day 45. In our study we therefore used the more invasive DOC strain of LCMV and we excluded any potential effect of differential clonal composition of B cells responding to acute and chronic infection by focusing on a monoclonal B cell population (KL25). In combination, these data suggest that murine antiviral B cells do not undergo a classical “exhaustion”, unlike T cells persistently exposed persistently to high levels of cognate antigen [410] [411].

As the present work shows, engrafting KL25 B cells at physiological-like precursor frequency similar or even lower than reported for VRCO1 anti-HIV class B cells in man [292], was key for the main observation reported. The very low numbers of KL25 cells but also their engraftment after infection was designed to mimic the response of new bone marrow emigrant B cells of antiviral specificity that are confronted with a persistent infection. Hence, this setting should further our understanding of viral immune subversion in the chronic phase of persistent viral infection rather than the response in the first, acute phase of the infection.

In conclusion, late deletion of B cells offers a novel mechanism whereby chronic infection subverts humoral defense. These insights should help tailoring intervention strategies aimed at furthering humoral immune control of persistent viral disease.

Figures

Figure 1. High-affinity B cells are deleted in the late phase of chronic viral infection

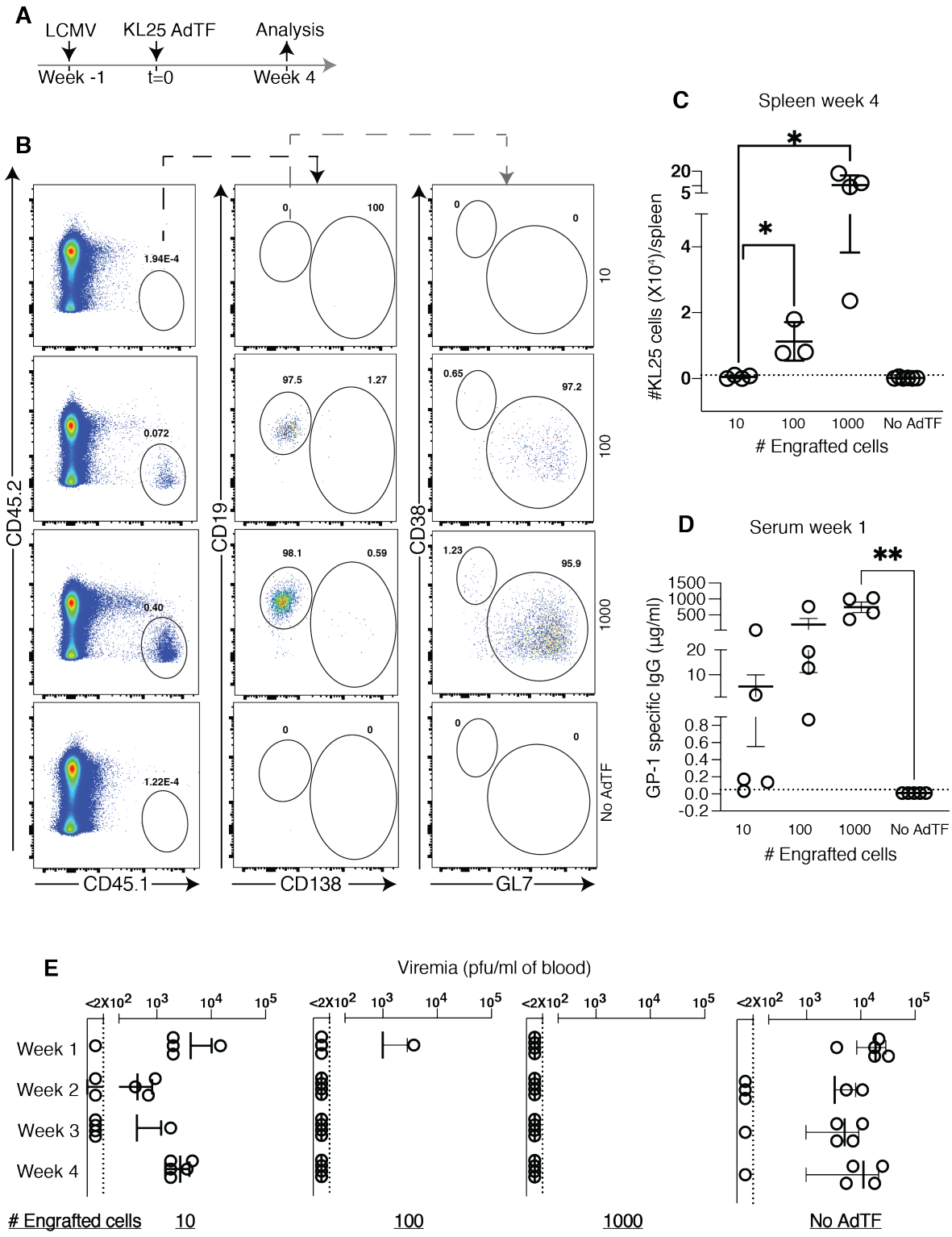

Figure 1. (A) We infected mice at week -1 with rCl13/WE prior to KL25 adoptive transfer (AdTF) at day t=0 of antiviral KL25 B cells, starting with 10, 100 and 1000 engrafted cells per mouse spleen. The animals were sacrificed 4 weeks later. (B) Representative flow cytometry plots showing the frequencies of KL25 B cells (CD45.1) amongst all groups. (C) Enumerated virus-specific KL25 B cells in the spleen. (D) GP-1-specific antibodies at week 1 after adoptive transfer and indicated individual KL25 values in µg/ml of mouse serum. (E) Viremia measured at weeks 1,2,3 and 4 in 10 cells, 100 cells and 1000 cells and NoAdTF (control) experimental groups. Data is displayed as mean±SD and symbols represent individual mice. Doted lines on graphs represent detection limit. Statistical analysis was performed with unpaired two-tailed Student's t tests for Figure 1 C and D. Significant p values (*,**,***,****) for $p < 0.05$; not statistically significant (n.s.) for $p \geq 0.05$, not statistically significant.

Figure 2. High-affinity B cells are deleted in the late phase of chronic viral infection (early analyses)

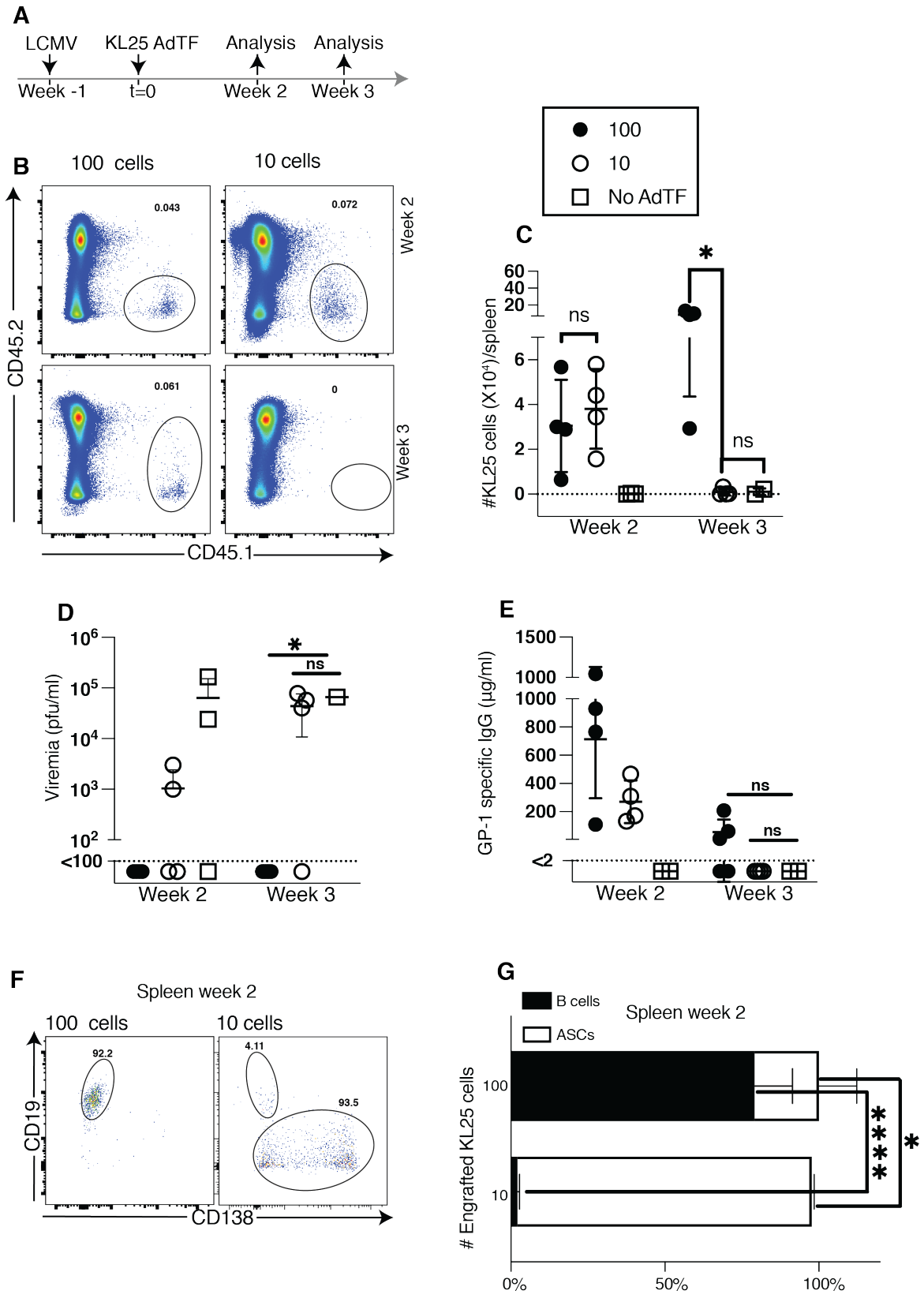

Figure 2. (A) We infected mice at week -1 prior to adoptive transfer (AdTF) and sacrificed the animals at the indicated time points. (B) Representative flow cytometry plots KL25 B cells from 10 and 100 engrafted cells groups. (C) Enumerated virus-specific KL25 B cells in the spleen from all groups. Viremia (D) and GP-1-specific antibodies (E) were monitored for the whole length of experiment. (F) Phenotypic analysis of KL25 B cells at week 2 from all groups. We calculated the percentage of B cells and ASCs at week 2 (G). Data is displayed as mean±SD and symbols represent individual mice. Doted lines on graphs represent detection limit. Statistical analysis was performed with one-way ANOVA for with multiple comparisons post-test (compared to control group No AdTF). Significant p values (*,**,***,****) for $p < 0.05$; not statistically significant (n.s.) for $p \geqq 0.05$, not statistically significant.

Figure 3. Chronic infection causes limited transcriptional changes in the antiviral KL25 B cells

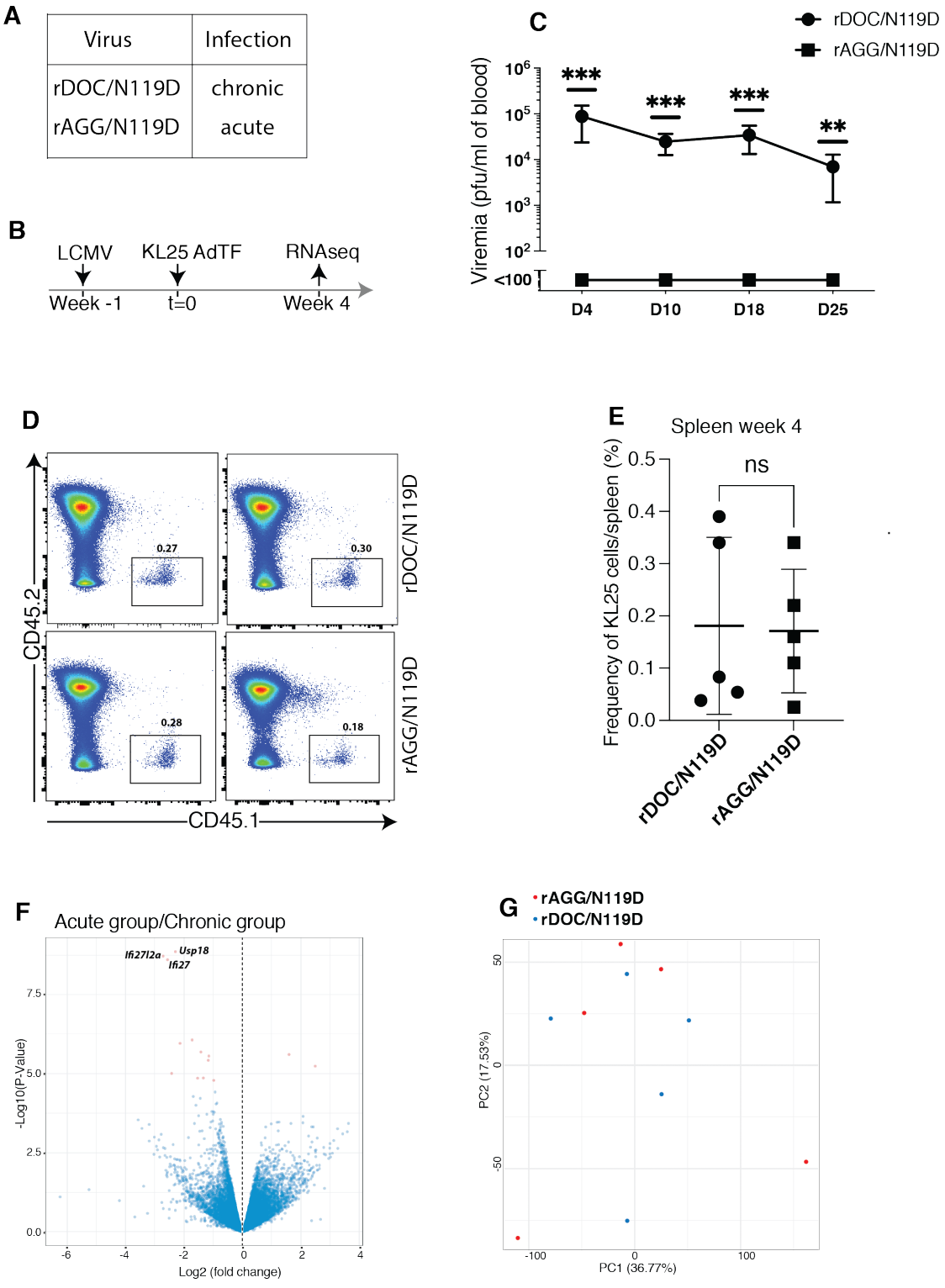

Figure 3. We infected mice with rDOC/N119D or rAGG/N119D (A) at week -1 prior to KL25 adoptive transfer (AdTF), resulting in 100 engrafted cells/spleen, and sacrificed the animals 4 weeks later and RNA sequencing of the KL25 B cells was performed. We monitored viremia over time (C). Representative flow cytometry plots showing KL25 progeny at week 4 (D) and calculated percentages of KL25 B cells in spleens at week 4 (E). Gene Set Enrichment Analysis (GSEA) (Figure 2F) and principal component analysis (PCA) in Figure 2G. Data is displayed as mean±SD in C and mean±SEM in E, and each symbol represent individual mice. Statistical analysis was performed with multiple unpaired two-tailed Student's *t* tests for viremia (C) and normal unpaired two-tailed Student's *t* tests for percentages of engrafted cells (E). Significant p values (*,**,***,****) for $p < 0.05$; not statistically significant (n.s.) for $p \geq 0.05$. (F) and (G) sequencing analysis was performed with limma_voom software with cut-off values for significantly differential gene expression set at 2.

Figure 4. BCR affinity rather than interferon-driven inflammation accounts for late deletion

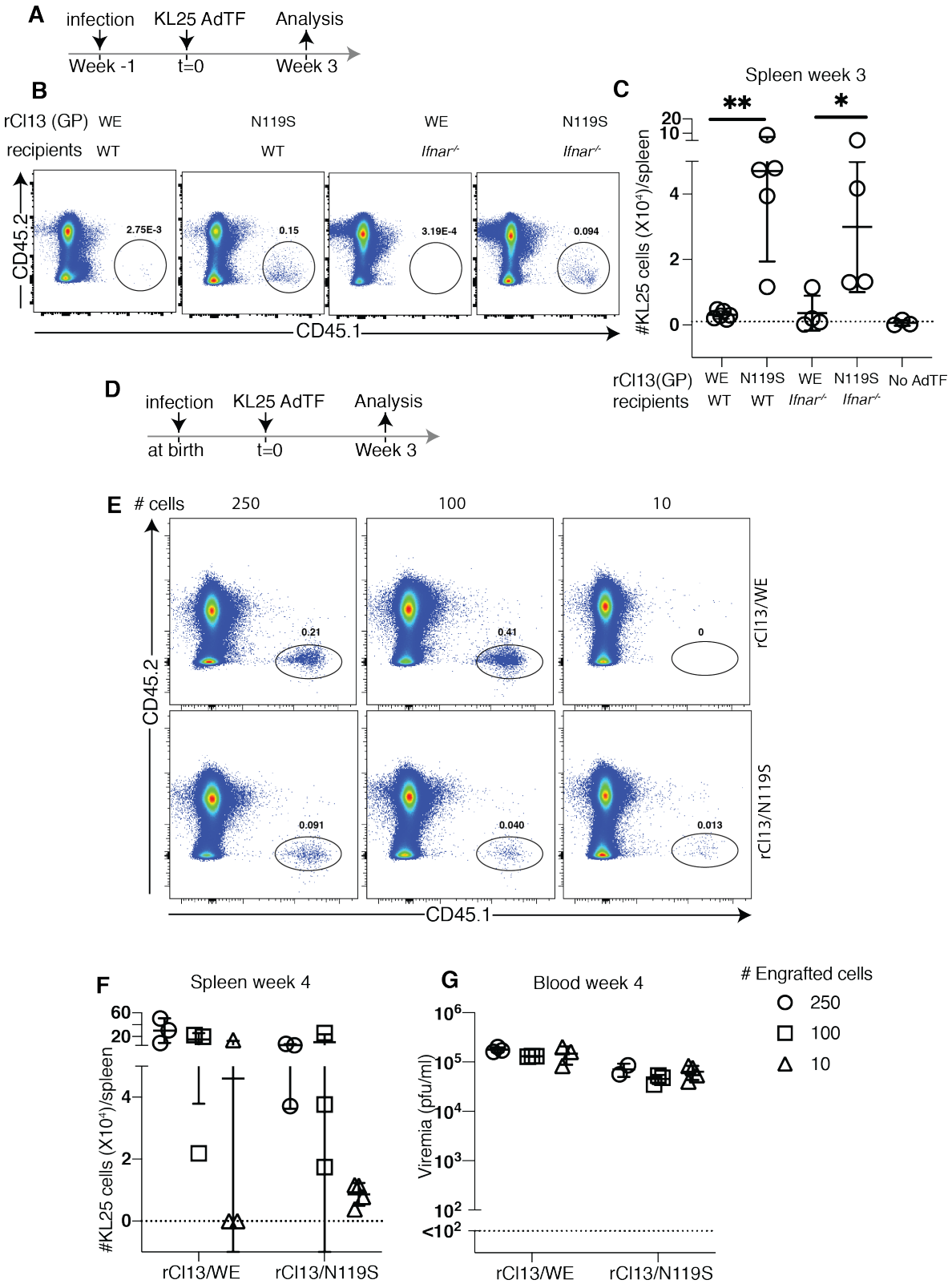

Figure 4. (A) WT or *Ifnar*$^{-/-}$ recipients were infected with rCl13/WE or rCl13/N119S viruses at week -1 prior to KL25 adoptive transfer (AdTF) at t=0 and analysed three weeks later. (B) Representative flow cytometry plots showing specific KL25 B cells (CD45.1) from all groups. (C) Enumerated virus-specific KL25 B cells at week 3. (D) Mice were infected at birth with rCl13/WE or rCl13/N119S viruses, adoptive transfer (AdTF) performed approximately 8 weeks later (t=0) and analyzed after four more weeks. (E) Representative flow cytometry plots showing specific KL25 B cells (CD45.1) from all groups. (F) Enumerated virus-specific KL25 B cells in all groups. (G) We measured last time point viremia for all groups (H). All data is displayed as mean±SD and symbol represent individual mice. Doted lines on graphs represent detection limit. Statistical analysis was performed with unpaired two-tailed Student's *t* tests. Significant p values (*,**,***,****) for $p < 0.05$; not statistically significant, n.s.: $p \geq 0.05$.

Figure 5. B cell receptor affinity governs late deletion of antiviral B cells in chronic infection

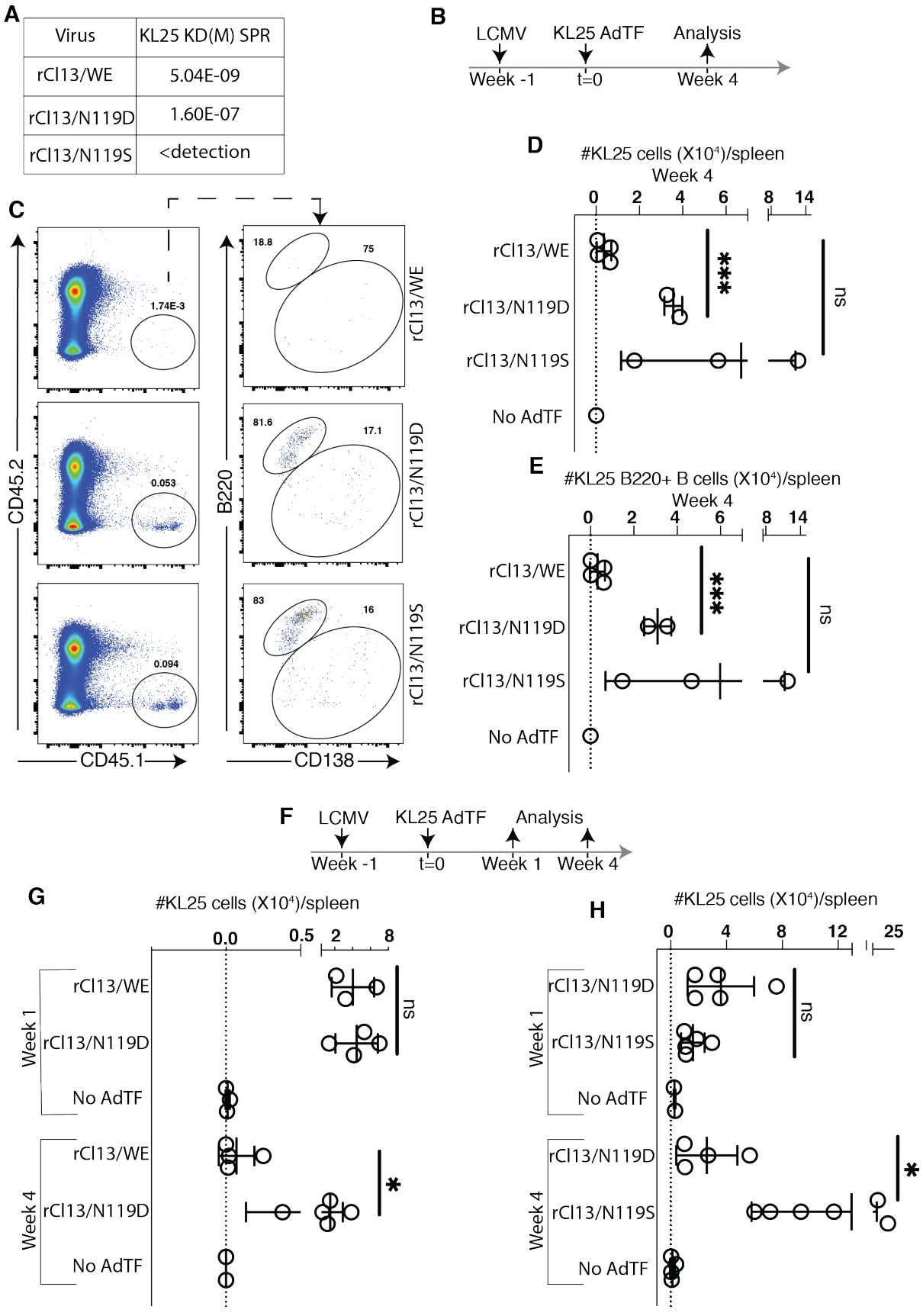

Figure 5. (A, B) Mice were infected with viruses with varying degree of affinity to the KL25 BCR at week -1 prior to KL25 AdTF (t=0) and sacrificed 4 weeks later. (C) Representative flow cytometry plots showing KL25 B cells. (D) Enumerated virus-specific KL25 cells, of which $B220^{+}CD138^{-}$ B cells (E). (F) Mice were infected with viruses with varying degree of affinity to the KL25 BCR at week -1 prior to AdTF (t=0) and sacrificed 1 or 4 weeks later. (G, H) Enumerated KL25 cells at week 1 and week 4 after transfer. All data is displayed as mean±SD and symbols represent individual mice. Doted lines on graphs represent detection limit. Statistical analysis was performed with unpaired two-tailed Student's *t* tests. Significant p values (*,**,***,****) for $p < 0.05$; not statistically significant, n.s.: $p \geqq 0.05$.

Figure 6. B cells of all affinities are maintained in self-limited acute viral infection

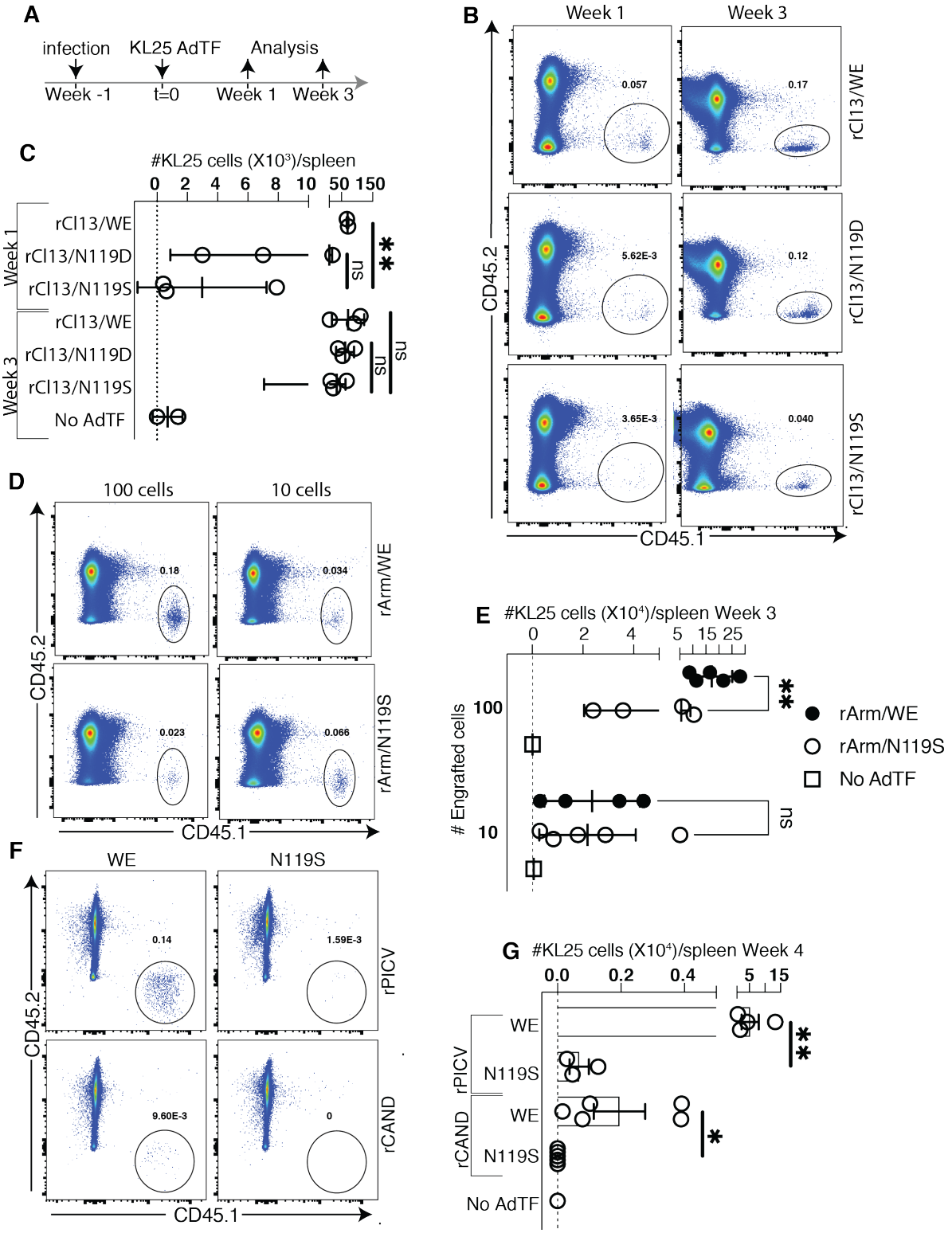

Figure 6. (A) Mice were infected with low dose (200pfu/recipient) Cl13 backbone viruses at week -1 prior to KL25 adoptive transfer (AdTF) (t=0) and analyzed 1 or 4 weeks later. (B) Representative flow cytometry plots showing KL25 B cells from all groups and time points. (C) Enumerated virus-specific KL25 B cells. (D) Mice were infected with Arm backbone viruses with WE GP or N11S GP at week -1 before engraftment of 100 or 10 KL25 B cells and analyzed 3 weeks later. (D) Representative flow cytometry plots at week 3. (E) Enumerated virus-specific KL25 B cells in all groups at week 3. A third infection model was performed using Candid and Pichinde backbone viruses, engineered with either WE GP or N119S GP. Infection and KL25 AdTF were performed as before. (F) Representative flow cytometry plots showing specific KL25 B cells (CD45.1) from all groups at week 4. (G) Enumerated virus-specific KL25 B cells 4 weeks after AdTF. All data is displayed as mean±SD, except Figure 5G which is displayed as mean±SEM and symbols represent individual mice. Doted lines on graphs represent detection limit. Statistical analysis was performed with unpaired two-tailed Student's *t* tests for figures C and G. In Figure 5G the two-tailed Student's *t* tests was performed after $\log_{10}$ conversion of data points. In Figure E, 2- way ANOVA with multiple comparisons was used with a simple effect within row post-test. Significant p values (*,**,***,****) for $p < 0.05$; not statistically significant, n.s.: $p \geqq 0.05$.

Figure 7. High-affinity B cells responding to chronic infection undergo terminal ASC differentiation

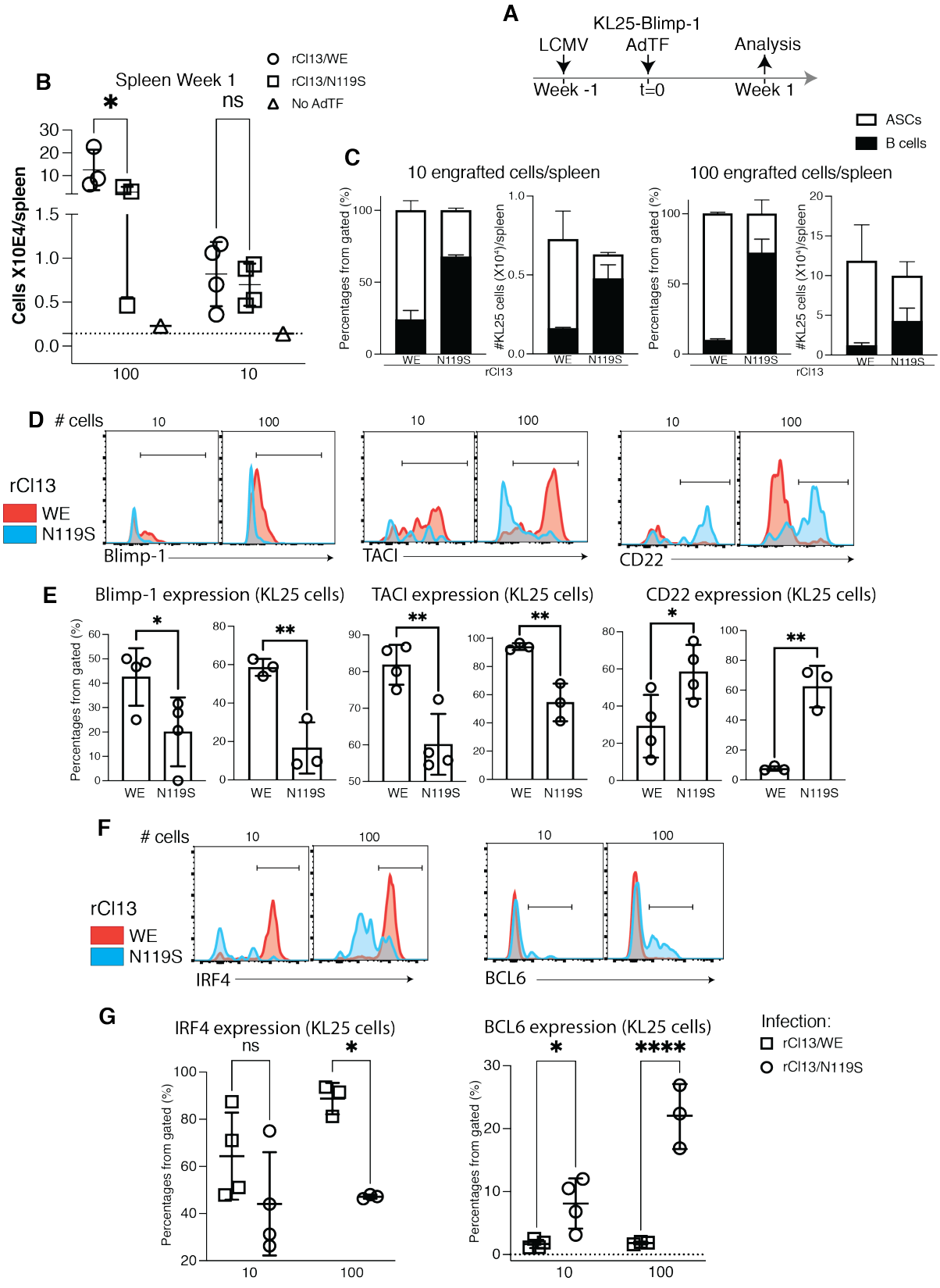

Figure 7. (A) Recipients were infected with high dose WE or N119S Cl13 backbone viruses at week -1 prior to adoptive transfer (AdTF) at t=0 of Blimp-KL25 cells and analyzed within 1 week. (B) Enumerated virus-specific KL25 B cells. (C) Percentages and total enumerated cells as B cells or ASCs from reporter KL25 B cells' progeny. Representative histograms are shown in (D) with the percentages of positive cells for transcription factor Blimp- 1 and surface proteins TACI and CD22. We additionally performed an intracellular staining (ICS) for IRF4 and BCL6 transcription factors for all samples. Representative histograms showing pre-gated KL25 are shown in (F) and the enumerated percentage positive cells in (G). All data is displayed as mean±SD or mean±SEM for Figure 6C. The symbols represent individual mice. Doted lines on graphs represent detection limit. Statistical analysis was performed with unpaired two-tailed Student's *t* tests for C and E. For B and G, 2-way ANOVA with multiple comparisons was used with a simple effect withing row post-test. Significant p values (*,**,***,****) for $p < 0.05$; not statistically significant, n.s.: $p \geqq 0.05$.

Figure S 1. Gating strategy for KL25 progeny

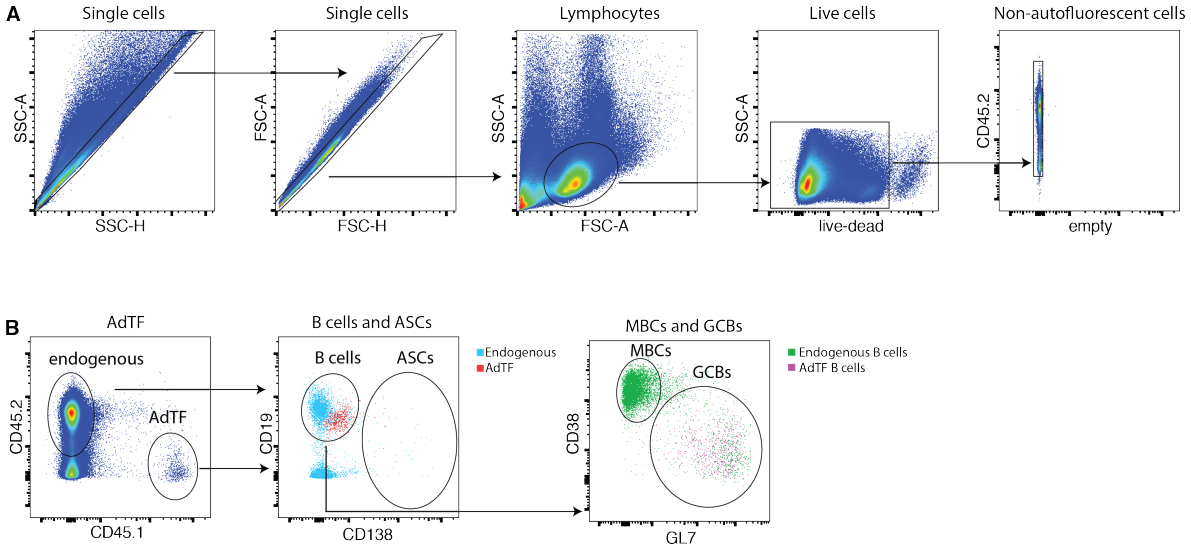

Figure S1. (A) Single cells were gated based on SSC-A and SSC-H, followed by FSC-A and FSC-H. Consequently, we gated on lymphocytes (SSC-A vs FSC-A), excluded dead cells with Zombie U.V. live-dead cells marker, and excluded autofluorescence cells (empty channel). (B) KL25 B cells were identified using CD45.1.1 syngeneic marker whereas endogenous population is CD45.2.2. For further analysis, we gated on B cells ($CD19^+$ or $B220^+$ $CD138^-$) or ASCs ($CD19^-$ or $B220^-CD138^+$) and we determined memory B cells (MBCs) by $GL7^-CD38^+$ and GC B cells by $GL7^+CD38^-$ surface expression.

Figure S 2. Engraftment of KL25 cells in naive spleens

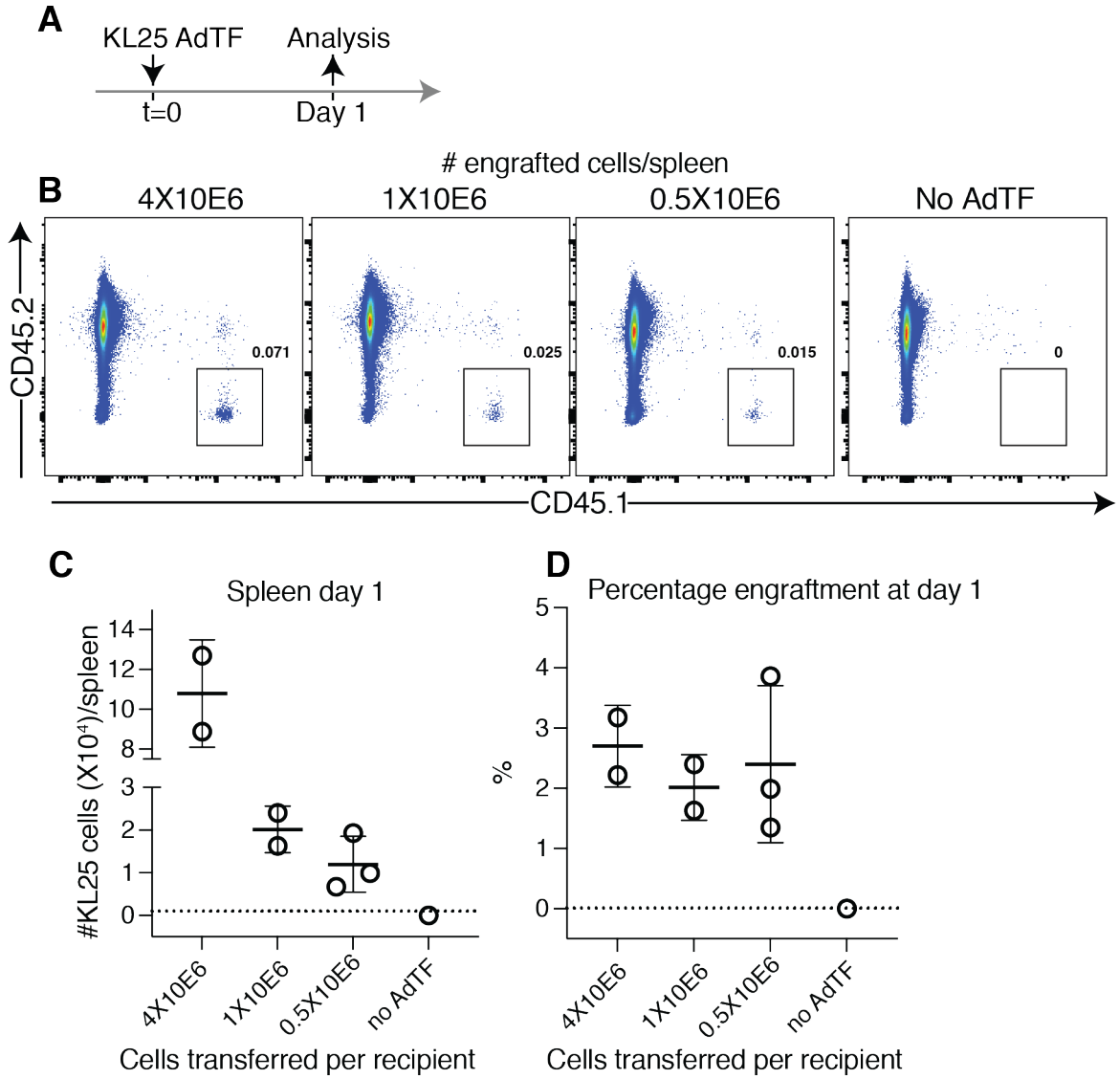

Figure S2. (A) We transferred KL25 B cells at various dilutions and analyzed the frequency of KL25 B cell population one day later. (B) Representative flow cytometry plots showing specific KL25 B cells (CD45.1) from all groups. (C) Enumerated virus-specific KL25 B cells in all groups. We calculated the percentage of engrafted cells amongst all groups 1 day after AdTF (D).

Figure S 3. Gating strategies for Blimp-1, CD22, TACI, BCL6 and IRF4

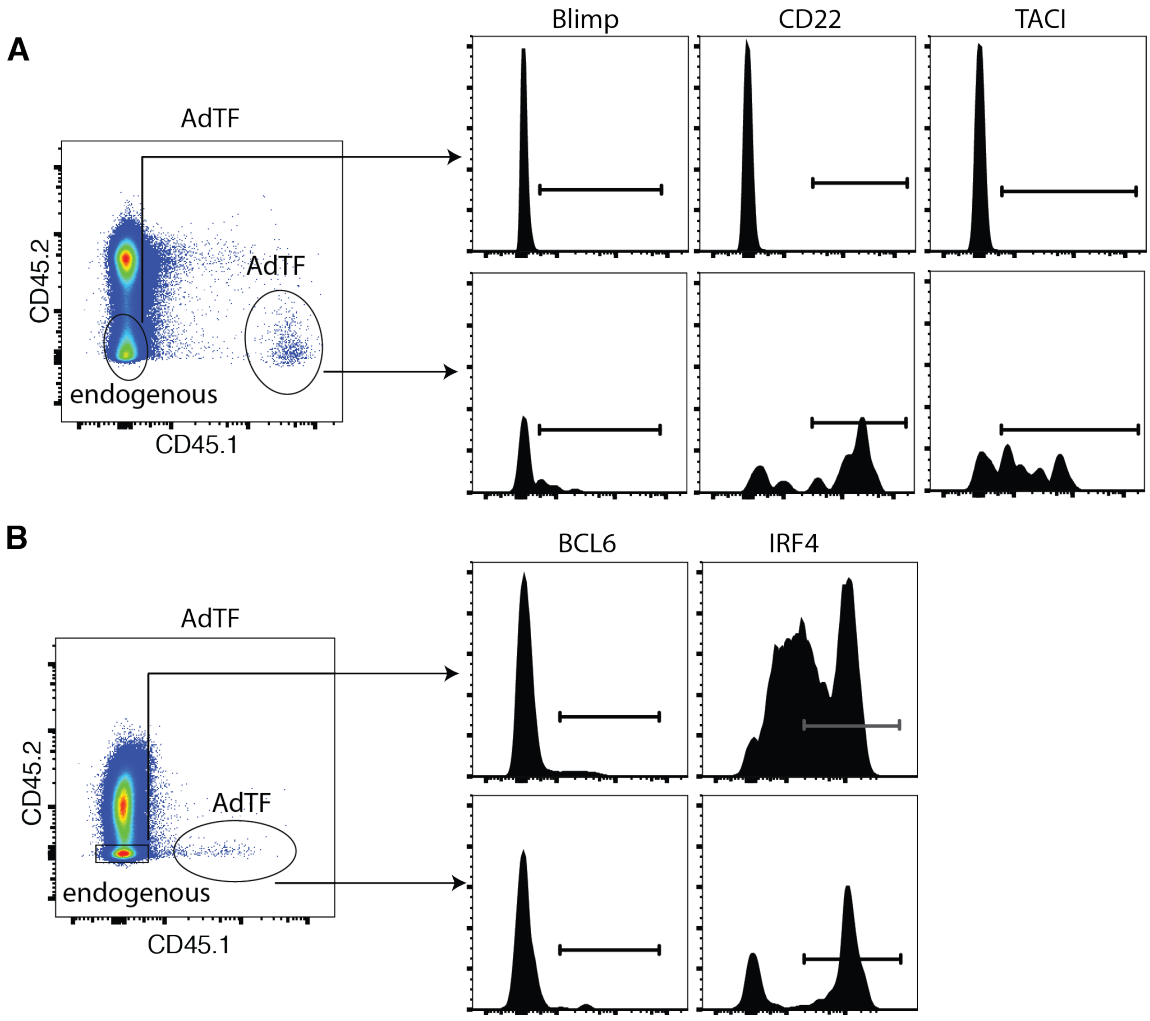

Figure S3. Single cells were gated based on SSC-A and SSC-H, followed by FSC-A and FSC-H. Consequently, we gated on lymphocytes (SSC-A vs FSC-A), excluded dead cells with Zombie U.V. live-dead cells marker, and excluded autofluorescence cells (empty channel). (A) KL25 B cells were identified using CD45.1.1 syngeneic marker while endogenous population is CD45.2.2. For further analysis, we gated on Blimp-1-GFP, CD22 and TACI by using a non-B non-ASC population as a negative control and staining controls as positive controls. (B) Alternatively, we performed an intracellular staining (ICS) and gated on CD45.1 KL25 cells. Gating on IRF4 or BCL6 was performed in a similar fashion as in (A).

Acknowledgements

We wish to thank Karsten Stauffer for excellent animal care work. We would like to also thank Dr. Florian Geier for RNA sequencing analysis. For critical discussion and great feedback, we would like to express our gratitude to all former and current lab members, especially Anna F. Marx, Katrin Martin, Peter Reuter, Lena Kastner, Lena Siewert and Weldy Bonilla Pinschewer. This work would not have been possible without the excellent technical support of Min Lu and Keren Cornille.

Funding

Author contributions

M.D. and D.D.P contributed to experimental design; M.D., K.N., Y.E. and D.D.P acquired, analyzed and/or interpreted the data; M.D. and D.D.P. drafted or critically revised the article for important intellectual content. M.F. and K.N. have contributed by creating the mouse models as outlined in Material and Methods section of this manuscript.

Conflict of interests

The authors report no conflict of interests.

Vaccine-elicited CD4 T cells prevent the deletion of antiviral B cells in chronic infection

Kerstin Narr[1], Yusuf, I. Ertuna[1], Benedict Fallet[1], Karen Cornille[1], Mirela Dimitrova[1], Anna Friederike Marx[1], Katrin Martin[1], Marco Künzli[2], David Schreiner[2], Tobias M. Brunner[3,4], Mario Kreutzfeldt[5,6], Florian Geier[7], Lukas Bestmann[8] , Max Löhning[3,4], Doron Merkler[5,6], Carolyn G. King[2] and Daniel D. Pinschewer[1,*]

[1] Division of Experimental Virology, Department of Biomedicine, University of Basel, 4003 Basel, Switzerland
[2] Immune Cell Biology Laboratory, Department of Biomedicine, University Hospital Basel, 4031 Basel, Switzerland
[3] Experimental Immunology and Osteoarthritis Research, Department of Rheumatology and Clinical Immunology, Charité - Universitätsmedizin Berlin, corporate member of Freie Universität Berlin, Humboldt-Universität zu Berlin, and Berlin Institute of Health, 10117 Berlin, Germany
[4] Pitzer Laboratory of Osteoarthritis Research, German Rheumatism Research Center (DRFZ), a Leibniz Institute, 10117 Berlin, Germany
[5] Division of Clinical Pathology, Geneva University Hospital, 1211 Geneva, Switzerland
[6] Department of Pathology and Immunology, Geneva Faculty of Medicine, Geneva University Hospital, 1211 Geneva, Switzerland
[7] Department of Biomedicine, Bioinformatics Core Facility, University Hospital Basel, 4031 Basel, Switzerland
[8] Bioanalytica, St. Anna-Strasse 36, 6006 Luzern, Switzerland

[*] Corresponding author:
Daniel D. Pinschewer, M.D.
Email: Daniel.Pinschewer@unibas.ch
Phone: +41-79-543 39 70

One Sentence Summary: Vaccination-induced Tfh memory CD4 cells prevent terminal plasmablast differentiation and clonal deletion of B cells responding to chronic viral challenge by instructing a germinal center transcriptional program.

Abstract

Chronic viral infections subvert protective B-cell immunity. An early interferon-driven bias to short-lived plasmablast differentiation leads to clonal deletion, so-called “decimation”, of antiviral memory B-cells. Therefore, prophylactic countermeasures against decimation remain an unmet need.
We show that vaccination-induced CD4 T cells prevented the decimation of naïve and memory B-cells in chronically LCMV-infected mice. Although these B-cell responses were T-independent, pre-existing T help assured their sustainability by instructing a germinal center B-cell transcriptional program. Prevention of decimation depended on T cell-intrinsic Bcl6 and Tfh progeny formation. Antigen presentation by B-cells, interactions with antigen-specific T helper cells and costimulation by CD40 and ICOS were also required. Importantly, B-cell-mediated virus control averted Th1-driven immunopathology in LCMV-challenged animals with pre-existing CD4 T cell immunity.
Our findings show that vaccination-induced Tfh cells represent a cornerstone of effective B-cell immunity to chronic virus challenge, pointing the way towards more effective B-cell-based vaccination against persistent viral diseases.

Introduction

CD4 T cell induction represents a key goal of vaccination and an important correlate of immunity to diseases of global importance such as tuberculosis [1]. Moreover, genetic deficiency in CD4 T cell defense or the loss thereof in AIDS allows the emergence of various microorganisms, resulting in life-threatening opportunistic infections [2, 3]. Significant gaps remain, however, in our understanding of how CD4 T cells contribute to protection against chronic viruses. While essential to contain established HIV or cytomegalovirus infection [4, 5, 6], the potential role of pre-existing CD4 T cell immunity in the prevention of viral persistence remains a matter of debate [7].

Observations made in the model of chronic lymphocytic choriomeningitis virus (LCMV) infection of mice indicate that vaccination-induced CD4 T cell immunity, similarly to adoptively transferred virus-specific CD4 T cells, can result in severe immunopathological disease instead of protection [8, 9, 10]. Th1-biased CD4 T cell memory – a type of CD4 T cell immunity commonly induced by bacterially and virally vectored vaccine delivery systems [11, 12, 13] – was found to trigger a pathogenic cytokine storm upon chronic virus challenge, thus questioning the utility of CD4 T cell-targeted vaccination for the prevention of chronic viral infection.

Humoral immune protection against acute viral disease commonly requires a critical titer of pre-existing serum antibodies, irrespective of B cell memory [14]. As an important exception, recall responses by vaccination-induced memory B cells have the capacity to prevent hepatitis B virus (HBV) persistence even after serum antibody immunity has waned [15, 16]. Similarly, rapid neutralizing antibody (nAb) responses to primary and, importantly, also secondary HCV infection are associated with spontaneous viral clearance [17, 18, 19, 20]. These findings highlight not only the tremendous potential of B cell-based protection, specifically in the context of chronic viral diseases, but also the need to better understand its functioning and the requirements for its optimal exploitation in vaccination.

When aiming to harness B cell-based immunity against persistent viral diseases, the subversion of early – and therefore timely - humoral immune responses to these viruses is a major hurdle. This is evident in a delayed and inadequate antibody response to HCV and HIV in man [21, 22, 23] and to LCMV in mice [24]. We and others have reported that antiviral B cells, whether naïve or antigen-experienced memory B cells (memB), undergo rapid terminal differentiation to short-lived antibody-secreting cells (ASCs) and near-total clonal deletion at the onset of chronic LCMV infection [25, 26, 27]. This process, referred to as “B cell decimation”, is driven by type I interferon- (IFN-I-) induced inflammation and may explain delayed antibody responses to persisting viruses [21, 22, 23, 24]. Antibody-mediated blockade of the IFN-I receptor (IFNAR) prevented B cell decimation and restored B cell transcription factor profiles of mature B cell stages [25], thus enabling a sustainable germinal center-based antiviral B cell response. These findings suggested the utility of IFNAR blockade as a therapeutic strategy to counter B cell decimation. The same treatment given to SIV-infected non-human primates resulted, however, in the animals’ rapid progression to AIDS, illustrating the superordinate importance of IFN-I signaling in antiviral defense [28]. Strategies to prevent B cell decimation and to enable effective primary and/or secondary B cell responses to chronic virus challenge remain, therefore, an important unmet need.

CD4 T cell help, notably in the form of follicular T helper cells (Tfh), is essential for germinal center (GC) reactions and thereby for B cell affinity maturation and long-term antibody as well as B cell memory formation [29, 30, 31]. Unlike protein-based immunization, several viruses have the capacity to trigger early antibody responses in a CD4-independent fashion [32, 33]. Accordingly, we have reported that under conditions of IFNAR blockade, thus when B cell decimation was prevented, the early B cell response to chronic LCMV challenge was CD4-independent [25]. In contrast to primary B cell responses, the dependence of memory B cell recall responses on primary and/or secondary CD4 T cell help remains a subject of controversy [34, 35]. Accordingly, the differential availability and quality of memory CD4 T cell help [36, 37] has been identified as a likely confounding variable across several recent studies on memB cell recall responses [38, 39, 40, 41, 42, 43].

Here we investigated the role of vaccination-induced CD4 T cell immunity in supporting primary and secondary B cell responses to chronic viral challenge. We found that early, cognate interactions of antiviral B cells with vaccination-induced CD4 T cells reversed the cellular and molecular hallmarks of B cell decimation, thereby enabling a robust and sustainable antibody response and the formation of B cell memory. In return, effective B cell-mediated control of viral replication prevented immunopathological complications of CD4 recall responses. These observations establish vaccination-induced CD4 T cell memory as an essential pillar of effective B cell immunity against persistent viral challenge.

Results

Pre-existing CD4 T cell help prevents decimation of naïve and memory B cells upon chronic virus challenge

To study the impact of pre-existing CD4 T cell help on B cell responses to chronic LCMV challenge we immunized mice with a recombinant Listeria monocytogenes (LM61) expressing from its transgene the immunodominant LCMV glycoprotein- (GP-) derived CD4 T cell epitope GP61-80. Non-transgenic LM was used for controls. Four weeks later, both groups of mice were given monoclonal GP-specific B cells (KL25HL B cells) by adoptive transfer and were challenged with a chronic strain and dose of LCMV (Fig. 1A). Five days into the LCMV response, splenic GP66-77 (GP66) tetramer-binding CD4 T cells of LM61-immunized mice were significantly more abundant than in LM-vaccinated controls, as expected (Figs. 1B, S1A). Intriguingly, however, LM61-immune mice harbored also >20-fold higher numbers of KL25HL progeny B cells and >200-fold higher numbers of antibody-secreting cells

(ASCs, Figs. 1C, S1B). Accordingly, they mounted >100-fold higher LCMV-nAb titers than LM-immunized controls (Fig. 1D). Altogether these findings suggested that pre-existing GP-specific CD4 help prevented GP-specific B cell decimation upon chronic viral challenge. When B cell transfer and LCMV challenge were conducted only nine days after LM61 pre-immunization, thus shortly after its clearance [44], GP66-specific CD4 T cell as well as KL25HL B cell responses were similarly augmented (Fig. 1E) and this effect was sustained for at least 20 days after chronic virus challenge (Fig. 1E-G). Importantly, LM61 immunization also augmented the number of KL25HL B cells with a GC phenotype (GL7+CD95+, Fig. 1G,H) and promoted their participation in GC reactions as evident from histological sections (Fig. 1I). As both naïve and memB cells are susceptible to decimation [25], we next assessed whether pre-existing CD4 T help enables robust memB cell recall responses to chronic viral challenge. KL25HL memB cells were generated in primary recipients, sorted and characterized (Fig. S1C,D), then adoptively transferred into either LM61- or LM-immune secondary recipients, followed by LCMV challenge (Fig. 1J). Seven days later, substantial progeny populations of KL25HL B cells and ASCs were recovered from LM61-immune mice, while KL25HL memB cells in LM-immune control recipients were largely decimated (Fig. 1K, S1E). This effect translated into ~100-fold higher LCMV-nAb and GP-binding antibody responses by memB cell progeny on day 7 (Fig. 1L,M), which at this early time point of analysis, were mostly found outside B cell follicles (Fig. 1N). Altogether, these observations indicated that pre-existing CD4 T help prevented the decimation of both naïve and memory B cells. Analogous effects on KL25HL B cell and antibody responses were observed when GP66-specific TCR-transgenic CD4 T cells (SM cells) from naïve donor animals were engrafted in numbers to approximate LM61-induced CD4 T cell responses (Fig. 1O-Q). RAG-deficient SM cells were similarly effective (Fig. S1F,G), indicating that truly naïve CD4 T cells, when provided in sufficient numbers [45], can help B cells and prevent their decimation.

LM61-induced CD4 responses are Th1-biased but comprise a Tfh-like population that expands upon recall

The prevention of B cell decimation by LM61-induced CD4 T cells was surprising in light of the reportedly pronounced Th1 bias of these responses [8], prompting us to investigate the heterogeneity of LM61-induced CD4 T cell responses by single cell RNA sequencing (scRNAseq). We profiled the transcriptome of GP66 tetramer-binding CD4 T cells, which we collected on day 9 after LM61 pre-immunization (day 9, Fig. 2A) and five days following subsequent KL25HL cell transfer and LCMV challenge (day 14, Fig. 2A). A principle component analysis (PCA) and hierarchical clustering evidenced five and four main cell clusters on day 9 and day 14, respectively (Fig. 2B,C,F,G). As expected, three Th1-like clusters dominated the response at both time points, but seven to eight percent of cells fell into a fourth cluster, which by comparison to published scRNAseq data, [46] exhibited a Tfh gene expression signature (Fig. 2D,E,H,I, Fig. S2A,B). This Tfh cell cluster was characterized by elevated mRNA levels of the master transcriptional regulators *Bcl6, Tcf1* (encoded by the *Tcf7* locus) and *Id3*, and of Tfh hallmark genes such as *Cxcr5* and *Il21* (Fig. 2E,I, Fig. S2A,B). In contrast, the expression of Th1-related genes such as *Tbx21* (encoding T-bet) and *Selplg* (encoding PSGL1) was lower in these cells. A fifth yet very minor Treg-like subset was only detected on day 9.

When analyzed by flow cytometry on day 9, vaccination with LM61 induced a population of ~1-2% GP66-Tet-binding $CD44^{hi}$ cells (Fig. 2J-L). Within this population a small but distinct subpopulation of cells co-expressed the Tfh markers CXCR5 and PD-1, mostly in combination with ICOS (Fig. 2J-L). The GP66-specific recall response to LCMV on day 14 contained ~15-20% $CXCR5^{+}PD\text{-}1^{+}$ cells (Fig. 2J-L). In keeping with a persisting Th1-bias, this proportion of Tfh-like cells was lower than in the primary GP66-specific response of LM control-immunized animals (~40-60%, Fig. 2L). Still, the total number of GP66-specific CD4 T cells in LM61 pre-immunized mice on day 14 exceeded the primary response of LM control-vaccinated animals ~15-fold. By consequence the $CXCR5^{+}PD\text{-}1^{+}$ Tfh-like subpopulation was also ~5-fold more abundant than in the respective population of LM-immune controls (Fig. 2L). Experiments in $IL\text{-}21^{gfp}$ reporter mice demonstrated that approximately two third of the Tfh-like ($CXCR5^{+}$) GP66-specific cells expressed IL-21 (Fig. 2M, Fig. S2C), an important Tfh signature cytokine that is not normally expressed by Th1 cells [47]. Altogether, these observations indicated that the LM61-induced GP66 response was Th1-biased but also contained a subpopulation of Tfh-differentiated CD4 T cells, which expanded upon LCMV challenge.

Bcl6-dependent CD4 response and Th2- but not Th1-polarized SM CD4 T cells prevent B cell decimation

We aimed to establish a functional link between CD4 T cell subset differentiation and the cells' ability to prevent B cell decimation. To assess whether Th1 differentiation was required for the prevention of B cell decimation we performed adoptive transfer experiments with SM cells lacking T-bet ($SMxTbx21^{-/-}$), the master transcriptional regulator of Th1 differentiation. These cells' expansion upon LCMV challenge and, importantly, also the expansion of co-transferred KL25HL B cells was comparable to control mice receiving T-bet-sufficient

SM cells (Fig. 3A,B). This finding indicated that T-bet-mediated Th1 differentiation was not required for CD4 T cells to prevent B cell decimation.

To test whether the Tfh-like subpopulation in the LM61-induced GP66 response was required for the prevention of B cell decimation, we exploited $Bcl6^{fl/fl}CD4^{Cre}$ mice with a T cell-specific deficiency in Bcl6, the master transcriptional regulator of Tfh differentiation [48, 49, 50]. When immunized with LM61 and subsequently challenged with LCMV, $Bcl6^{fl/fl}CD4^{Cre}$ mice mounted a CD4 recall response that significantly exceeded the primary response of LM control-vaccinated wt and $Bcl6^{fl/fl}CD4^{Cre}$ mice (Fig. 3C). However, as expected, the number of $CXCR5^{+}PD\text{-}1^{+}$ Tfh-like CD4 T cells in $Bcl6^{fl/fl}CD4^{Cre}$ mice did not exceed the respective primary responses in LM-immune controls (Fig. 3D). Consistent with the lack of Tfh cells in $Bcl6^{fl/fl}CD4^{Cre}$ mice, there was an almost complete absence of the $T\text{-}bet^{low/neg}CXCR5^{+}$ subpopulation (Fig. 3F,G), which in control mice expressed elevated levels of Bcl6 (Fig. 3H). Most importantly, Bcl6-deficient T help failed to prevent B cell decimation. Unlike in wt mice, where LM61 pre-immunization augmented KL25HL B cell and ASC progeny ~10 and ~50-fold, respectively, immunization of $Bcl6^{fl/fl}CD4^{Cre}$ mice failed to exert any discernible effect on KL25HL B cell progeny (Fig. 3E).

To formally determine whether *bona fide* Th1 cells have the capacity to prevent KL25HL B cell decimation we subjected SM CD4 T cells to two consecutive rounds of in vitro activation and polarization to either a Th1 or a Th2 phenotype (SM-Th1, SM-Th2, Fig. S3). When transferred into naïve recipients alongside with KL25HL B cells and challenged with LCMV, SM-Th2 cells expanded substantially less than SM-Th1 cells (Fig. 3I). Yet SM-Th2 but not SM-Th1 cells formed a sizeable population of CXCR5+PD-1+ Tfh-like progeny (Fig. 3J,M) and they acquired only low to intermediate T-bet levels, whereas SM-Th1 cells were uniformly $T\text{-}bet^{hi}$, as expected (Fig. 3L). In keeping with superior plasticity and the resulting Tfh phenotype, SM-Th2 but not SM-Th1 cells prevented the decimation of KL25HL B cells (Fig. 3K).

Altogether, these observations support the concept that the LM61-induced CD4 T cell response comprised a Bcl6-dependent Tfh-like population of $CXCR5^{+}PD\text{-}1^{+}T\text{-}bet^{low/neg}$ CD4 T cells, which was accountable for the prevention of B cell decimation upon LCMV recall.

T help prevents B cell decimation in an antigen-specific and MHC class II-dependent manner

Antigen-specific but also nonspecific bystander interactions between T and B cell can contribute to humoral immune responses [51]. To test whether activated CD4 T cells prevent B cell decimation in a bystander fashion, we transferred either vesicular stomatitis virus (VSV) specific TCR-transgenic CD4 T cells (L7 cells) or SM cells, followed by KL25HL B cell transfer and co-infection with VSV and LCMV (Fig. 4A). L7 cells expanded vigorously and secreted cytokines upon peptide restimulation (Fig. 4B), a response that equalled or exceeded the response of SM cells (Fig. 4C). Still, the KL25HL B cell response in L7 cell recipients did not exceed the one of control recipients without CD4 T cell transfer, indicating that bystander L7 T help failed to prevent B cell decimation (Fig. 4D).

To investigate whether KL25HL B cells establish contacts with virus-specific SM CD4 T cells we analyzed histological sections of spleens prepared 24 and 48 hours after LCMV challenge. SM cells and KL25HL cells were frequently juxtaposed (Fig. 4E). A computational assessment confirmed that the contact ratio of KL25HL cells with virus-specific SM cells vastly exceeded the same B cells' contact ratio with polyclonal endogenous and thus mostly virus-unspecific CD4 T cells (Fig. 4F), altogether suggesting early cognate T – B cell interactions.

T help induced by LM61 immunization targets the same epitope as adoptively transferred SM cells. To determine whether another antiviral CD4 T cell specificity could prevent B cell decimation similarly to GP61-specific SM cells, we assessed the effect of adoptively transferred LCMV nucleoprotein- (NP-) specific TCR-transgenic CD4 T cells (NIP cells). NIP cells are predicted to provide help to KL25HL B cells that capture entire LCMV particles and present virus-internal NP fragments on MHC class II (MHC-II) [52]. When challenged with LCMV, NIP cells expanded somewhat less than SM cells (Fig. 4G). Nevertheless, they were at least partially effective in preventing B cell decimation (Fig. 4H).

We next assessed whether the prevention of B cell decimation required direct antigen presentation by the respective antiviral B cells [53]. LM61 pre-immunization (Fig. 4I) prevented the decimation of MHC-II-sufficient but not of MHC-II-deficient KL25HL cells (Fig. 4J). In contrast, MHC-II-deficient KL25HL cells expanded vigorously when LCMV challenge was conducted in non-decimating $IFNAR^{-/-}$ hosts (Fig. 4J), confirming their intrinsic ability to mount T-independent responses to LCMV[25]. Taken together, these observations indicated that the prevention of B cell decimation by pre-existing T help relies on cellular interactions that involve MHC-II on the responding B cell.

T help prevents B cell decimation in a CD40- and ICOS-dependent manner

Since CD4 T cells provide help to B cells in the form of costimulatory receptor engagement as well as cytokines, we examined these signals in the context of T help-mediated prevention of B cell decimation. ICOS blockade during LCMV challenge did not interfere with the expansion of LM61 pre-primed CD4 T cells (Fig. 5A,B) but it largely abrogated their ability to prevent B cell decimation (Fig. 5C). This indicated an essential role for ICOS – ICOSL interactions in the prevention of B cell decimation. Similarly and despite GP66-specific CD4 T cell responses of normal magnitude, LM61 pre-immunization of CD40L-deficient recipients failed to prevent the decimation of KL25HL cells (Fig. 5D,E). Consistent with these observations, CD40L-deficient SM cells also responded vigorously to LCMV challenge but could not restore KL25HL B cell responses (Fig. S4A). Importantly, LM61 pre-immunization failed to prevent the decimation of CD40-deficient KL25HL B cells (Fig. 5F,G). Altogether, these observations established an essential role for direct CD40 – CD40L interactions by virus-specific CD4 T cells and B cells, respectively, to prevent decimation of the latter.

We also assessed a potential role of individual helper T cell cytokines in this process. Adoptively transferred IL- 4- or IFN-y-deficient SM CD4 T cells were as effective at preventing B cell decimation as their wildtype counterparts (Fig. S4B,C). In a complementary approach we performed LM61 pre-immunization experiments in either IL-10- or IL-21-deficient hosts but failed to reveal an essential individual contribution of either one of these cytokines to the prevention of B cell decimation (Fig. S4D,E). These observations indicated that IL-4, IL-10, IL-21 and IFN-y were either dispensable for T help-mediated prevention of B cell decimation or played a largely redundant role in this process.

The above experiments identified CD40L as a key signal preventing the decimation of naïve B cells, but the CD40L-dependence of primary immune responses can differ from recall responses [54]. Hence we tested whether the prevention of memB cell decimation by T help (compare Fig. 1I-K) was similarly dependent on CD40L signals. We generated KL25HL memB cells in LCMV-infected primary recipients, then sorted and adoptively transferred the cells into LM61 pre-immunized secondary recipients, which were either wildtype or CD40L-deficient (Fig. 5H). GP66-specific CD4 T cell responses of LM61 pre-primed CD40L-deficient mice were of near-normal magnitude but they failed to prevent the decimation of KL25HL memB cells upon LCMV challenge (Fig. 5I,J). Hence, prevention of memB cell decimation by T help depended on CD40L signalling, analogously to primary B cell responses.

Taken together, our results reveal that pre-existing CD4 T help prevents B cell decimation in an antigen-specific manner, which involves direct B cell – T cell contact with essential engagement of the costimulatory receptors ICOS and CD40 as well as MHC class II-dependent antigen presentation by B cells.

Pre-existing CD4 T help antagonizes inflammation and instructs a germinal center B cell program

We previously reported that IFNAR blockade promotes transcription factor expression profiles of mature B cell stages thereby antagonizing ASC differentiation and decimation [25]. Here we profiled the transcriptome of KL25HL B cells on day 4 after LCMV challenge (Fig. 6A,B, S5). Pre-existing T help, provided either by LM61 pre-immunization or by SM cell transfer, augmented the expression of transcription factors characteristically upregulated in GC B cells [55]. Amongst them were master regulators of the GC B cell program such as Bcl6 and Mef2b [56, 57]. Intriguingly, these effects of T cell help on GC transcription factor profiles closely mimicked analogous effects of IFNAR blockade on the B cell transcriptome (Fig. 6A,B). Both T help and IFNAR blockade repressed inflammation-related hallmark gene sets such as interferon-a response, interferon-y response and TNF-α signaling (Fig. 6C, S6). In addition, they augmented proliferation-related gene sets such as E2F targets and G2M checkpoints but also metabolism-related gene sets such as genes associated with oxidative phosphorylation (Fig. 6C, S6). To further investigate the functional impact of pre-existing CD4 T help on the GC program of B cells undergoing chronic viral challenge we made use of KL25HL donor mice expressing an AID fate mapping reporter (KL25HL-AID^{rep} [58]). KL25HL-AID^{rep} mice carry one allele of an engineered *aicda* locus (encoding for activation-induced deaminase, AID), which drives a tamoxifen (TAM)-inducible Cre recombinase (Cre-ERT2). In conjunction with a Cre-inducible EYFP reporter gene, TAM administration induces EYFP expression in approximately 10%–20% of AID^{rep} GC B cells [39, 58]. KL25HL-AID^{rep} B cells were transferred into recipient mice immunized with either LM61 or LM, or into a third cohort that was given IFNAR blockade instead of pre-immunization. Upon LCMV challenge, TAM was administered and KL25HL-AID^{rep} B cells were analyzed five days later (Fig. 6D). LM61 pre-immunization as well as IFNAR blockade significantly augmented both the absolute number and the proportion of KL25HL-AID^{rep} B cell progeny that reported AID (EYFP, Fig. 6E). This effect of pre-existing T help was also evident on histological sections (Fig. 6F). AID-reporting (EYFP+) B cells populated the B cell follicles of LM61 pre-primed or IFNAR-blocked recipients while only individual scattered cells were found in

LM-immune controls (Fig. 6F). These results suggested that pre-existing T help, analogous to IFNAR blockade [25], prevents B cell decimation by instructing a GC B cell transcriptional program.

KL25HL B cells control viremia and prevent CD4 T cell-driven immunopathology upon chronic viral challenge

The above results suggested that effective B cell immunity to chronic viral challenge requires not only a suitable repertoire of antiviral B cells but also pre-existing CD4 T cells with the capacity to prevent decimation of the former. This concept raised the question of whether combined B cell- and CD4 T cell-based immunity was associated with a risk of severe immunopathological disease as has been reported for vaccination-induced CD4 T cell memory in the absence of virus-neutralizing B cells [8]. Mice were immunized with LM61 and prior to LCMV challenge were given KL25HL cells by adoptive transfer while control animals were left without cell transfer (Fig. 7A). As expected[8], LM61 pre-immunized and LCMV challenged control mice evidenced signs of immunopathology such as weight loss as well as elevated serum alanine and aspartate aminotransferase (AST, ALT) levels (Fig. 7B-D). Importantly, these signs of immunopathological disease were largely absent in mice that had received KL25HL B cells prior to LCMV challenge. A rapid and potent neutralizing antibody response in LM61 pre-immunized KL25HL cell recipients (Fig. 7E) resulted in complete suppression of viremia (Fig. 7F). This observation was in line with earlier findings that suppression of LCMV viral loads by passively administered neutralizing antibodies prevented immunopathological disease induction by vaccination-elicited CD4 T cells[8].

Discussion

The present work defines effective B cell immunity against chronic viral challenge as a synergy between two cellular compartments: B cells of a protective antiviral specificity as well as CD4 T cells with the capacity to provide early cognate help to the former. The mutual interdependence of these two cell types in the chronic infection context differs in key aspects from their co-operation in classical T-dependent B cell responses [59]. In line with earlier CD4 T cell depletion data [25] we show that KL25HL B cell have the intrinsic capacity of responding to LCMV in a T-independent manner. It therefore appears that T help, which in classical T-dependent B cell responses is essential for B cell activation, expansion and affinity maturation, serves an additional key role in the context of chronic virus challenge. It assures the clonal survival and thereby the sustainability of antiviral B cell responses when at risk of IFN-I-driven decimation. However, vaccination-induced CD4 T cell immunity bears the risk of fatal immunopathology. Here we show the latter can be averted by antiviral B cells that – with support from the same pre-existing CD4 T cells - mount a timely and protective antibody response to control viral loads. The finding that T help prevents B cell decimation by instructing a germinal center B cell program, analogously to IFNAR blockade, provides additional support to our postulate that B cell decimation reflects a biased, unsustainable plasmablast response [25]. Studies in mice with B cell-specific Blimp1 deletion and a resulting defect in ASC differentiation have also demonstrated that in hapten-carrier immunization, ASC differentiation inevitably occurs at the expense of GC cellularity [60]. It therefore appears that productive and sustainable B cell responses reflect a delicate balance of GC and ASC differentiation, a balance which is tilted by IFN-I-driven inflammation to culminate in B cell decimation. As reported herein, not only IFNAR blockade but also pre-existing T help can readjust this balance to ensure both rapid antibody-mediated virus control as well as long-term sustained GC B cell responses. Whether and how pre-existing T help may additionally affect other postulated pathways of B cell decimation remains to be investigated [26, 27].

Thus far IFNAR blockade has represented the only known intervention for the prevention of B cell decimation, but from a practical perspective, vaccination-induced CD4 T cell immunity offers key advantages. Firstly, IFNAR blockade can result in unwanted side-effects owing to inhibition of a main pathway of innate antiviral defense [28]. Secondly, as our earlier studies suggested [25], IFNAR blockade would likely have to be administered within the first two days if not within hours after a viral encounter, an occurrence that commonly goes unnoticed. CD4 T cell memory can be induced prophylactically with potentially long-lived effects [61], and strategies for its induction in clinical vaccination programs are well established [62]. The present findings suggest pre-existing T help and memory Tfh cells in particular represent a rate-limiting component of protective B cell memory to persisting viruses. Vaccination strategies against HIV or HCV that focus on the induction of affinity-matured, broadly neutralizing memB cells [63] may, therefore, only succeed if combined with modalities that elicit potent and long-lived Tfh memory. With critical support from Tfh memory cells during the earliest phase of infection, timely and sustained memB cell responses may critically curb or even eliminate chronic viruses [64] and thereby may prevent viral sequence diversification from outpacing the host germinal center response [65, 66].

The molecular interactions and signals we identified as essential for CD4 T cells to prevent B cell decimation at the onset of chronic infection – cognate antigen, MHC-II, CD40 and ICOS – closely resemble those required for

classical T-dependent B cell responses [59]. Somewhat more surprisingly, not only IFN-γ but also IL-4, IL-10 and IL-21 each individually appeared dispensable. Importantly, however, this observation does not exclude a supportive yet redundant role of these cytokines in the prevention of early B cell decimation. Moreover, these cytokines and even combinations thereof clearly are essential for effective CD4 T help to B cells during later stages of chronic LCMV infection [67]. Interestingly, the key role of CD40 signals in preventing B cell decimation aligns well with the observation that CD40 ligation potently antagonizes ASC differentiation in human B cell cultures [68].

In our standard experimental setting the number of adoptively transferred naïve KL25HL B cells resulted in a splenic B cell precursor frequency of ~$2x10^{-4}$ (see Methods). This corresponds to the physiological range of B cells specific for proteins such as phycoerythrin, *B. anthracis* protective antigen or influenza hemagglutinin, which range from ~$9x10^{-4}$-$6x10^{-5}$ [69, 70]. In contrast, naïve precursor frequencies as low as ~$3x10^{-6}$ have been reported for VRC01 class antibodies that target a specific neutralizing epitope on the HIV envelope [71]. For such rare specificities, KL25 B cell precursor frequencies as established in our above experiments may thus be more reflective of memB cell populations upon vaccination [72], which we show are similarly rescued from decimation by pre-existing T help.

We confirm earlier observations that LM61-induced CD4 T cell responses are largely Th1-biased [8]. In vivo generated polyclonal CD4 T cell responses, however, commonly comprise several differentiation patterns [61, 73]. Accordingly, we detect a small but clearly discernible Tfh-like subpopulation in the primary response to LM61 and a population of ~15-20% such cells in the recall response to LCMV. It seems likely that the latter are descendants of the former analogously differentiated cells, with their Tfh differentiation likely supported by the antiviral B cell response ensuing in parallel [74]. In light of the considerable plasticity of CD4 T cell subsets in the context of viral infection [75] we acknowledge, however, that Tfh trans-differentiation of other LM61-induced CD4 T cell subpopulations remains a not mutually exclusive possibility.

Taken together our findings reveal and characterize very early yet essential interactions of antiviral memory B cells with pre-existing CD4 T helper cells, which provide key signals to prevent decimation and thereby subversion of the antiviral B cell response at the onset of chronic infection. These insights establish CD4 T cell memory as an essential cornerstone of B cell immunity to chronic viral challenge and should help in leveraging the full potential of B cell-based protection in the fight against persisting human pathogens such as HIV and HCV.

Material and Methods

Mice and animal experimentation

KL25HL B cells express the LCMV-neutralizing KL25 antibody as monoclonal B cell receptor. The KL25 heavy chain is expressed from a VDJ knock-in in the immunoglobulin heavy chain locus [76]. The light chain of KL25HL cells is delivered by a previously described transgene, which is linked to a Thy1.1 reporter (KL25L) [25, 58], or from an analogous newly generated transgenic line devoid of the Thy1.1 reporter (BasL36). KL25HL-AID^{rep} mice [58] have been described, KL25HLx$CD40^{-/-}$ and KL25HLx$MHC\text{-}II^{-/-}$ lines were obtained by intercrossing KL25HL mice with the $CD40^{-/-}$ [77] and $MHC\text{-}II^{-/-}$ lines [78], respectively. KL25HL mice and crosses thereof were maintained on a CD45.1 background. SMx$Tbx21^{-/-}$, SMx$IFN\text{-}\gamma^{-/-}$, SMx$IL4^{-/-}$, SMx$RAG2^{-/-}$, were generated by intercrossing SM mice with the respective gene knockout lines [79, 80, 81, 82]. The SM [83], $CD40^{-/-}$ [77], $CD40L^{-/-}$ [84], $MHC\text{-}II^{-/-}$ [78], $IFNAR^{-/-}$ [85], $IL\text{-}10^{-/-}$ [86], $TCR\beta^{-/-}$ [87] and L7 [88] lines were obtained from the Swiss Immunological Mouse Repository (SwImMR). The AID^{rep} strain (also referred to as AID-Cre-EYFP [39]) was donated by Drs. J.-C. Weill and C.-A. Reynaud, SM mice on a Thy1.1 background by Dr. P. Aichele, $Bcl6^{fl/fl}CD4^{Cre}$ [89] and NIP mice [90] by Dr. S. Crotty, $IL21^{-/-}$ mice [91] by Dr. M. Kopf, $IL\text{-}21^{GFP}$ reporter animals [92] by Dr. S. Nutt. All mice were on a C57BL/6 background and were kept under specific-pathogen-free (SPF) conditions for colony maintenance and experiments. Breeding was conducted at the Laboratory Animal Services Center (LASC) of the University of Zurich and at the University of Basel. Experiments were performed at the University of Basel in accordance with the Swiss law for animal protection and with authorization by the Cantonal Veterinary Office Basel-Stadt.

Bacteria, viruses, virus titrations, infections and immunizations

A genetically engineered LCMV Clone 13 was used, expressing the WE strain glycoprotein [93]. It was propagated on either BHK-21 (ECACC) or 293-F cells (Invitrogen). Viral stocks and viral titers in mouse blood were determined by immunofocus assay on 3T3 cells using an anti-LCMV-NP antibody for detection [94]. Mice were infected intravenously at a dose of $2x10^6$ PFU.

The recombinant *Listeria monocytogenes* expressing the LCMV glycoprotein-derived epitope gp61-80 [8, 95, 96] was originally from Dr. H. Shen and was donated by Dr. P. Penaloza-MacMaster. The bacteria were harvested during

the exponential growth phase and washed with PBS. For infection of mice a dose of $2x10^5$ CFU was administered intravenously.

Flow cytometry and intracellular cytokine assays

Spleens were digested enzymatically with collagenase D (Roche) and DNase I (Sigma-Aldrich). The resulting cells in suspension were counted using an Immunospot S6 ultimate UV analyzer (C.T.L.). FACS buffer and cell culture media were adjusted to mouse osmolarity. Surface markers were stained at 4°C for 15 minutes using the following antibody-fluorophore conjugates (antibody clones in brackets): B220-PECy7 (RA-3-6B2), CD19-PE (1D3), CD138-APC (281-2), CD45.1-BV421 (A20), CD45.2-AF700 (104), CD4-BV605 (RM4-5), F4/80-PerCP (BM8), PD1-BV711 (29F.1A12), ICOS-PE (C398.4A) GL7-APC (GL7) (all from BioLegend), B220-PerCP (RA-3-6B2), CD8a-PerCP (53-6.7), CD44-FITC (IM7), CD95- (Fas-) PECy7 (Jo2) from BectonDickinson, CXCR3-PerCPCy5.5 (CXCR3-172), CD62L-PECy7 (MEL-14) from (eBioscience) and CD25-APC (pC61.5), CD44-Pacific Blue (IM7) were produced inhouse at the DRFZ, Berlin.

CXCR5 was surface stained using anti-CXCR5-BV421 or -BV605 conjugates (L138D7, BD) for 1h at room temperature. The following reagents were obtained through the NIH Tetramer Core Facility: H-2IA^b tetramers loaded with the LCMV glycoprotein-derived GP66-77 epitope (DIYKGVYQFKSV) as well as negative control tetramers loaded with an irrelevant human CLIP 87-101 peptide (PVSKMRMATPLLMQA), both of them coupled to APC, PE and BV421. Staining was performed for 1h at 37°C. Intracellular transcription factor staining was done using the FoxP3/Transcription Factor Staining Buffer set (eBioscience): T-bet-PE (4B10), GATA3-eFLuor660 (TWAJ) (both from eBioscience), Bcl6-AF647 (K112-91, BD), were used.

To assess epitope-specific CD4 T cell responses by intracellular cytokine staining, splenocytes were stimulated for 1h at 37°C using either the LCMV glycoprotein-derived peptide epitope GP64-79 (GPDIYKGVYQFKSVEF) or the VSVG-derived P8 peptide (Aa. 415-433; SSKHQVFEHPHIQDAASQL) at a concentration of 10^{-6}M or PMA and Ionomycin (Sigma) at a final concentration of 5ng/ml and 500ng/ml respectively, then Brefeldin A (final conc. 10ug/ml) was added and cells were incubated for another 4h. Surface staining was performed as above, then the cells were fixed (4% PFA) and permeabilized (1% Saponin, Fluka), followed by intracellular staining using IFN-γ-APC (XMG1.2), IL2-PE (JES6-5H4), TNF-α-PECy7 (MP6-XT22) (all from BioLegend) or IL-4-PE (11B11), IL-13-A488 (eBio13A), IFN-γ-eFluor450 (SMG1.2), IL-10-APC (JES5-16E3), TNF-α-eFluor450 (MP6-XT22) (all from eBioscience) IL-2-APC (JES6-5H4) (BectonDickinson). Live-dead staining was performed using the Zombie UV Fixable viability kit (BioLegend). Samples were acquired on an LSRFortessa (BectonDickinson).

Immunohistochemistry and image analysis

Spleen tissue was fixed in HEPES glutamic acid buffer-mediated organic solvent protection effect (HOPE, DCS Innovative) and embedded in low melting paraffin following the manufacturer's instructions. 1 µm-think sections were cut and dewaxed prior to staining and slides were mounted using Fluoprep. All staining steps were performed at room temperature if not otherwise stated.

For co-staining of CD45.1, B220 and PNA, Slides were blocked with 10% normal mouse serum (Jackson ImmunoResearch, 015-000-001) in PBS. FITC-labelled anti-mouse CD45.1 antibody (Biolegend 110705, clone A20) was applied (1:50) simultaneously with AF467-labelled anti-mouse-B220 antibody (Biolegend 103229, clone RA3-682; 1:100) in PBS supplemented with 10% PBS, followed by 3h of incubation. FITC was visualized using a rabbit anti-FITC antibody (Life Technologies, 71-1900) followed by AF555 anti-rabbit (H+L) antibody (Life Technologies, A21429), both diluted 1:200 in PBS/5%FCS and incubated for 1h. Lectin PNA-AF488 (Life Technologies, L21409) was incubated (1:50 diluted) together with DAPI as nuclear stain for 30min in PBS.

For co-staining of IgD, GFP and PNA, slides were blocked with 10% normal mouse serum (Jackson Immuno Research, 015-000-001) diluted in PBS, followed by 10% normal rat serum (Jackson Immuno Research, 012-000-001) diluted in PBS. PE-labelled anti-mouse IgD antibody (eBioscience 12-5993-81) was applied 1:50 together with rabbit anti-GFP (Cell Signaling, 29565; diluted 1:100) in DAKO diluent (DAKO, S2022) and incubated overnight at 4°C. PE was visualized using a biotinylated mouse anti-PE antibody (Biolegend, 408103) followed by Cy3-streptavidin (Biolegend, 405215), both diluted 1:100 in PBS and incubated for 1h. GFP was visualized using AF647-conjugated anti-rabbit (H+L) antibody (Life Technologies, A31573; diluted 1:100 in PBS) and incubated for 1h. Lectin PNA-AF488 (Life Technologies, L21409) was incubated together with DAPI as nuclear stain for 30min in PBS.

For co-staining of CD45.1, Thy1.1 and CD4, slides were blocked with mouse Fab fragments (Jackson Immuno Research, 115-007-003; diluted 1:100) and incubated for 30 minutes followed by blocking with 10% FCS (both diluted in PBS) for 15 minutes. Anti-mouse CD4 antibody (BD Pharmingen, 550280) was applied 1:25 in DAKO diluent (DAKO, S2022) overnight at 4°C. Bound CD4 antibody was visualized using AF647-conjugated anti-rat

(H+L) antibody (Jackson Immuno Research, 712-545-153; diluted 1:200 in PBS) and incubated for 1h. Tissue was blocked using 10% normal mouse serum and normal rat serum in PBS for 30 minutes before applying PE-labelled anti-mouse CD90.1 antibody (Biolegend, 202523; 1:100 diluted) and FITC-labelled anti-mouse CD45.1 (Biolegend, 110706) in DAKO diluent (DAKO, S2022) and incubating for 2h. PE was visualized using a biotinylated mouse anti-PE antibody (Biolegend, 408103) followed by Cy3-streptavidin (Biolegend, 405215), both diluted 1:100 in PBS and incubated for 1h. FITC was visualized using a rabbit anti-FITC antibody (Life Technologies, 71-1900) followed by AF555 anti-rabbit (H+L) antibody (Life Technologies, A21429), both diluted 1:200 in PBS/5%FCS and incubated for 1h.
Slides were scanned with a P250 Flash II whole slide scanner (3DHistech, Hungary) using a 20x objective resulting in a resolution of 0.325 µm/pixel. To determine cell-to-cell contacts between KL25HL and SM cells, images were analyzed using a custom ruleset in Definiens Developer XD Version 2.7.0 (Definiens, Germany). As a first step, total tissue was detected. Endogenous and transferred CD4 T cell and B cells were detected based on their respective markers. Cells were considered in "contact" if their object borders were closer than 20µm and the total number of contacts was determined for each cell.

Next generation RNA sequencing and bioinformatic data analyses
Single cell RNA sequencing: $CD44^{hi}GP66\text{-}Tet^{+}$ CD4 T cells were FACS sorted (FACSAria II, BD) at the given timepoint in RPMI with 60% FCS or pure FCS. Samples went immediately for cell capture and library preparation using the 10x Genomics Chromium Controller and Chromium Single Cell 3' Reagent kits v3 according to the manufacture's instruction. PE 28/8/0/91 sequencing was performed with the NovaSeq 6000 (Illumina) using an S1 Reagent Kit v1 (100 cycles) at the Genomics Facility Basel.
Sequencing data was processed using 10X Genomics' cellranger software version 3.1.0 and transcriptome reference mm10-3.0.0. Raw molecule info from cellranger output was initially filtered leniently, discarding cells with fewer than 100 UMI counts, as well as those with more than 60000 to account for possible doublets. The resulting UMI matrix was further filtered to keep only cells with log library size > 3.3, log number of features > 3.0, percent mitochondrial reads <= 5, and percent ribosomal protein reads >= 20. Normalization was done using the R package scran's deconvolution method. Technical noise within gene expression was modeled using scran, and biologically relevant highly variable genes were calculated after separating the technical from biological variance, using FDR < 0.05 and biological variance > 0.1. PCA was run on the normalized data using the top 500 most variable genes by biological variance, and the PCA was denoised to account for the modelled technical variation. *t*-distributed stochastic neighbor embedding (t-SNE) was calculated using a perplexity of 75. Cells were clustered hierarchically using Ward's method on the distance matrix of the PCA. Default dendrogram cut height using the R package dynamicTreeCut resulted in clusterings that also mapped to the highest average silhouette width. Data subsets, e.g. LM61 d14, were subjected to the same pipeline after subsetting. Cluster-defining genes were found using the R package limma and comparing cells in each cluster to cells in all other clusters. For LM61 d9, a sub'cluster (5) of putative regulatory T cells characterized by high *Foxp3* expression was manually defined as a distinct cluster.
Bulk RNA sequencing: $CD45.1^{+}B220^{+}CFSE^{low}$ B cells were sorted directly in TRI Reagent IS (Sigma-Aldrich) using a FACSAria II (BectonDickinson). RNA was extracted using Direct-zol RNA MicroPrep Kit (Zymo Research). Library preparation was performed, starting from 100ng total RNA, using the TruSeq Stranded mRNA Library Prep Kit High Throughput (Cat# RS-122-2103, Illumina, San Diego, CA, USA) and the TruSeq RNA CD Index Plate (Cat# 20019792, Illumina). 15 cycles of PCR were performed. Libraries were quality-checked on the Fragment Analyzer (Advanced Analytical, Ames, IA, USA) using the Standard Sensitivity NGS Fragment Analysis Kit (Cat# DNF-473, Advanced Analytical) revealing excellent quality of libraries (average concentration was 70±18 nmol/L and average library size was 344±11 base pairs). Samples were pooled to equal molarity. The pool was quantified by Fluorometry Libraries were sequenced Single-reads 76 bases (in addition: 8 bases for index 1 and 8 bases for index 2) during 3 sequencing runs on NextSeq 500 High Output Kit 75-cycles (Illumina, Cat# FC-404-1005) loaded at 1.8pM, 3.6pM, 3.6pM respectively, including 1% PhiX in order to generate on average a total of 43.5±3.5 millions of reads per sample.
Reads were aligned to the mouse genome (UCSC version mm10) with STAR using the multi-map settings '--outFilterMultimapNmax 10 --outSAMmultNmax 1' [97]. Mapped reads were assigned to genes based on the UCSC refGene annotation (downloaded 2015-12-18) using the function qCount of the R/Bioconductor package QuasR [98, 99]. Genes with zero counts were removed resulting in n=18824 detected RefSeq genes. Differential gene expression analysis between the genotypes relied on functions from the R/Bioconductor package edgeR [100]. Specifically, function 'estimateGLMRobustDisp' was used for estimating gene-wise dispersions, and functions 'glmFit' and 'glmLRT' were used for testing the contrast of interest. Differential regulation of all hallmark gene sets from MSigDB [101] was evaluated using the function 'camera' from edgeR with extra options 'inter.gene.cor =

0.01'. The average absolute log fold change (absLog2FC) of a gene set was used as a proxy for its strength of regulation. Specific gene sets published by Shi et al. [55] were tested using the function 'mroast' with extra options ` set.statistic = "mean", nrot=1e5`.

Adoptive cell transfer, fluorescent cell labeling and FACS sorting

For KL25HL cell transfer, single cell suspensions were prepared from spleens of KL25HL donor mice. The cells were labeled with CFSE (Sigma-Aldrich) and $2x10^5$ cells were routinely administered to recipients intravenously. Spleens of KL25HL donor mice contain ~40% B cells, which in conjunction with an engraftment rate of ~5% [102, 103, 104] resulted in ~4'000 engrafted KL25HL B cells per recipient spleen, corresponding to a precursor frequency in the range of $2x10^{-4}$. For experiments involving the histological analysis of adoptively transferred naïve B cells (Fig. 1E-I), ~50'000 KL25HL B cells were engrafted.

For transfer of purified B cells (when generating KL25HL memB cells, for immunohistochemical co-localization studies and analysis on d20 after infection), KL25HL B cells were purified using magnetic-activated cell sorting (EasySep™ Mouse Pan-B cell Isolation Kit, StemCell or Pan B cell Isolation Kit, Miltenyi Biotec). Purity (>95%) was checked before transfer by FACS. For CD4 T cell transfer, CD4 T cells were isolated from splenocytes using (EasySep™ Mouse Naïve CD4 T or EasySep™ Mouse CD4 T cell isolation kit). Purity (>95%) was addressed before transfer. KL25HL memB cells were sorted on a FACSAria II (BectonDickinson) and $4x10^4$ – 10^5 cells were re-transferred intravenously to recipients. Naïve and in vitro polarized TCR-transgenic $CD4^+$ T cells were adoptively transferred by the i.v. route (10^6 cells per recipient).

C57BL/6J wildtype mice served as recipients for short-term analyses, whereas KL25L mice were used as recipients to avoid anti-idiotypic rejection [25, 58], notably when analyses were performed more than seven days after adoptive transfer.

In vivo cell depletion, antibody blockade and Tamoxifen administration

For in vivo blockade of the interferon type I receptor (IFNAR), 1mg of MAR1-5A3 antibody (BioXCell) was injected intraperitoneally (i.p.) on day -1 of infection. For ICOS blockade, 200 µg 7E.17G9 antibody (BioXCell) was administered i.p. on day -1, 1 and 2 of infection. Tamoxifen (Novadex, AstraZeneca) was administered to mice at a dose of 2.5mg, dissolved in 20% Clinoleic (Baxter).

Neutralizing and GP binding antibody responses, and serum transaminase measurements

Microtainer tubes (BectonDickinson) were used for serum collection. LCMV neutralizing antibodies were detected by immunofocus reduction assays [94] and GP1-binding antibodies were measured by ELISA as described in [105].

For determination of serum AST and ALT activities, sera were diluted 1 in 10 in water and were measured by Bioanalytica (Switzerland) on a Roche/Hitachi Modular Analytics system according to the recommendations of the International Federation of Clinical Chemistry with pyridoxal phosphate activation at 37 °C [106].

In vitro differentiation of SM-Th1 and SM-Th2 cells

Naive $CD4^+$ $CD25^-CXCR3^-CD62L^{hi}CD44^{lo}$ T cells were isolated from spleens and lymph nodes of LCMV-TCR transgenic SM mice by FACS to a purity of >98%. Sorted T cells were cultured in the presence of LCMV-GP_{64-80} peptide (1 µg/ml) and irradiated splenocytes from TCR□$8^{-/-}$ mice in RPMI1640 + GlutaMax I supplemented with fetal calf serum (10% v/v; Gibco), penicillin (100 U/ml, Gibco), streptomycin (100 mg/ml, Gibco), gentamycin (10 ug/ml, Sigma Aldrich) and ß-mercaptoethanol (50 ng/ml, Sigma Aldrich). Th1 polarization was achieved by addition of IL-12 (10 ng/ml), IL-2 (5 ng/ml) and anti-IL-4 (11B11; 10 µg/ml). For Th2 differentiation, IL-4 (10 ng/ml), IL-2 (5 ng/ml), anti-IL-12 (C17.8; 10 µg/ml) and anti-IFN-γ (AN18.17.24, 10 µg/ml) were added. Cells were split after 3 days of culture and replenished with fresh medium containing IL-2 (5 ng/ml). After 5 days, T cells were harvested by Histopaque density centrifugation and re-plated with freshly prepared, irradiated splenocytes in the same conditions for a second round of culture.

Statistical analysis

Statistical analyses were performed using Graph Pad Prism software. For comparison of two groups two-tailed unpaired Student's *t* test was used, whereas for single measurement comparisons of more than two groups one-way ANOVA with Tukey's post-tests was performed. For comparison to a reference group Dunnett's post-test was used. For multiple comparison of more than one parameter between more than two groups, two-way ANOVA with Tukey's post-test was used, for comparisons of two groups Bonferroni's post-test was performed. When comparing to a reference group Dunnett's post-test was used. Viral load, antibody titers and absolute cell

numbers were log-converted to obtain a near-normal distribution for statistical analysis. *P* values <0.05 were considered significant, $p<0.01$ as highly significant, and $p>0.05$ was considered as not statistically significant (ns).

Data availability

Bulk RNAseq and single cell RNAseq data are deposited with the National Center for Biotechnology Information Gene Expression Omnibus (GEO) under the accession numbers GSE160294 and GSE161356, respectively. Additional raw data sets will be provided by the authors upon request.

References

1. Nunes-Alves C, Booty MG, Carpenter SM, Jayaraman P, Rothchild AC, Behar SM. In search of a new paradigm for protective immunity to TB. *Nat Rev Microbiol* **12**, 289-299 (2014).

2. Reith W, Mach B. The bare lymphocyte syndrome and the regulation of MHC expression. *Annu Rev Immunol* **19**, 331-373 (2001).

3. Kovacs JA, Masur H. Prophylaxis against opportunistic infections in patients with human immunodeficiency virus infection. *N Engl J Med* **342**, 1416-1429 (2000).

4. Buranapraditkun S*, et al.* Preservation of Peripheral T Follicular Helper Cell Function in HIV Controllers. *J Virol* **91**, (2017).

5. Dyer WB*, et al.* Mechanisms of HIV non-progression; robust and sustained CD4+ T-cell proliferative responses to p24 antigen correlate with control of viraemia and lack of disease progression after long-term transfusion-acquired HIV-1 infection. *Retrovirology* **5**, 112 (2008).

6. Komanduri KV*, et al.* Restoration of cytomegalovirus-specific CD4+ T-lymphocyte responses after ganciclovir and highly active antiretroviral therapy in individuals infected with HIV-1. *Nat Med* **4**, 953-956 (1998).

7. Streeck H, D'Souza MP, Littman DR, Crotty S. Harnessing CD4(+) T cell responses in HIV vaccine development. *Nat Med* **19**, 143-149 (2013).

8. Penaloza-MacMaster P*, et al.* Vaccine-elicited CD4 T cells induce immunopathology after chronic LCMV infection. *Science* **347**, 278-282 (2015).

9. Hunziker L*, et al.* Antagonistic variant virus prevents wild-type virus-induced lethal immunopathology. *J Exp Med* **196**, 1039-1046 (2002).

10. Oxenius A, Zinkernagel RM, Hengartner H. Comparison of activation versus induction of unresponsiveness of virus-specific CD4+ and CD8+ T cells upon acute versus persistent viral infection. *Immunity* **9**, 449-457 (1998).

11. van der Fits L*, et al.* Adenovector 26 encoded prefusion conformation stabilized RSV-F protein induces long-lasting Th1-biased immunity in neonatal mice. *NPJ Vaccines* **5**, 49 (2020).

12. Puissant-Lubrano B*, et al.* Control of vaccinia virus skin lesions by long-term-maintained IFN-gamma+TNF-alpha+ effector/memory CD4+ lymphocytes in humans. *J Clin Invest* **120**, 1636-1644 (2010).

13. Hsieh CS, Macatonia SE, Tripp CS, Wolf SF, O'Garra A, Murphy KM. Development of TH1 CD4+ T cells through IL-12 produced by Listeria-induced macrophages. *Science* **260**, 547-549 (1993).

14. Plotkin SA. Correlates of protection induced by vaccination. *Clin Vaccine Immunol* **17**, 1055-1065 (2010).

15. Immunity ECGoHB. Are booster immunisations needed for lifelong hepatitis B immunity? European Consensus Group on Hepatitis B Immunity. *Lancet* **355**, 561-565 (2000).

16. West DJ, Calandra GB. Vaccine induced immunologic memory for hepatitis B surface antigen: implications for policy on booster vaccination. *Vaccine* **14**, 1019-1027 (1996).

17. Kinchen VJ*, et al.* Broadly Neutralizing Antibody Mediated Clearance of Human Hepatitis C Virus Infection. *Cell Host Microbe* **24**, 717-730 e715 (2018).

18. Pestka JM*, et al.* Rapid induction of virus-neutralizing antibodies and viral clearance in a single-source outbreak of hepatitis C. *Proc Natl Acad Sci U S A* **104**, 6025-6030 (2007).

19. Osburn WO*, et al.* Clearance of hepatitis C infection is associated with the early appearance of broad neutralizing antibody responses. *Hepatology* **59**, 2140-2151 (2014).

20. Raghuraman S, Park H, Osburn WO, Winkelstein E, Edlin BR, Rehermann B. Spontaneous clearance of chronic hepatitis C virus infection is associated with appearance of neutralizing antibodies and reversal of T-cell exhaustion. *J Infect Dis* **205**, 763-771 (2012).

21. Chen M*, et al.* Limited humoral immunity in hepatitis C virus infection. *Gastroenterology* **116**, 135-143 (1999).

22. Cox AL*, et al.* Prospective evaluation of community-acquired acute-phase hepatitis C virus infection. *Clin Infect Dis* **40**, 951-958 (2005).

23. Cohen MS, Shaw GM, McMichael AJ, Haynes BF. Acute HIV-1 Infection. *N Engl J Med* **364**, 1943-1954 (2011).

24. Pinschewer DD*, et al.* Kinetics of protective antibodies are determined by the viral surface antigen. *J Clin Invest* **114**, 988-993 (2004).

25. Fallet B*, et al.* Interferon-driven deletion of antiviral B cells at the onset of chronic infection *Sci Immunol* **1**, eaah6817 (2016).

26. Sammicheli S*, et al.* Inflammatory monocytes hinder antiviral B cell responses. *Sci Immunol* **1**, (2016).

27. Moseman EA, Wu T, de la Torre JC, Schwartzberg PL, McGavern DB. Type I interferon suppresses virus-specific B cell responses by modulating CD8(+) T cell differentiation. *Sci Immunol* **1**, (2016).

28. Sandler NG*, et al.* Type I interferon responses in rhesus macaques prevent SIV infection and slow disease progression. *Nature* **511**, 601-605 (2014).

29. Crotty S. Follicular helper CD4 T cells (TFH). *Annu Rev Immunol* **29**, 621-663 (2011).

30. Vinuesa CG, Linterman MA, Yu D, MacLennan IC. Follicular Helper T Cells. *Annu Rev Immunol* **34**, 335-368 (2016).

31. Qi H. T follicular helper cells in space-time. *Nat Rev Immunol* **16**, 612-625 (2016).

32. Lee BO*, et al.* CD4 T cell-independent antibody response promotes resolution of primary influenza infection and helps to prevent reinfection. *J Immunol* **175**, 5827-5838 (2005).

33. Ochsenbein AF, Pinschewer DD, Odermatt B, Carroll MC, Hengartner H, Zinkernagel RM. Protective T cell-independent antiviral antibody responses are dependent on complement. *J Exp Med* **190**, 1165-1174 (1999).

34. Vieira P, Rajewsky K. Persistence of memory B cells in mice deprived of T cell help. *Int Immunol* **2**, 487-494 (1990).

35. Hebeis BJ*, et al.* Activation of virus-specific memory B cells in the absence of T cell help. *J Exp Med* **199**, 593-602 (2004).

36. Asrir A, Aloulou M, Gador M, Perals C, Fazilleau N. Interconnected subsets of memory follicular helper T cells have different effector functions. *Nat Commun* **8**, 847 (2017).

37. MacLeod MK, David A, McKee AS, Crawford F, Kappler JW, Marrack P. Memory CD4 T cells that express CXCR5 provide accelerated help to B cells. *J Immunol* **186**, 2889-2896 (2011).

38. McHeyzer-Williams LJ, Dufaud C, McHeyzer-Williams MG. Do Memory B Cells Form Secondary Germinal Centers? Impact of Antibody Class and Quality of Memory T-Cell Help at Recall. *Cold Spring Harb Perspect Biol* **10**, (2018).

39. Dogan I*, et al.* Multiple layers of B cell memory with different effector functions. *Nat Immunol* **10**, 1292-1299 (2009).

40. Krishnamurty AT*, et al.* Somatically Hypermutated Plasmodium-Specific IgM(+) Memory B Cells Are Rapid, Plastic, Early Responders upon Malaria Rechallenge. *Immunity* **45**, 402-414 (2016).

41. Pape KA, Taylor JJ, Maul RW, Gearhart PJ, Jenkins MK. Different B cell populations mediate early and late memory during an endogenous immune response. *Science* **331**, 1203-1207 (2011).

42. Zuccarino-Catania GV*, et al.* CD80 and PD-L2 define functionally distinct memory B cell subsets that are independent of antibody isotype. *Nat Immunol* **15**, 631-637 (2014).

43. McHeyzer-Williams LJ, Milpied PJ, Okitsu SL, McHeyzer-Williams MG. Class-switched memory B cells remodel BCRs within secondary germinal centers. *Nat Immunol* **16**, 296-305 (2015).

44. Porter BB, Harty JT. The onset of CD8+-T-cell contraction is influenced by the peak of Listeria monocytogenes infection and antigen display. *Infect Immun* **74**, 1528-1536 (2006).

45. Duffy D, Yang CP, Heath A, Garside P, Bell EB. Naive T-cell receptor transgenic T cells help memory B cells produce antibody. *Immunology* **119**, 376-384 (2006).

46. Choi YS*, et al.* LEF-1 and TCF-1 orchestrate T(FH) differentiation by regulating differentiation circuits upstream of the transcriptional repressor Bcl6. *Nat Immunol* **16**, 980-990 (2015).

47. Tangye SG. Advances in IL-21 biology - enhancing our understanding of human disease. *Curr Opin Immunol* **34**, 107-115 (2015).

48. Yu D*, et al.* The transcriptional repressor Bcl-6 directs T follicular helper cell lineage commitment. *Immunity* **31**, 457-468 (2009).

49. Nurieva RI*, et al.* Bcl6 mediates the development of T follicular helper cells. *Science* **21**, 1001-1005 (2009).

50. Johnston RJ*, et al.* Bcl6 and Blimp-1 Are Reciprocal and Antagonistic Regulators of T Follicular Helper Cell Differentiation. *Science* **325**, 1006-1010 (2009).

51. Wan Z, Lin Y, Zhao Y, Qi H. TFH cells in bystander and cognate interactions with B cells. *Immunol Rev* **288**, 28-36 (2019).

52. Scherle PA, Gerhard W. Functional analysis of influenza-specific helper T cell clones in vivo. T cells specific for internal viral proteins provide cognate help for B cell responses to hemagglutinin. *J Exp Med* **164**, 1114-1128 (1986).

53. Lanzavecchia A. Antigen-specific interaction between T and B cells. *Nature* **314**, 537-539 (1985).

54. Hernandez MG, Shen L, Rock KL. CD40 on APCs is needed for optimal programming, maintenance, and recall of CD8+ T cell memory even in the absence of CD4+ T cell help. *J Immunol* **180**, 4382-4390 (2008).

55. Shi W*, et al.* Transcriptional profiling of mouse B cell terminal differentiation defines a signature for antibody-secreting plasma cells. *Nat Immunol* **16**, 663-673 (2015).

56. Brescia P*, et al.* MEF2B Instructs Germinal Center Development and Acts as an Oncogene in B Cell Lymphomagenesis. *Cancer Cell* **34**, 453-465 e459 (2018).

57. Dent AL, Shaffer AL, Yu X, Allman D, Staudt LM. Control of inflammation, cytokine expression, and germinal center formation by BCL-6. *Science* **276**, 589-592 (1997).

58. Fallet B*, et al.* Chronic Viral Infection Promotes Efficient Germinal Center B Cell Responses. *Cell Rep* **30**, 1013-1026 e1017 (2020).

59. Cyster JG, Allen CDC. B Cell Responses: Cell Interaction Dynamics and Decisions. *Cell* **177**, 524-540 (2019).

60. Shapiro-Shelef M, Lin KI, McHeyzer-Williams LJ, Liao J, McHeyzer-Williams MG, Calame K. Blimp-1 is required for the formation of immunoglobulin secreting plasma cells and pre-plasma memory B cells. *Immunity* **19**, 607-620 (2003).

61. Kunzli M*, et al.* Long-lived T follicular helper cells retain plasticity and help sustain humoral immunity. *Sci Immunol* **5**, (2020).

62. Hill DL*, et al.* The adjuvant GLA-SE promotes human Tfh cell expansion and emergence of public TCRbeta clonotypes. *J Exp Med* **216**, 1857-1873 (2019).

63. Burton DR*, et al.* A Blueprint for HIV Vaccine Discovery. *Cell Host Microbe* **12**, 396-407 (2012).

64. Liu J*, et al.* Antibody-mediated protection against SHIV challenge includes systemic clearance of distal virus. *Science* **353**, 1045-1049 (2016).

65. Doria-Rose NA*, et al.* Developmental pathway for potent V1V2-directed HIV-neutralizing antibodies. *Nature* **509**, 55-62 (2014).

66. Liao HX*, et al.* Co-evolution of a broadly neutralizing HIV-1 antibody and founder virus. *Nature* **496**, 469-476 (2013).

67. Xin G*, et al.* Single-cell RNA sequencing unveils an IL-10-producing helper subset that sustains humoral immunity during persistent infection. *Nat Commun* **9**, 5037 (2018).

68. Arpin C*, et al.* Generation of memory B cells and plasma cells in vitro. *Science* **268**, 720-722 (1995).

69. Pape KA, Maul RW, Dileepan T, Paustian AS, Gearhart PJ, Jenkins MK. Naive B Cells with High-Avidity Germline-Encoded Antigen Receptors Produce Persistent IgM(+) and Transient IgG(+) Memory B Cells. *Immunity* **48**, 1135-1143 e1134 (2018).

70. Kuraoka M*, et al.* Complex Antigens Drive Permissive Clonal Selection in Germinal Centers. *Immunity* **44**, 542-552 (2016).

71. Jardine JG*, et al.* Minimally Mutated HIV-1 Broadly Neutralizing Antibodies to Guide Reductionist Vaccine Design. *PLoS Pathog* **12**, e1005815 (2016).

72. Huang D*, et al.* B cells expressing authentic naive human VRC01-class BCRs can be recruited to germinal centers and affinity mature in multiple independent mouse models. *Proc Natl Acad Sci U S A* **117**, 22920-22931 (2020).

73. Marzo AL, Vezys V, Williams K, Tough DF, Lefrancois L. Tissue-level regulation of Th1 and Th2 primary and memory CD4 T cells in response to Listeria infection. *J Immunol* **168**, 4504-4510 (2002).

74. Ise W*, et al.* Memory B cells contribute to rapid Bcl6 expression by memory follicular helper T cells. *Proc Natl Acad Sci U S A* **111**, 11792-11797 (2014).

75. Hegazy AN*, et al.* Interferons direct Th2 cell reprogramming to generate a stable GATA-3(+)T-bet(+) cell subset with combined Th2 and Th1 cell functions. *Immunity* **32**, 116-128 (2010).

76. Hangartner L*, et al.* Antiviral immune responses in gene-targeted mice expressing the immunoglobulin heavy chain of virus-neutralizing antibodies. *Proc Natl Acad Sci U S A* **100**, 12883-12888 (2003).

77. Kawabe T*, et al.* The immune responses in CD40-deficient mice: impaired immunoglobulin class switching and germinal center formation. *Immunity* **1**, 167-178 (1994).

78. Cosgrove D*, et al.* Mice lacking MHC class II molecules. *Cell* **66**, 1051-1066 (1991).

79. Szabo SJ, Sullivan BM, Stemmann C, Satoskar AR, Sleckman BP, Glimcher LH. Distinct effects of T-bet in TH1 lineage commitment and IFN-gamma production in CD4 and CD8 T cells. *Science* **295**, 338-342 (2002).

80. Huang S*, et al.* Immune response in mice that lack the interferon-gamma receptor. *Science* **259**, 1742-1745 (1993).

81. Kuhn R, Rajewsky K, Muller W. Generation and analysis of interleukin-4 deficient mice. *Science* **254**, 707-710 (1991).

82. Hao Z, Rajewsky K. Homeostasis of peripheral B cells in the absence of B cell influx from the bone marrow. *J Exp Med* **194**, 1151-1164 (2001).

83. Oxenius A, Bachmann MF, Zinkernagel RM, Hengartner H. Virus-specific MHC-class II-restricted TCR-transgenic mice: effects on humoral and cellular immune responses after viral infection. *Eur J Immunol* **28**, 390-400 (1998).

84. Renshaw BR*, et al.* Humoral immune responses in CD40 ligand-deficient mice. *J Exp Med* **180**, 1889-1900 (1994).

85. Muller U*, et al.* Functional role of type I and type II interferons in antiviral defense. *Science* **264**, 1918-1921 (1994).

86. Kuhn R, Lohler J, Rennick D, Rajewsky K, Muller W. Interleukin-10-deficient mice develop chronic enterocolitis. *Cell* **75**, 263-274 (1993).

87. Mombaerts P*, et al.* Peripheral lymphoid development and function in TCR mutant mice. *Int Immunol* **6**, 1061-1070 (1994).

88. Maloy KJ*, et al.* Qualitative and quantitative requirements for CD4+ T cell-mediated antiviral protection. *J Immunol* **162**, 2867-2874 (1999).

89. Kaji T*, et al.* Distinct cellular pathways select germline-encoded and somatically mutated antibodies into immunological memory. *J Exp Med* **209**, 2079-2097 (2012).

90. Nance JP, Belanger S, Johnston RJ, Takemori T, Crotty S. Cutting edge: T follicular helper cell differentiation is defective in the absence of Bcl6 BTB repressor domain function. *J Immunol* **194**, 5599-5603 (2015).

91. Sonderegger I, Kisielow J, Meier R, King C, Kopf M. IL-21 and IL-21R are not required for development of Th17 cells and autoimmunity in vivo. *Eur J Immunol* **38**, 1833-1838 (2008).

92. Luthje K*, et al.* The development and fate of follicular helper T cells defined by an IL-21 reporter mouse. *Nat Immunol* **13**, 491-498 (2012).

93. Sommerstein R*, et al.* Arenavirus Glycan Shield Promotes Neutralizing Antibody Evasion and Protracted Infection. *PLoS Pathog* **11**, e1005276 (2015).

94. Battegay M, Cooper S, Althage A, Banziger J, Hengartner H, Zinkernagel RM. Quantification of lymphocytic choriomeningitis virus with an immunological focus assay in 24- or 96-well plates. *J Virol Methods* **33**, 191-198 (1991).

95. Way SS, Havenar-Daughton C, Kolumam GA, Orgun NN, Murali-Krishna K. IL-12 and type-I IFN synergize for IFN-gamma production by CD4 T cells, whereas neither are required for IFN-gamma production by CD8 T cells after Listeria monocytogenes infection. *J Immunol* **178**, 4498-4505 (2007).

96. Shen H, Slifka MK, Matloubian M, Jensen ER, Ahmed R, Miller JF. Recombinant Listeria monocytogenes as a live vaccine vehicle for the induction of protective anti-viral cell-mediated immunity. *Proc Natl Acad Sci U S A* **92**, 3987-3991 (1995).

97. Dobin A*, et al.* STAR: ultrafast universal RNA-seq aligner. *Bioinformatics* **29**, 15-21 (2013).

98. Huber W*, et al.* Orchestrating high-throughput genomic analysis with Bioconductor. *Nat Methods* **12**, 115-121 (2015).

99. Gaidatzis D, Lerch A, Hahne F, Stadler MB. QuasR: quantification and annotation of short reads in R. *Bioinformatics* **31**, 1130-1132 (2015).

100. McCarthy DJ, Chen Y, Smyth GK. Differential expression analysis of multifactor RNA-Seq experiments with respect to biological variation. *Nucleic Acids Res* **40**, 4288-4297 (2012).

101. Liberzon A, Birger C, Thorvaldsdottir H, Ghandi M, Mesirov JP, Tamayo P. The Molecular Signatures Database (MSigDB) hallmark gene set collection. *Cell Syst* **1**, 417-425 (2015).

102. Dosenovic P*, et al.* Anti-HIV-1 B cell responses are dependent on B cell precursor frequency and antigen-binding affinity. *Proc Natl Acad Sci U S A* **115**, 4743-4748 (2018).

103. Abbott RK*, et al.* Precursor Frequency and Affinity Determine B Cell Competitive Fitness in Germinal Centers, Tested with Germline-Targeting HIV Vaccine Immunogens. *Immunity* **48**, 133-146 e136 (2018).

104. Taylor JJ, Pape KA, Steach HR, Jenkins MK. Humoral immunity. Apoptosis and antigen affinity limit effector cell differentiation of a single naive B cell. *Science* **347**, 784-787 (2015).

105. Eschli B*, et al.* Early antibodies specific for the neutralizing epitope on the receptor binding subunit of the lymphocytic choriomeningitis virus glycoprotein fail to neutralize the virus. *J Virol* **81**, 11650-11657 (2007).

106. Bergthaler A, Merkler D, Horvath E, Bestmann L, Pinschewer DD. Contributions of the lymphocytic choriomeningitis virus glycoprotein and polymerase to strain-specific differences in murine liver pathogenicity. *J Gen Virol* **88**, 592-603 (2007).

Acknowledgments

We wish to thank Christian Beisel and Tobias Schär from the Genomics Facility Basel of the University of Basel and D-BSSE of ETH Zurich for single-cell RNA-seq library preparation and next generation RNA sequencing; Julien Roux from the DBM Bioinformatics Core Facility of the University of Basel for single-cell RNA-Seq analysis; Philippe Demougin from the Life Sciences Training Facility of the University of Basel Pharmacenter for bulk RNA

sequencing; Karsten Stauffer for experimental support in animal handling and care; Ingrid Wagner and Karim Hammad for immunohistochemistry; Telma Lopes, Danny Labes, Lorenzo Raeli and Emmanuel Traunecker from the DBM flow cytometry core facility for FACS sorting; Jean-Claude Weill, Claude-Agnès Reynaud, Peter Aichele, Shane Crotty, Manfred Kopf and Stephen Nutt for generously donating mouse strains; Pablo Penaloza, Dan Barouch and Hao Shen for providing recombinant Listeria; the NIH tetramer core facility for MHC class II tetramers and the entire Experimental Virology lab for helpful discussions. All bioinformatic calculations were performed at the sciCORE (http://scicore.unibas.ch/) scientific computing center at University of Basel.

Funding

This work was supported by the European Research Council (ERC grants No. 310962 to D.D.P.), by the Swiss National Science Foundation (project grants No. 310030_173132 to D.D.P and No. 310030_173010 to D.M., and project No. 323630_151472 to B.F.)

Author contributions

K.N, Y.I.E, B.F., M.Kü., D.S., F.G., D.M, C.K, and D.D.P, contributed to experimental conception and design; K.N, Y.I.E. B.F, K.C. M.D, A.F.M., K.M., M.Kü., D.S., T.B., M.Kr., F.G., L.B., M.L., D.M., C.K. and D.D.P acquired, analyzed and/or interpreted the data; K.N. D.S. C.K. and D.D.P. drafted or critically revised the article for important intellectual content.

Conflict of interests statement

D.D.P. is a founder, shareholder and consultant and serves as scientific advisor to the CEO of Hookipa Pharma Inc. commercializing arenavirus-based vector technology. D.M. and D.D.P. are inventors on patents describing arenavirus-based vector technology. The remaining authors declare that they have no competing interests.

Figures

Figure 1

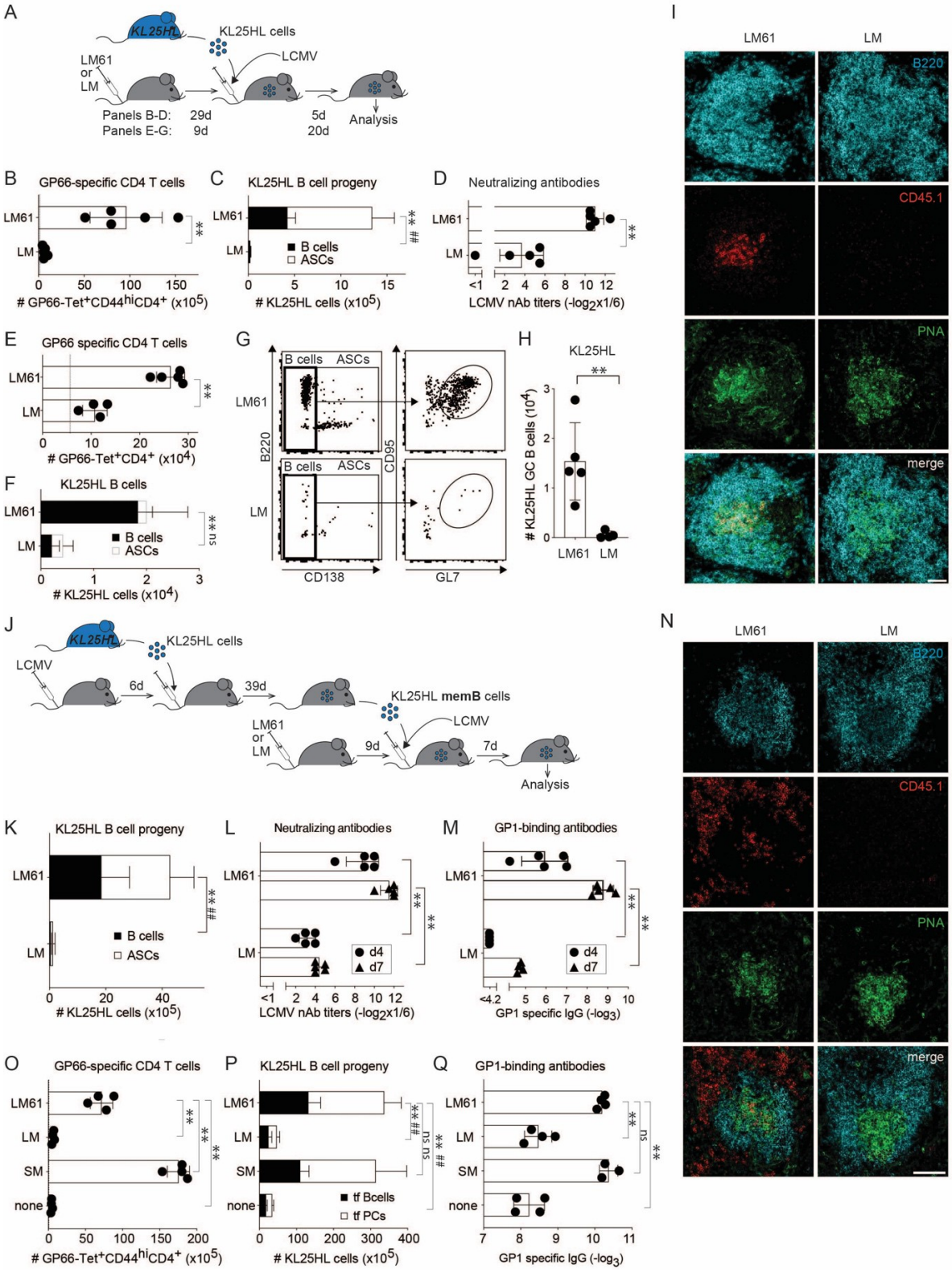

Figure 1. Pre-existing CD4 T cell help prevents decimation of naïve and memory B cells upon chronic virus challenge

A-I: Schematic of the experimental design to panels B-I. Recipients were pre-immunized with LM61 or LM. 29 days (B-D) or 9 days later (E-I) they received KL25 B cells transfer and LCMV infection. Immune responses were analyzed another 5 days (B-D) or 20 days (E-I) later. GP66-Tet$^+$ CD4 T cells (B,E) and KL25HL B cell progeny (C,F) were enumerated and nAb titers in serum (D) were determined. Exemplary FACS plots analyzing KL25HL B cell progeny are shown in (G). For details on flow cytometry gating see Fig. S1A,B. GL7$^+$CD95$^+$ KL25HL GC B cells are enumerated in (H). KL25HL B cell progeny (CD45.1+) inside GCs (PNA) of splenic B cell follicles (B220) were visualized by histology (scale bars: 100 µm) (I).

J-N: Schematic of the experimental layout to panels K-N. KL25HL cells were adoptively transferred into LCMV-infected primary recipients. 39 days later progeny memB cells were purified from spleen (see Fig. S1C,D) and were adoptively transferred into LM61- or LM-pre-immunized secondary recipients, followed by LCMV challenge. KL25HL memB cell progeny were analyzed 7 days later (K), neutralizing (L) and GP-1-binding (M) antibody titers were determined four and seven days later. Histological spleen sections (N) localized KL25HL memB cell progeny (CD45.1$^+$) mostly outside B cell follicles (B220) and GCs (PNA; scale bars: 100 µm).

O-Q: SM CD4 T cells were adoptively transferred to recipients one day prior to KL25HL cell transfer and LCMV challenge. Instead of SM transfer, controls were LMgp61-pre-immunized (LM61) LM-pre-immunized (LM) or received neither CD4 T cell transfer nor pre-immunization (none). GP66-Tet-binding CD4 T cells (O), KL25HL B cell progeny (P) and GP1-binding antibodies (Q) were analyzed 5 days after LCMV challenge.

Symbols and bars represent means±SD. Number of biological replicates (*n*)=5 (B-D, K-N), *n*=4-5 (E-I), *n*=4 (O-Q), Number of independent experiments (*N*)=2-3. Unpaired two-tailed Students's *t* test (B, D-E, H), two-way analysis of variance (ANOVA) with Bonferroni's (C, F, K-M) or Dunnett's (P) post-test for multiple comparison and ordinary one-way ANOVA with Dunnett's post-test for multiple comparisons (O, Q). ns: not significant; **,##: $p<0.01$; when used next to each other ** compares B cells and ## compares ASCs.

Figure 2

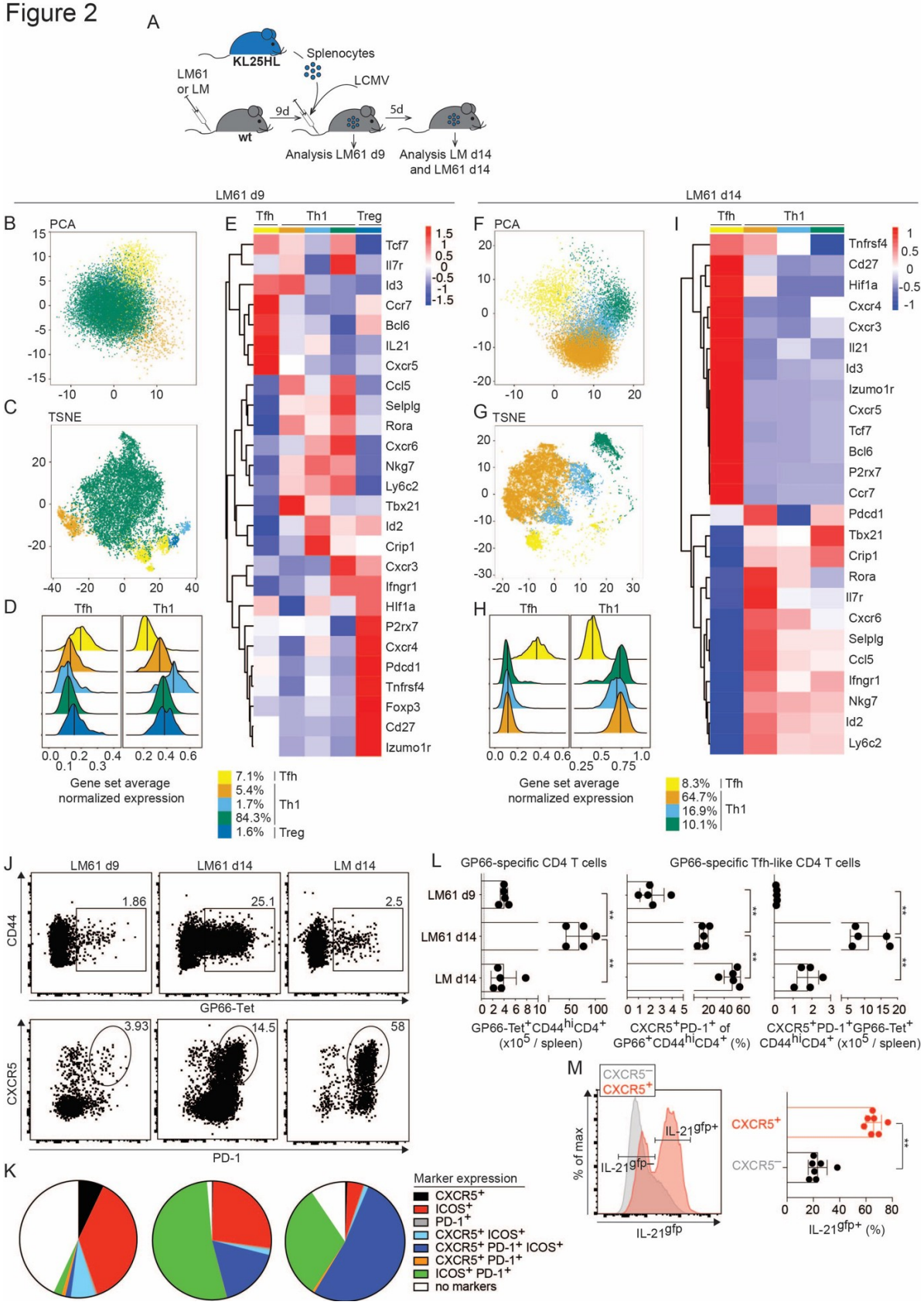
A
KL25HL
Splenocytes
LCMV
LM61 or LM
wt
9d
5d
Analysis LM61 d9
Analysis LM d14 and LM61 d14
LM61 d9
LM61 d14
B PCA
C TSNE
D
Tfh
Th1
Gene set average normalized expression
E
Tfh
Th1
Treg
Tcf7
Il7r
Id3
Ccr7
Bcl6
IL21
Cxcr5
Ccl5
Selplg
Rora
Cxcr6
Nkg7
Ly6c2
Tbx21
Id2
Crip1
Cxcr3
Ifngr1
Hlf1a
P2rx7
Cxcr4
Pdcd1
Tnfrsf4
Foxp3
Cd27
Izumo1r
7.1% Tfh
5.4%
1.7% Th1
84.3%
1.6% Treg
F PCA
G TSNE
H
Gene set average normalized expression
8.3% Tfh
64.7%
16.9% Th1
10.1%
I
Tnfrsf4
Cd27
Hif1a
Cxcr4
Cxcr3
Il21
Id3
Izumo1r
Cxcr5
Tcf7
Bcl6
P2rx7
Ccr7
Pdcd1
Tbx21
Crip1
Rora
Il7r
Cxcr6
Selplg
Ccl5
Ifngr1
Nkg7
Id2
Ly6c2
J
LM61 d9
LM61 d14
LM d14
CD44
GP66-Tet
CXCR5
PD-1
1.86
25.1
2.5
3.93
14.5
58
K
Marker expression
CXCR5+
ICOS+
PD-1+
CXCR5+ ICOS+
CXCR5+ PD-1+ ICOS+
CXCR5+ PD-1+
ICOS+ PD-1+
no markers
L
GP66-specific CD4 T cells
GP66-specific Tfh-like CD4 T cells
LM61 d9
LM61 d14
LM d14
GP66-Tet+CD44hiCD4+ (x10^5 / spleen)
CXCR5+PD-1+ of GP66+CD44hiCD4+ (%)
CXCR5+PD-1+GP66-Tet+ CD44hiCD4+ (x10^5 / spleen)
M
CXCR5−
CXCR5+
% of max
IL-21gfp+
IL-21gfp−
IL-21gfp
CXCR5+
CXCR5−
IL-21gfp+ (%)

Figure 2. LM61-induced CD4 responses are Th1-biased but comprise a Tfh-like population that expands upon recall

A: Schematic of the experimental design to panels B-L. Mice were pre-immunized with LM61 or LM on d0, followed by KL25HL cell transfer and LCMV challenge on d9. GP66-Tet+ CD4 T cell responses in spleen were analyzed on d9 and d14 of the experiment.

B-I: scRNAseq data from cells recovered on d9 (B-E; 14'459 cells from two mice) or d14 (F-I: 13'478 cells from two mice). Principle component analyses (PCA; B,F) and t-distributed stochastic neighbor embedding (t-SNE, C,G), normalized expression of gene sets [46] (D,H) and expression levels of select Tfh and Th1 hallmark genes (E,I) are shown.

J-L: Representative FACS plots of the indicated immunization groups and time points show $CD44^{hi}GP66\text{-}Tet^{+}$ CD4 T cells (pre-gated as shown in Fig. S1A) and these cells' expression of CXCR5 and PD-1 (J). Co-expression of these markers together with ICOS is displayed in (K). Total $CD44^{hi}GP66\text{-}Tet^{+}$ CD4 T cells, the percentage thereof expressing both CXCR5 and PD-1, and the total number of the latter subset are displayed in (L, left to right).

M: We immunized IL-21^{gfp} reporter mice with LM61 and challenged them with LCMV as outlined in (A), and on d14 compared the IL-21 reporting by the $CXCR5^{+}$ Tfh-like and $CXCR5^{-}$ Th1-like subsets of $CD44^{hi}GP66\text{-}Tet^{+}$ CD4 T cells. The percentage of IL-21^{gfp}-positive cells in each subset is indicated in the bar chart.

Numbers in exemplary FACS plots indicate percentages of gated cells. Symbols and bars represent means±SD, Number of biological replicates *(n)*=5 (J-K) and *n*=7 (M). Number of independent experiments *(N)*=1 (B-I), *N*=2 (J-M). Ordinary one-way ANOVA with Dunnett's post-test for multiple comparisons (L), unpaired two-tailed Student's *t* test (M). **: $p<0.01$.

Figure 3

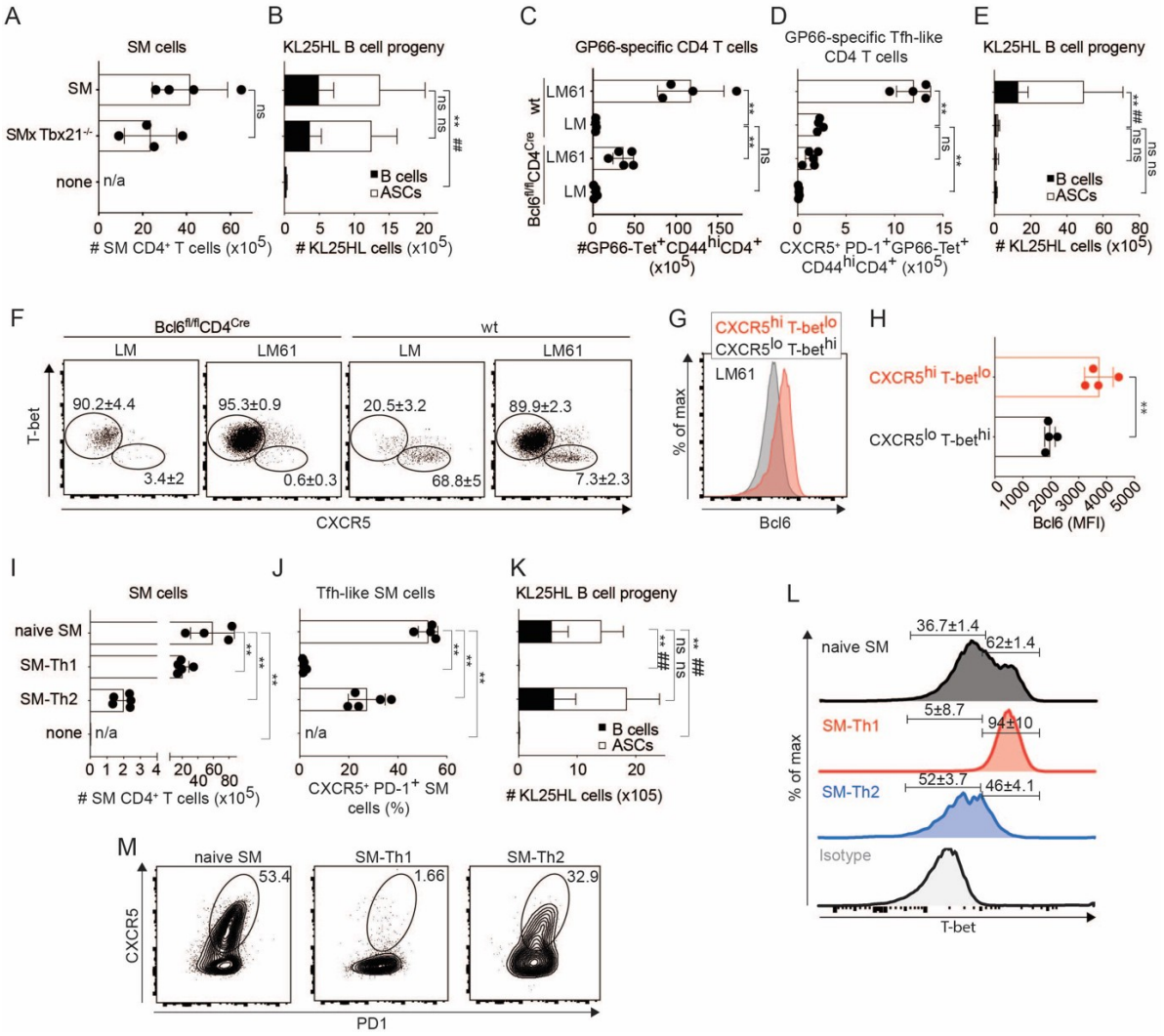
A
SM cells
SM
SMx Tbx21-/-
none
n/a
ns
0 20 40 60
SM CD4+ T cells (x10^5)
B
KL25HL B cell progeny
ns ns
**
B cells
ASCs
0 5 10 15 20
KL25HL cells (x10^5)
C
GP66-specific CD4 T cells
wt
Bcl6fl/flCD4Cre
LM61
LM
LM61
LM
**
**
ns
0 50 100 150
#GP66-Tet+CD44hiCD4+ (x10^5)
D
GP66-specific Tfh-like CD4 T cells
**
ns
**
0 5 10 15
CXCR5+ PD-1+GP66-Tet+ CD44hiCD4+ (x10^5)
E
KL25HL B cell progeny
** ns
ns
ns ns
B cells
ASCs
0 20 40 60 80
KL25HL cells (x10^5)
F
Bcl6fl/flCD4Cre
wt
LM
LM61
LM
LM61
T-bet
90.2±4.4
3.4±2
95.3±0.9
0.6±0.3
20.5±3.2
68.8±5
89.9±2.3
7.3±2.3
CXCR5
G
CXCR5hi T-betlo
CXCR5lo T-bethi
LM61
% of max
Bcl6
H
CXCR5hi T-betlo
CXCR5lo T-bethi
**
0 1000 2000 3000 4000 5000
Bcl6 (MFI)
I
SM cells
naive SM
SM-Th1
SM-Th2
none
n/a
** **
** **
0 1 2 3 4 20 40 60 80
SM CD4+ T cells (x10^5)
J
Tfh-like SM cells
** **
** **
n/a
0 20 40 60
CXCR5+ PD-1+ SM cells (%)
K
KL25HL B cell progeny
**
ns ns
**
B cells
ASCs
0 10 20
KL25HL cells (x105)
L
naive SM
36.7±1.4
62±1.4
SM-Th1
5±8.7
94±10
SM-Th2
52±3.7
46±4.1
Isotype
% of max
T-bet
M
naive SM
SM-Th1
SM-Th2
53.4
1.66
32.9
CXCR5
PD1

Figure 3. Bcl6-dependent CD4 response and Th2- but not Th1-polarized SM CD4 T cells prevent B cell decimation
A,B: On day -1 we transferred either T-bet-sufficient or T-bet-deficient SM CD4 T cells (SMxTbx21$^{-/-}$) to naïve recipients, followed by KL25HL cell transfer and LCMV challenge on d0. Controls were left without CD4 T cell transfer. Five days later we enumerated the progeny of adoptively transferred CD4 T cells (A) and KL25HL B cells (B) in spleen.
C-H: CD4^{Cre}Bcl6^{fl} mice and wt controls were pre-immunized with either LM61 or LM on day -9, followed by KL25HL cell transfer and LCMV challenge on d0. On d5 we determined CD44^{hi}GP66-Tet^{+} CD4 T cells (C), the CXCR5^{+}PD-1^{+} Tfh subset comprised therein (D) as well as KL25HL cell progeny (E) in spleen. Exemplary FACS plots characterizing T-bet^{hi}CXCR5^{lo} Th1 and T-bet$^{low/neg}$CXCR5^{hi} Tfh cell subsets amongst the CD44^{hi}GP66-Tet^{+} CD4 T cells enumerated in (C). Bcl6 levels of the aforementioned Th1 and Tfh cell subsets in LM61 pre-immunized wt control mice are displayed (G) and quantified (H).
I-M: SM cells were polarized to either a Th1 (SM-Th1) or a Th2 phenotype (SM-Th2) using the appropriate *in vitro* culture conditions (see also Fig. S3) and were adoptively transferred to syngeneic recipients on d-1. Control mice were either given naïve SM cells or were left without SM cell transfer ("none"). On d0 all mice were given KL25HL cells and were challenged with LCMV. We analyzed the expanded SM cells (I), Tfh-differentiated CXCR5+PD-1+ SM cells (J) and KL25HL progeny (K) from spleen on d5. T-bet expression levels (L) of transferred SM cells including an isotype control stain as well as exemplary FACS plot of CXCR5 and PD-1 expression are shown (M). Percentage values in (L) are shown as mean±SD.
Numbers in exemplary FACS plots indicate the mean±SD (F) or the percentage of gated cells (M). Symbols and bars represent means±SD, number of biological replicates *(n)*=4 (A-B) *n*=4-5 (C-M). Number of independent experiments *(N)*=2 (A-M). Unpaired two-tailed Students's *t* test (A, H), two-way ANOVA with Dunnett's post-test for multiple comparison (B,E,K). Ordinary one-way ANOVA with Dunnett's post-test for multiple comparisons (C-D,I-J),. ns: not significant*;* **,##: $p<0.01$; when used next to each other, ** compares B cells and ## compares ASCs.

Figure 4

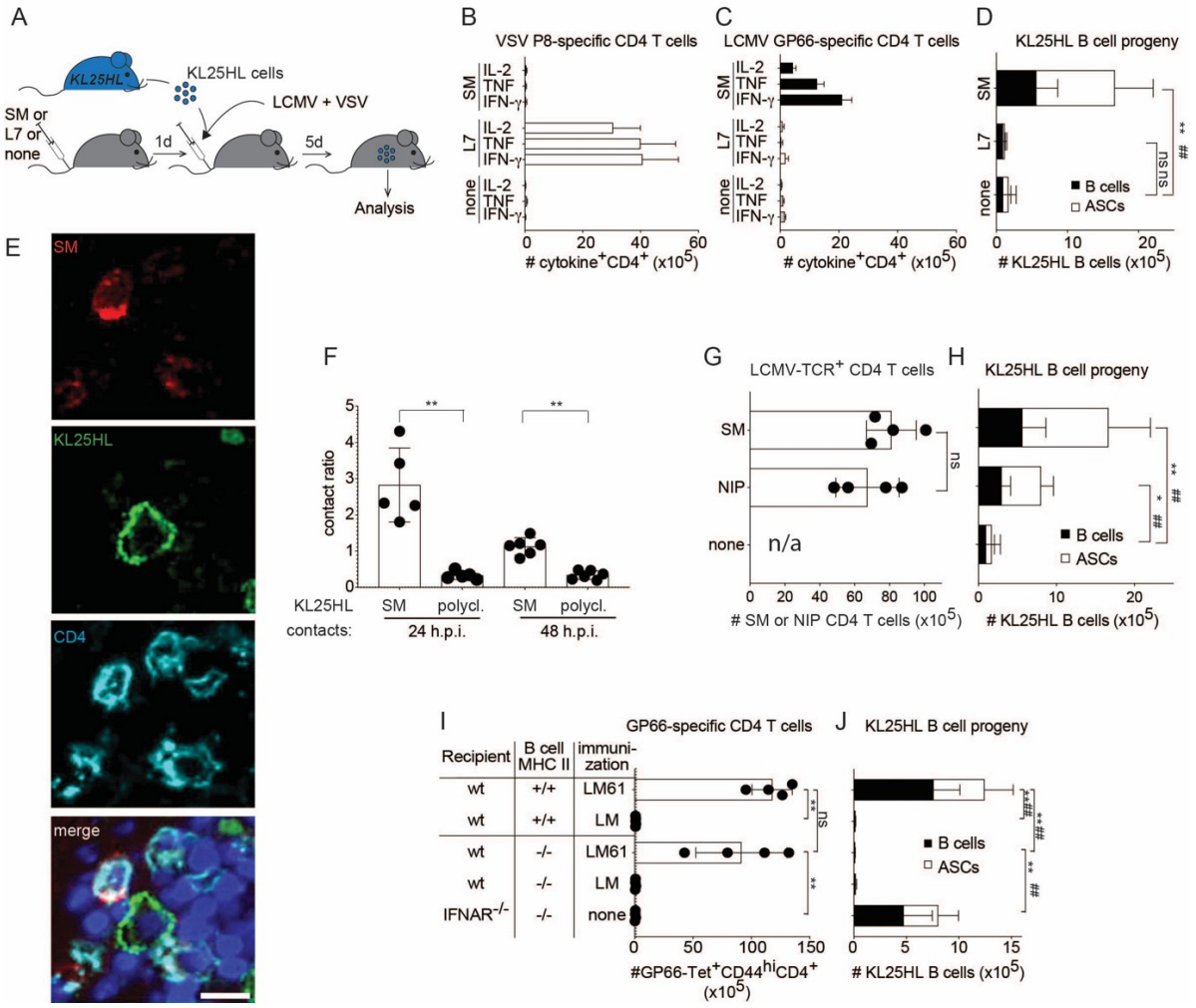
A
KL25HL
KL25HL cells
LCMV + VSV
SM or
L7 or
none
1d
5d
Analysis
B
VSV P8-specific CD4 T cells
SM
L7
none
IL-2
TNF
IFN-γ
cytokine+CD4+ (x10^5)
C
LCMV GP66-specific CD4 T cells
cytokine+CD4+ (x10^5)
D
KL25HL B cell progeny
ns
ns
B cells
ASCs
KL25HL B cells (x10^5)
E
SM
KL25HL
CD4
merge
F
contact ratio
KL25HL contacts:
SM
polycl.
24 h.p.i.
48 h.p.i.
G
LCMV-TCR+ CD4 T cells
NIP
n/a
ns
SM or NIP CD4 T cells (x10^5)
H
KL25HL B cell progeny
B cells
ASCs
KL25HL B cells (x10^5)
I
GP66-specific CD4 T cells
Recipient
B cell MHC II
immuni-zation
wt
+/+
LM61
LM
-/-
IFNAR-/-
none
ns
#GP66-Tet+CD44hiCD4+ (x10^5)
J
KL25HL B cell progeny
B cells
ASCs
KL25HL B cells (x10^5)

Figure 4. T help prevents B cell decimation in an antigen-specific and MHC class II-dependent manner
A-D: Schematic of the experimental design to (B-D). Recipient mice were given either LCMV-specific SM CD4 T cells or VSV-specific L7 CD4 T cells or no CD4 T cells on -d1. On day 0 they received KL25HL cells and were infected the same day with both LCMV and VSV. On day 5 we measured VSV P8-specific (B) and LCMV GP66-specific CD4 T cell responses (C) in spleen by intracellular cytokine assay and enumerated KL25HL progeny (D).
E,F: We transferred SM cells (Thy1.1$^+$) on day -1, followed by KL25HL cell transfer (CD45.1$^+$) and LCMV challenge on d0. 24 and 48 hours later we collected spleens for histological analysis. Exemplary image showing co-localization of SM and KL25HL cells (magnification bar: 10 µm). Contact ratios of KL25HL B cells with either LCMV-specific SM CD4 T cells or polyclonal endogenous CD4 T cells. Each dot represents one mouse (average contact ratio calculated from ≥2250 KL25HL cells for each mouse).
G,H: We transferred GP-specific SM CD4 T cells or NP-specific NIP CD4 T cells on d-1, followed by KL25HL cell transfer and LCMV challenge on d0. Controls were left without T cell transfer ("none"). Adoptively transferred CD4 T cells (G) and KL25HL cell progeny (H) were enumerated on d5.
I,J: Wt and IFNAR-/- recipients were pre-immunized on d-9 as indicated (LM61, LM or none), and on d0 received either MHC-II-deficient or – sufficient KL25HL cells simultaneously with LCMV challenge. CD44^{hi}GP66-Tet$^+$ CD4 T cells (I) and KL25HL progeny (J) were enumerated on d5 in spleen.
Symbols and bars represent means±SD, number of biological replicates *(n)*=4 (A-D,G-H) *n*=5-6 (E-F) *n*=4-5 (I-J). Number of independent experiments *(N)*=2-3 (A-J). Unpaired two-tailed Students's *t* test (F, G), two-way ANOVA with Dunnett's post-test for multiple comparison (D,H), two-way ANOVA with Tukey's post-test for multiple comparison (J), Ordinary one-way ANOVA with Tukey's post-test for multiple comparisons (I),. ns: not significant*;* *: $p<0.05$;**,##: $p<0.01$; when used next to each other, ** compares B cells and ## compares ASCs. Datasets in (A-D) are from the same experiment as (G-H).

Figure 5

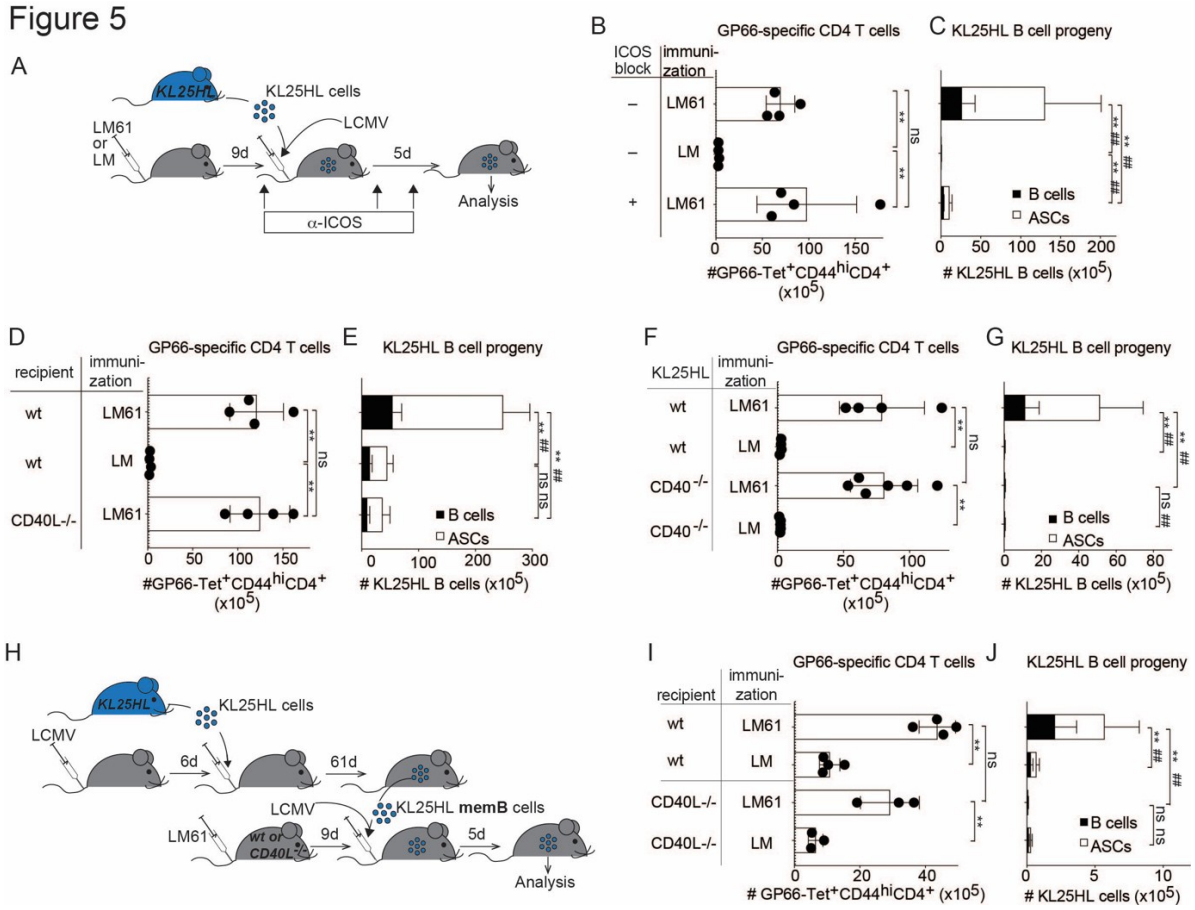
A
KL25HL
KL25HL cells
LCMV
LM61 or LM
9d
5d
Analysis
α-ICOS
B
GP66-specific CD4 T cells
C KL25HL B cell progeny
ICOS block
immuni-zation
LM61
LM
B cells
ASCs
#GP66-Tet+CD44hiCD4+ (x10^5)
KL25HL B cells (x10^5)
D
E
recipient
wt
CD40L-/-
F
G
KL25HL
CD40-/-
H
6d
61d
KL25HL memB cells
wt or CD40L-/-
I
J

Figure 5. T help prevents B cell decimation in a CD40- and ICOS-dependent manner

A-C: Schematic of the experimental design to (B,C). On d-9 mice were pre-immunized as indicated and challenged with LCMV on d0. ICOS-blocking antibody was administered to the indicated group of mice on d-1, d1 and d2. $CD44^{hi}GP66\text{-}Tet^{+}$ CD4 T cells (B) and KL25HL progeny (C) were enumerated on d5 in spleen.

D,E: On d-9 wt and CD40L-/- recipients were pre-immunized as indicated and challenged with LCMV on d0. $CD44^{hi}GP66\text{-}Tet^{+}$ CD4 T cells (D) and KL25HL progeny (E) were enumerated on d5 in spleen.

F,G: Wt recipients were pre-immunized on d-9 as indicated. On d0 they received either CD40-sufficient or –deficient KL25HL cells simultaneously with LCMV challenge. $CD44^{hi}GP66\text{-}Tet^{+}$ CD4 T cells (F) and KL25HL progeny (G) were enumerated on d5 in spleen.

H-J: Schematic of the experimental design to (I,J). KL25HL cells were adoptively transferred into LCMV-infected primary recipients. 61 days later progeny memB cells were purified from spleen (compare Fig. S1C,D) and were adoptively transferred into LM61-pre-immunized secondary recipients, either wt or CD40L-deficient, followed by LCMV challenge and analysis seven days later. $CD44^{hi}GP66\text{-}Tet^{+}$ CD4 T cells (I) and KL25HL progeny (J) were enumerated in spleen.

Symbols and bars represent means±SD, number of biological replicates *(n)*=4 (A-E) *n*=4-6 (F-G) *n*=3-4 (H-J). Number of independent experiments *(N)*=2-3 (A-J). Ordinary one-way ANOVA with Tukey's post-test for multiple comparisons (B,D, F, I) and two-way ANOVA with Tukey's post-test for multiple comparison (C, E, G, J),. ns: not significant;**,##: $p<0.01$; when used next to each other, ** compares B cells and ## compares ASCs.

Figure 6

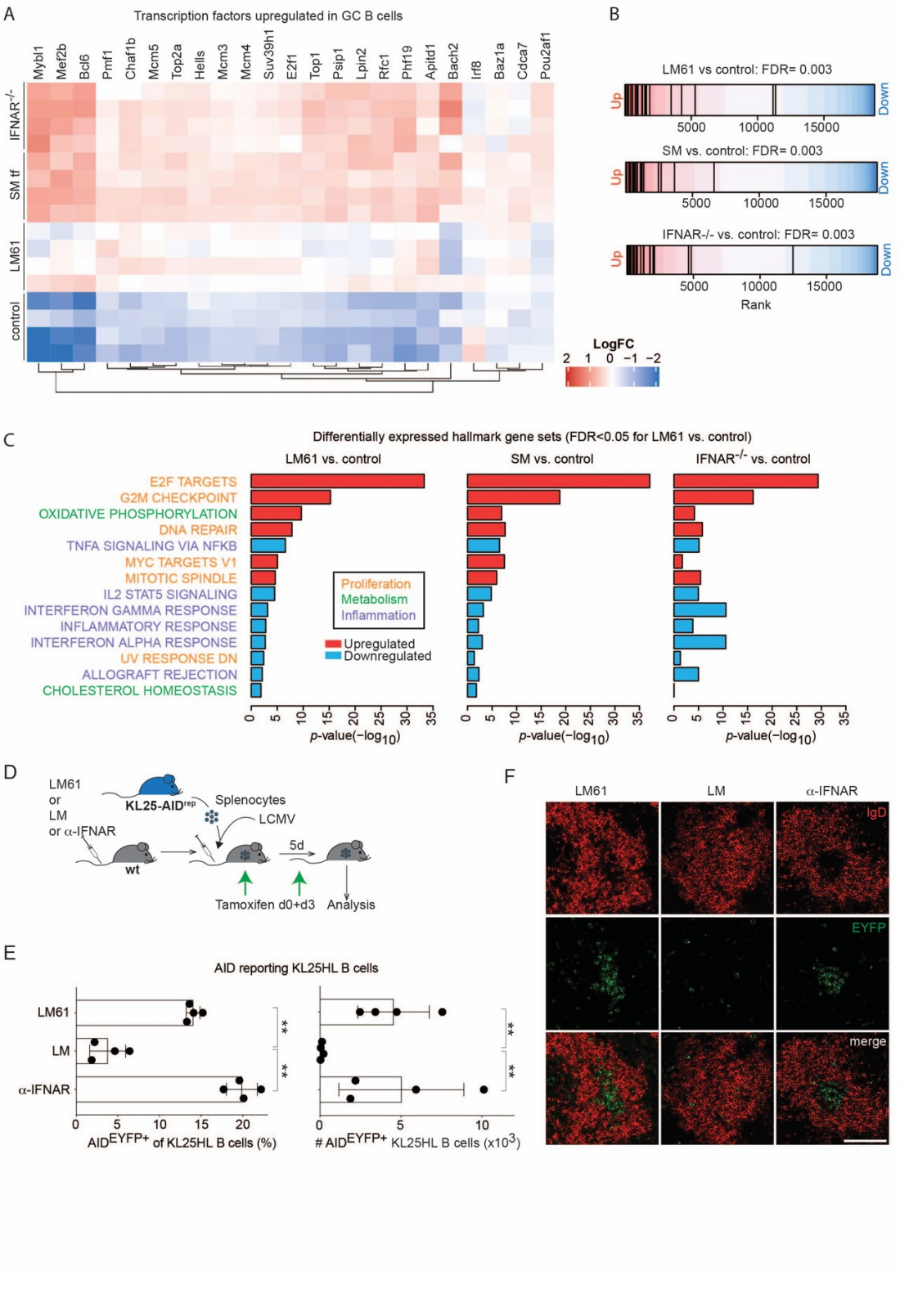
A
Transcription factors upregulated in GC B cells
Mybl1
Mef2b
Bcl6
Pmf1
Chaf1b
Mcm5
Top2a
Hells
Mcm3
Mcm4
Suv39h1
E2f1
Top1
Psip1
Lpin2
Rfc1
Phf19
Apitd1
Bach2
Irf8
Baz1a
Cdca7
Pou2af1
IFNAR-/-
SM tf
LM61
control
LogFC
2 1 0 −1 −2
B
LM61 vs control: FDR= 0.003
SM vs. control: FDR= 0.003
IFNAR-/- vs. control: FDR= 0.003
Up
Down
5000
10000
15000
Rank
C
Differentially expressed hallmark gene sets (FDR<0.05 for LM61 vs. control)
LM61 vs. control
SM vs. control
IFNAR-/- vs. control
E2F TARGETS
G2M CHECKPOINT
OXIDATIVE PHOSPHORYLATION
DNA REPAIR
TNFA SIGNALING VIA NFKB
MYC TARGETS V1
MITOTIC SPINDLE
IL2 STAT5 SIGNALING
INTERFERON GAMMA RESPONSE
INFLAMMATORY RESPONSE
INTERFERON ALPHA RESPONSE
UV RESPONSE DN
ALLOGRAFT REJECTION
CHOLESTEROL HOMEOSTASIS
Proliferation
Metabolism
Inflammation
Upregulated
Downregulated
p-value(−log10)
D
LM61
or
LM
or α-IFNAR
KL25-AIDrep
Splenocytes
LCMV
wt
5d
Tamoxifen d0+d3
Analysis
E
AID reporting KL25HL B cells
LM61
LM
α-IFNAR
**
AIDEYFP+ of KL25HL B cells (%)
AIDEYFP+ KL25HL B cells (x10^3)
F
LM61
LM
α-IFNAR
IgD
EYFP
merge

Figure 6. Pre-existing CD4 T help antagonizes inflammation and instructs a germinal center B cell program
A-C: Wt recipients were either pre-immunized with LM61 ("LM61") or LM ("control") on d-9 or were given SM CD4 T cells by adoptive transfer ("SM") on d-1. $IFNAR^{-/-}$ recipients were left untreated. KL25HL cell transfer and LCMV challenge were conducted on d0. On d4 KL25HL B cell progeny (CD45.1+B220+) were purified by FACS sorting (Fig. S5) and subject to RNAseq. Heatmap displaying expression levels of GC B cell transcription factors as determined by Shi et al. [55]. Pair-wise self-contained gene set testing for the same set of genes is shown in (B). Hallmark gene sets, which are significantly differentially expressed (FDR <0.05) in KL25HL B cells from LM61-preimmunized and LM-preimmunized control mice are displayed in (C). *P*-values obtained when assessing the same gene sets but comparing either SM vs. control or $IFNAR^{-/-}$ vs. control are also shown.
D-F: Schematic of the experimental design to (E,F). Recipients were pre-immunized with LM61 or LM on d9 or were given IFNAR-blocking antibody. On d0 KL25HL-AID^{rep} B cells were adoptively transferred simultaneously with LCMV challenge. Tamoxifen was administered on d0 and d3 and AID^{EYFP}-reporting KL25HL-AID^{rep} cells were determined on d5 in spleen (E) and are expressed as a percentage of all KL25HL-AID^{rep} cells and also in absolute numbers. Histological sections prepared at the same time point revealed clusters of AID^{EYFP}-reporting KL25HL-AID^{rep} cells in the splenic B cell zone (IgD) of LM61 pre-immunized and IFNAR-blocked mice but not in LM-pre-immunized controls. Magnification bar: 100 µm.
Symbols and bars represent means±SD, number of biological replicates *(n)*=4 (D-F). Number of independent experiments *(N)*=2 (D-F). Ordinary one-way ANOVA with Dunnett's post-test for multiple comparisons (E),**: $p<0.01$.

Figure 7

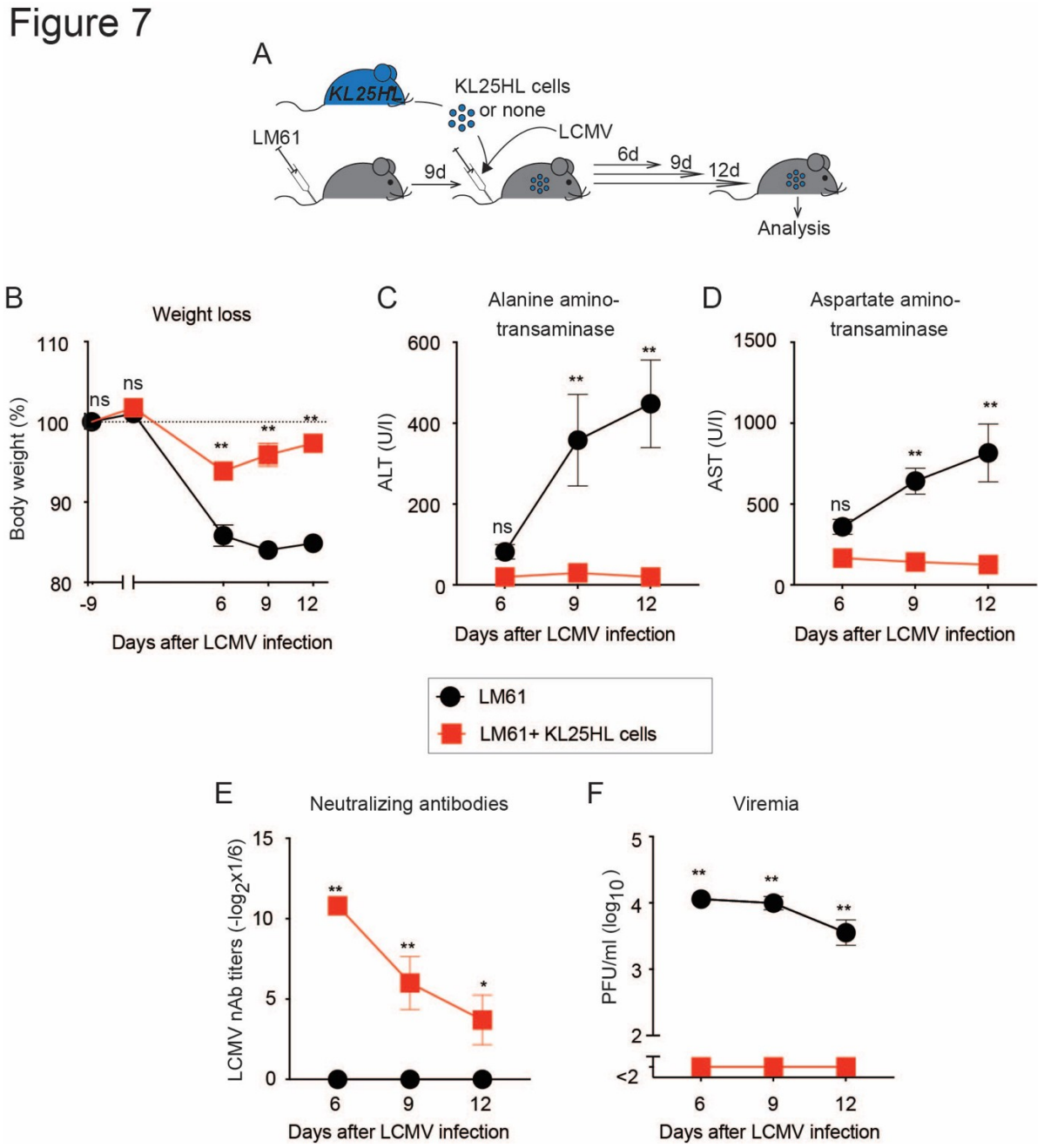
A
KL25HL
KL25HL cells
or none
LCMV
LM61
9d
6d
9d
12d
Analysis
B
Weight loss
Body weight (%)
110
100
90
80
ns
ns
**
**
**
-9
6
9
12
Days after LCMV infection
C
Alanine amino-transaminase
ALT (U/l)
600
400
200
0
ns
**
**
6
9
12
Days after LCMV infection
D
Aspartate amino-transaminase
AST (U/l)
1500
1000
500
0
ns
**
**
6
9
12
Days after LCMV infection
LM61
LM61+ KL25HL cells
E
Neutralizing antibodies
LCMV nAb titers (-log2x1/6)
15
10
5
0
**
**
*
6
9
12
Days after LCMV infection
F
Viremia
PFU/ml (log10)
5
4
3
2
<2
**
**
**
6
9
12
Days after LCMV infection

Figure 7. KL25HL B cells control viremia and prevent CD4 T cell-driven immunopathology upon chronic viral challenge

A: Schematic of the experimental design in (B-F). Two groups of mice were pre-immunized with LM61 on d-9 and on d0 were challenged with LCMV. One of these groups was given KL25HL B cells simultaneously with LCMV challenge. Body weight was monitored on the indicated time points to determine weight loss (B). Serum alanine aminotransaminase activity (C) serum aspartate aminotransaminase activity (D), LCMV-neutralizing antibody titers (E) and viremia (F) were determined on d6, d9 and d12.

Symbols represent means±SEM, number of biological replicates *(n)*=5 (B-F). Number of independent experiments *(N)*=3 (B-F). Two-way ANOVA with Bonferroni's post-test for multiple comparisons (B-F), ns: not significant*;* *: $p<0.05$;**: $p<0.01$.

Figure S1

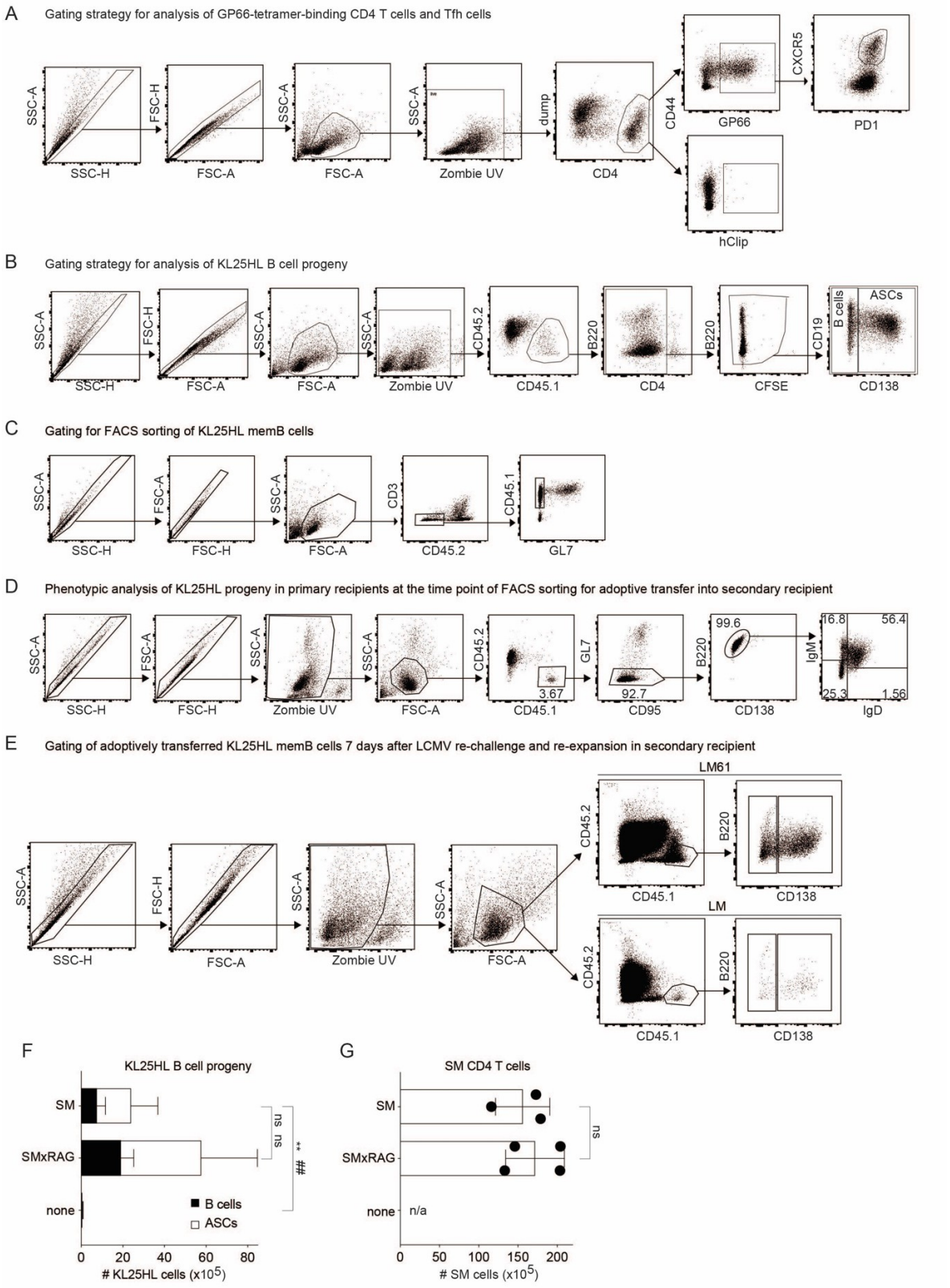
A
Gating strategy for analysis of GP66-tetramer-binding CD4 T cells and Tfh cells
SSC-A
SSC-H
FSC-H
FSC-A
SSC-A
FSC-A
SSC-A
Zombie UV
dump
CD4
CD44
GP66
CXCR5
PD1
hClip
B
Gating strategy for analysis of KL25HL B cell progeny
SSC-A
SSC-H
FSC-H
FSC-A
SSC-A
FSC-A
SSC-A
Zombie UV
CD45.2
CD45.1
B220
CD4
B220
CFSE
CD19
B cells
ASCs
CD138
C
Gating for FACS sorting of KL25HL memB cells
SSC-A
SSC-H
FSC-A
FSC-H
SSC-A
FSC-A
CD3
CD45.2
CD45.1
GL7
D
Phenotypic analysis of KL25HL progeny in primary recipients at the time point of FACS sorting for adoptive transfer into secondary recipient
SSC-A
SSC-H
FSC-A
FSC-H
SSC-A
Zombie UV
SSC-A
FSC-A
CD45.2
CD45.1
3.67
GL7
92.7
CD95
B220
99.6
CD138
IgM
16.8
56.4
25.3
1.56
IgD
E
Gating of adoptively transferred KL25HL memB cells 7 days after LCMV re-challenge and re-expansion in secondary recipient
LM61
SSC-A
SSC-H
FSC-H
FSC-A
SSC-A
Zombie UV
SSC-A
FSC-A
CD45.2
CD45.1
B220
CD138
LM
CD45.2
CD45.1
B220
CD138
F
KL25HL B cell progeny
SM
SMxRAG
none
B cells
ASCs
ns
ns
**
##
0
20
40
60
80
KL25HL cells (x10^5)
G
SM CD4 T cells
SM
SMxRAG
none
n/a
ns
0
50
100
150
200
SM cells (x10^5)

Figure S1: Flow cytometry gating strategies, KL25 memB cell FACS sorting and characterization, and prevention of B cell decimation by RAG-deficient SM cells

A: General gating strategy used throughout the study for the analysis and enumeration of polyclonal GP66-specific CD4 T cells by MHC class II tetramer staining. A dump gate exclusion contained B220, CD8, F4/80. A control sample was stained with an hClip peptide-loaded MHC class II tetramer serving as specificity control.

B: General gating strategy used throughout the study for the analysis and enumeration of adoptively transferred KL25HL cell progeny.

C: Gating strategy used throughout the study for sorting of KL25HL memB cells from primary recipients and subsequent re-transfer into secondary recipients.

D: Characterization of immunoglobulin isotype profile of adoptively transferred memB cells.

E: Gating strategy used throughout the study for gating of KL25HL memB cell progeny in LCMV-challenged secondary recipients.

F,G: SM CD4 T cells or RAG-deficient SM CD4 T cells (SMxRAG) were adoptively transferred to recipients one day prior to KL25HL cell transfer and LCMV challenge. Control mice were left without CD4 T cell transfer ("none"). KL25HL B cell progeny (F) and SM / SMxRAG CD4 T cells (G) were analyzed in spleen 5 days after LCMV challenge. Symbols and bars represent means±SD, number of biological replicates *(n)*=3-4 (F,G). Number of independent experiments *(N)*=2 (F-G). Two-way ANOVA with Dunnett's post-test for multiple comparison (F), unpaired two-tailed Students's *t* test (G), ns: not significant*;* **,##: $p<0.01$; when used next to each other, ** compares B cells and ## compares ASCs. n/a: not assessed

Figure S2

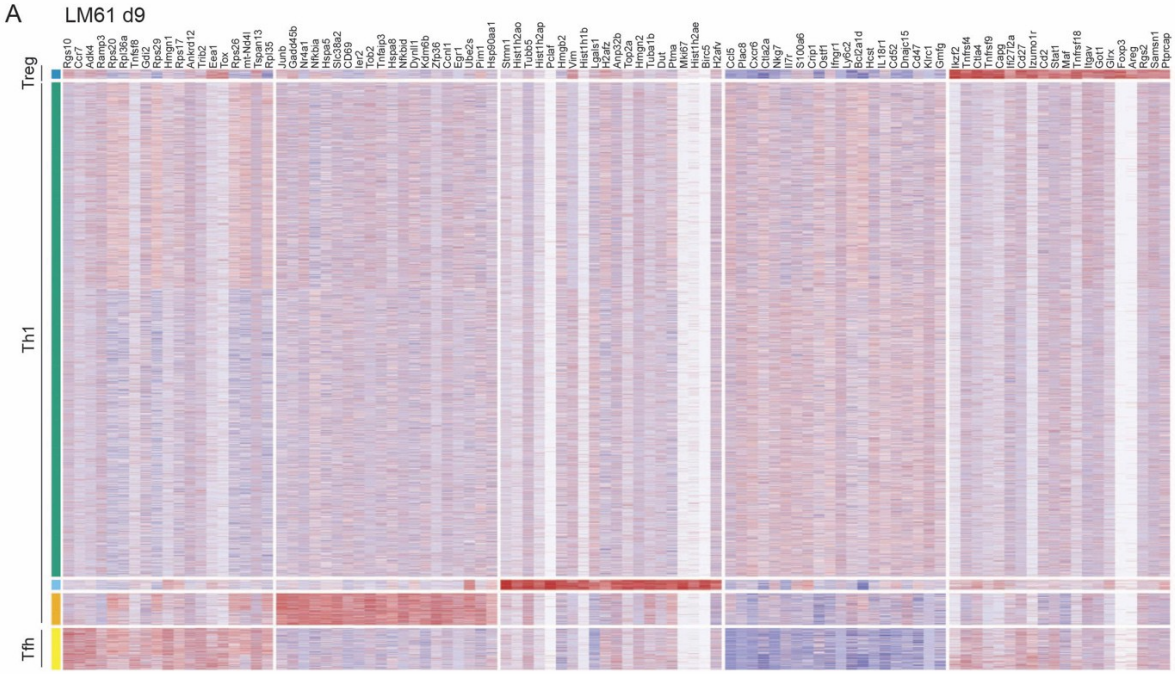

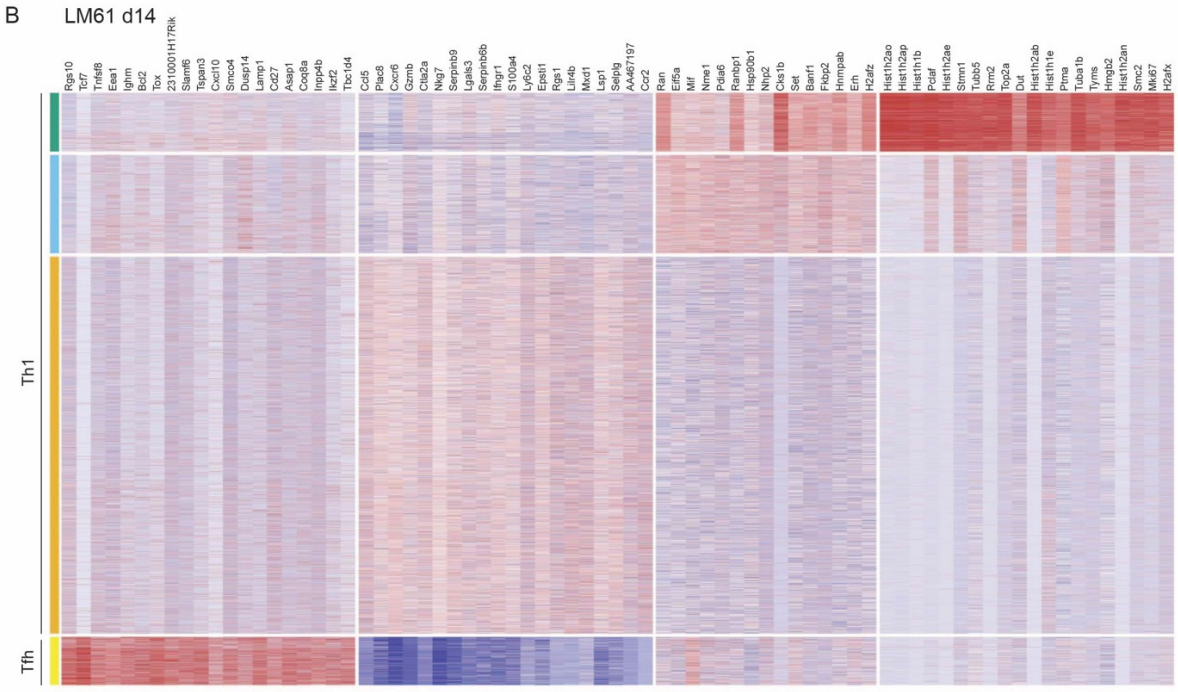

C

Gating strategy for the analysis of IL-21-reporting GP66-tetramer-binding Tfh and non-Tfh CD4 T cells in IL-21^{gfp} reporter mice

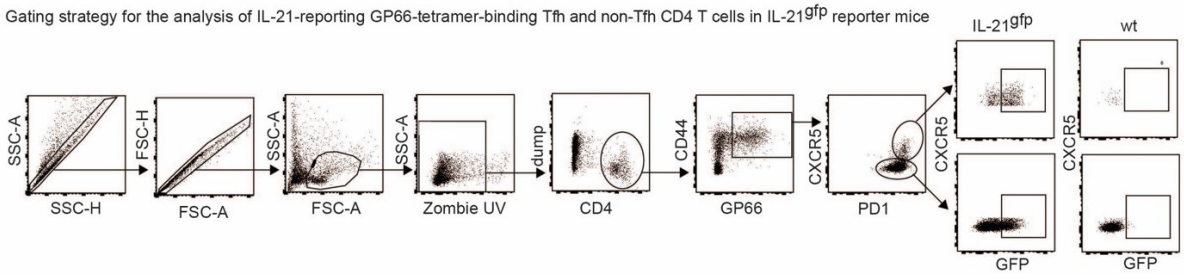

Figure S2: Single cell RNAseq analysis of GP66-specific CD4 T cell recall responses in LM61-preimmunized and LCMV challenged mice.
A,B: Mice were pre-immunized with LM61, followed by KL25HL cell transfer and LCMV challenge as outlined in Fig. 2A (same data set as in Fig. 2B-I). GP66-specific CD4 T cells were isolated on d9 (prior to LCMV challenge; A) and on d14 (5 days after LCMV challenge; B). The expression of the indicated genes is displayed for 14'459 cells collected on d9 (A) and for 13'478 cells collected on d14 (B), with each row corresponding to an individual cell. Cells are vertically clustered as detailed in Fig. 2B-I (one cluster of Tfh-differentiated cells, three subclusters of Th1-differentiated cells and a minor population of Treg-like cells found only on d9).
C: Gating strategy for the analysis and enumeration of IL-21^{gfp} reporting, polyclonal GP66-specific CD4 T cells, either Tfh (CXCR5^{+}) or non-Tfh (CXCR5^{-}), by MHC class II tetramer staining. IL-21^{gfp} reporter mice were compared to non-reporting littermate controls (wt). A dump gate exclusion contained B220, CD8, F4/80.

Figure S3

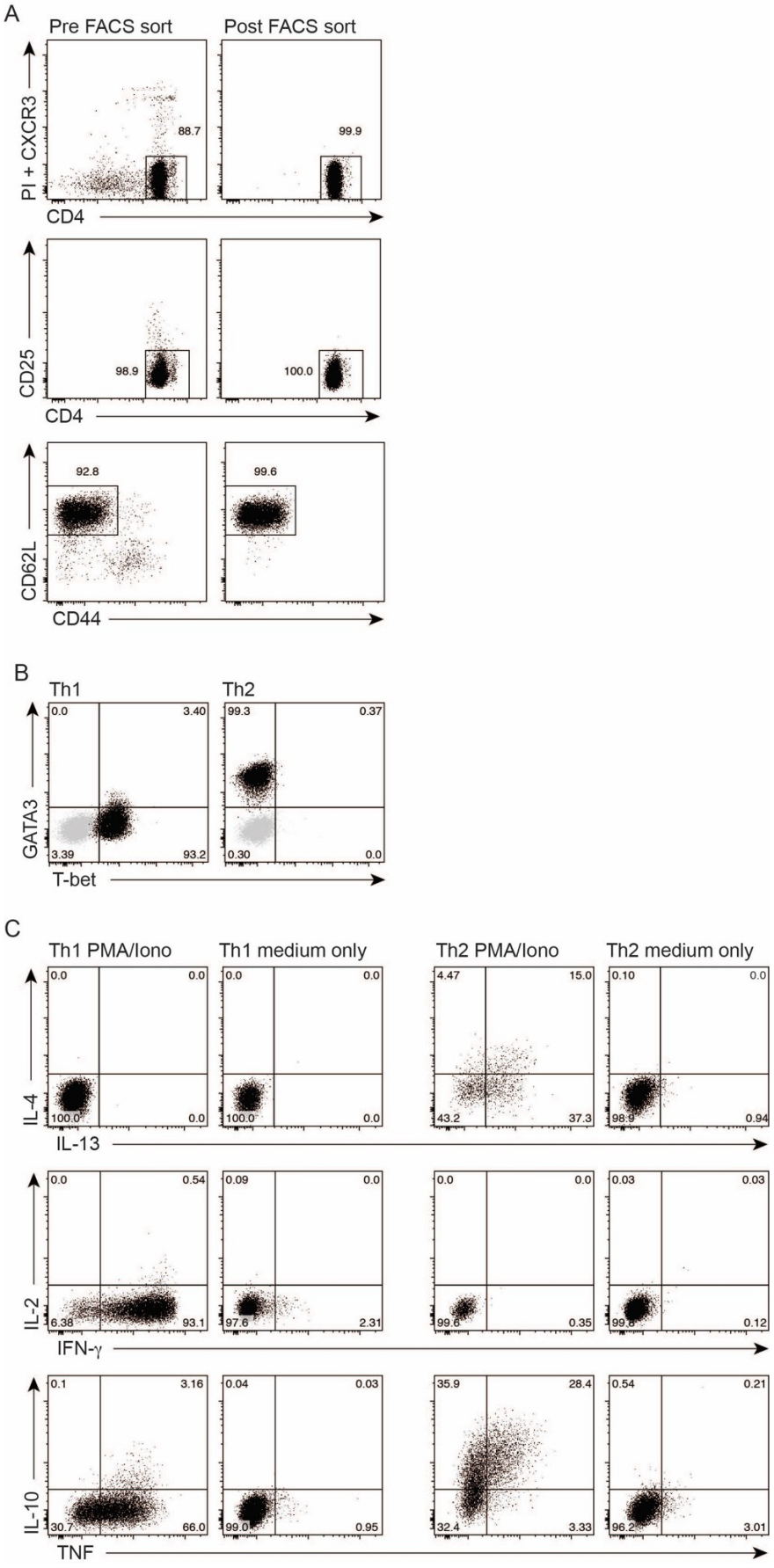
A
Pre FACS sort
Post FACS sort
PI + CXCR3
CD4
88.7
99.9
CD25
CD4
98.9
100.0
CD62L
CD44
92.8
99.6
B
Th1
Th2
GATA3
T-bet
0.0
3.40
3.39
93.2
99.3
0.37
0.30
0.0
C
Th1 PMA/Iono
Th1 medium only
Th2 PMA/Iono
Th2 medium only
IL-4
IL-13
IL-2
IFN-γ
IL-10
TNF
0.0
0.0
100.0
0.0
0.0
0.54
6.38
93.1
0.09
0.0
97.6
2.31
0.1
3.16
30.7
66.0
0.04
0.03
99.0
0.95
4.47
15.0
43.2
37.3
0.0
0.0
99.6
0.35
35.9
28.4
32.4
3.33
0.10
0.0
98.9
0.94
0.03
0.03
99.6
0.12
0.54
0.21
96.2
3.01

Figure S3: Characterization of SM cells prior to and after *in vitro* Th1/Th2 differentiation
A: Naïve $PI^{-}CXCR3^{-}CD25^{-}CD44^{-}CD62L^{+}CD4^{+}$ SM cells were FACS-sorted from the spleen of SM TCR-transgenic donor mice. Representative quality control stains of pre-sort and post-sort SM cells are shown.
B: Representative transcription factor expression profiles of differentiated Th1 and Th2 cells at day 10 of *in vitro* culture under Th1- or Th2- polarizing conditions, respectively. Isotype control stains are depicted in grey.
C: Representative cytokine production profiles of differentiated Th1 and Th2 cells at day 10 of *in vitro* culture under Th1- or Th2- polarizing conditions, respectively, upon stimulation with either PMA/ionomycin or medium control, as indicated.

Figure S4

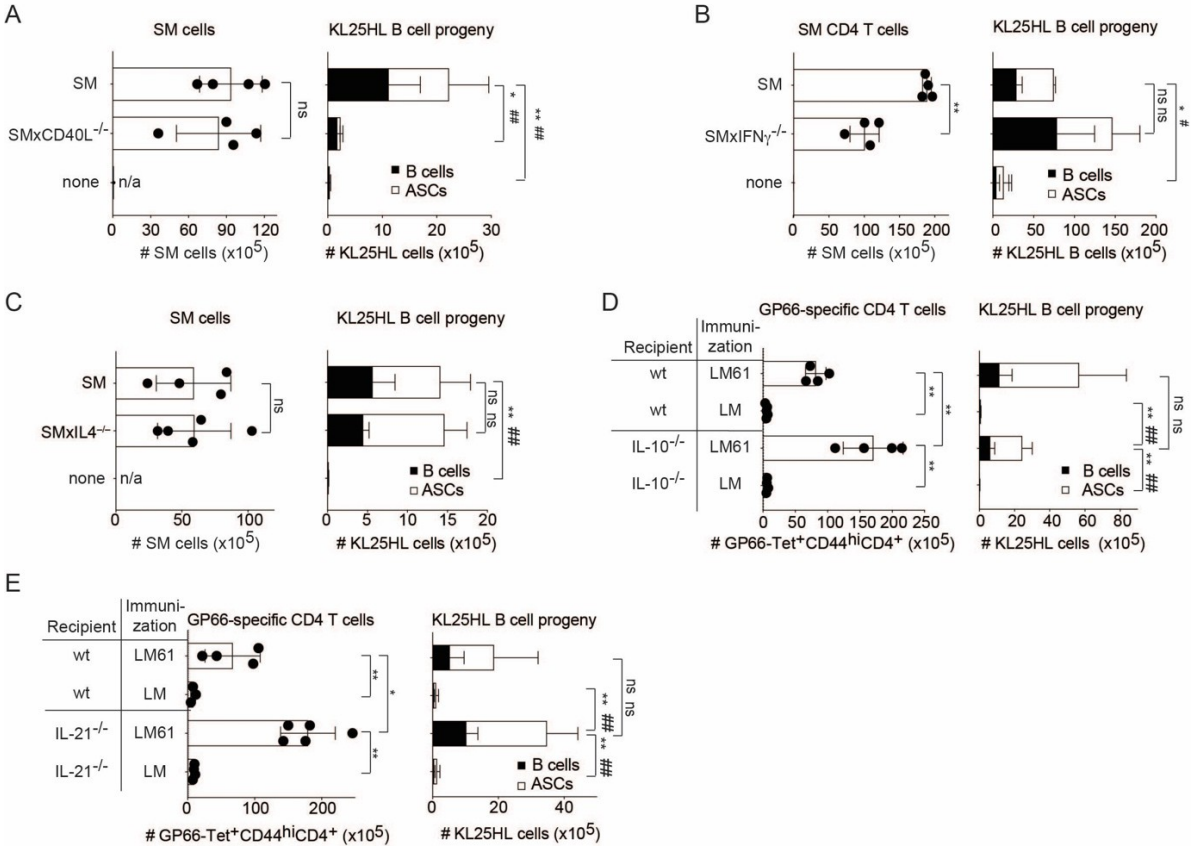
A
SM cells
KL25HL B cell progeny
SM
SMxCD40L-/-
none
n/a
ns
* ## ** ##
B cells
ASCs
SM cells (x10^5)
KL25HL cells (x10^5)
B
SM CD4 T cells
KL25HL B cell progeny
SM
SMxIFNγ-/-
none
**
ns ns
* #
B cells
ASCs
SM cells (x10^5)
KL25HL B cells (x10^5)
C
SM cells
KL25HL B cell progeny
SM
SMxIL4-/-
none
n/a
ns
ns ns
** ##
B cells
ASCs
SM cells (x10^5)
KL25HL cells (x10^5)
D
GP66-specific CD4 T cells
KL25HL B cell progeny
Recipient
Immuni-zation
wt
LM61
wt
LM
IL-10-/-
LM61
IL-10-/-
LM
** **
** **
ns ns
** ##
** ##
B cells
ASCs
GP66-Tet+CD44hiCD4+ (x10^5)
KL25HL cells (x10^5)
E
Recipient
Immuni-zation
GP66-specific CD4 T cells
KL25HL B cell progeny
wt
LM61
wt
LM
IL-21-/-
LM61
IL-21-/-
LM
** *
**
ns ns
** ##
** ##
B cells
ASCs
GP66-Tet+CD44hiCD4+ (x10^5)
KL25HL cells (x10^5)

Figure S4: Prevention of B cell decimation depends on CD4 T cell-intrinsic CD40L but not on IFN-y or IL-4 and works in the absence of IL-10 or IL-21.

A-C: SM CD4 T cells (SM), CD40L-deficient SM cells (SMxCD40L$^{-/-}$), IFN-y-deficient SM cells (SMx IFN-y$^{-/-}$) and IL-4-deficient SM cells (SMxIL4$^{-/-}$) were adoptively transferred to recipients one day prior to KL25HL cell transfer and LCMV challenge. Control groups were left without CD4 T cell transfer ("none"). The progeny of adoptively transferred SM cells and the respective knockout versions thereof (SM CD4 T cells) as well as KL25HL B cell progeny were enumerated in spleen five days after LCMV challenge.

D,E: Wt, IL-10$^{-/-}$ and IL-21$^{-/-}$ mice were pre-immunized with LM61 on d-9. On d0 they were given KL25HL cells by adoptive transfer simultaneously with LCMV challenge. GP66-Tet-binding CD4 T cells and KL25HL B cell progeny were enumerated in spleen on d5. Symbols and bars represent means±SD, number of biological replicates *(n)*=4 (A-B), n=4-5 (C-D), *n*=3-5 (E). Number of independent experiments *(N)*=2 (A-B,E), *N*=1 (C-D). Unpaired two-tailed Students's *t* test (A-C).Two-way ANOVA with Dunnett's post-test for multiple comparison (A-E), ordinary one-way ANOVA with Tukey's post-test for multiple comparisons (D-E), ns: not significant*;* *,#: $p<0.05$**,##: $p<0.01$; when used next to each other, ** compares B cells and ## compares ASCs. The SM and "none" control groups in (C) are the same as the ones shown in Fig. 3I-M.

Figure S5

Gating for FACS sorting of KL25HL B cells to be processed for bulk RNAseq

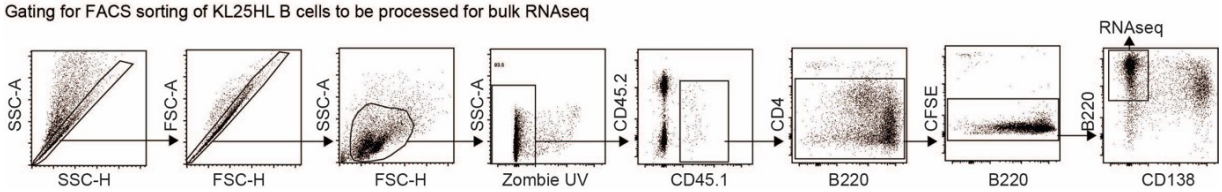

Figure S5: Gating strategy for FACS sorting of B cells in the experiment to Fig. 5A-C
Recipients were pre-immunized on d-9 as outlined for Fig. 5A-C. KL25HL cell transfer and LCMV challenge were conducted on d0. On d4 KL25HL B cell progeny (CD45.1+B220+) were purified by FACS sorting following the gating strategy as displayed.

Figure S6

A

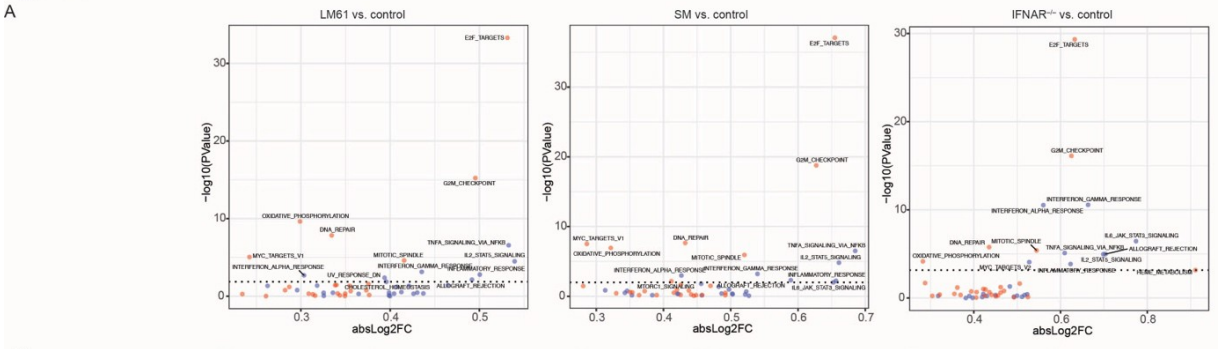

B

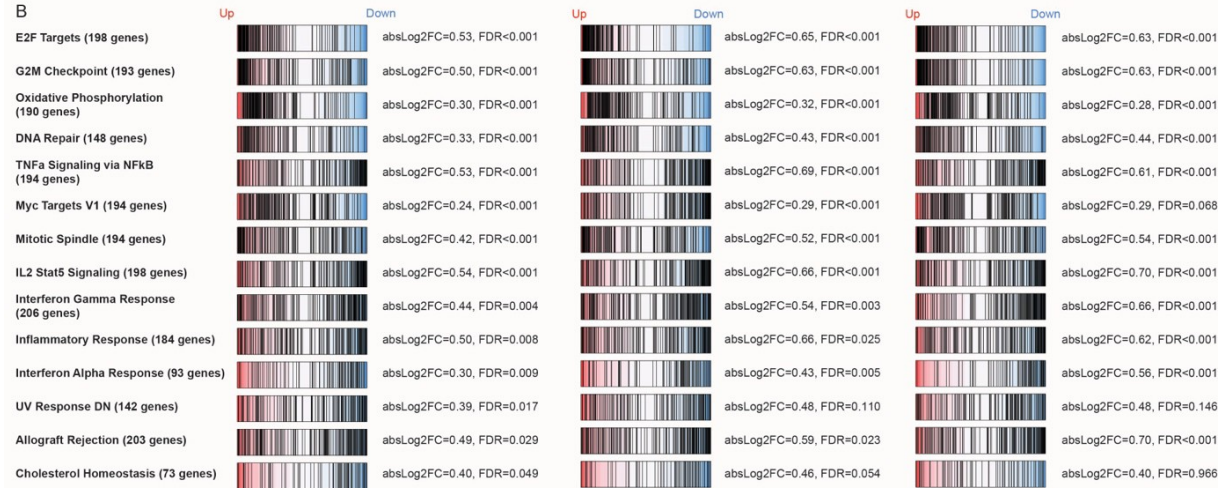

Figure S6: Hallmark gene sets differentially expressed in KL25HL cells responding to LCMV in the presence of pre-existing T help or in the absence of interferon-driven inflammation
A: Volcano plot display of the hallmark gene set analyses shown in Fig. 5C.
B: Pair-wise self-contained gene set testing for the indicated set of genes.

Vectored antibody gene delivery restores host B and T cell control of persistent viral infection

Yusuf I. Ertuna[1], Benedict Fallet[1], Anna F. Marx[1], Mirela Dimitrova[1] and Daniel D. Pinschewer[1]*

Affiliations
[1] University of Basel, Department of Biomedicine – Haus Petersplatz, Division of Experimental Virology, 4009 Basel, Switzerland.

* Corresponding author:
Daniel D. Pinschewer, M.D.
Department of Biomedicine – Haus Petersplatz, Division of Experimental Virology, University of Basel,
4009 Basel, Switzerland.
Email: Daniel.Pinschewer@unibas.ch
Phone: +41 79 543 39 70

Abstract

Passive antibody therapy and vectored antibody gene delivery (VAGD) in particular offer an innovative approach to combat persistent viral diseases. Here we exploited a small animal model to investigate synergies of VAGD with the host's endogenous immune defense for treating chronic viral infection.

An adeno-associated viral (AAV) vector delivering the lymphocytic choriomeningitis virus (LCMV)-neutralizing antibody KL25 (AAV-KL25) established protective antibody titers for >200 days. When therapeutically administered to chronically infected immunocompetent wildtype mice, AAV-KL25 afforded sustained viral load control. In contrast, viral mutational escape thwarted therapeutic AAV-KL25 effects when mice were unable to mount LCMV-specific antibody responses or lacked $CD8^+$ T cells. VAGD therapy reduced inhibitory receptor expression levels on antiviral $CD8^+$ T cells and augmented antiviral germinal center B cell and antibody-secreting cell responses.

These results indicate VAGD augments and synergizes with host B cell and CD8 T cell responses to restore immune control of chronic viral infection.

One sentence summary

Vectored antibody gene delivery augments germinal center reactions and reverts T cell exhaustion to restore host immune control of a persisting virus.

Introduction

Several decades after von Behring and Kitasato's first description of passive antibody therapy [412], the advent of monoclonal antibody (mAb) technology [413] and recombinant antibody engineering [414] paved the way to the revolutionary role antibodies play in modern medicine. Considerable potential for antibody-based therapies looms also in the context of persistent viral diseases such as HIV, where the identification of broadly HIV-neutralizing antibodies (bnAbs [415, 416]) has opened up new horizons in the long-standing quest for a functional cure [417]. When administered to SHIV-infected non-human primates (NHPs) early after infection, viral loads were suppressed for prolonged periods of time [418-421]. Human trials co-administering two or more bnAbs to target different viral epitopes have demonstrated that HIV load suppression can be sustained for more than 30 weeks [422]. Such a functional cure would, however, require life-long, continually repeated infusions of bnAbs to sustain critical antibody concentrations. Costs of goods and logistics of re-administration therefore pose a significant challenge for long-term use at the global scale. Somatic antibody gene therapy based on adenovirus-associated viral (AAV) vector delivery may offer an elegant solution to this challenge [423], although further refinement is needed before widespread human use can be envisaged [424-426]. When used prophylactically in animal models, AAV-vectored antibody gene delivery (VAGD) has demonstrated efficacy against a vast range of microbes including HIV, Hepatitis C (HCV), influenza, Ebola and malaria parasites [427-433]. In a therapeutic setting, VAGD cleared HCV infection from immunodeficient mice with a human liver graft [430]. Sustained therapeutic effects of AAV-delivered bnAbs on viral loads were also observed in HIV-infected humanized mice [434] and more recently in a chronically SHIV-infected macaque that suppressed SHIV loads for at least three years after VAGD [435].

Mutational viral escape even from bnAbs is commonly observed in persistent viral infections of mice, monkeys and man, posing a formidable challenge to antibody therapy [189, 434, 436, 437]. Observations from animal studies suggest, however, that the host immune response contributes to virus control in the context of passive antibody therapy and has potential to prevent mutational viral escape [419, 435, 436]. CD8 T cells were essential to viral load control in long-term bnAb-treated NHPs [419, 438]. Similarly, the host's endogenous antibody response can exhibit neutralizing activity against bnAb escape variants and may contribute to viral load suppression [436]. Besides synergistic antiviral effects, passive antiviral antibody administration can improve the host's antibody response to persisting viruses [439-442]. Moreover, studies on CD8 and CD4 T cell responses to HIV and SHIV infection, respectively, suggest the immune enhancing effect of passive antibody therapy comprises both arms of adaptive immune defense [443, 444].

The lack of a suitable immunocompetent small animal model for HIV or HCV research has, however, precluded a systemic and comprehensive mechanistic assessment of the several axes of potential synergy between VAGD and the host's adaptive immune response in the context of chronic viremia. Specifically, a potential impact of passive antibody delivery on the host's germinal center B cell response remains to be investigated.

Chronic infection of mice with lymphocytic choriomeningitis virus (LCMV) is widely studied as a model to decipher basic principles of virus – host interactions in persistent viral infection. Over the past decades LCMV research has contributed several important and widely validated concepts of antiviral immunity and immune evasion by persisting viral pathogens. Prominent examples comprise T cell-mediated control of viral infection [445] viral mutational escape from T cell selection pressure [302], T cell exhaustion as a consequence of chronic viral antigen exposure [94, 446-448] and its restoration by immune checkpoint inhibitors [449]. Additional commonalities of the LCMV model with human HIV and HCV infection consist in weak and delayed neutralizing antibody formation as a consequence of the viral envelope protein's glycan shield on the outer globular domain of its envelope glycoprotein (GP-1) [192, 195] and the virus' rapid mutational escape from antibody selection pressure [437].

Here we establish an experimental setting in which chronic LCMV infection of mice can be treated by means of an AAV vector (AAV-KL25) delivering one of the most potent LCMV-neutralizing antibodies (KL25). Combining this tool with genetically engineered mouse strains and cell subset depletion we systematically dissect how CD8 T cells and antiviral B cells contribute to AAV-KL25-mediated control of chronic infection and prevent viral mutational escape. Additionally, our study reveals distinct effects of VAGD on CD8 T cell exhaustion, CD4 Tfh responses and, intriguingly, we document that VAGD improves antiviral germinal center B cell and antibody-secreting cell responses.

Materials and Methods

Mice and animal experimentation

C57BL/6 wild-type (from Charles River Laboratories), T11μMT [450], $K^bD^{b-/-}$ [451] and MD4 mice [452] were bred at the Laboratory Animal Services Center of the University of Zurich. Animals were housed under specific-pathogen-free (SPF) conditions throughout. All experiments were conducted at the University of Basel in accordance with the Swiss law for animal protection and with authorization from the Cantonal veterinary office.

Viruses, cells, focus formation assay, plaque reduction neutralization test and TaqMan RT-PCR

The reverse engineered LCMV strain Clone 13 virus expressing the LCMV-WE glycoprotein (rCl13) has been described previously [195, 365]. rCl13 stocks were produced on BHK-21 cells (ECACC). The LCMV strain Docile [453] was propagated on MDCK cells (ATCC). Titers of viral stocks and infectivity in mouse blood and tissue samples were determined by focus forming assays on 3T3 cells (ATCC) and LCMV nAb titers were determined by plaque reduction neutralization tests as described previously [367]. Mice were infected with a dose of $2\text{-}3x10^6$ plaque forming units (PFU) intravenously (i.v.) into the tail vein. For a quantitative assessment of LCMV Docile RNA in liver tissue we performed TaqMan RT-PCR using the nucleoprotein sequence-binding primers 5'-AGTTTGTCTTTCAGGTGAGGG-3' and 5'-GGGTGAGTTAGCTACAGGTTTC-3' with the probe 5'-FAM-ATTGTGGGAAGGGCATGGGAGAA-3'-BHQ-1 (Microsynth AG, Switzerland).

Production of AAV-KL25 and its administration to mice

The AAV-KL25 genome is based on AAV2 inverted terminal repeats (ITR) flanking a chicken beta-actin-driven expression cassette (pENN.AAV.CB7.CI) obtained from the PENN Vector Core (Perelman School of Medicine, University of Pennsylvania, PA, USA). Into this expression cassette we inserted a construct allowing for the monocystronic expression of the KL25 antibody (synthesized by Genscript). It contains in sequential order the KL25 heavy chain cDNA [155], a furin recognition site (R-K-R-R), a spacer (S-G-S-G), the foot-and-mouth-disease virus 2A peptide (F2A) for autocatalytic cleavage and the KL25 light chain cDNA. Recombinant AAV particles with an AAV8 capsid were produced and genome copy (GC) titer were assessed by a droplet digital (dd) PCR-based method at the PENN Vector Core [454]. rAAV particles were administered intramuscularly (i.m.) into the thigh of mice at a dose of $1x10^{11}$ GC in PBS. Control mice were administered PBS i.m or were left untreated.

Flow cytometry

Single cell suspensions were obtained by pushing spleens through a metal mesh using a syringe plunger. Mouse osmolarity-adjusted media were used throughout [371]. Staining of blood and spleen samples was performed in PBS containing 2% FCS, 5mM ethylenediaminetetraacetic acid (EDTA) and 0.05% sodium azide (staining buffer). For staining of spleen cell subsets, the following antibodies and clones were used: F4/80 (BM8), CD4 (RM4-5), CD107a (1D4B), TNF-α (MP6-XT22), IFN-γ (XMG1.2), CD38 (90), GL7 (GL7), IgD (11-26c.2a), CD138 (281-2), CD8α (53-6.7), CD4 (RM4-5), CD45R/B220 (RA3-6B2), CD244.2 (2B4; m2B4 (B6) 458.1), CD279 (PD1, 29F.1A12), CXCR5 (CD185, L138D7) from BioLegend (CA, USA) or against anti-IgM (II/41), CD223 (LAG-3, C9B7W) from eBioscience (CA, USA). Antibodies against CD44 (IM7), CD366 (TIM-3, 5D12/TIM-3) were purchased from Becton Dickinson (BD) Biosciences (NJ, USA). The Zombie UV™ Fixable viability kit (BioLegend) was used to exclude dead cells as described in the manufacturer`s protocol. $CD8^+$ and $CD4^+$ T cells specific for the LCMV epitopes $GP_{33\text{-}41}$ and $GP_{66\text{-}77}$ were identified by H-$2D^b$ and I-A^b tetramers, respectively, $hCLIP_{87\text{-}101}$ epitope-loaded I-A^b tetramers were used as specificity control (generously provided by the NIH tetramer core, Emory University Vaccine Center, GA, USA). For the detection of NP-specific B cells, cells were stained with bacterially expressed fluorochrome-conjugated recombinant LCMV nucleoprotein (rNP) [195] as previously described [200, 455].
For intracellular cytokine staining of CD4 and CD8 T cells, spleen cell suspensions were incubated with anti-CD107a antibody (LAMP-1), and restimulated with the LCMV-GP derived $GP_{64\text{-}79}$ and $GP_{33\text{-}41}$ peptides (1 μg/ml) for 5 hours at 37°C in a 5% CO_2 incubator. Brefeldin A (5 μg/ml) was added to the cells 1 hour after the addition of peptide, followed by additional 4 hours of incubation. After the full 5-hour stimulation period, the cells were fixed with 2% PFA for 5 min. Fixation was followed by permeabilization using staining buffer supplemented with 0.05% saponin (Sigma-Merck, Germany). Stained cells were measured on a BD LSRFortessa™ (BD Biosciences) flow cytometer and data were analyzed using FlowJo software (FlowJo LLC, version 10.5.3).

In vivo cell subset depletion

Mouse anti mouse-CD8α/Lyt-2 (YTS 169.4) (Absolute Antibody, MA, USA) was administered at a dose of 200µg/ml intraperitoneally (i.p.) to mice on days -3, -1 and day 0, and biweekly thereafter until analysis on day 50. Mouse IgG2a anti-fluorescein antibody (4-4-20e) (Absolute Antibody) was administered as isotype control CD4-depletion antibody (YTS 191) (BioXCell) at a dose of 200 µg was administered i.p. 3 days and 1 day prior to infection.

Enzyme-linked immunosorbent assay (ELISA)

LCMV GP-1-specific antibodies were measured by enzyme-linked immunosorbent assay (ELISA) using a recombinant fusion protein consisting of the outer globular GP-1 domain of the LCMV-WE glycoprotein fused to the human IgG constant domain (GP1-Fc) [374]. The analogous construct for the Docile GP-1 sequence was generated by cDNA synthesis (GenScript) and was subject to site-directed mutagenesis to generate expression plasmids for the GP-1^{N119Y} and GP-1^{N119S} variants. IgG1 and IgG2c isotype-specific ELISAs were conducted to differentiate AAV-delivered and endogenous antibody responses, respectively. To perform isotype specific ELISAs, 96-well high-binding plates were coated with anti-human Fc-specific antibody (JacksonImmunoResearch Europe Ltd, UK) in coating buffer (15 mM Na_2CO_3 35mM $NaHCO_3$ dissolved in ddH_20, pH: 9.6) and incubated overnight at 4°C. The following day, the coating solution was flicked off and the plate was incubated with blocking buffer (5% milk powder PBS-Tween-20 (5%) (PBS-T) (Merk, Germany) at RT for 2 hours. Then, the blocking buffer was flicked off and the respective glycoproteins (GP1^{N119S}-Fc or GP1^{N119Y}-Fc) were diluted in blocking buffer and added to the plates, followed by incubation at RT for 1 hour. Plates were washed 3X with PBS-T. Then, mouse sera were serially diluted and transferred to coated and blocked plates, followed 1 hours of incubation at RT. Then the plates were washed 3X with PBS-T. HRP-conjugated anti-IgG2c (Bethyl Laboratories, TX, USA) or HRP-conjugated anti-IgG1 (ThermoFischer) antibodies were diluted in blocking buffer and were added to the plates for detection of bound serum antibodies. The plates were washed 3X with PBS-T and once with PBS. The color reaction solution was prepared by mixing 2.8 ml 0.1 M citric acid (Sigma Aldrich), 2.2 ml of 0.2 M Na_2HPO_4 (Sigma Aldrich), 5ml of ddH_20, 10µl H_20_2 and 10mg ABTS (2,2'-Azino-bis(3-ethylbenzothiazoline-6-sulfonic acid) diammonium salt, Sigma Aldrich). It was added to the wells and 15 minutes later absorbance was measured on an ELISA reader (Safire II™, Tecan Group Ltd, Switzerland). Naïve serum was used to determine technical backgrounds.

Enzyme-linked immunospot (ELISpot) assay

ELISpot assays were used to quantify the NP-specific antibody secreting cells (ASCs) in the bone marrow and in spleens of mice as described [455]. In brief, single cell suspensions of bone marrow (BM) and splenocytes were prepared. Erythrocytes were lysed and 96-well Multiscreen assay plates (Millipore, Merck) were activated with 35% EtOH. Plates were coated with rNP (3µg/ml) by overnight incubation. Plates were blocked with medium and 2 hours later the cells were plated with 10^6 cells/well followed by 3-fold dilutions. Horseradish peroxidase labeled rabbit-anti mouse Fcγ-specific antibody was used as detection antibody. As substrate, the 3-amino-9-ethylcarbazole substrate kit was used (BD Biosciences). Spots were counted on an ImmunoSpot reader (C.T.L. Europe GmbH, Germany).

Viral RNA isolation, cDNA synthesis and sequencing

For viral RNA isolation and sequencing, BHK-21 cells were infected with the viremic serum of infected mice and virus-containing supernatant was harvested 48 hours later. Viral RNA was extracted using the QIAamp Viral RNA Mini Kit (QIAGEN) in accordance with the manufacturer`s protocol. cDNA synthesis and PCR amplification of the complete LCMV-Docile GP coding region was performed using the OneStep RT-PCR kit (QIAGEN) according to the manufacturer`s protocol. An additional round of PCR amplification was performed using the Phusion High-Fidelity DNA Polymerase (New England Biolabs). The amplicons were run on a 1.5% agarose gel, were excised and then were purified using the QIAquick Gel Extraction Kit (QIAGEN) for direct Sanger sequencing (Microsynth AG, Switzerland). The primers used for amplification and sequencing were 5'-GCTGGCTTGTCACTAATGGCTC-3' and 5'-TCAGCGTCTTTTCCAGATAG-3'.

Data and statistical analysis

In order to compare a single parameter between two experimental groups, we have performed unpaired two-tailed Student`s t test. To compare a single parameter between multiple groups, one-way analysis of variance (ANOVA) was performed. To compare antibody responses between groups over time we have used two-way ANOVA. Statistical tests were performed using Prism 8 for MacOS (version 8.1.1 (224)). ELISA titers were calculated using Gen5^{TM} (BioTek^{TM}) software and were log-converted in order to reach a near-normal distribution for statistical analysis. *P* values <0.05 were considered statistically significant (*), *P* values <0.01 highly significant (**). FlowJo software (FlowJo LLC, version 10.5.3) was used for the analysis of the flow cytometry data.

Results

VAGD affords long-term protection and curbs viremia when administered early after viral challenge

For our studies on VAGD in LCMV infection we constructed an AAV vector carrying a chicken beta actin promoter-driven cassette for monocistronic expression of the heavy and light chain genes of the LCMV-neutralizing GP-1-specific mAb KL25 (AAV-KL25, Fig. 1A). Upon intramuscular administration to mice, KL25 was detectable in serum by day 4 (Fig. 1B,C). Peak titers were reached within about two weeks and persisted at stable levels for more than 200 days. Accordingly, mouse serum collected on day 243 after AAV-KL25 administration potently neutralized LCMV in cell culture (Fig. 1D). On day 245 we challenged these animals and control mice devoid of AAV-KL25 prophylaxis with LCMV. A genetically engineered LCMV Clone 13 was used, which expresses the glycoprotein (GP) of the KL25-sensitive WE strain (rCl13) [195, 365]. Viremia was high on day 5 after challenge of control mice but was significantly suppressed by AAV-KL25 prophylaxis given 250 days earlier (Fig. 1E). This indicated that AAV-KL25 afforded long-term protection against LCMV challenge.

Next, we infected mice with rCl13 and 4 days later administered either AAV-KL25 or control (PBS) to test whether vectored antibody gene delivery would curtail LCMV infection in a therapeutic fashion (Fig. 1F,G). By day 11 of the experiment (seven days after AAV-KL25 administration) rCl13 loads were significantly suppressed and viremia subsided earlier than in control-treated mice. In infected mice without AAV-KL25 administration, GP-1 binding IgG titers remained close to technical background throughout the observation period and rCl13-nAbs were undetectable on day 31 (Fig. 1H,I). In contrast, GP1-binding antibodies were readily detected in AAV-KL25-treated mice from day 22 onwards, and sera collected on day 31 neutralized rCl13. Of note, however, GP-1-binding antibodies and nAb titers in AAV-KL25-treated rCl13-infected mice were lower than in a control group of mice receiving AAV-KL25 in the absence of rCl13 infection. This observation suggested that LCMV antigen "consumed" some of the AAV-delivered antiviral antibody, supposedly by immune complex formation. Irrespective thereof, this set of experiments demonstrated the utility of AAV-KL25 for curbing LCMV infection.

Therapeutic VAGD synergizes with host antibody responses for sustained suppression of chronic infection

rCl13 persists in the blood of adult C57BL/6 (WT) mice for only about 30 days (compare Fig. 1G). To investigate a potential impact of AAV-KL25 when administered around three weeks after infection, i.e. in the chronic phase of infection when T cell exhaustion is established [94, 447-449, 456, 457] we used the KL25-sensitive but more invasive Docile variant of LCMV-WE (DOC [458]). We administered AAV-KL25 on day 19 after DOC infection of WT mice, resulting in significantly suppressed viremia from day 41 onwards (Fig. 2A,B). When the experiment was terminated on day 82, splenic viral titers of AAV-KL25-treated mice were below the detection limit whereas high levels of virus persisted in PBS-treated control mice (Fig. 2C). These effects of AAV-KL25 on systemic viral loads were further corroborated by TaqMan RT-PCR measurements from liver tissue of mice (Fig. S1A). From day 41 onwards AAV-KL25-derived GP-1-specific IgG was clearly detectable in serum (Fig. 2D), which timewise coincided with virus control. This sustained antiviral effect of AAV-KL25 was somewhat unexpected in light of earlier observations on rapid viral mutational escape from KL25 in life-long LCMV carrier mice [437]. Hence, we hypothesized that the host's endogenous antibody and/or CD8 T cell response synergized with AAV-delivered KL25 for long-term suppression of viremia. To address this possibility we tested the efficacy of AAV-KL25 therapy in DOC-infected mice that lacked either CD8 T cells due to MHC class I-deficiency (K^bD^b-/- mice [451]) or were unable to mount LCMV-specific antibody responses owing to a quasi-monoclonal B cell receptor (BCR) repertoire directed against the LCMV-unrelated vesicular stomatitis virus (T11µMT mice [175, 450]). Unlike in WT mice and despite substantial titers of AAV-delivered GP-1-binding antibodies (Fig. 2D), AAV-KL25 therapy of $K^bD^{b-/-}$ and T11µMT mice resulted in an only modest and very transient suppression of viremia on day 41 (Fig. 2B), and splenic viral loads on day 82 were comparable to controls (Fig. 2C). Analogous observations were made in MD4-transgenic mice expressing a monoclonal BCR specific for Hen egg lysozyme [452] and in mice depleted of CD4 T cells (Fig. S1B-E), which suppresses LCMV-GP-specific antibody responses [455]. Taken together, these findings suggested that AAV-KL25 therapy synergized with host endogenous B cell and CD8 T cell responses for sustained control of chronic LCMV infection.

When determining the glycoprotein sequence of the viruses persisting in the various groups of mice, we found that in untreated animals, irrespective of their genotype, the consensus sequence of the persisting virus remained identical to the inoculum, i.e. no KL25 escape mutations were detectable. In contrast, all viruses persisting in AAV-KL25-treated $K^bD^{b-/-}$, T11µMT, MD4 and CD4-depleted mice exhibited characteristic mutations at position N119 of GP-1, indicating KL25 escape (N119Y, N119S; Fig. 2E,F, Fig. S1F, Table S1, [437]) and explaining the eventual failure of AAV-KL25 therapy in these mice. Additional GP-1 mutations previously linked

to LCMV antibody evasion [459] were found in some AAV-KL25-treated $K^bD^{b-/-}$ mice (Table S1). Intriguingly, N119-mutant sequences were also found in six out of thirteen WT mice analyzed at the last time point prior to AAV-induced viral load suppression ("pre-extinction" viruses; e.g. day 33 in Fig. 2B). Thus, we hypothesized that endogenous antibody responses and/or CD8 T cells of WT mice controlled KL25 escape variants that emerged upon AAV-KL25 therapy. To test whether the endogenous antibody response in AAV-KL25-treated mice covered KL25 escape variants and to discriminate AAV-delivered antibody from host B cell responses we relied on the observation that LCMV-specific antibody responses consists mostly of IgG2a/c [460] whereas AAV-delivered KL25 was of the IgG1 isotype. On day 82 after infection the sera of AAV-KL25-treated WT mice contained substantial Docile-GP-1^{WT}-specific IgG2c titers whereas T11µMT mice were devoid of such responses, as expected (Fig. 2G). These endogenous antibody responses of WT mice recognized also the escape variants GP-1^{N119Y} and GP-1^{N119S}, which arose in AAV-KL25-treated $K^bD^{b-/-}$, T11µMT, MD4 and CD4-depleted mice (Fig. 2F-I, Fig. S1F, Table S1), lending further support to the concept that host-endogenous antibody responses contributed to sustained virus control in AAV-KL25-treated WT mice. Only marginal and transient effects of AAV-KL25 therapy in $K^bD^{b-/-}$ mice suggested that CD8 T cell responses were also required for sustained virus control upon vectored antibody gene delivery. Unexpectedly and for unknown reasons, however, the endogenous antibody responses of AAV-KL25-treated $K^bD^{b-/-}$ mice were lower than those of WT mice (Fig. 2G-I), prompting us to further scrutinize the contribution of CD8 T cells to successful AAV-KL25 therapy.

Therapeutic VAGD synergizes with CD8 T cells for sustained suppression of chronic LCMV infection

We sought a second independent experimental setting to assess the contribution of CD8 T cells to AAV-KL25-induced viral load control in persistent DOC infection (Fig. 3A). Repeated administration of a murinized monoclonal anti-CD8 antibody allowed for a virtually complete depletion of CD8 T cells throughout a 50-day observation period (Fig. 3B). AAV-KL25 was administered on day 19 after DOC infection and by day 30 resulted in a significant viral load reduction in both CD8-depleted and isotype control antibody-treated mice (Fig. 3C). By day 50, however, viremia in AAV-KL25-treated and CD8 T cell-depleted mice had rebounded, reaching the levels of control animals without AAV-KL25 therapy. In contrast and in keeping with the results reported in Fig. 2B, viral load control in isotype control-treated animals with AAV-KL25 therapy was sustained up to day 50. Analogously to $K^bD^{b-/-}$ mice, rebound viremia in AAV-KL25-treated and CD8-depleted mice was accompanied by mutational escape (Table S1). Unlike in CD8 T cell-deficient $K^bD^{b-/-}$ mice (compare Fig. 2G), GP-1-specific antibody responses of CD8-depleted and AAV-KL25-treated mice were comparable to those of AAV-KL25-treated mice given isotype antibody control treatment. These findings indicated that sustained viral load control upon AAV-KL25 therapy required not only endogenous antiviral antibody responses but also host CD8 T cells.

Therapeutic VAGD partially reverts CD8 T cell exhaustion

Persistent LCMV infection represent the classical model to study CD8 T cell exhaustion, which can manifest in functional adaptation or even deletion of antiviral CD8 T cells and is often associated with inhibitory receptor expression [94, 447-449, 456, 457]. Here we assessed whether AAV-KL25 therapy influenced the magnitude and phenotype of antiviral CD8 T cell responses. We infected WT mice with DOC on day 0 followed by AAV-KL25 therapy on day 19 (analogous to Fig. 2A). On day 50 of the experiment the overall size of the splenic $CD8^+$ T cell compartment was unaffected by AAV-KL25 therapy (Fig. 4A) and the frequency of $CD8^+$ T cells (CTLs) specific for the immunodominant LCMV glycoprotein-derived epitope GP33 remained unaltered (Fig. 4B, Fig. S2). Moreover, intracellular cytokine stains detecting the frequency of GP33-specific cytolytic granule-releasing ($CD107a^+$), IFN-γ- and TNF-α -secreting CD8 T cells did not reveal any clear differences between AAV-KL25-treated mice and controls (Fig. 4D, Fig. S3). Interestingly, however, AAV-KL25 therapy consistently reduced the expression levels of the inhibitory receptors programmed cell death protein 1 (PD-1), lymphocyte-activation gene 3 (LAG3) and T cell immunoglobulin and mucin domain-containing protein 3 (TIM-3) on GP33-specific CD8 T cells (Fig. 4E,F). These findings indicated that AAV-KL25 therapy counteracted select features of CD8 T cell exhaustion, presumably by lowering viral loads [446].

Therapeutic VAGD results in reduced numbers of LCMV-specific follicular T helper cells

An assessment of splenic CD4+ T cell numbers on day 50 did not reveal clear AAV-KL25-induced changes (Fig. 5A). Neither did AAV-KL25 exert clear effects on the number of CD4 T cells that secreted the Th1 cytokines IFN-γ or TNF-α upon stimulation with the immunodominant LCMV-derived epitope GP66 (Fig. 5B, Fig. S3). Interestingly, however, AAV-KL25-treated mice exhibited a statistically significant ~2-fold reduction in the number of GP66-tetramer-binding CD4 T cells (Fig. 5C,D, Fig. S4). A somewhat more pronounced reduction was

observed in the GP66-specific CD4+ T follicular helper cell subset (PD-1$^+$ CXCR5$^+$; Tfh, Fig. 5E,F). Taken together, these findings suggested a modest reduction of the overall LCMV-specific CD4 T cell population in AAV-KL25-treated mice, which was mostly accounted for by a reduction in antiviral CD4 Tfh cells.

Therapeutic VAGD augments antiviral germinal center B cell and antibody-secreting cell response

Next, we investigated a potential impact of VAGD on the host's endogenous B cell response. We noted that AAV-KL25-treated mice mounted significantly higher GP1^{WT}-specific IgG2c titers than controls (Fig. 6A, B). An analogous trend, albeit not statistically significant, was noted for antibody responses to the escape variant envelope proteins GP-1^{N119Y} while GP-1^{N119S}-binding responses seemed virtually unaffected by VAGD (Fig. 6C,D). Thus, we sought to investigate the cellular correlates of AAV-KL25-driven enhancement of humoral immune responses to LCMV. The total numbers of splenic B cells, isotype-switched B cells (swIg B cells; IgM$^-$IgD$^-$) and antibody-secreting cells were unaltered in animals with KL25-AAV therapy (ASCs, Fig. 6E-G). To specifically assess virus-specific B cell responses we used recently developed flow cytometry methodology, which is based on recombinantly expressed and fluorescently tagged LCMV nucleoprotein (NP) as a staining reagent (Fig. S5) [200, 455]. Intriguingly, we found that NP-specific swIg B cells were ~6-fold more abundant in mice with VAGD than in controls (Fig. 6H,I). Within the population of NP-specific swIg B cells, the proportional representation of germinal center (GC) B cells (CD38$^-$GL7$^+$) and memory B cells (CD38$^+$GL7$^-$) was comparable in AAV-KL25-treated and control animals (Fig. 6J). Accordingly, there were approx. 6-fold higher total numbers of NP-specific GC B cells in spleens of mice with VAGD than in controls (Fig. 6K). To corroborate and extend the observation of VAGD-driven enhancement of antiviral humoral immune responses we performed ELISpot assays. VAGD significantly augmented the number of NP-specific antibody secreting cells (ASCs) in spleen but not in bone marrow (Fig. 6L). Taken together these results indicated that virus-specific GC B cell and ASC responses were augmented upon AAV-KL25 therapy, providing a cellular correlate of augmented antibody responses upon VAGD.

Discussion

The present study provides a comprehensive analysis of the synergy between VAGD and the host's adaptive immune response in persistent viral infection, which likely can be extrapolated to passive antibody therapy in general. We demonstrate that not only CD8 T cell but also B cell responses are essential for sustained viral load control upon VAGD. In the absence of either one of these responses, the therapeutic effect of VAGD was thwarted by promptly arising mAb escape variants. While an essential contribution of CD8 T cells to bnAb-induced suppression of SHIV infection has been documented [419, 438], the present work formally establishes an essential role of the host B cell response in containing VAGD escape variants and preventing viral rebound. Thereby we confirm and extend earlier correlative studies on the role of host antibody responses in the context of bnAb-treated SHIV infection [436].

An independent and equally important finding of our study consists in the profound impact of VAGD on host T and B cell responses to the persisting virus. Most importantly, we establish a cellular correlate of enhanced endogenous antibody responses upon passive antibody therapy [439]. Specifically, VAGD resulted in 6-fold higher numbers of virus-specific B cells overall and in a proportionally augmented GC B cell compartment, which in conjunction with elevated numbers of antiviral ASC numbers offers a compelling explanation for earlier observations of augmented and broadened nAb responses in bnAb-treated HIV patients [439]. AAV-KL25 augmented predominantly the antibody response against the originally inoculated virus while antibody titers against KL25 escape variants were less affected. A limited duration of infection prior to VAGD and, therefore, only modest viral genetic diversification in LCMV-infected WT mice may, on average (compare Tbl. S1), have offered only limited B cell exposure to KL25 escape variants in successfully VAGD-treated WT mice. The mechanisms underlying augmented antiviral GC B cell responses in VAGD-treated mice requires further investigation. Several not mutually exclusive mechanisms may contribute including direct beneficial effects of reduced viral antigen loads on GC reactions [409], conformational epitope unmasking on antibody-bound antigens [461, 462] and improved delivery and/or retention of antibody-bound viral antigen by Fcγ- and complement-receptors inside GCs [463-465].

VAGD reduced the levels of inhibitory receptor expression on LCMV-specific CD8 T cells, suggesting at least partial reversion of T cell exhaustion. This is in line with the concept that persistently high antigenic load, which is suppressed by VAGD, accounts for this T cell phenotype [446]. A complete loss of inhibitory receptor expression could not be expected, since inhibitory receptors are indicative of a differentiation program that persists even when CD8 T cells from chronically infected mice are adoptively transferred into completely antigen-free hosts [466]. Overall, our observations on CD8 T cell exhaustion are in line with and complement a recent report on bnAb-treated HIV patients [443]. While the latter study documented increased frequencies of cytokine-secreting human CD8 T cells, the present data from mice evidence a more pronounced effect of VAGD on the cells' phenotype. In either case, future work should address the possibility that VAGD-mediated reversion of exhaustion may augment the cells' antiviral efficacy, which in a positive feedback loop should facilitate VAGD-induced virus control.

VAGD diminished rather than augmented antiviral Tfh numbers, which is in line with chronic antigen load as a potent driver of Tfh differentiation and population expansion [467-470]. The negative impact of VAGD on Tfh population size was, however, modest and still compatible with potent antiviral GC B cell responses. Moreover, a potential beneficial effect of VAGD on Tfh functionality [468] remains to be investigated. In contrast and for currently unknown reasons we failed to observe a clear effect of VAGD on cytokine-secreting Th1 responses as reported from SIV-infected NHPs [444].

We are aware that augmented antiviral antibody titers in VAGD-treated mice could be the result of "consumption" by high antigen levels and therefore a relative lack of detection rather than elevated production. The augmentation of antiviral B cells as determined by flow cytometry and, most notably, the augmentation of splenic ASC numbers in VAGD-treated animals indicates, however, that VAGD effects on humoral immune responses extend beyond potential "antibody unmasking". We acknowledge that LCMV infection of mice can only recreate some but clearly not all relevant immunological features of chronic viral diseases of humans such as HIV, HCV or HBV infection. The gradual loss of CD4 T cells with progression to AIDS, for example, is likely to curtail the synergy of VAGD with endogenous immune defense. Similarly, the excessive abundance of HBs in the serum of congenital HBV carriers may trigger mechanisms of humoral immune subversion, which are not recreated in LCMV infection [255, 471]

In summary, the present work in immunocompetent animals with established chronic infection highlights previously underestimated VAGD effects on the host's endogenous immune defense and resulting virus control. By revealing multiple layers of reciprocal interactions between passively administered antibodies with host GC

B cell and CD8+ T cell responses our findings should help to better position and leverage passive antibody therapy and VAGD in particular as innovative new tools in the combat against persistent viral diseases.

References

Balazs, A.B., J. Chen, C.M. Hong, D.S. Rao, L. Yang, and D. Baltimore. 2012. Antibody-based protection against HIV infection by vectored immunoprophylaxis. *Nature* 481:81-84.

Balazs, A.B., Y. Ouyang, C.M. Hong, J. Chen, S.M. Nguyen, D.S. Rao, D.S. An, and D. Baltimore. 2014. Vectored immunoprophylaxis protects humanized mice from mucosal HIV transmission. *Nature Medicine* 20:296-300.

Barber, D.L., E.J. Wherry, D. Masopust, B. Zhu, J.P. Allison, A.H. Sharpe, G.J. Freeman, and R. Ahmed. 2006. Restoring function in exhausted CD8 T cells during chronic viral infection. *Nature* 439:682-687.

Barouch, D.H., J.B. Whitney, B. Moldt, F. Klein, T.Y. Oliveira, J. Liu, K.E. Stephenson, H.-W. Chang, K. Shekhar, S. Gupta, J.P. Nkolola, M.S. Seaman, K.M. Smith, E.N. Borducchi, C. Cabral, J.Y. Smith, S. Blackmore, S. Sanisetty, J.R. Perry, M. Beck, M.G. Lewis, W. Rinaldi, A.K. Chakraborty, P. Poignard, M.C. Nussenzweig, and D.R. Burton. 2013. Therapeutic efficacy of potent neutralizing HIV-1-specific monoclonal antibodies in SHIV-infected rhesus monkeys. *Nature* 503:224-228.

Batista, F.D., and N.E. Harwood. 2009. The who, how and where of antigen presentation to B cells. *Nature Reviews Immunology* 9:15-27.

Battegay, M., S. Cooper, A. Althage, J. Banziger, H. Hengartner, and R.M. Zinkernagel. 1991. Quantification of lymphocytic choriomeningitis virus with an immunological focus assay in 24- or 96-well plates. *J Virol Methods* 33:191-198.

Behring, E.v., Shibasaburo Kitasato. 1890. Ueber Das Zustandekommen Der Diphtherie-Immunität Und Der Tetanus-Immunität Bei Thieren. *Deutsch. Med. Woch.* 49:1113-1114.

Bergthaler, A., L. Flatz, A. Verschoor, A.N. Hegazy, M. Holdener, K. Fink, B. Eschli, D. Merkler, R. Sommerstein, E. Horvath, M. Fernandez, A. Fitsche, B.M. Senn, J.S. Verbeek, B. Odermatt, C.-A. Siegrist, and D.D. Pinschewer. 2009. Impaired Antibody Response Causes Persistence of Prototypic T Cell–Contained Virus. *PLOS Biology* 7:e1000080.

Blackburn, S.D., H. Shin, W.N. Haining, T. Zou, C.J. Workman, A. Polley, M.R. Betts, G.J. Freeman, D.A.A. Vignali, and E.J. Wherry. 2009. Coregulation of CD8+ T cell exhaustion by multiple inhibitory receptors during chronic viral infection. *Nature Immunology* 10:29-37.

Burton, A.R., L.J. Pallett, L.E. McCoy, K. Suveizdyte, O.E. Amin, L. Swadling, E. Alberts, B.R. Davidson, P.T.F. Kennedy, U.S. Gill, C. Mauri, P.A. Blair, N. Pelletier, and M.K. Maini. 2018. Circulating and intrahepatic antiviral B cells are defective in hepatitis B. *The Journal of Clinical Investigation* 128:4588-4603.

Carroll, Michael C., and David E. Isenman. 2012. Regulation of Humoral Immunity by Complement. *Immunity* 37:199-207.

Coutelier, J.P., J.T. van der Logt, F.W. Heessen, G. Warnier, and J. Van Snick. 1987. IgG2a restriction of murine antibodies elicited by viral infections. *The Journal of Experimental Medicine* 165:64-69.

Crawford, A., Jill M. Angelosanto, C. Kao, Travis A. Doering, Pamela M. Odorizzi, Burton E. Barnett, and E.J. Wherry. 2014. Molecular and Transcriptional Basis of CD4+ T Cell Dysfunction during Chronic Infection. *Immunity* 40:289-302.

de Jong, Y.P., M. Dorner, M.C. Mommersteeg, J.W. Xiao, A.B. Balazs, J.B. Robbins, B.Y. Winer, S. Gerges, K. Vega, R.N. Labitt, B.M. Donovan, E. Giang, A. Krishnan, L. Chiriboga, M.R. Charlton, D.R. Burton, D. Baltimore, M. Law, C.M. Rice, and A. Ploss. 2014. Broadly neutralizing antibodies abrogate established hepatitis C virus infection. *Science Translational Medicine* 6:254ra129-254ra129.

Eschli, B., R.M. Zellweger, A. Wepf, K.S. Lang, K. Quirin, J. Weber, R.M. Zinkernagel, and H. Hengartner. 2007. Early Antibodies Specific for the Neutralizing Epitope on the Receptor Binding Subunit of the Lymphocytic Choriomeningitis Virus Glycoprotein Fail To Neutralize the Virus. *Journal of Virology* 81:11650-11657.

Fahey, L.M., E.B. Wilson, H. Elsaesser, C.D. Fistonich, D.B. McGavern, and D.G. Brooks. 2011. Viral persistence redirects CD4 T cell differentiation toward T follicular helper cells. *The Journal of Experimental Medicine* 208:987-999.

Fallet, B., Y. Hao, M. Florova, K. Cornille, A.V. de los Aires, G. Girelli Zubani, Y.I. Ertuna, V. Greiff, U. Menzel, K. Hammad, D. Merkler, S.T. Reddy, J.-C. Weill, C.-A. Reynaud, and D.D. Pinschewer. 2020. Chronic Viral Infection Promotes Efficient Germinal Center B Cell Responses. *Cell Reports* 30:1013-1026.e1017.

Fallet, B., K. Narr, Y.I. Ertuna, M. Remy, R. Sommerstein, K. Cornille, M. Kreutzfeldt, N. Page, G. Zimmer, F. Geier, T. Straub, H. Pircher, K. Larimore, P.D. Greenberg, D. Merkler, and D.D. Pinschewer. 2016. Interferon-driven deletion of antiviral B cells at the onset of chronic infection. *Science Immunology* 1:eaah6817.

Fuchs, S.P., J.M. Martinez-Navio, M. Piatak, Jr., J.D. Lifson, G. Gao, and R.C. Desrosiers. 2015. AAV-Delivered Antibody Mediates Significant Protective Effects against SIVmac239 Challenge in the Absence of Neutralizing Activity. *PLOS Pathogens* 11:e1005090.
Fung-Leung, W.P., T.M. Kündig, R.M. Zinkernagel, and T.W. Mak. 1991. Immune response against lymphocytic choriomeningitis virus infection in mice without CD8 expression. *Journal of Experimental Medicine* 174:1425-1429.
Gallimore, A., A. Glithero, A. Godkin, A.C. Tissot, A. Plückthun, T. Elliott, H. Hengartner, and R. Zinkernagel. 1998. Induction and Exhaustion of Lymphocytic Choriomeningitis Virus–specific Cytotoxic T Lymphocytes Visualized Using Soluble Tetrameric Major Histocompatibility Complex Class I–Peptide Complexes. *The Journal of Experimental Medicine* 187:1383-1393.
Gardner, M.R., C.H. Fellinger, L.M. Kattenhorn, M.E. Davis-Gardner, J.A. Weber, B. Alfant, A.S. Zhou, N.R. Prasad, H.R. Kondur, W.A. Newton, K.L. Weisgrau, E.G. Rakasz, J.D. Lifson, G. Gao, N. Schultz-Darken, and M. Farzan. 2019. AAV-delivered eCD4-Ig protects rhesus macaques from high-dose SIVmac239 challenges. *Science Translational Medicine* 11:eaau5409.
Goodnow, C.C., J. Crosbie, S. Adelstein, T.B. Lavoie, S.J. Smith-Gill, R.A. Brink, H. Pritchard-Briscoe, J.S. Wotherspoon, R.H. Loblay, K. Raphael, R.J. Trent, and A. Basten. 1988. Altered immunoglobulin expression and functional silencing of self-reactive B lymphocytes in transgenic mice. *Nature* 334:676-682.
Gros, L., H. Dreja, A.L. Fiser, M. Plays, M. Pelegrin, and M. Piechaczyk. 2005. Induction of Long-Term Protective Antiviral Endogenous Immune Response by Short Neutralizing Monoclonal Antibody Treatment. *Journal of Virology* 79:6272-6280.
Haigwood, N.L., D.C. Montefiori, W.F. Sutton, J. McClure, A.J. Watson, G. Voss, V.M. Hirsch, B.A. Richardson, N.L. Letvin, S.-L. Hu, and P.R. Johnson. 2004. Passive Immunotherapy in Simian Immunodeficiency Virus-Infected Macaques Accelerates the Development of Neutralizing Antibodies. *Journal of Virology* 78:5983-5995.
Harker, J.A., G.M. Lewis, L. Mack, and E.I. Zuniga. 2011. Late Interleukin-6 Escalates T Follicular Helper Cell Responses and Controls a Chronic Viral Infection. *Science* 334:825-829.
Hioe, C.E., M.L. Visciano, R. Kumar, J. Liu, E.A. Mack, R.E. Simon, D.N. Levy, and M. Tuen. 2009. The use of immune complex vaccines to enhance antibody responses against neutralizing epitopes on HIV-1 envelope gp120. *Vaccine* 28:352-360.
Horwitz, J.A., A. Halper-Stromberg, H. Mouquet, A.D. Gitlin, A. Tretiakova, T.R. Eisenreich, M. Malbec, S. Gravemann, E. Billerbeck, M. Dorner, H. Büning, O. Schwartz, E. Knops, R. Kaiser, M.S. Seaman, J.M. Wilson, C.M. Rice, A. Ploss, P.J. Bjorkman, F. Klein, and M.C. Nussenzweig. 2013. HIV-1 suppression and durable control by combining single broadly neutralizing antibodies and antiretroviral drugs in humanized mice. *Proceedings of the National Academy of Sciences* 110:16538-16543.
Hunziker, L., A. Ciurea, M. Recher, H. Hengartner, and R.M. Zinkernagel. 2003. Public versus personal serotypes of a viral quasispecies. *Proceedings of the National Academy of Sciences* 100:6015-6020.
Iseda, S., N. Takahashi, H. Poplimont, T. Nomura, S. Seki, T. Nakane, M. Nakamura, S. Shi, H. Ishii, S. Furukawa, S. Harada, T.K. Naruse, A. Kimura, T. Matano, and H. Yamamoto. 2016. Biphasic CD8⁺ T-Cell Defense in Simian Immunodeficiency Virus Control by Acute-Phase Passive Neutralizing Antibody Immunization. *Journal of Virology* 90:6276-6290.
Kisalu, N.K., L.D. Pereira, K. Ernste, Y. Flores-Garcia, A.H. Idris, M. Asokan, M. Dillon, S. MacDonald, W. Shi, X. Chen, A. Pegu, A. Schön, F. Zavala, A.B. Balazs, J.R. Francica, and R.A. Seder. 2021. Enhancing durability of CIS43 monoclonal antibody by Fc mutation or AAV delivery for malaria prevention. *JCI Insight* 6:
Klein, F., L. Nogueira, Y. Nishimura, G. Phad, A.P. West, A. Halper-Stromberg, J.A. Horwitz, A. Gazumyan, C. Liu, T.R. Eisenreich, C. Lehmann, G. Fätkenheuer, C. Williams, M. Shingai, M.A. Martin, P.J. Bjorkman, M.S. Seaman, S. Zolla-Pazner, G.B. Karlsson Hedestam, and M.C. Nussenzweig. 2014. Enhanced HIV-1 immunotherapy by commonly arising antibodies that target virus escape variants. *The Journal of Experimental Medicine* 211:2361-2372.
Klein, M.A., R. Frigg, E. Flechsig, A.J. Raeber, U. Kalinke, H. Bluethmann, F. Bootz, M. Suter, R.M. Zinkernagel, and A. Aguzzi. 1997. A crucial role for B cells in neuroinvasive scrapie. *Nature* 390:687-690.
Köhler, G., and C. Milstein. 1975. Continuous cultures of fused cells secreting antibody of predefined specificity. *Nature* 256:495-497.
Kumar, R., M. Tuen, J. Liu, A. Nàdas, R. Pan, X. Kong, and C.E. Hioe. 2013. Elicitation of broadly reactive antibodies against glycan-modulated neutralizing V3 epitopes of HIV-1 by immune complex vaccines. *Vaccine* 31:5413-5421.
Leborgne, C., E. Barbon, J.M. Alexander, H. Hanby, S. Delignat, D.M. Cohen, F. Collaud, S. Muraleetharan, D. Lupo, J. Silverberg, K. Huang, L. van Wittengerghe, B. Marolleau, A. Miranda, A. Fabiano, V. Daventure, H. Beck, X.M. Anguela, G. Ronzitti, S.M. Armour, S. Lacroix-Desmazes, and F. Mingozzi. 2020. IgG-cleaving endopeptidase

enables in vivo gene therapy in the presence of anti-AAV neutralizing antibodies. *Nature Medicine* 26:1096-1101.
Lewis, A.D., R. Chen, D.C. Montefiori, P.R. Johnson, and K.R. Clark. 2002. Generation of Neutralizing Activity against Human Immunodeficiency Virus Type 1 in Serum by Antibody Gene Transfer. *Journal of Virology* 76:8769-8775.
Lock, M., M.R. Alvira, S.-J. Chen, and J.M. Wilson. 2013. Absolute Determination of Single-Stranded and Self-Complementary Adeno-Associated Viral Vector Genome Titers by Droplet Digital PCR. *Human Gene Therapy Methods* 25:115-125.
Martinez-Navio, J.M., S.P. Fuchs, S.N. Pantry, W.A. Lauer, N.N. Duggan, B.F. Keele, E.G. Rakasz, G. Gao, J.D. Lifson, and R.C. Desrosiers. 2019. Adeno-Associated Virus Delivery of Anti-HIV Monoclonal Antibodies Can Drive Long-Term Virologic Suppression. *Immunity* 50:567-575.e565.
Mendoza, P., H. Gruell, L. Nogueira, J.A. Pai, A.L. Butler, K. Millard, C. Lehmann, I. Suárez, T.Y. Oliveira, J.C.C. Lorenzi, Y.Z. Cohen, C. Wyen, T. Kümmerle, T. Karagounis, C.-L. Lu, L. Handl, C. Unson-O'Brien, R. Patel, C. Ruping, M. Schlotz, M. Witmer-Pack, I. Shimeliovich, G. Kremer, E. Thomas, K.E. Seaton, J. Horowitz, A.P. West, P.J. Bjorkman, G.D. Tomaras, R.M. Gulick, N. Pfeifer, G. Fätkenheuer, M.S. Seaman, F. Klein, M. Caskey, and M.C. Nussenzweig. 2018. Combination therapy with anti-HIV-1 antibodies maintains viral suppression. *Nature* 561:479-484.
Moskophidis, D., M. Battegay, M. van den Broek, E. Laine, U. Hoffmann-Rohrer, and R.M. Zinkernagel. 1995. Role of virus and host variables in virus persistence or immunopathological disease caused by a non-cytolytic virus. *Journal of General Virology* 76:381-391.
Moskophidis, D., F. Lechner, H. Pircher, and R.M. Zinkernagel. 1993. Virus persistence in acutely infected immunocompetent mice by exhaustion of antiviral cytotoxic effector T cells. *Nature* 362:758-761.
Mueller, S.N., and R. Ahmed. 2009. High antigen levels are the cause of T cell exhaustion during chronic viral infection. *Proc Natl Acad Sci U S A* 106:8623-8628.
Ng, C.T., J.P. Jaworski, P. Jayaraman, W.F. Sutton, P. Delio, L. Kuller, D. Anderson, G. Landucci, B.A. Richardson, D.R. Burton, D.N. Forthal, and N.L. Haigwood. 2010. Passive neutralizing antibody controls SHIV viremia and enhances B cell responses in infant macaques. *Nature Medicine* 16:1117.
Niessl, J., A.E. Baxter, P. Mendoza, M. Jankovic, Y.Z. Cohen, A.L. Butler, C.-L. Lu, M. Dubé, I. Shimeliovich, H. Gruell, F. Klein, M. Caskey, M.C. Nussenzweig, and D.E. Kaufmann. 2020. Combination anti-HIV-1 antibody therapy is associated with increased virus-specific T cell immunity. *Nature Medicine* 26:222-227.
Nishimura, Y., O.K. Donau, J. Dias, S. Ferrando-Martinez, E. Jesteadt, R. Sadjadpour, R. Gautam, A. Buckler-White, R. Geleziunas, R.A. Koup, M.C. Nussenzweig, and M.A. Martin. 2020. Immunotherapy during the acute SHIV infection of macaques confers long-term suppression of viremia. *Journal of Experimental Medicine* 218:
Nishimura, Y., R. Gautam, T.-W. Chun, R. Sadjadpour, K.E. Foulds, M. Shingai, F. Klein, A. Gazumyan, J. Golijanin, M. Donaldson, O.K. Donau, R.J. Plishka, A. Buckler-White, M.S. Seaman, J.D. Lifson, R.A. Koup, A.S. Fauci, M.C. Nussenzweig, and M.A. Martin. 2017. Early antibody therapy can induce long-lasting immunity to SHIV. *Nature* 543:559-563.
Penaloza-MacMaster, P., D.L. Barber, E.J. Wherry, N.M. Provine, J.E. Teigler, L. Parenteau, S. Blackmore, E.N. Borducchi, R.A. Larocca, K.B. Yates, H. Shen, W.N. Haining, R. Sommerstein, D.D. Pinschewer, R. Ahmed, and D.H. Barouch. 2015. Vaccine-elicited CD4 T cells induce immunopathology after chronic LCMV infection. *Science* 347:278-282.
Pérarnau, B., M.-F. Saron, B.R. San Martin, N. Bervas, H. Ong, M.J. Soloski, A.G. Smith, J.M. Ure, J.E. Gairin, and F.A. Lemonnier. 1999. Single H2Kb, H2Db and double H2KbDb knockout mice: peripheral CD8+ T cell repertoire and antilymphocytic choriomeningitis virus cytolytic responses. *European Journal of Immunology* 29:1243-1252.
Pfau, C.J., J.K. Valenti, D.C. Pevear, and K.D. Hunt. 1982. Lymphocytic choriomeningitis virus killer T cells are lethal only in weakly disseminated murine infections. *The Journal of Experimental Medicine* 156:79-89.
Phan, T.G., J.A. Green, E.E. Gray, Y. Xu, and J.G. Cyster. 2009. Immune complex relay by subcapsular sinus macrophages and noncognate B cells drives antibody affinity maturation. *Nature Immunology* 10:786-793.
Pinschewer, D.D., M. Perez, E. Jeetendra, T. Bächi, E. Horvath, H. Hengartner, M.A. Whitt, J.C. de la Torre, and R.M. Zinkernagel. 2004. Kinetics of protective antibodies are determined by the viral surface antigen. *The Journal of Clinical Investigation* 114:988-993.
Pircher, H., D. Moskophidis, U. Rohrer, K. Bürki, H. Hengartner, and R.M. Zinkernagel. 1990. Viral escape by selection of cytotoxic T cell-resistant virus variants in vivo. *Nature* 346:629-633.
Priddy, F.H., D.J.M. Lewis, H.C. Gelderblom, H. Hassanin, C. Streatfield, C. LaBranche, J. Hare, J.H. Cox, L. Dally, D. Bendel, D. Montefiori, E. Sayeed, J. Ackland, J. Gilmour, B.C. Schnepp, J.F. Wright, and P. Johnson. 2019. Adeno-associated virus vectored immunoprophylaxis to prevent HIV in healthy adults: a phase 1 randomised controlled trial. *The Lancet HIV* 6:e230-e239.

Robert, M.-A., N. Nassoury, P.S. Chahal, M.-H. Venne, T. Racine, X. Qiu, G. Kobinger, A. Kamen, R. Gilbert, and B. Gaillet. 2017. Gene Transfer of ZMapp Antibodies Mediated by Recombinant Adeno-Associated Virus Protects Against Ebola Infections. *Human Gene Therapy* 29:452-466.
Salimzadeh, L., N. Le Bert, C.-A. Dutertre, U.S. Gill, E.W. Newell, C. Frey, M. Hung, N. Novikov, S. Fletcher, P.T.F. Kennedy, and A. Bertoletti. 2018. PD-1 blockade partially recovers dysfunctional virus–specific B cells in chronic hepatitis B infection. *The Journal of Clinical Investigation* 128:4573-4587.
Scheid, J.F., H. Mouquet, B. Ueberheide, R. Diskin, F. Klein, T.Y.K. Oliveira, J. Pietzsch, D. Fenyo, A. Abadir, K. Velinzon, A. Hurley, S. Myung, F. Boulad, P. Poignard, D.R. Burton, F. Pereyra, D.D. Ho, B.D. Walker, M.S. Seaman, P.J. Bjorkman, B.T. Chait, and M.C. Nussenzweig. 2011. Sequence and Structural Convergence of Broad and Potent HIV Antibodies That Mimic CD4 Binding. *Science* 333:1633-1637.
Schoofs, T., F. Klein, M. Braunschweig, E.F. Kreider, A. Feldmann, L. Nogueira, T. Oliveira, J.C.C. Lorenzi, E.H. Parrish, G.H. Learn, A.P. West, P.J. Bjorkman, S.J. Schlesinger, M.S. Seaman, J. Czartoski, M.J. McElrath, N. Pfeifer, B.H. Hahn, M. Caskey, and M.C. Nussenzweig. 2016. HIV-1 therapy with monoclonal antibody 3BNC117 elicits host immune responses against HIV-1. *Science* 352:997-1001.
Schweier, O., U. Aichele, A.-F. Marx, T. Straub, J.S. Verbeek, D.D. Pinschewer, and H. Pircher. 2019. Residual LCMV antigen in transiently CD4+ T cell-depleted mice induces high levels of virus-specific antibodies but only limited B-cell memory. *European Journal of Immunology* 49:626-637.
Seiler, P., B.M. Senn, M.-A. Bründler, R.M. Zinkernagel, H. Hengartner, and U. Kalinke. 1999. In Vivo Selection of Neutralization-Resistant Virus Variants But No Evidence of B Cell Tolerance in Lymphocytic Choriomeningitis Virus Carrier Mice Expressing a Transgenic Virus-Neutralizing Antibody. *The Journal of Immunology* 162:4536-4541.
Shingai, M., Y. Nishimura, F. Klein, H. Mouquet, O.K. Donau, R. Plishka, A. Buckler-White, M. Seaman, M. Piatak, J.D. Lifson, D. Dimitrov, M.C. Nussenzweig, and M.A. Martin. 2013. Antibody-mediated immunotherapy of macaques chronically infected with SHIV suppresses viraemia. *Nature* 503:277-280.
Sommerstein, R., L. Flatz, M.M. Remy, P. Malinge, G. Magistrelli, N. Fischer, M. Sahin, A. Bergthaler, S. Igonet, J. ter Meulen, D. Rigo, P. Meda, N. Rabah, B. Coutard, T.A. Bowden, P.-H. Lambert, C.-A. Siegrist, and D.D. Pinschewer. 2015. Arenavirus Glycan Shield Promotes Neutralizing Antibody Evasion and Protracted Infection. *PLOS Pathogens* 11:e1005276.
Staupe, R.P., L.A. Vella, S. Manne, J.R. Giles, W. Meng, R.S. Herati, O. Khan, J.E. Wu, A.E. Baxter, E.T.L. Prak, and E.J. Wherry. 2019. Chronic viral infection promotes early germinal center exit of B cells and impaired antibody development. *bioRxiv* 849844.
Trkola, A., H. Kuster, P. Rusert, B. Joos, M. Fischer, C. Leemann, A. Manrique, M. Huber, M. Rehr, A. Oxenius, R. Weber, G. Stiegler, B. Vcelar, H. Katinger, L. Aceto, and H.F. Günthard. 2005. Delay of HIV-1 rebound after cessation of antiretroviral therapy through passive transfer of human neutralizing antibodies. *Nature Medicine* 11:615-622.
Trono, D., C. Van Lint, C. Rouzioux, E. Verdin, F. Barré-Sinoussi, T.-W. Chun, and N. Chomont. 2010. HIV Persistence and the Prospect of Long-Term Drug-Free Remissions for HIV-Infected Individuals. *Science* 329:174-180.
Utzschneider, D.T., A. Legat, S.A. Fuertes Marraco, L. Carrié, I. Luescher, D.E. Speiser, and D. Zehn. 2013. T cells maintain an exhausted phenotype after antigen withdrawal and population reexpansion. *Nature Immunology* 14:603.
van Lieshout, L.P., G. Soule, D. Sorensen, K.L. Frost, S. He, K. Tierney, D. Safronetz, S.A. Booth, G.P. Kobinger, X. Qiu, and S.K. Wootton. 2018. Intramuscular Adeno-Associated Virus–Mediated Expression of Monoclonal Antibodies Provides 100% Protection Against Ebola Virus Infection in Mice. *The Journal of Infectious Diseases* 217:916-925.
Wherry, E.J., J.N. Blattman, K. Murali-Krishna, R. van der Most, and R. Ahmed. 2003. Viral Persistence Alters CD8 T-Cell Immunodominance and Tissue Distribution and Results in Distinct Stages of Functional Impairment. *Journal of Virology* 77:4911-4927.
Williams, N., N. Kraft, and K. Shortman. 1972. The separation of different cell classes from lymphoid organs. VI. The effect of osmolarity of gradient media on the density distribution of cells. *Immunology* 22:885-899.
Winter, G. 2019. Harnessing Evolution to Make Medicines (Nobel Lecture). *Angewandte Chemie International Edition* 58:14438-14445.
Wu, X., Z.-Y. Yang, Y. Li, C.-M. Hogerkorp, W.R. Schief, M.S. Seaman, T. Zhou, S.D. Schmidt, L. Wu, L. Xu, N.S. Longo, K. McKee, S. O'Dell, M.K. Louder, D.L. Wycuff, Y. Feng, M. Nason, N. Doria-Rose, M. Connors, P.D. Kwong, M. Roederer, R.T. Wyatt, G.J. Nabel, and J.R. Mascola. 2010. Rational Design of Envelope Identifies Broadly Neutralizing Human Monoclonal Antibodies to HIV-1. *Science* 329:856-861.

Xin, G., R. Zander, D.M. Schauder, Y. Chen, J.S. Weinstein, W.R. Drobyski, V. Tarakanova, J. Craft, and W. Cui. 2018. Single-cell RNA sequencing unveils an IL-10-producing helper subset that sustains humoral immunity during persistent infection. *Nature Communications* 9:5037.
Yamamoto, T., N. Iwamoto, H. Yamamoto, T. Tsukamoto, T. Kuwano, A. Takeda, M. Kawada, Y. Tsunetsugu-Yokota, and T. Matano. 2009. Polyfunctional CD4⁺ T-Cell Induction in Neutralizing Antibody-Triggered Control of Simian Immunodeficiency Virus Infection. *Journal of Virology* 83:5514-5524.
Zajac, A.J., J.N. Blattman, K. Murali-Krishna, D.J. Sourdive, M. Suresh, J.D. Altman, and R. Ahmed. 1998. Viral immune evasion due to persistence of activated T cells without effector function. *The Journal of experimental medicine* 188:2205-2213.
Acknowledgments
We wish to thank Karsten Stauffer for excellent animal handling and care.

Funding
This work was supported by the Swiss National Science Foundation project grant No. 310030_173132 to D.D.P.

Author contributions
YIE, BF and DDP contributed to experimental conception and design. YIE, BF, AFM and MD performed experiments. YIE, BF and DDP analyzed and/or interpreted the data. YIE and DDP wrote the manuscript.

Conflict of interests
D.D.P. is a founder, shareholder and consultant of Hookipa Pharma Inc. commercializing arenavirus-based vector technology.

Figures

Figure 1

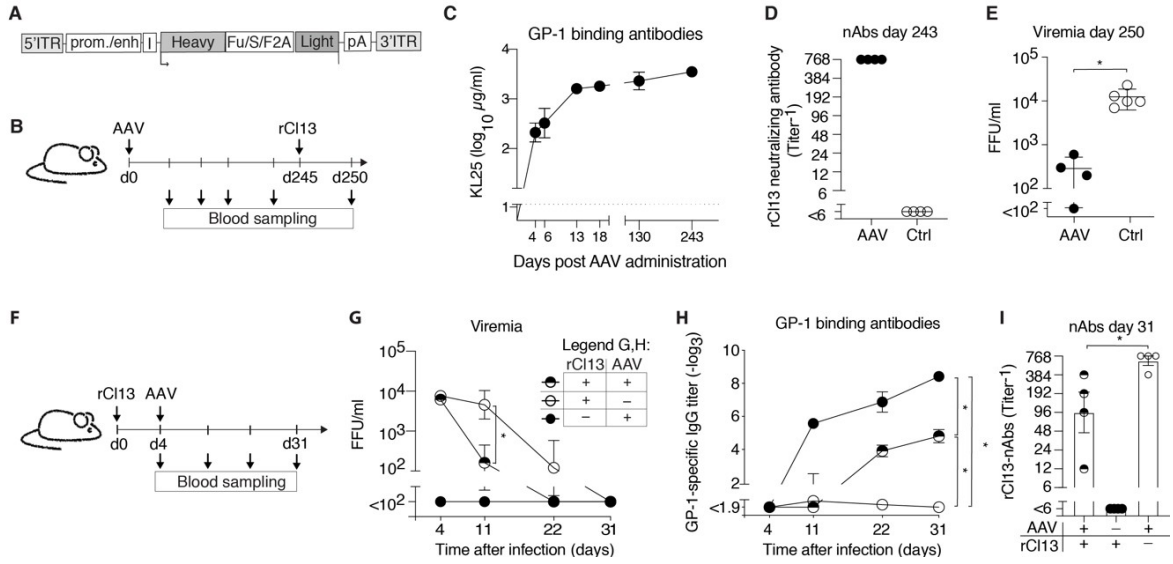

Figure 1: VAGD affords long-term protection and curbs viremia when administered early after viral challenge. (A) Schematic of the AAV-KL25 genome. 5'ITR and 3'ITR: AAV genomic 5' and 3' inverted terminal repeats; Prom./enh: promoter and enhancer; heavy: KL25 heavy chain; Fu/S/F2A: furin cleavage site, spacer and F2A peptide; Light: KL25 light chain; pA: polyadenylation site. (B) We administered AAV-KL25 to WT mice on d0. On d245, these animals and previously untreated controls were challenged with rCl13. We measured KL25 serum concentrations over time (C) and tested the neutralizing activity in serum on d243 (D). (E) 5 days after virus challenge (d250) we determined viremia. (F) We infected WT mice with rCl13 on d0, followed by AAV-KL25 administration on d4. We measured viremia (G) and LCMV GP-1-specific serum Ig titers over time (H) and determined rCl13-nAbs on day 31 (I). Symbols in C, G, H represent the mean±SEM of 4 mice. Symbols in D, E, I show individual animals, error bars denote the mean±SEM. Number of independent experiments (*N*) = 2 (C-E, G-I), Data were analyzed by unpaired two-tailed Student's *t* tests (D-E), by two-way ANOVA followed by Tukey's post-test for individual time points (G-H) and by one-way ANOVA followed by Tukey's post-test for (I). * p <0.05.

Figure 2

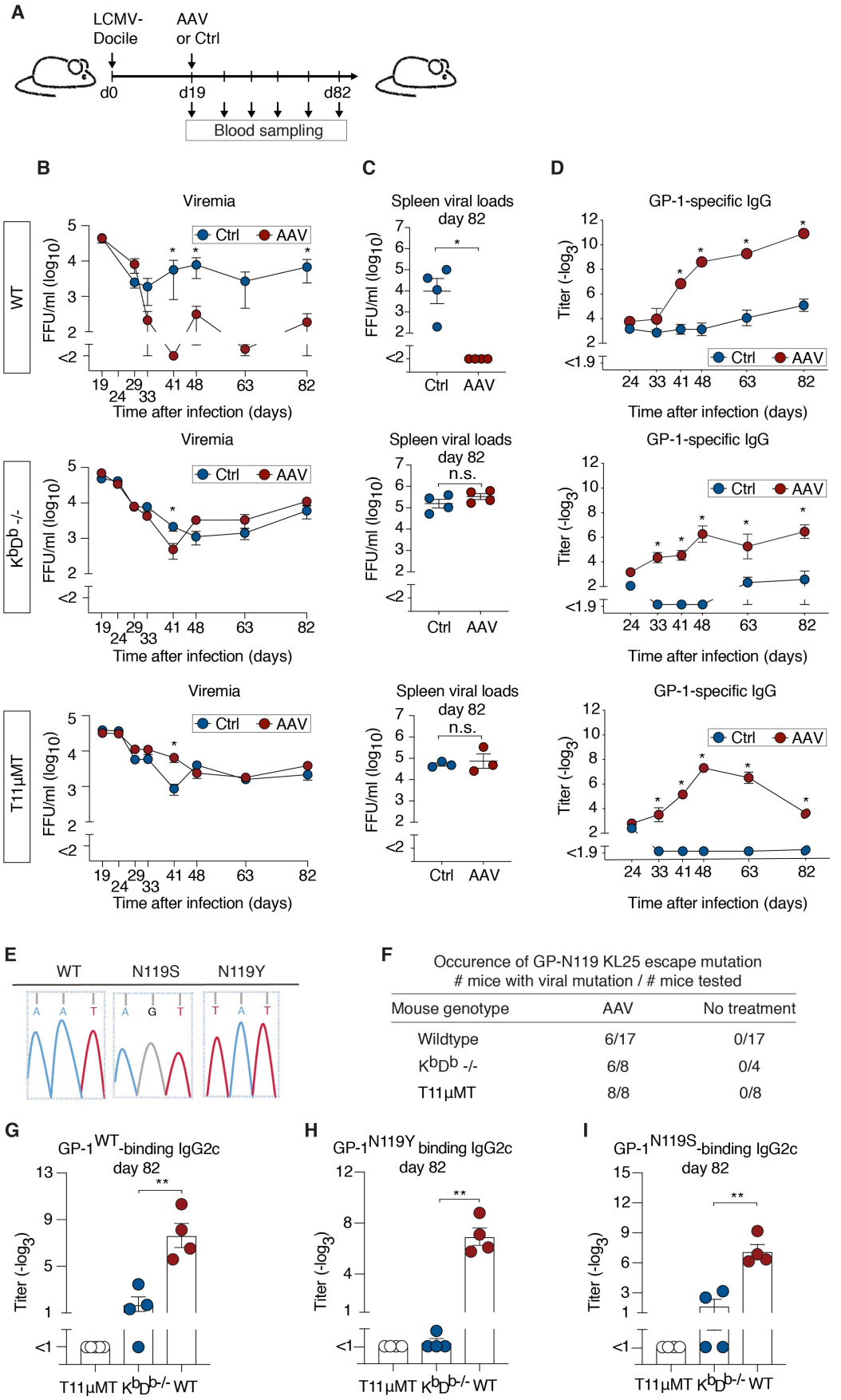

Mouse genotype	AAV	No treatment
Wildtype	6/17	0/17
K^bD^b -/-	6/8	0/4
T11µMT	8/8	0/8

Figure 2: Therapeutic VAGD synergizes with host antibody responses for sustained suppression of chronic infection.

(A) We infected WT, $K^bD^{b-/-}$ and T11µMT mice with LCMV-DOC on d0, followed by AAV-KL25 therapy or control (PBS) on d19. (B) Viremia was assessed on the indicated time points. (C) Viral titers in the spleen were measured on day 82. (D) LCMV GP-1 specific antibody titers were determined by ELISA. (E) Illustrative chromatograms of sequencing reactions performed to determine Aa119 of LCMV-Docile and of two commonly found escape variants. (F) Occurrence of N119 escape mutations in AAV-KL25-treated and untreated WT, $K^bD^{b-/-}$ and T11µMT mice (see also Supplementary Table I). To determine host-endogenous GP-1-specific antibody responses we measured serum IgG2c titers against $GP\text{-}1^{WT}$ (F), $GP\text{-}1^{N119Y}$ (G) and $GP\text{-}1^{N119S}$ (H) by ELISA. Symbols in (B-D) and bars in (G-I) represent the mean ± SEM of 3-4 mice, symbols in (C, G-I) show individual mice. *N* = 2 D, G-I). Data were analyzed by unpaired two-tailed Student's *t* test (B, C, G-I) and by two-way ANOVA followed by Tukey's post-test for individual time points (D). **p* < 0.05, ***p* < 0.01, n.s.: p≧0.05, not statistically significant.

(B)

Figure 3

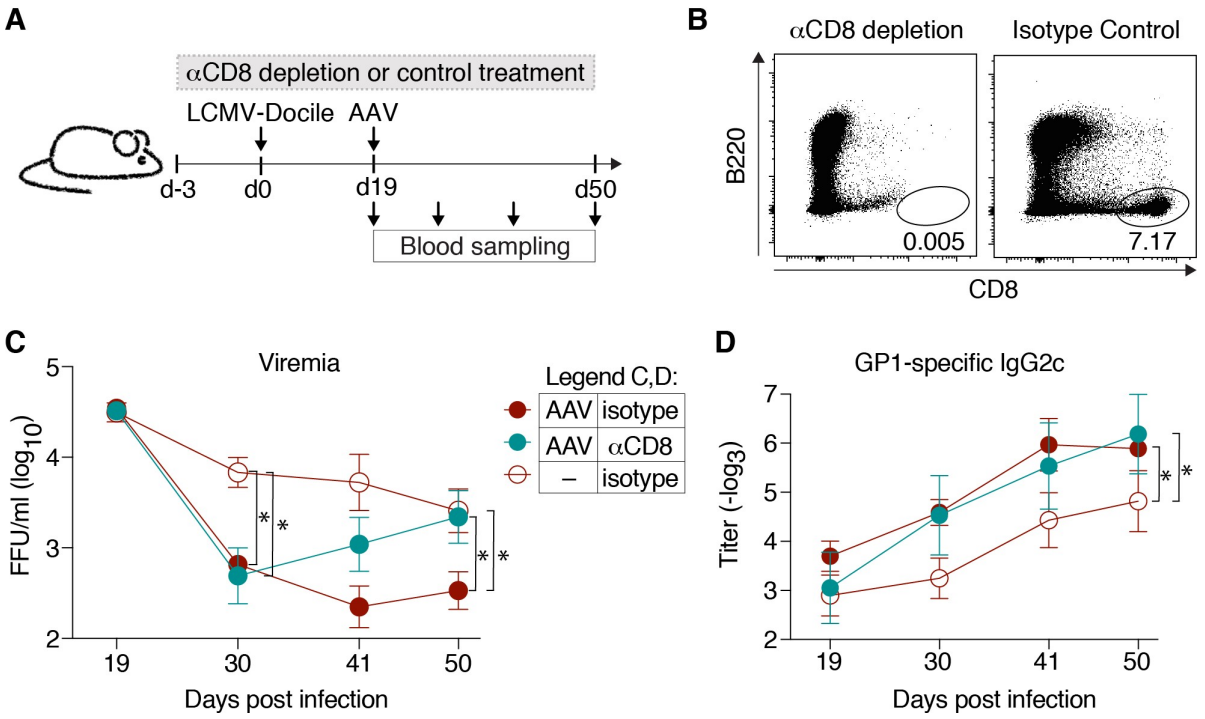

Figure 3: Therapeutic VAGD synergizes with CD8 T cells for sustained suppression of chronic LCMV infection.
(A) Mice were depleted of CD8 T cells from d-3 until d50 or were given isotype control antibody. On d0 they were infected with LCMV-Docile, AAV-KL25 therapy was administered on d19. (B) Representative FACS plots showing quasi-complete depletion of CD8 T cells in peripheral blood of anti-CD8a antibody-treated but not isotype control antibody-treated mice on d50 of the experiment (analogous results on d15 and d30). We monitored viremia (C) and host-derived GP-1-binding IgG2c titers in serum (D) over time. Symbols show the mean ± SEM of 5 mice (C-D). *N* = 2 (B-D). Data in (C-D) were analyzed by two-way ANOVA using group and time point of analysis (limited to post AAV-KL25, i.e. d30, d41, d50) as variables and the untreated group as reference for multiple comparisons using Dunnett's post-test to assess between-group differences at individual time points (C), or to compare curves overall (C,D). **p* < 0.05.

Figure 4

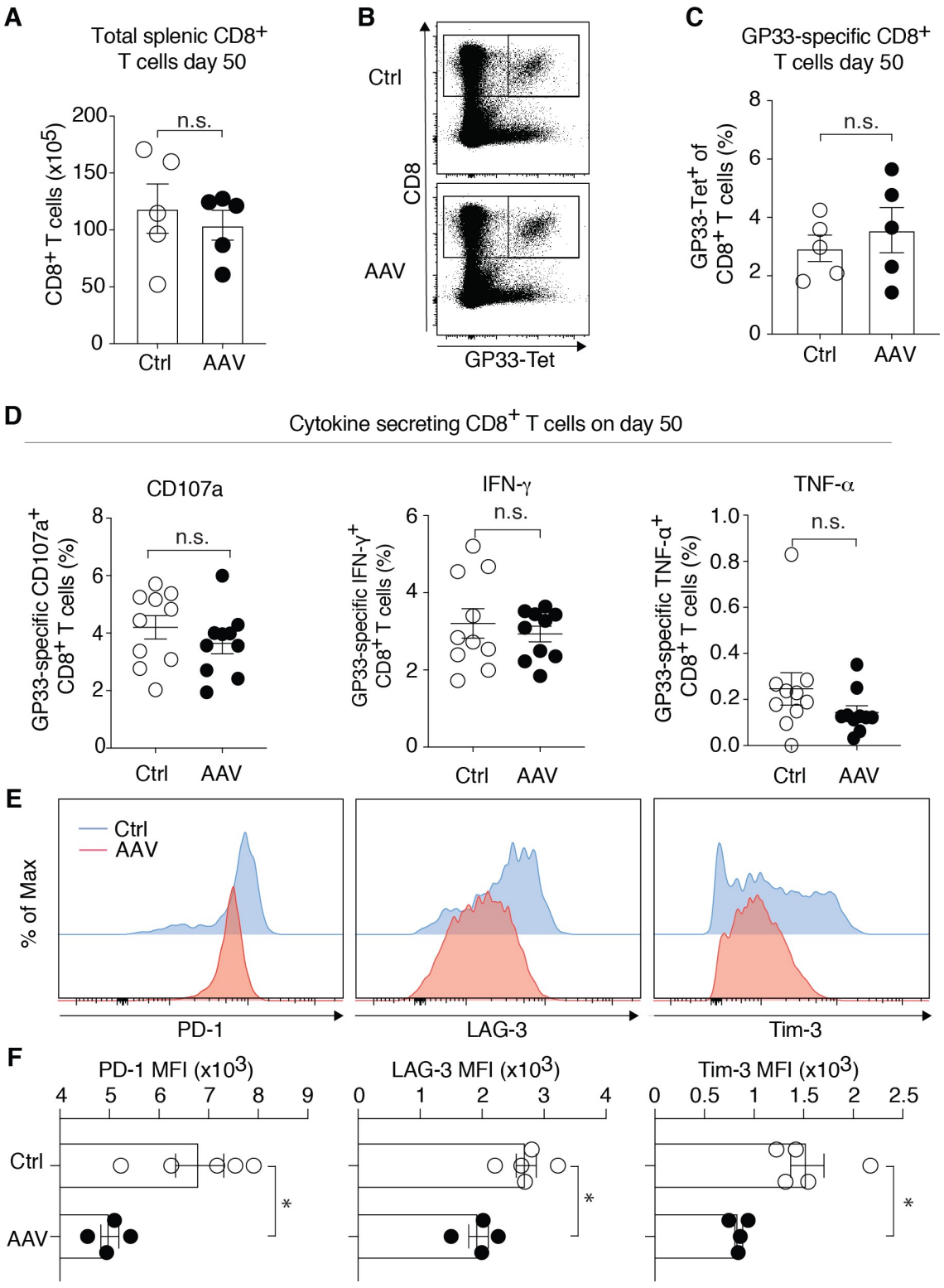
A
Total splenic CD8+ T cells day 50
CD8+ T cells (x10^5)
200
150
100
50
0
n.s.
Ctrl
AAV
B
Ctrl
AAV
CD8
GP33-Tet
C
GP33-specific CD8+ T cells day 50
GP33-Tet+ of CD8+ T cells (%)
8
6
4
2
0
n.s.
Ctrl
AAV
D
Cytokine secreting CD8+ T cells on day 50
CD107a
GP33-specific CD107a+ CD8+ T cells (%)
n.s.
IFN-γ
GP33-specific IFN-γ+ CD8+ T cells (%)
n.s.
TNF-α
GP33-specific TNF-α+ CD8+ T cells (%)
1.0
0.8
0.6
0.4
0.2
0.0
n.s.
Ctrl
AAV
E
Ctrl
AAV
% of Max
PD-1
LAG-3
Tim-3
F
PD-1 MFI (x10^3)
4 5 6 7 8 9
LAG-3 MFI (x10^3)
0 1 2 3 4
Tim-3 MFI (x10^3)
0 0.5 1 1.5 2 2.5
Ctrl
AAV
*
*
*

Figure 4: Therapeutic VAGD partially reverts CD8 T cell exhaustion.
We infected WT mice with LCMV-Docile, followed by AAV-KL25 or control (PBS) treatment on day 19 (compare Fig. 2A). On d50 we enumerated total $CD8^+$ T cells in spleen (A) and determined GP33-specific CD8 T cell frequencies using MHC class I tetramer staining (B,C). Representative FACS plots of AAV-KL25-treated (bottom) and control-treated mice (top) are shown in (B). We performed intracellular cytokine staining upon GP33 peptide stimulation to determine the frequency of cytolytic granule-releasing ($CD107a^+$), IFN-γ- and TNF-α -secreting CD8 T cells (D). GP33-tetramer-binding CD8 T cells were characterized for their expression levels of the inhibitory receptors PD-1, LAG-3 and Tim-3 (E,F). Representative histogram plots are shown in (E) and mean fluorescence intensity is displayed in (F). Bars in (A,C,F) represent the mean±SEM. Symbols in (A,C,D,F) represent individual mice. $N = 2$ (A-F). Data in (A,C,D,F) were analyzed by unpaired two-tailed Student's *t* test. $^*p < 0.05$. n.s.: $p \geqq 0.05$, not statistically significant.

Figure 5

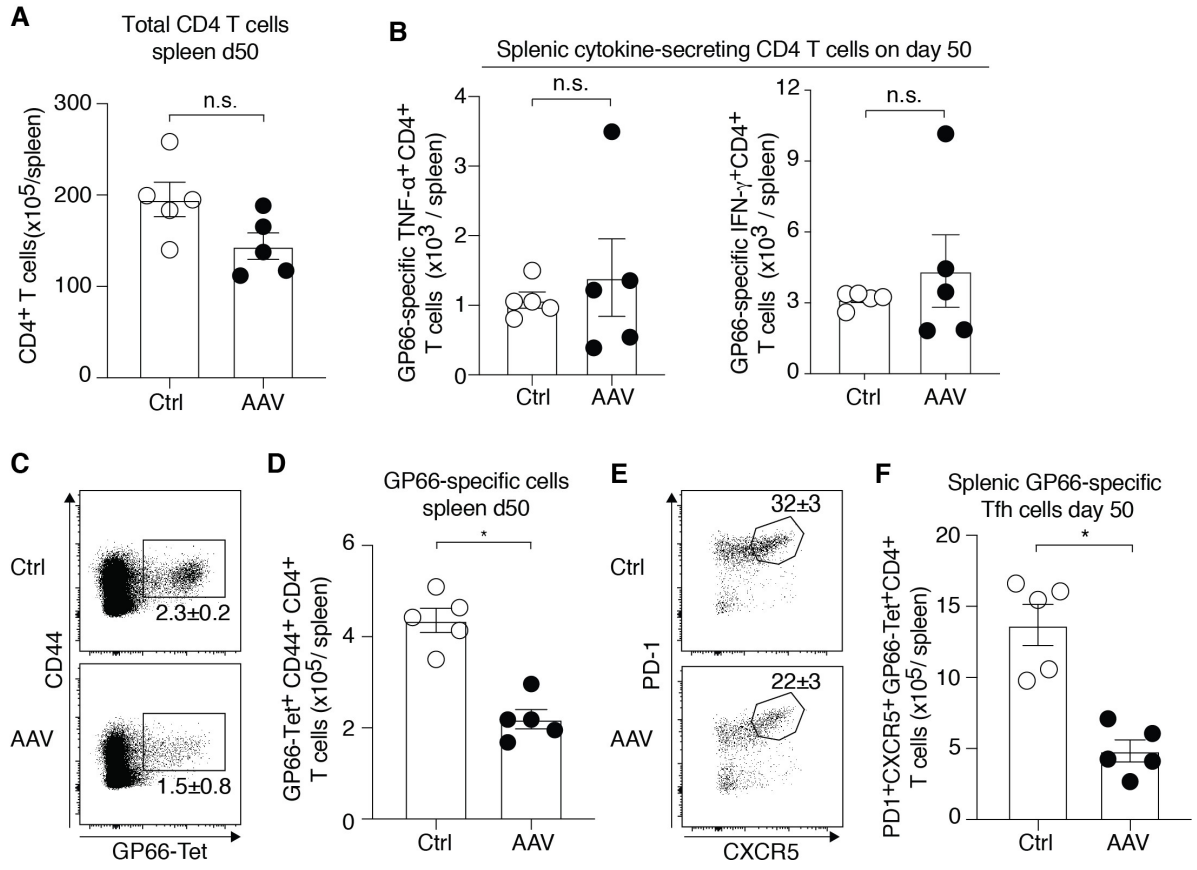

Figure 5: Therapeutic VAGD results in reduced numbers of LCMV-specific follicular T helper cells.
We infected WT mice with LCMV-Docile, followed by AAV-KL25 or control (PBS) treatment on day 19 (compare Fig. 2A). On d50 we enumerated total CD4$^+$ T cells in spleen (A) and determined the number of GP66-specific IFN-y- and TNF-α -secreting CD4$^+$ Th1 cells by intracellular cytokine assays (B). The total compartment of GP66-specific CD4 T cells was determined by MHC class II tetramer staining (C,D). Representative FACS plots from AAV-KL25-treated (bottom) and control-treated mice (top) are shown in (C). GP66-specific Tfh CD4$^+$ T cells (PD-1$^+$ CXCR5$^+$) were enumerated in (C,D) with representative FACS plots shown in (D). Bars show the mean±SEM, symbols in (A,B,D,F) represent individual mice. *N* = 2 (A-F). Data in (A,B,D,F) were analyzed by unpaired two-tailed Student's *t* test. *: $p < 0.05$. n.s.: p≧0.05, not statistically significant.

Figure 6

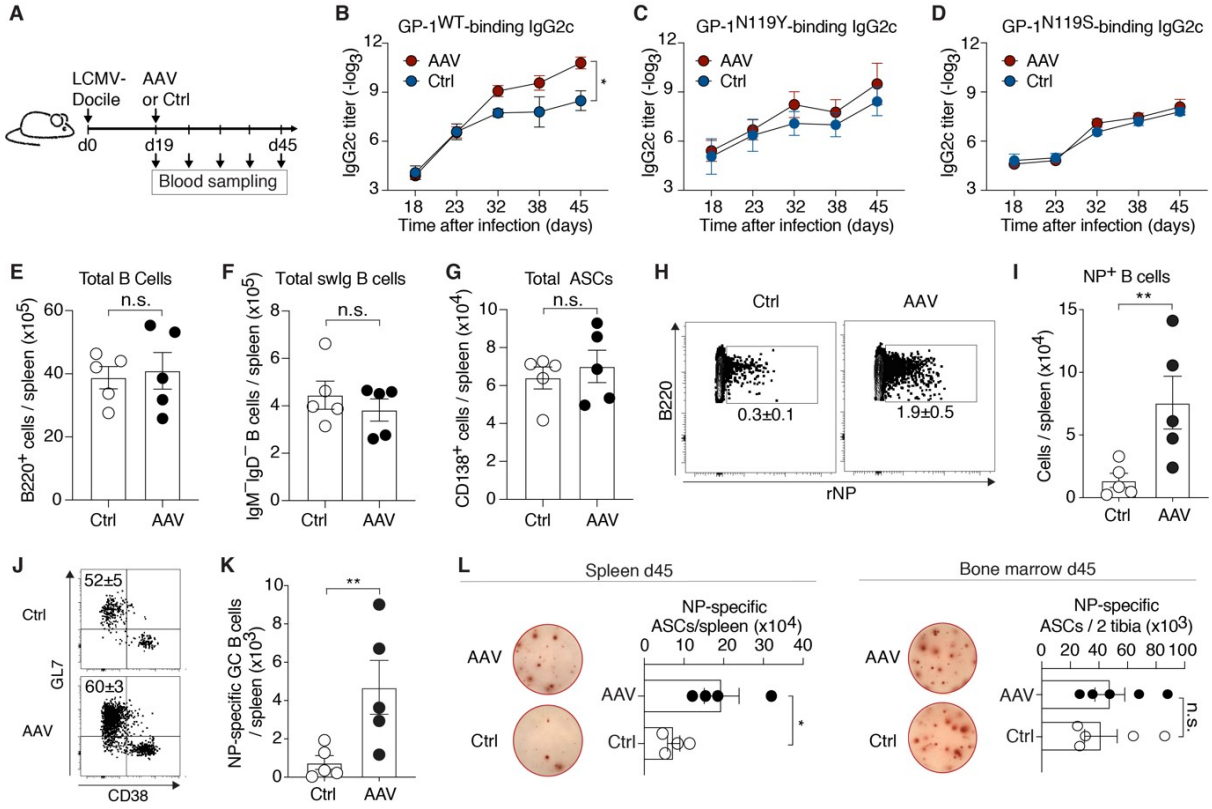

Figure 6: Therapeutic VAGD augments antiviral germinal center B cell and antibody-secreting cell response. We infected WT mice with LCMV-Docile on d0, AAV-KL25 was administered on d19 (A). We measured host-derived IgG2c responses to GP-1^{WT} (B), GP-1^{N119Y} (C) and GP-1^{N119S} (D) over time. On d50 we determined the total number of $B220^+$ B cells (E), swIg ($IgM^{neg}IgD^{neg}$) B cells (F) and $CD138^+$ ASCs in spleen (G). We enumerated swIg B cells ($B220^+$ $CD138^{neg}$ IgM^{neg} IgD^{neg} , Fig. S5) binding to recombinant LCMV-NP (rNP; H,I). Representative FACS plots of rNP binding are shown in (H). Within the population of rNP-binding swIg B cells we analyzed the representation of GC B cells ($GL7^+CD38^-$) and memory B cells ($GL7^-CD38^+$) (J; representative FACS plots are shown) and enumerated rNP-binding GC B cells (K). (L) LCMV NP-specific ASCs were enumerated in the spleen (left panel) and in bone marrow (BM, right panel) by ELISpot. Illustrative cell culture wells are shown. Symbols in (B-D) and bars in (E-G,I,K,L) display the mean±SEM of 5 mice, symbols in (E-G,I,K,L) show individual animals. *N* = 2 (B-L). Data in (B-D) were analyzed by two-way ANOVA using group and time point of analysis (limited to time points after AAV-KL25 treatment, i.e. d23, d32, d38 and d45) as variables with Dunnett's post-test to compare entire curves. Data in (E-G, I, K and L) were analyzed using unpaired two-tailed Student's *t* tests. **p* < 0.05; ***p* < 0.01; n.s.: p≧0.05, not statistically significant.

Figure S1

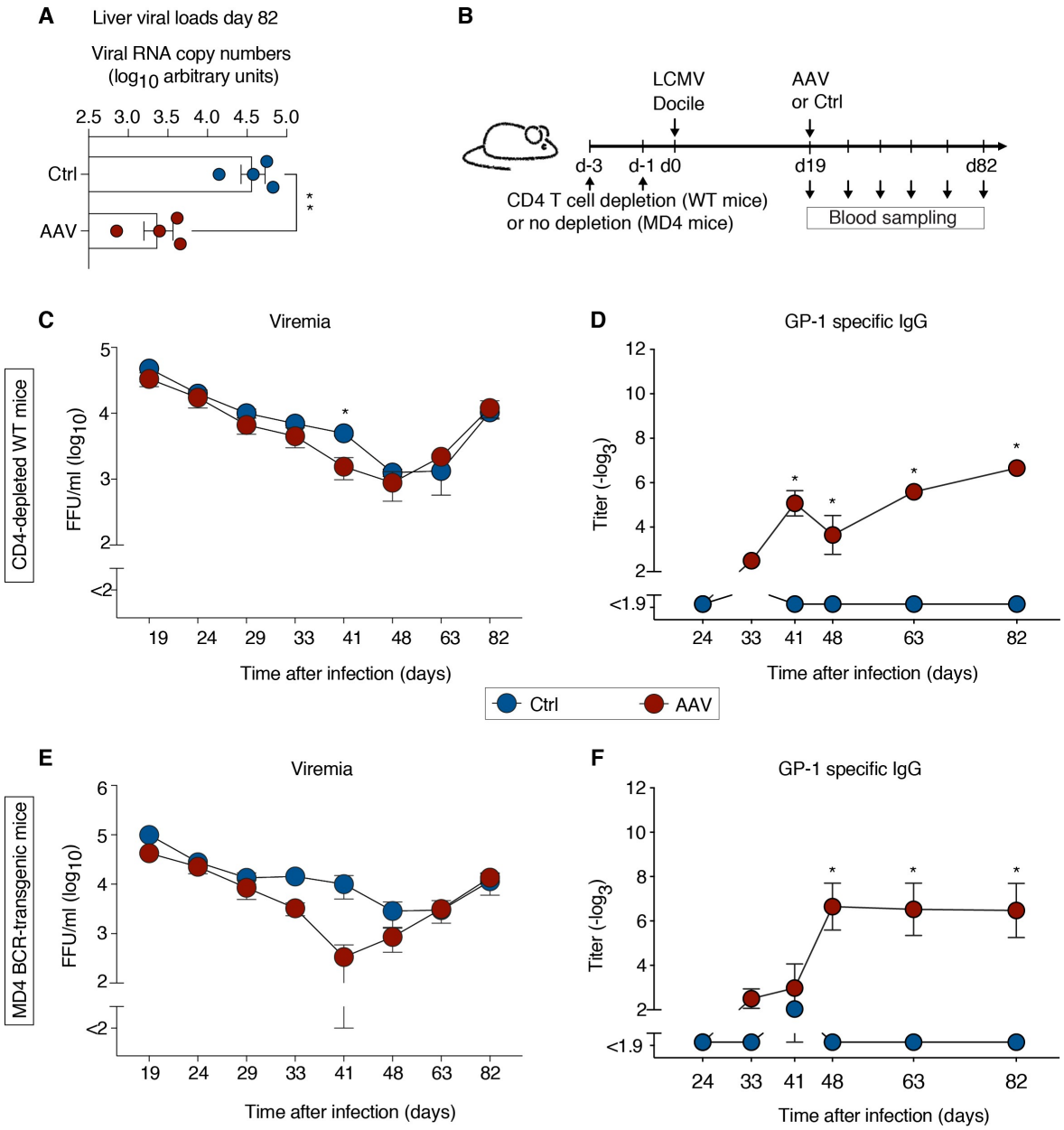

G

Occurrence of N119 KL25 escape mutation
(# mice with viral mutation / # mice tested)

Mouse genotype	AAV	Control
MD4	3/3	0/2
CD4-depleted	3/3	0/3

Figure S1: Therapeutic VAGD synergizes with host antibody responses and depends on CD4 T cells for sustained suppression of chronic infection.
(A) Arbitrary units of LCMV RNA copies in the livers of WT mice shown in Figure 2C were determined by TaqMan RT-PCR. (B) We depleted WT mice of CD4 T cells on d-3 and d-1 and left MD4 BCR-transgenic mice undepleted. Both groups of mice were infected with LCMV-DOC on d0, followed by AAV-KL25 therapy or control (PBS) on d19 (performed in parallel to the experimental groups displayed in Fig. 2). (C,D) Viremia was assessed on the indicated time points. (E,F) GP-1 specific antibody titers were determined by ELISA. (G) Occurrence of N119 escape mutations in AAV-KL25-treated and untreated CD4-depleted WT mice and undepleted MD4 mice (see also Supplementary Table I). Symbols represent the mean±SEM of 2 (control MD4 mice) to 3 mice (all other groups). *N* = 1 (C-F). Liver Viral RNA titers and d41 viremia titers were compared using unpaired two-tailed Student's *t* test (A,C,D), antibody titers by two-way ANOVA followed by Bonferroni's post-test for individual time points (E,F). **p* < 0.05; ***p* < 0.01; p≧0.05, not statistically significant.

Figure S2

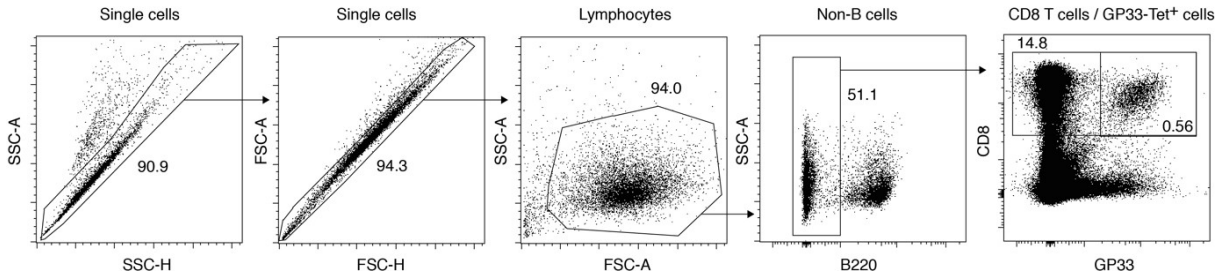

Figure S2: Flow cytometry gating strategy related to the analyses reported in Figures 3B and 4A-F.
Single cells were gated based on SSC-A and SSC-H followed by FSC-A and FSC-H. Subsequently, lymphocytes were gated according to their SSC-A / FSC-A profile and were further analyzed as displayed in Fig. 3B. For the analyses presented in Fig. 4A-G we next excluded $B220^+$ cells and then determined $CD8^+$ single-positive and $CD8^+GP33\text{-}tet^+$ double-positive cells, to calculate the percentage of GP33-tet-binding cells amongst $CD8^+$ cells.

Figure S3

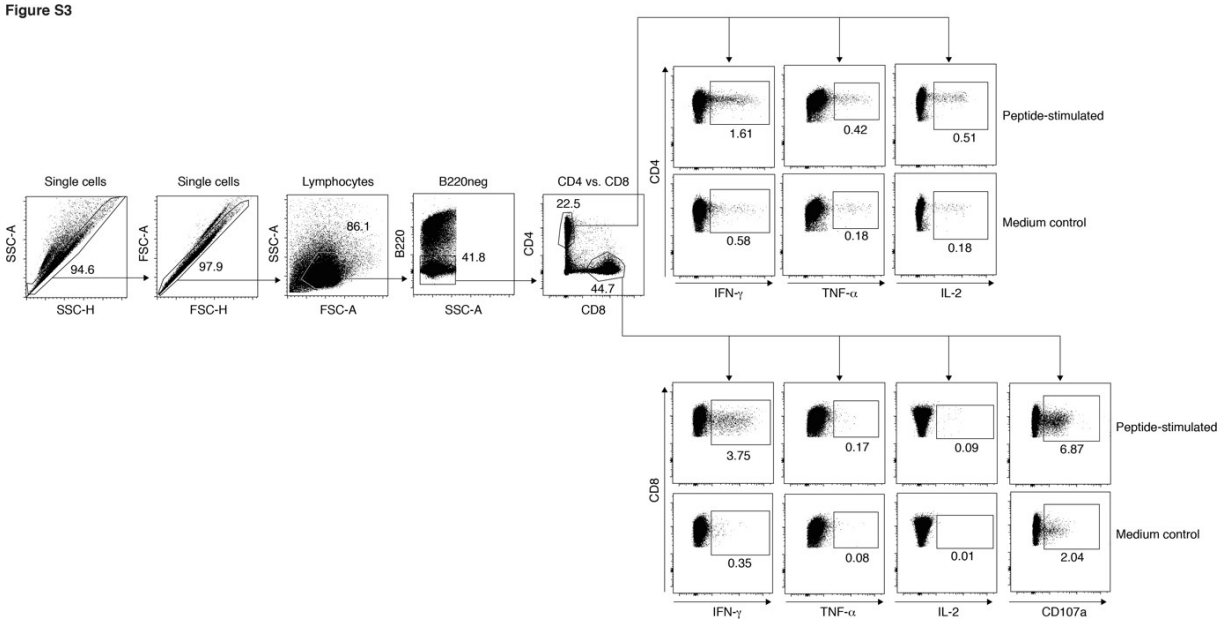

Figure S3: Flow cytometry gating strategy related to the analyses reported in Figure 4D and Figure 5F.
Single cells were gated based on SSC-A and SSC-H followed by FSC-A and FSC-H. Subsequently, lymphocytes were gated according to their SSC-A / FSC-A profile. After exclusion of $B220^+$ cells $CD8^+$ and $CD4^+$ single-positive cells were identified. CD107a surface expression and intracellular IFN-y, TNF-α and IL-2 levels were determined for either peptide-stimulated or medium control-stimulated $CD4^+$ and $CD8^+$ T cell populations were further gated for IFN-y, TNF-α and IL-2, respectively for both peptide stimulated and medium control samples as indicated. The difference between peptide- and medium-stimulated responses are reported in Figure 4D and F5 for $CD8^+$ and $CD4^+$ T cells, respectively.

Figure S4

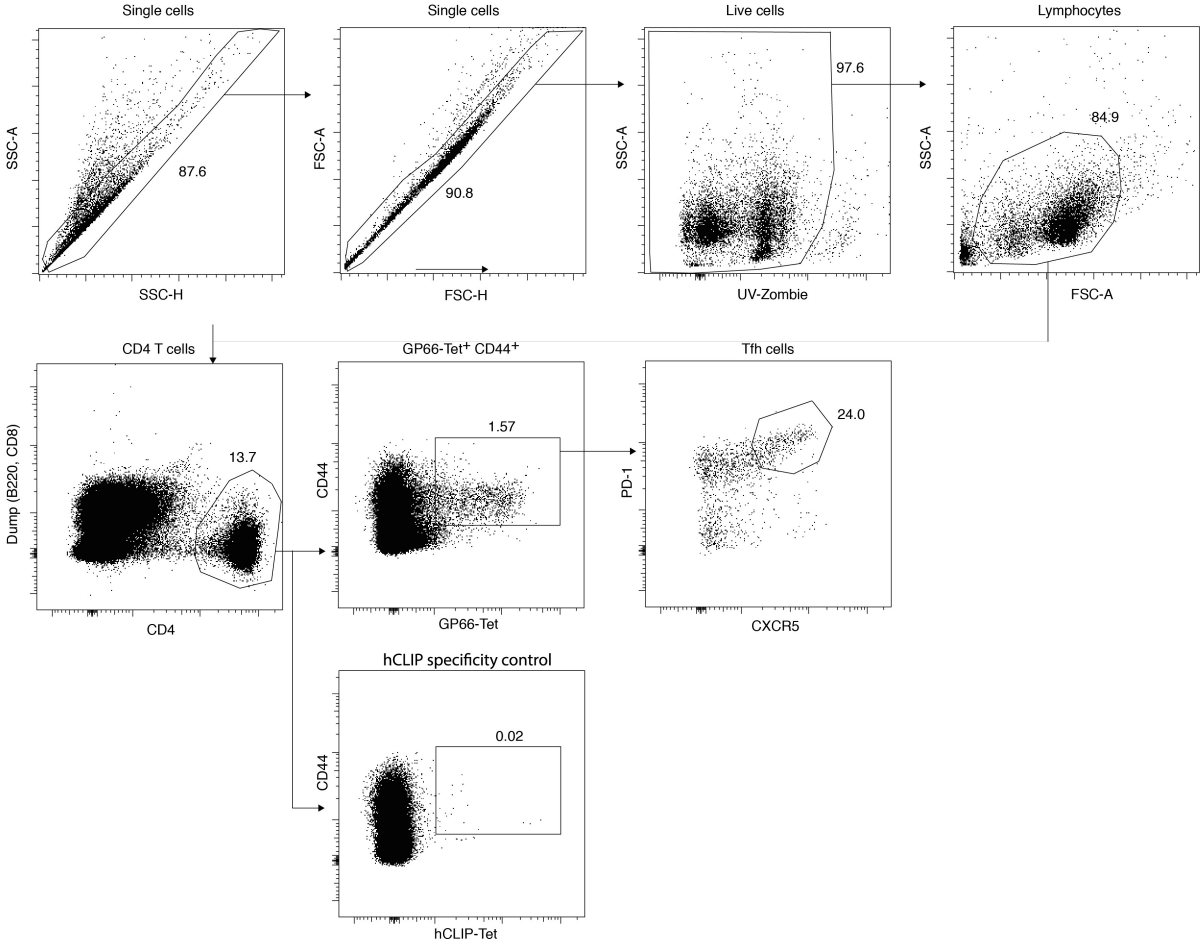

Figure S4: Flow cytometry gating strategy related to the analyses reported in Figure 5A-F.
Single cells were gated based on SSC-A and SSC-H followed by FSC-A and FSC-H. Subsequently, Zombie-UV positive (dead cells) were excluded and lymphocytes identified based on the cells' SSC-A / FSC-A profile. $CD4^+$ T cells were identified as $CD4^+CD8^-B220^-$ cells within the lymphocyte population. Then, the GP66-specific ($CD44^+$GP66-Tet^+) $CD4^+$ population was gated. hCLIP-Tet staining served as specificity control. Finally, $CXCR5^+PD\text{-}1^+$ cells within the $CD44^+$GP66-Tet^+ CD4 T cell population were identified as Tfh cells.

Figure S5

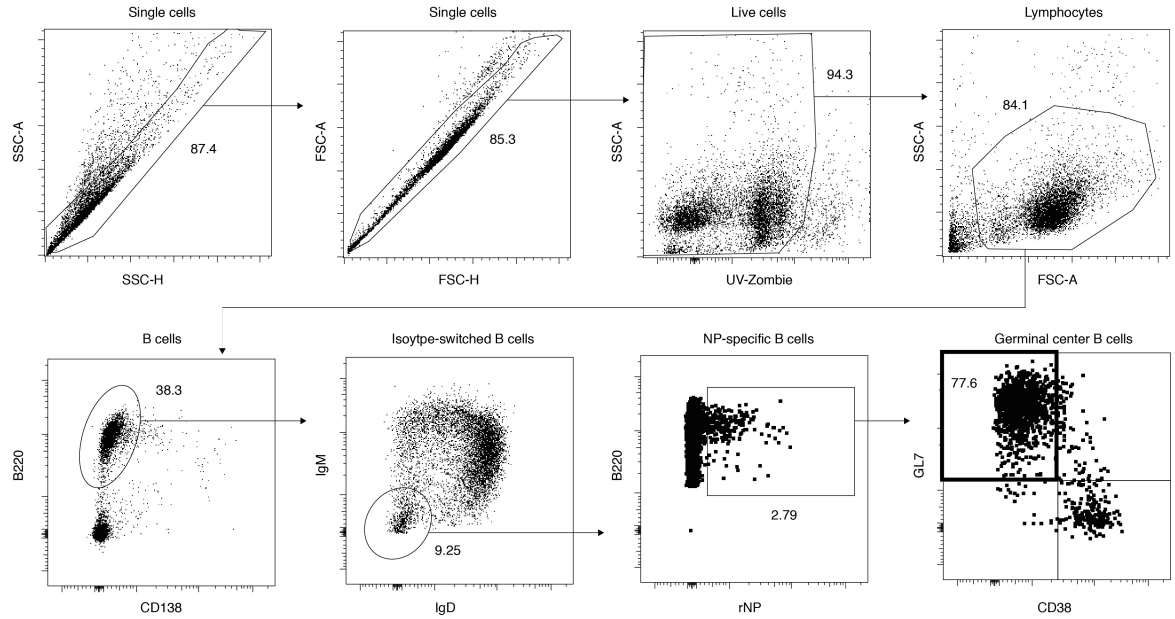

Figure S5: Flow cytometry gating strategy related to the FACS analyses reported in Figure 6E-K.
Single cells were gated based on SSC-A and SSC-H followed by FSC-A and FSC-H. Subsequently, Zombie-UV positive (dead cells) were excluded and lymphocytes gated based on the cells' SSC-A / FSC-A profile. Amongst the lymphocytes, B cells ($B220^{+}CD138^{neg}$) and, as a subset, isotype-switched cells (swIg; $IgM^{-}IgD^{-}$) were identified. rNP-binding cells amongst swIg B cells were gated and within this population we differentiated GC cells ($GL7^{+}$ $CD38^{-}$).

General discussion

We aimed to understand the role of antiviral B cells in chronic viral infections in greater detail than before. Such studies are essential to gain more knowledge about immune responses to chronic pathogens and may give us a clue how to design successful therapies and vaccines to tackle persistent infections. Our data showed that high-affinity antiviral B cells undergo deletion in response to persistent antigen stimulation. The process was IFN-I- and inflammation-independent and was the result of terminal differentiation of the antiviral B cells into short-lived ASCs. To our knowledge, this is the first time such type of perturbation of the B cell compartment in chronic infection has been described. It is a valuable discovery that may pave the way to new vaccine strategies to fight chronic infectious diseases.

We have established a strategy to engraft precursor-like numbers of KL25 B cells [291, 292, 407] in mouse spleen and follow them during infection using congenic markers CD45. Physiological-like engraftments of KL25 B cells, close to VRCO1 precursor numbers in HIV [292, 472] and the time of engrafting were both designed to mimics the interaction between newly-egressed bone marrow B cell emigrants [200, 472] [324], challenged with persistent antigen. This setting allows us to identify individual antiviral B cell clones being recruited to GCs as the infection progresses to chronic phase rather than focusing on the early, acute phase of the infection.

We observe a late deletion of virus-specific B KL25 B cells that seems to be driven by two parameters: i) high BCR affinity to the LCMV GP and ii) chronic exposure to antigen. [389-392]. In contrast to early decimation [200], the mechanism of late deletion is independent of IFN-I-inflammation. Overexpression of plasma cell-related surface markers and transcription factors indicates that late deletion is a result of B cells terminal differentiation into short-lived ASCs. The observed late clonal deletion of B cells, described in this thesis, may explain the late appearance of nAbs against LCMV [175, 193, 320], alongside with destroyed lymphoid organization [327] and IFN-mediated decimation of virus-specific B cells [155, 351, 352].

Our study showed that there was only limited differential gene regulation between monoclonal B cells, challenged with chronic pathogen, and those, challenged with acute strain of LCMV. Usp18, a ubiquitin-specific peptidase and a potent inhibitor of interferon signaling [382] [473], was upregulated in chronic LCMV in comparison to acute infection. The absence of USP18 leads to stronger IFN-I signaling which, in turn, inhibits viral replication and antigen presentation. As a consequence, *Usp18 -/-* mice survive intracerebral LCMV and VSV challenges, while WT mice do not [384]. Moreover, interferonopathy was prevented by Usp18 in mouse microglial cells [474]. Many antiviral genes, cytokines, chemokines and antigen presenting genes are expressed in the absence of Usp18, leading to better viral control [475]. The overexpression of these IFN-I-stimulated molecules, however, may drive pathological immune overactivation [476]. *Usp18* plays a role at balancing out this malignant response to infection, as described for chronic HCV [477]. The other two overexpressed genes in response to chronic infection in our study are *Ifi27* and *Ifi27l2a*, Interferon-stimulated genes (ISGs). These ISGs have been associated with protection against viral infection (anti-viral proteins) and with cancer [478-480]. Ifi27l2a plays a role in restricting West Nile virus propagation in the brain through inhibition of viral translation and Ifi27 (ISG12) is an important modulator of innate immune responses in murine sepsis model [481]. The simultaneous expression of these genes may indicate the unique features of B cells in chronic infection. It is plausible that upon IFN-I production in response to invading pathogens, cells react by ISGs upregulation, a process which may result in death for the B cells via terminal differentiation [200, 351, 352] or interferonopathy in microglia [474]. Usp18 counteracts this process by inhibiting IFN-I downstream signaling. Possibly, it is a matter of timing and dose of IFN-I which dictate for the fate of B cell in chronic infection. We could speculate that if the cells sense too much IFN-I, as at the onset of chronic Clone 13 infection [200], they have little time to upregulate protective inhibitors of interferon signaling, such as Usp18, and succumb to terminal differentiation and death. If the dose of IFN-I is relatively low, as in our RNAseq experiment, the B cells may not suffer the interferon-induced shock and may be fit enough to induce the IFN-I counteracting genes such as Usp18.

Contrary to our observations, Staupe *et al.* (2020) reported substantial differential gene expression among LCMV-specific B cells, recovered from chronic or acute LCMV infection [409]. The greatest difference was detectable at day 15 in GC B cells. At day 45, however, the antiviral B cells from either chronic or acute infection were not transcriptionally different anymore. Combined, these data suggest that murine LCMV-specific B cells do not undergo a classical “exhaustion” pathway, defined by phenotypic and functional changes as their T cell counterparts [410] [411]. On the contrary, it seems that with the progression of chronic LCMV the humoral immune responses increase, whereas T cell responses undergo exhaustion. Recent papers show that chronic LCMV infection results in successful GC reaction, culminating in a late nAbs production, while acute infection rarely produce any neutralizing antibody titer [155, 482]. One main observation is, however, that nAbs arise only once virus is suppressed i.e., when antigenic burden is low after day 40. Taken together, these data suggest that as long viremia is of a high titer, the B cell clones with high affinity the viral GP can neither survive long enough,

nor could they expand sufficiently in order to exert antibody-mediated control on the pathogen. We speculate that in the late phase of chronic infection, non-neutralizing antibodies start to exert pressure on the virus, leading to escape mutations in viral GP [175]. Effectively, at this time point the viral loads of the founder virus may have fallen to very low titers, prompting the survival and expansion of those B cells clones, carrying a high-affinity BCR against that founder. Once these high-affinity clones are able to survive and produce nAbs, the infection may be greatly suppressed. It is possible that many rounds of antibody maturation such as this lead to successful clearance of all viral quasispecies from host. One could imagine that these are the processes that underline to development of broad neutralizing Abs in HIV as it was shown that length of infection, or the time of antibody maturation, is a main correlate to develop neutralizing breath [201].
Our observations may explain why the mammalian immune system is failing to clear persistent-prone pathogens. It is possible that this is a coping mechanism for a fast production of antibodies upon infection, resulting, however, in the specific loss of the B cells clone with neutralizing affinity. From evolutionary standpoint, when challenged with life-threatening acute infection, a bias towards ASCs differentiation of high-affinity B cells clones that can rapidly suppress the pathogen, would seem highly beneficial for the host. Conversely, such a differentiation bias jeopardizes the sustainability of adequate humoral response in chronic viral infections. Our lab showed that this bias may occur throughout the chronic infection. First, this occurs at the very onset of the infection when IFN-I drives terminal differentiation of all antiviral B cells, independent of their affinity for the virus and causes dramatic obliteration of the B cell compartment, termed decimation [351, 352, 483]. The cells are eventually reconstituted by newly-egressed bone marrow B cell emigrants [200, 472] [324] and a second wave of antiviral B cells deletion begins, this time targeting solely the B cell clones carrying BCR of neutralizing affinity for the dominant circulating viral variant. The late clonal deletion of B cells seems to continue as long as viremia is above a certain threshold. Interestingly, late deletion “spares” the low- and average-affinity antiviral B cells clones, as those accumulate throughout the GC reaction in chronic infection [155, 482]. As mentioned above, pressure from those B cell clones may eventually curb viremia and allow B cell clones of high BCR affinity to survive.

Outlook

KL25 antibody treatment early during chronic viral infection: This work showed that chronic antigen exposure is one of the driving mechanisms for late deletion of high-affinity antiviral B cells. We also showed that high-affinity B cells are selectively maintained in acute infection and vaccination. In order to corroborate our results, we could test the survival of KL25 B cells upon suppression of viral loads by passive KL25 antibody administration. We hypothesize that early decrease in viral loads would prevent terminal ASCs differentiation of high-affinity KL25 B cells and would result in their survival.
Preventing the differentiation of KL25 B cells into short lived ASCs: As a follow-up of our Blimp-1 reporter we could test the differentiation of KL25 B cells lacking this transcription factor. In short, in Figure 7 we observed high expression of Blimp-1 in KL25 cells in rCl13/WE group, whereas rCl13/N119S infection caused only limited upregulation of Blimp-1. We know that Blimp-1 expression is required for the differentiation of KL25 B cells into ASCs as it acts as a master transcription factor in that process [217, 218, 231, 236, 484]. We hypothesize, therefore, that KL25 cells which lack the ability of differentiating into plasmablasts/plasma cells would be able to survive chronic rCl13/WE infection. To this end, we plan to Blimp-1-KO KL25 cells as described in [217]. We hypothesize that the inability of the KL25 cells to differentiate into short-lived ASCs due to the functional KO Blimp-1 TF should result in maintenance of this cell population upon transfer in chronic rCl13/WE recipients. This key experiment would provide us with mechanistic insides of the late deletion of high-affinity antiviral B cells.
Unmutated ancestor of KL25: We are in the process of engineering a KI mouse which carries a lower affinity BCR for the WE glycoprotein, KL25 Low Affinity (KL25^{LA}). We can transfer these KL25^{LA} cells as “low affinity” donor cells in Cl13/WE chronic infection and follow their differentiation. We hypothesize that, due to the low binding of the KL25^{LA} BCR to the viral GP, the KL25^{LA} cells will not differentiate into short-lived ASCs and will be maintained in rCl13/WE-infected recipient
Sequencing viruses and cells to look at viral escape mutants or rare cellular adaptations of the KL25 cells: We suspect that, in the rare event of survival of KL25 cell in chronic rCl13/WE infection, either the virus or the B cells mutated rapidly and thus allowed a low-affinity interaction between KL25 BCR and WE GP. If cellular, the escape would present as mutations in the heavy and light chains of the KL25 BCR as shown in [155]. The HC and LC could be co-expressed as natural antibody and tested for its capacity to neutralize virus with methods well-established in lab.

Viral escape mutations could also possibly arise. In order to prevent late deletion of the KL25, the majority of the virus quasispecies would need to accumulate mutations in the GP WE, like the ones we use throughout this manuscript, N119S, N119D and some in the proximity such as N121K [176]. It remains an open question if this is possible in a timely manner, allowing the KL25 B cells to survive.

Limitations of the study

While extremely valuable immunological tool for modelling chronic infections that occur in man, "chronic" LCMV Clone 13 and Docile are spontaneously cleared from adult infected C57/B6 mice which we used in our research. HIV in man is virtually a lifelong infection due to both the nature of the virus and the host's immune system. I good measure of caution is required, therefore, when interpreting biological events taking place in LCMV model.

Related work

Our work would not have been possible without the development of BCR-engineered mouse strains. We performed physiological-like engraftments of KL25 B cells, close to VRCO1 precursor numbers in HIV [292, 472]. Engrafting the KL25 cells after infection mimics the interaction between newly-egressed bone marrow B cell emigrants [200, 472] [324] and the virus.

The current work is tightly inked to other studies performed in the lab, addressing various aspects of humoral immunity against chronic viral infections.

We showed that antiviral B cells can be rescued from IFN-I-decimation by inducing Tfh virus-specific response in the manuscript by Narr *et al*. Logically, we could argue that CD4-mediated rescue of KL25 B cells may apply in the newly-described late deletion of high-affinity KL25 B cells which is the focus of this thesis work. Unfortunately, one limitation of our study was its focus on B cells without simultaneous analysis of the CD4+ compartment. During the past years, however, a few studies have documented the essential contribution of Tfh cells to GC responses during chronic LCMV infection and viral control [131, 468, 485]. We know from the work by Narr *et al.* that GP66-specific CD4+ T cells are induced early after immunization with *Listeria monocytogenes* (LM), expressing LCMV-derived glycoprotein 61-80, for short LM61. Previous work showed that LCMV-specific Tfh (SMARTA) cells are induced early after Cl13 infection, with 10E5 SMARTA cells at day 9 post-infection [469]. A week into the chronic infection, we could assume that LCMV-specific Tfh exist in sufficient numbers to provide timely help to the cognate LCMV-specific B cells that we engraft and do not limit the immune response [486, 487]. Moreover, we could assume with high certainty that there is no significant difference between the T help induced in chronic rCl13/WE infection compared to chronic rCl13/N119S infection because both viruses have absolutely identical T cell epitopes. Chronic rCl13 infection, regardless of carrying wt or mutant GP, results in similar viral loads and persist for the same amount of time, suggesting that the T help response would be induced with similar potency across experimental groups. One could conclude from these findings, that despite existing Tfh help, our high-affinity precursor-like B cells are still deleted late in the course of the chronic LCMV infection due to overwhelming activation. This is in a strong contrast to the work of Narr *et al*., again showing that early decimation and late deletion of KL25 B cells are two entirely different pathways for subversion of the host's immune response to persistent pathogens.

VAGD success at resolving chronicity in LCMV is yet another powerful tool to fight chronic pathogens, as exemplified by the work of Ertuna et al. VAGD therapy could improve the deleterious outcome for high-affinity KL25 B cells in chronic viral infection, described in this thesis. Timely administration of AAV-KL25 could potentially prevent deletion of the adoptively engrafted cells. We could test the VAGD therapy in resolving viremia early during infection and preventing deletion of high-affinity KL25 B cells. The observations, made by Ertuna *et al*., on improved GC responses upon VAGD therapy may be a result of the survival of LCMV-specific high-affinity B cells clones from the endogenous B cells compartment. As we discussed, reducing viral loads relatively early in the chronic infection may reduce the chances for high-affinity antiviral B cells to undergo late deletion. This survival should reflect in improved GC responses and antiviral antibodies, as shown by Ertuna *et al.*, thus indirectly confirming our observations on the deletion of high-affinity B cells in the late phase of chronic viral infection.

In conclusion, our study offers new insights in the field of chronic infectious diseases and may explain some of the immune perturbations associated with chronic viral diseases. As mentioned before, detailed knowledge about B cells' role in chronic infections is still limited, despite the best efforts. We offer a new mechanism of subversion of the immune system in the context of persistent infection, namely the clonal deletion of antiviral B cells. Understanding the humoral perturbations, such as the one described in this thesis, could provide us with new strategies to prevent and cure chronic infections. Such knowledge may be implemented into vaccine design for chronic pathogens, a field of vaccinology which proved to be extremely challenging.

General References

This reference list contains all references used in the manuscript “Selective deletion of high-affinity B cells in the late phase of chronic viral infection”, as well as in the General Introduction and General Discussion of this thesis.

Websites

https://www.nobelprize.org/prizes/medicine/1996/summary/ ,accessed on 05.May.2021

https://www.nobelprize.org/prizes/medicine/2018/press-release/, accessed on 14.May.2021

World Health Organization (WHO)

a. https://www.who.int/health-topics/hiv-aids/#tab=tab_1
b. https://www.who.int/news-room/fact-sheets/detail/hepatitis-b
c. https://www.who.int/news-room/fact-sheets/detail/hepatitis-c

1. Charrel, R.N. and X. de Lamballerie, *Arenaviruses other than Lassa virus.* Antiviral Res, 2003. **57**(1-2): p. 89-100.
2. Tesh, R.B., et al. , *Field studies on the epidemiology of Venezuelan hemorrhagic fever: implication of the cotton rat Sigmodon alstoni as the probable rodent reservoir.* Am J Trop Med Hyg, 1993. **49**(2): p. 227-35.
3. Mills, J.N., et al. , *Prevalence of infection with Junin virus in rodent populations in the epidemic area of Argentine hemorrhagic fever.* Am J Trop Med Hyg, 1994. **51**(5): p. 554-62.
4. Vanzee, B.E., et al. , *Lymphocytic choriomeningitis in University Hospital personnel: Clinical features.* The American Journal of Medicine, 1975. **58**(6): p. 803-809.
5. Dräger, S., et al. , *Lymphocytic choriomeningitis virus meningitis after needlestick injury: a case report.* Antimicrob Resist Infect Control, 2019. **8**: p. 77.
6. Brisse, M.E. and H. Ly, *Hemorrhagic Fever-Causing Arenaviruses: Lethal Pathogens and Potent Immune Suppressors.* Frontiers in immunology, 2019. **10**: p. 372-372.
7. Zinkernagel, R.M. and P.C. Doherty, *Immunological surveillance against altered self components by sensitised T lymphocytes in lymphocytes choriomeningitis.* Nature, 1974. **251**(5475): p. 547-548.
8. Zinkernagel, R.M. and P.C. Doherty, *Restriction of in vitro T cell-mediated cytotoxicity in lymphocytic choriomeningitis within a syngeneic or semiallogeneic system.* Nature, 1974. **248**(5450): p. 701-702.
9. Blaskovic, P.J. and M.S. Mahdy, *Tacaribe-Vero-electron microscopy: model for laboratory diagnosis of arenavirus infection.* Can Med Assoc J, 1978. **118**(10): p. 1193-4.
10. Auperin, D.D., R.W. Compans, and D.H. Bishop, *Nucleotide sequence conservation at the 3' termini of the virion RNA species of New World and Old World arenaviruses.* Virology, 1982. **121**(1): p. 200-3.
11. Salvato, M., E. Shimomaye, and M.B.A. Oldstone, *The primary structure of the lymphocytic choriomeningitis virus L gene encodes a putative RNA polymerase.* Virology, 1989. **169**(2): p. 377-384.
12. Young, P.R. and C.R. Howard, *Fine Structure Analysis of Pichinde Virus Nucleocapsids.* Journal of General Virology, 1983. **64**(4): p. 833-842.
13. Hass, M., et al. , *Mutational Analysis of the Lassa Virus Promoter.* Journal of Virology, 2006. **80**(24): p. 12414.
14. Perez, M., R.C. Craven, and J.C. de la Torre, *The small RING finger protein Z drives arenavirus budding: Implications for antiviral strategies.* Proceedings of the National Academy of Sciences, 2003. **100**(22): p. 12978.

15. Auperin, D.D., M. Galinski, and D.H.L. Bishop, *The sequences of the N protein gene and intergenic region of the S RNA of pichinde arenavirus.* Virology, 1984. **134**(1): p. 208-219.
16. Bishop, D.H.L., *Arenaviruses have ambisense S RNA.* Medical Microbiology and Immunology, 1986. **175**(2): p. 61-62.
17. Salvato, M.S. and E.M. Shimomaye, *The completed sequence of lymphocytic choriomeningitis virus reveals a unique RNA structure and a gene for a zinc finger protein.* Virology, 1989. **173**(1): p. 1-10.
18. Buchmeier, M.J., et al. , *Site-specific antibodies define a cleavage site conserved among arenavirus GP-C glycoproteins.* Journal of Virology, 1987. **61**(4): p. 982.
19. Kunz, S., et al. , *Mechanisms for lymphocytic choriomeningitis virus glycoprotein cleavage, transport, and incorporation into virions.* Virology, 2003. **314**(1): p. 168-178.
20. Lenz, O., et al. , *The Lassa virus glycoprotein precursor GP-C is proteolytically processed by subtilase SKI-1/S1P.* Proceedings of the National Academy of Sciences, 2001. **98**(22): p. 12701.
21. Wilson, S.M. and J.C.S. Clegg, *Sequence analysis of the S RNA of the African Arenavirus Mopeia: An unusual secondary structure feature in the intergenic region.* Virology, 1991. **180**(2): p. 543-552.
22. Meyer, B.J. and P.J. Southern, *Concurrent sequence analysis of 5' and 3' RNA termini by intramolecular circularization reveals 5' nontemplated bases and 3' terminal heterogeneity for lymphocytic choriomeningitis virus mRNAs.* Journal of Virology, 1993. **67**(5): p. 2621.
23. Meyer, B.J. and P.J. Southern, *Sequence heterogeneity in the termini of lymphocytic choriomeningitis virus genomic and antigenomic RNAs.* Journal of virology, 1994. **68**(11): p. 7659-7664.
24. Tortorici, M.A., et al. , *Arenavirus nucleocapsid protein displays a transcriptional antitermination activity in vivo.* Virus Research, 2001. **73**(1): p. 41-55.
25. Pinschewer, D.D., M. Perez, and J.C. de la Torre, *Dual role of the lymphocytic choriomeningitis virus intergenic region in transcription termination and virus propagation.* Journal of virology, 2005. **79**(7): p. 4519-4526.
26. Singh, M.K., et al. , *Analysis of the genomic l rna segment from lymphocytic choriomeningitis virus.* Virology, 1987. **161**(2): p. 448-456.
27. Southern, P.J., et al. , *Molecular characterization of the genomic S RNA segment from lymphocytic choriomeningitis virus.* Virology, 1987. **157**(1): p. 145-155.
28. Garcin, D. and D. Kolakofsky, *A novel mechanism for the initiation of Tacaribe arenavirus genome replication.* Journal of virology, 1990. **64**(12): p. 6196-6203.
29. Raju, R., et al. , *Nontemplated bases at the 5' ends of Tacaribe virus mRNAs.* Virology, 1990. **174**(1): p. 53-9.
30. Olschewski, S., S. Cusack, and M. Rosenthal, *The Cap-Snatching Mechanism of Bunyaviruses.* Trends in Microbiology, 2020. **28**(4): p. 293-303.
31. Iwasaki, M., et al. , *Efficient Interaction between Arenavirus Nucleoprotein (NP) and RNA-Dependent RNA Polymerase (L) Is Mediated by the Virus Nucleocapsid (NP-RNA) Template.* Journal of virology, 2015. **89**(10): p. 5734-5738.
32. Pinschewer, D.D., M. Perez, and J.C. de la Torre, *Role of the Virus Nucleoprotein in the Regulation of Lymphocytic Choriomeningitis Virus Transcription and RNA Replication.* Journal of Virology, 2003. **77**(6): p. 3882-3887.

33. Fuller-Pace, F.V. and P.J. Southern, *Detection of virus-specific RNA-dependent RNA polymerase activity in extracts from cells infected with lymphocytic choriomeningitis virus: in vitro synthesis of full-length viral RNA species.* Journal of virology, 1989. **63**(5): p. 1938-1944.
34. Garcin, D. and D. Kolakofsky, *Tacaribe arenavirus RNA synthesis in vitro is primer dependent and suggests an unusual model for the initiation of genome replication.* Journal of virology, 1992. **66**(3): p. 1370-1376.
35. Kranzusch, P.J. and S.P.J. Whelan, *Architecture and regulation of negative-strand viral enzymatic machinery.* RNA biology, 2012. **9**(7): p. 941-948.
36. Leung, W.C., M.F. Leung, and W.E. Rawls, *Distinctive RNA transcriptase, polyadenylic acid polymerase, and polyuridylic acid polymerase activities associated with Pichinde virus.* Journal of virology, 1979. **30**(1): p. 98-107.
37. Salvato, M.S., et al. , *Biochemical and immunological evidence that the 11 kDa zinc-binding protein of lymphocytic choriomeningitis virus is a structural component of the virus.* Virus Res, 1992. **22**(3): p. 185-98.
38. Strecker, T., et al. , *Lassa virus Z protein is a matrix protein and sufficient for the release of virus-like particles [corrected].* Journal of virology, 2003. **77**(19): p. 10700-10705.
39. Cornu, T.I. and J.C. de la Torre, *RING Finger Z Protein of Lymphocytic Choriomeningitis Virus (LCMV) Inhibits Transcription and RNA Replication of an LCMV S-Segment Minigenome.* Journal of Virology, 2001. **75**(19): p. 9415.
40. Cornu, T.I. and J.C. de la Torre, *Characterization of the arenavirus RING finger Z protein regions required for Z-mediated inhibition of viral RNA synthesis.* Journal of virology, 2002. **76**(13): p. 6678-6688.
41. Cornu, T.I., H. Feldmann, and J.C. de la Torre, *Cells expressing the RING finger Z protein are resistant to arenavirus infection.* Journal of virology, 2004. **78**(6): p. 2979-2983.
42. Garcin, D., S. Rochat, and D. Kolakofsky, *The Tacaribe arenavirus small zinc finger protein is required for both mRNA synthesis and genome replication.* Journal of virology, 1993. **67**(2): p. 807-812.
43. Kranzusch, P.J. and S.P.J. Whelan, *Arenavirus Z protein controls viral RNA synthesis by locking a polymerase-promoter complex.* Proceedings of the National Academy of Sciences of the United States of America, 2011. **108**(49): p. 19743-19748.
44. López, N., R. Jácamo, and M.T. Franze-Fernández, *Transcription and RNA replication of tacaribe virus genome and antigenome analogs require N and L proteins: Z protein is an inhibitor of these processes.* Journal of virology, 2001. **75**(24): p. 12241-12251.
45. Rojek, J.M., et al. , *Site 1 protease is required for proteolytic processing of the glycoproteins of the South American hemorrhagic fever viruses Junin, Machupo, and Guanarito.* J Virol, 2008. **82**(12): p. 6045-51.
46. Beyer, W.R., et al. , *Endoproteolytic processing of the lymphocytic choriomeningitis virus glycoprotein by the subtilase SKI-1/S1P.* J Virol, 2003. **77**(5): p. 2866-72.
47. Borrow, P. and M.B. Oldstone, *Characterization of lymphocytic choriomeningitis virus-binding protein(s): a candidate cellular receptor for the virus.* J Virol, 1992. **66**(12): p. 7270-81.
48. Eschli, B., et al. , *Identification of an N-terminal trimeric coiled-coil core within arenavirus glycoprotein 2 permits assignment to class I viral fusion proteins.* J Virol, 2006. **80**(12): p. 5897-907.

49. Igonet, S., et al. , *X-ray structure of the arenavirus glycoprotein GP2 in its postfusion hairpin conformation.* Proceedings of the National Academy of Sciences, 2011. **108**(50): p. 19967.
50. Parsy, M.L., et al. , *Crystal structure of Venezuelan hemorrhagic fever virus fusion glycoprotein reveals a class 1 postfusion architecture with extensive glycosylation.* J Virol, 2013. **87**(23): p. 13070-5.
51. Hastie, K.M., et al. , *Crystal structure of the prefusion surface glycoprotein of the prototypic arenavirus LCMV.* Nature structural & molecular biology, 2016. **23**(6): p. 513-521.
52. Parekh, B.S. and M.J. Buchmeier, *Proteins of lymphocytic choriomeningitis virus: Antigenic topography of the viral glycoproteins.* Virology, 1986. **153**(2): p. 168-178.
53. Borrow, P. and M.B.A. Oldstone, *Mechanism of Lymphocytic Choriomeningitis Virus Entry into Cells.* Virology, 1994. **198**(1): p. 1-9.
54. Martinez, M.G., S.M. Cordo, and N.A. Candurra, *Characterization of Junin arenavirus cell entry.* J Gen Virol, 2007. **88**(Pt 6): p. 1776-1784.
55. Vela, E.M., et al. , *Arenavirus entry occurs through a cholesterol-dependent, non-caveolar, clathrin-mediated endocytic mechanism.* Virology, 2007. **369**(1): p. 1-11.
56. Rojek, J.M., M. Perez, and S. Kunz, *Cellular entry of lymphocytic choriomeningitis virus.* Journal of virology, 2008. **82**(3): p. 1505-1517.
57. Quirin, K., et al. , *Lymphocytic choriomeningitis virus uses a novel endocytic pathway for infectious entry via late endosomes.* Virology, 2008. **378**(1): p. 21-33.
58. Leung, W.C., H.P. Ghosh, and W.E. Rawls, *Strandedness of Pichinde virus RNA.* Journal of virology, 1977. **22**(1): p. 235-237.
59. Burri, D.J., et al. , *Molecular characterization of the processing of arenavirus envelope glycoprotein precursors by subtilisin kexin isozyme-1/site-1 protease.* Journal of virology, 2012. **86**(9): p. 4935-4946.
60. Burri, D.J., et al. , *The role of proteolytic processing and the stable signal peptide in expression of the Old World arenavirus envelope glycoprotein ectodomain.* Virology, 2013. **436**(1): p. 127-133.
61. Urata, S. and J. Yasuda, *Molecular mechanism of arenavirus assembly and budding.* Viruses, 2012. **4**(10): p. 2049-2079.
62. Lee, K.J., et al. , *Identification of the lymphocytic choriomeningitis virus (LCMV) proteins required to rescue LCMV RNA analogs into LCMV-like particles.* Journal of virology, 2002. **76**(12): p. 6393-6397.
63. Urata, S., et al. , *Cellular Factors Required for Lassa Virus Budding.* Journal of Virology, 2006. **80**(8): p. 4191.
64. Perez, M., D.L. Greenwald, and J.C. de la Torre, *Myristoylation of the RING finger Z protein is essential for arenavirus budding.* J Virol, 2004. **78**(20): p. 11443-8.
65. Ziegler, C.M., et al. , *NEDD4 family ubiquitin ligases associate with LCMV Z's PPXY domain and are required for virus budding, but not via direct ubiquitination of Z.* PLOS Pathogens, 2019. **15**(11): p. e1008100.
66. Flatz, L., et al. , *Recovery of an arenavirus entirely from RNA polymerase I/II-driven cDNA.* Proceedings of the National Academy of Sciences of the United States of America, 2006. **103**(12): p. 4663.
67. Sánchez, A.B. and J.C. de la Torre, *Rescue of the prototypic Arenavirus LCMV entirely from plasmid.* Virology, 2006. **350**(2): p. 370-80.

68. Lee, K.J., et al. , *NP and L proteins of lymphocytic choriomeningitis virus (LCMV) are sufficient for efficient transcription and replication of LCMV genomic RNA analogs.* J Virol, 2000. **74**(8): p. 3470-7.
69. Lee, K.J., et al. , *Identification of the lymphocytic choriomeningitis virus (LCMV) proteins required to rescue LCMV RNA analogs into LCMV-like particles.* J Virol, 2002. **76**(12): p. 6393-7.
70. Perez, M. and J.C. de la Torre, *Characterization of the Genomic Promoter of the Prototypic Arenavirus Lymphocytic Choriomeningitis Virus.* Journal of Virology, 2003. **77**(2): p. 1184.
71. Albariño, C.G., et al. , *Efficient Rescue of Recombinant Lassa Virus Reveals the Influence of S Segment Noncoding Regions on Virus Replication and Virulence.* Journal of Virology, 2011. **85**(8): p. 4020.
72. Hass, M., et al. , *Replicon System for Lassa Virus.* Journal of Virology, 2004. **78**(24): p. 13793.
73. Krammer, F., et al. , *Influenza.* Nature Reviews Disease Primers, 2018. **4**(1): p. 3.
74. Hu, B., et al. , *Characteristics of SARS-CoV-2 and COVID-19.* Nature Reviews Microbiology, 2021. **19**(3): p. 141-154.
75. Pantaleo, G., C. Graziosi, and A.S. Fauci, *The Immunopathogenesis of Human Immunodeficiency Virus Infection.* New England Journal of Medicine, 1993. **328**(5): p. 327-335.
76. Spearman, C.W., et al. , *Hepatitis C.* The Lancet, 2019. **394**(10207): p. 1451-1466.
77. Schröder, A.R.W., et al. , *HIV-1 Integration in the Human Genome Favors Active Genes and Local Hotspots.* Cell, 2002. **110**(4): p. 521-529.
78. Mitchell, R.S., et al. , *Retroviral DNA Integration: ASLV, HIV, and MLV Show Distinct Target Site Preferences.* PLOS Biology, 2004. **2**(8): p. e234.
79. Zinkernagel, R.M., et al. , *Susceptibility to murine lymphocytic choriomeningitis maps to class I MHC genes—a model for MHC/disease associations.* Nature, 1985. **316**(6031): p. 814-817.
80. Ahmed, R., et al. , *Selection of genetic variants of lymphocytic choriomeningitis virus in spleens of persistently infected mice. Role in suppression of cytotoxic T lymphocyte response and viral persistence.* J Exp Med, 1984. **160**(2): p. 521-40.
81. Wherry, E.J., et al. , *Viral Persistence Alters CD8 T-Cell Immunodominance and Tissue Distribution and Results in Distinct Stages of Functional Impairment.* Journal of Virology, 2003. **77**(8): p. 4911.
82. Bergthaler, A., et al. , *Viral replicative capacity is the primary determinant of lymphocytic choriomeningitis virus persistence and immunosuppression.* Proc Natl Acad Sci U S A, 2010. **107**(50): p. 21641-6.
83. Ahmed, R., B.D. Jamieson, and D.D. Porter, *Immune therapy of a persistent and disseminated viral infection.* Journal of virology, 1987. **61**(12): p. 3920-3929.
84. Byrne, J.A., R. Ahmed, and M.B. Oldstone, *Biology of cloned cytotoxic T lymphocytes specific for lymphocytic choriomeningitis virus. I. Generation and recognition of virus strains and H-2b mutants.* J Immunol, 1984. **133**(1): p. 433-9.
85. Fung-Leung, W.P., et al. , *Immune response against lymphocytic choriomeningitis virus infection in mice without CD8 expression.* J Exp Med, 1991. **174**(6): p. 1425-9.
86. Jamieson, B.D., L.D. Butler, and R. Ahmed, *Effective clearance of a persistent viral infection requires cooperation between virus-specific Lyt2+ T cells and nonspecific bone marrow-derived cells.* J Virol, 1987. **61**(12): p. 3930-7.

87. Lehmann-Grube, F., et al. , *Mechanism of recovery from acute virus infection. I. Role of T lymphocytes in the clearance of lymphocytic choriomeningitis virus from spleens of mice.* J Immunol, 1985. **134**(1): p. 608-15.
88. Zinkernagel, R.M. and P.C. Doherty, *MHC-Restricted Cytotoxic T Cells: Studies on the Biological Role of Polymorphic Major Transplantation Antigens Determining T-Cell Restriction-Specificity, Function, and Responsiveness*, in *Advances in Immunology*, H.G. Kunkel and F.J. Dixon, Editors. 1979, Academic Press. p. 51-177.
89. Blattman, J.N., et al. , *Estimating the precursor frequency of naive antigen-specific CD8 T cells.* The Journal of experimental medicine, 2002. **195**(5): p. 657-664.
90. Kägi, D., et al. , *Cytotoxicity mediated by T cells and natural killer cells is greatly impaired in perforin-deficient mice.* Nature, 1994. **369**(6475): p. 31-7.
91. Zimmermann, C., et al. , *Kinetics of the response of naive and memory CD8 T cells to antigen: similarities and differences.* European Journal of Immunology, 1999. **29**(1): p. 284-290.
92. Zimmerman, C., et al. , *Visualization, characterization, and turnover of CD8+ memory T cells in virus-infected hosts.* Journal of Experimental Medicine, 1996. **183**(4): p. 1367-1375.
93. Wherry, E.J. and R. Ahmed, *Memory CD8 T-cell differentiation during viral infection.* J Virol, 2004. **78**(11): p. 5535-45.
94. Moskophidis, D., et al. , *Virus persistence in acutely infected immunocompetent mice by exhaustion of antiviral cytotoxic effector T cells.* Nature, 1993. **362**(6422): p. 758- 761.
95. Zajac, A.J., et al. , *Viral Immune Evasion Due to Persistence of Activated T Cells Without Effector Function.* The Journal of Experimental Medicine, 1998. **188**(12): p. 2205-2213.
96. Ou, R., et al. , *Critical role for alpha/beta and gamma interferons in persistence of lymphocytic choriomeningitis virus by clonal exhaustion of cytotoxic T cells.* J Virol, 2001. **75**(18): p. 8407-23.
97. Fuller, M.J. and A.J. Zajac, *Ablation of CD8 and CD4 T Cell Responses by High Viral Loads.* The Journal of Immunology, 2003. **170**(1): p. 477.
98. Wherry, E.J., et al. , *Molecular Signature of CD8+ T Cell Exhaustion during Chronic Viral Infection.* Immunity, 2007. **27**(4): p. 670-684.
99. Moskophidis, D., et al. , *Mechanism of recovery from acute virus infection: treatment of lymphocytic choriomeningitis virus-infected mice with monoclonal antibodies reveals that Lyt-2+ T lymphocytes mediate clearance of virus and regulate the antiviral antibody response.* Journal of Virology, 1987. **61**(6): p. 1867.
100. Ahmed, R., L.D. Butler, and L. Bhatti, *T4+ T helper cell function in vivo: differential requirement for induction of antiviral cytotoxic T-cell and antibody responses.* Journal of Virology, 1988. **62**(6): p. 2102.
101. Rahemtulla, A., et al. , *Normal development and function of CD8+ cells but markedly decreased helper cell activity in mice lacking CD4.* Nature, 1991. **353**(6340): p. 180-184.
102. Matloubian, M., R.J. Concepcion, and R. Ahmed, *CD4+ T cells are required to sustain CD8+ cytotoxic T-cell responses during chronic viral infection.* J Virol, 1994. **68**(12): p. 8056-63.
103. Battegay, M., et al. , *Enhanced establishment of a virus carrier state in adult CD4+ T-cell-deficient mice.* J Virol, 1994. **68**(7): p. 4700-4.

104. Brooks, D.G., et al. , *Intrinsic functional dysregulation of CD4 T cells occurs rapidly following persistent viral infection.* J Virol, 2005. **79**(16): p. 10514-27.
105. Brooks, D.G., D.B. McGavern, and M.B.A. Oldstone, *Reprogramming of antiviral T cells prevents inactivation and restores T cell activity during persistent viral infection.* The Journal of Clinical Investigation, 2006. **116**(6): p. 1675-1685.
106. Elsaesser, H., K. Sauer, and D.G. Brooks, *IL-21 is required to control chronic viral infection.* Science, 2009. **324**(5934): p. 1569-72.
107. Fröhlich, A., et al. , *IL-21R on T cells is critical for sustained functionality and control of chronic viral infection.* Science, 2009. **324**(5934): p. 1576-80.
108. Yi, J.S., M. Du, and A.J. Zajac, *A Vital Role for Interleukin-21 in the Control of a Chronic Viral Infection.* Science, 2009. **324**(5934): p. 1572.
109. Cyster, J.G., *B cell follicles and antigen encounters of the third kind.* Nat Immunol, 2010. **11**(11): p. 989-96.
110. Schulz, O., et al. , *Chemokines and Chemokine Receptors in Lymphoid Tissue Dynamics.* Annu Rev Immunol, 2016. **34**: p. 203-42.
111. Kosco-Vilbois, M.H., et al. , *Follicular dendritic cells help resting B cells to become effective antigen-presenting cells: induction of B7/BB1 and upregulation of major histocompatibility complex class II molecules.* The Journal of experimental medicine, 1993. **178**(6): p. 2055-2066.
112. Kranich, J., et al. , *Follicular dendritic cells control engulfment of apoptotic bodies by secreting Mfge8.* The Journal of experimental medicine, 2008. **205**(6): p. 1293-1302.
113. Heesters, B.A., et al. , *Endocytosis and recycling of immune complexes by follicular dendritic cells enhances B cell antigen binding and activation.* Immunity, 2013. **38**(6): p. 1164-75.
114. Aydar, Y., et al. , *Altered Regulation of FcγRII on Aged Follicular Dendritic Cells Correlates with Immunoreceptor Tyrosine-Based Inhibition Motif Signaling in B Cells and Reduced Germinal Center Formation.* The Journal of Immunology, 2003. **171**(11): p. 5975.
115. Aydar, Y., et al. , *The Influence of Immune Complex-Bearing Follicular Dendritic Cells on the IgM Response, Ig Class Switching, and Production of High Affinity IgG.* The Journal of Immunology, 2005. **174**(9): p. 5358.
116. Ansel, K.M., et al. , *A chemokine-driven positive feedback loop organizes lymphoid follicles.* Nature, 2000. **406**(6793): p. 309-314.
117. Suto, H., et al. , *CXCL13 production by an established lymph node stromal cell line via lymphotoxin-beta receptor engagement involves the cooperation of multiple signaling pathways.* International Immunology, 2009. **21**(4): p. 467-476.
118. Coelho, F.M., et al. , *Naive B-cell trafficking is shaped by local chemokine availability and LFA-1–independent stromal interactions.* Blood, 2013. **121**(20): p. 4101-4109.
119. Cremasco, V., et al. , *B cell homeostasis and follicle confines are governed by fibroblastic reticular cells.* Nature Immunology, 2014. **15**(10): p. 973-981.
120. Gatto, D., et al. , *Guidance of B Cells by the Orphan G Protein-Coupled Receptor EBI2 Shapes Humoral Immune Responses.* Immunity, 2009. **31**(2): p. 259-269.
121. Pereira, J.P., et al. , *EBI2 mediates B cell segregation between the outer and centre follicle.* Nature, 2009. **460**(7259): p. 1122-1126.
122. Schwab, S.R. and J.G. Cyster, *Finding a way out: lymphocyte egress from lymphoid organs.* Nature Immunology, 2007. **8**(12): p. 1295-1301.

123. Chan, E.Y.T. and I.C.M. Maclennan, *Only a small proportion of splenic B cells in adults are short-lived virgin cells.* European Journal of Immunology, 1993. **23**(2): p. 357-363.
124. Pape, K.A., et al. , *The humoral immune response is initiated in lymph nodes by B cells that acquire soluble antigen directly in the follicles.* Immunity, 2007. **26**(4): p. 491-502.
125. Carrasco, Y.R. and F.D. Batista, *B cells acquire particulate antigen in a macrophage-rich area at the boundary between the follicle and the subcapsular sinus of the lymph node.* Immunity, 2007. **27**(1): p. 160-71.
126. Junt, T., et al. , *Subcapsular sinus macrophages in lymph nodes clear lymph-borne viruses and present them to antiviral B cells.* Nature, 2007. **450**(7166): p. 110-114.
127. Suzuki, K., et al. , *Visualizing B cell capture of cognate antigen from follicular dendritic cells.* Journal of Experimental Medicine, 2009. **206**(7): p. 1485-1493.
128. Jaiswal, A.I. and M. Croft, *CD40 ligand induction on T cell subsets by peptide-presenting B cells: implications for development of the primary T and B cell response.* J Immunol, 1997. **159**(5): p. 2282-91.
129. Ware, C.F., et al. , *Expression of surface lymphotoxin and tumor necrosis factor on activated T, B, and natural killer cells.* J Immunol, 1992. **149**(12): p. 3881-8.
130. Harris, D.P., et al. , *Reciprocal regulation of polarized cytokine production by effector B and T cells.* Nat Immunol, 2000. **1**(6): p. 475-82.
131. Harker, J.A., et al. , *Late interleukin-6 escalates T follicular helper cell responses and controls a chronic viral infection.* Science (New York, N.Y.), 2011. **334**(6057): p. 825-829.
132. Whitmire, J.K., et al. , *Requirement of B cells for generating CD4+ T cell memory.* Journal of immunology (Baltimore, Md. : 1950), 2009. **182**(4): p. 1868-1876.
133. Kräutler, N.J., et al. , *Differentiation of germinal center B cells into plasma cells is initiated by high-affinity antigen and completed by Tfh cells.* Journal of Experimental Medicine, 2017. **214**(5): p. 1259-1267.
134. Okada, T., et al. , *Antigen-engaged B cells undergo chemotaxis toward the T zone and form motile conjugates with helper T cells.* PLoS Biol, 2005. **3**(6): p. e150.
135. Taylor, J.J., K.A. Pape, and M.K. Jenkins, *A germinal center-independent pathway generates unswitched memory B cells early in the primary response.* The Journal of experimental medicine, 2012. **209**(3): p. 597-606.
136. Papillion, A.M., et al. , *Early derivation of IgM memory cells and bone marrow plasmablasts.* PLOS ONE, 2017. **12**(6): p. e0178853.
137. Flemming, W., *Studien über Regeneration der Gewebe.* Archiv für mikroskopische Anatomie, 1884. **24**(1): p. 50-91.
138. Jacob, J., R. Kassir, and G. Kelsoe, *In situ studies of the primary immune response to (4-hydroxy-3-nitrophenyl)acetyl. I. The architecture and dynamics of responding cell populations.* J Exp Med, 1991. **173**(5): p. 1165-75.
139. Liu, Y.J., et al. , *Sites of specific B cell activation in primary and secondary responses to T cell-dependent and T cell-independent antigens.* Eur J Immunol, 1991. **21**(12): p. 2951-62.
140. Benson, M.J., et al. , *Affinity of antigen encounter and other early B-cell signals determine B-cell fate.* Curr Opin Immunol, 2007. **19**(3): p. 275-80.
141. Dal Porto, J.M., et al. , *Antigen drives very low affinity B cells to become plasmacytes and enter germinal centers.* J Immunol, 1998. **161**(10): p. 5373-81.

142. Dal Porto, J.M., et al. , *Very low affinity B cells form germinal centers, become memory B cells, and participate in secondary immune responses when higher affinity competition is reduced.* J Exp Med, 2002. **195**(9): p. 1215-21.
143. Paus, D., et al. , *Antigen recognition strength regulates the choice between extrafollicular plasma cell and germinal center B cell differentiation.* J Exp Med, 2006. **203**(4): p. 1081-91.
144. Shih, T.A., et al. , *Role of BCR affinity in T cell dependent antibody responses in vivo.* Nat Immunol, 2002. **3**(6): p. 570-5.
145. de Vinuesa, C.G., et al. , *Germinal centers without T cells.* J Exp Med, 2000. **191**(3): p. 485-94.
146. Chan, T.D., et al. , *Antigen affinity controls rapid T-dependent antibody production by driving the expansion rather than the differentiation or extrafollicular migration of early plasmablasts.* J Immunol, 2009. **183**(5): p. 3139-49.
147. McBride, K.M., et al. , *Regulation of class switch recombination and somatic mutation by AID phosphorylation.* The Journal of experimental medicine, 2008. **205**(11): p. 2585-2594.
148. Shinkura, R., et al. , *Separate domains of AID are required for somatic hypermutation and class-switch recombination.* Nat Immunol, 2004. **5**(7): p. 707-12.
149. Schwickert, T.A., et al. , *A dynamic T cell-limited checkpoint regulates affinity-dependent B cell entry into the germinal center.* The Journal of experimental medicine, 2011. **208**(6): p. 1243-1252.
150. Gitlin, A.D., et al. , *HUMORAL IMMUNITY. T cell help controls the speed of the cell cycle in germinal center B cells.* Science (New York, N.Y.), 2015. **349**(6248): p. 643-646.
151. Liu, D., et al. , *T-B-cell entanglement and ICOSL-driven feed-forward regulation of germinal centre reaction.* Nature, 2015. **517**(7533): p. 214-8.
152. Weisel, F.J., et al. , *A Temporal Switch in the Germinal Center Determines Differential Output of Memory B and Plasma Cells.* Immunity, 2016. **44**(1): p. 116-130.
153. Griffiths, G.M., et al. , *Somatic mutation and the maturation of immune response to 2-phenyl oxazolone.* Nature, 1984. **312**(5991): p. 271-5.
154. Staudt, L.M. and W. Gerhard, *Generation of antibody diversity in the immune response of BALB/c mice to influenza virus hemagglutinin. I. Significant variation in repertoire expression between individual mice.* Journal of Experimental Medicine, 1983. **157**(2): p. 687-704.
155. Fallet, B., et al. , *Chronic Viral Infection Promotes Efficient Germinal Center B Cell Responses.* Cell Reports, 2020. **30**(4): p. 1013-1026.e7.
156. Georgiev, I.S., et al. , *Antibodies VRC01 and 10E8 Neutralize HIV-1 with High Breadth and Potency Even with Ig-Framework Regions Substantially Reverted to Germline.* The Journal of Immunology, 2014. **192**(3): p. 1100.
157. Jardine, J.G., et al. , *Minimally Mutated HIV-1 Broadly Neutralizing Antibodies to Guide Reductionist Vaccine Design.* PLOS Pathogens, 2016. **12**(8): p. e1005815.
158. Simonich, C.A., et al. , *HIV-1 Neutralizing Antibodies with Limited Hypermutation from an Infant.* Cell, 2016. **166**(1): p. 77-87.
159. Wiehe, K., et al. , *Functional Relevance of Improbable Antibody Mutations for HIV Broadly Neutralizing Antibody Development.* Cell Host & Microbe, 2018. **23**(6): p. 759-765.e6.
160. Xiao, X., et al. , *Germline-like predecessors of broadly neutralizing antibodies lack measurable binding to HIV-1 envelope glycoproteins: Implications for evasion of*

immune responses and design of vaccine immunogens. Biochemical and Biophysical Research Communications, 2009. **390**(3): p. 404-409.
161. Nutt, S.L., et al. , *The generation of antibody-secreting plasma cells.* Nature Reviews Immunology, 2015. **15**(3): p. 160-171.
162. Manz, R.A., et al. , *Humoral immunity and long-lived plasma cells.* Curr Opin Immunol, 2002. **14**(4): p. 517-21.
163. Manz, R.A., A. Thiel, and A. Radbruch, *Lifetime of plasma cells in the bone marrow.* Nature, 1997. **388**(6638): p. 133-134.
164. Tangye, S.G., D.T. Avery, and P.D. Hodgkin, *A division-linked mechanism for the rapid generation of Ig-secreting cells from human memory B cells.* J Immunol, 2003. **170**(1): p. 261-9.
165. Tangye, S.G., et al. , *Intrinsic differences in the proliferation of naive and memory human B cells as a mechanism for enhanced secondary immune responses.* J Immunol, 2003. **170**(2): p. 686-94.
166. Arpin, C., J. Banchereau, and Y.-J. Liu, *Memory B Cells Are Biased Towards Terminal Differentiation: A Strategy That May Prevent Repertoire Freezing.* Journal of Experimental Medicine, 1997. **186**(6): p. 931-940.
167. Kindler, V. and R.H. Zubler, *Memory, but not naive, peripheral blood B lymphocytes differentiate into Ig-secreting cells after CD40 ligation and costimulation with IL-4 and the differentiation factors IL-2, IL-10, and IL-3.* J Immunol, 1997. **159**(5): p. 2085-90.
168. Bernasconi, N.L., E. Traggiai, and A. Lanzavecchia, *Maintenance of Serological Memory by Polyclonal Activation of Human Memory B Cells.* Science, 2002. **298**(5601): p. 2199.
169. Good, K.L., D.T. Avery, and S.G. Tangye, *Resting human memory B cells are intrinsically programmed for enhanced survival and responsiveness to diverse stimuli compared to naive B cells.* J Immunol, 2009. **182**(2): p. 890-901.
170. Toellner, K.M., et al. , *Low-level hypermutation in T cell-independent germinal centers compared with high mutation rates associated with T cell-dependent germinal centers.* J Exp Med, 2002. **195**(3): p. 383-9.
171. García de Vinuesa, C., et al. , *T-independent type 2 antigens induce B cell proliferation in multiple splenic sites, but exponential growth is confined to extrafollicular foci.* Eur J Immunol, 1999. **29**(4): p. 1314-23.
172. Hasbold, J., et al. , *Evidence from the generation of immunoglobulin G–secreting cells that stochastic mechanisms regulate lymphocyte differentiation.* Nature Immunology, 2004. **5**(1): p. 55-63.
173. Paus, D., et al. , *Antigen recognition strength regulates the choice between extrafollicular plasma cell and germinal center B cell differentiation.* Journal of Experimental Medicine, 2006. **203**(4): p. 1081-1091.
174. Planz, O., et al. , *A critical role for neutralizing-antibody-producing B cells, CD4(+) T cells, and interferons in persistent and acute infections of mice with lymphocytic choriomeningitis virus: implications for adoptive immunotherapy of virus carriers.* Proceedings of the National Academy of Sciences of the United States of America, 1997. **94**(13): p. 6874-6879.
175. Bergthaler, A., et al. , *Impaired Antibody Response Causes Persistence of Prototypic T Cell–Contained Virus.* PLOS Biology, 2009. **7**(4): p. e1000080.
176. Hangartner, L., et al. , *Nonneutralizing antibodies binding to the surface glycoprotein of lymphocytic choriomeningitis virus reduce early virus spread.* The Journal of Experimental Medicine, 2006. **203**(8): p. 2033-2042.

177. Ciurea, A., et al. , *Viral persistence in vivo through selection of neutralizing antibody-escape variants.* Proceedings of the National Academy of Sciences, 2000. **97**(6): p. 2749.
178. Plotkin, S.A., *Correlates of protection induced by vaccination.* Clinical and vaccine immunology : CVI, 2010. **17**(7): p. 1055-1065.
179. Sok, D. and D.R. Burton, *Recent progress in broadly neutralizing antibodies to HIV.* Nature immunology, 2018. **19**(11): p. 1179-1188.
180. Landais, E. and P.L. Moore, *Development of broadly neutralizing antibodies in HIV-1 infected elite neutralizers.* Retrovirology, 2018. **15**(1): p. 61.
181. Kouyos, R.D., et al. , *Tracing HIV-1 strains that imprint broadly neutralizing antibody responses.* Nature, 2018. **561**(7723): p. 406-410.
182. Subbaraman, H., M. Schanz, and A. Trkola, *Broadly neutralizing antibodies: What is needed to move from a rare event in HIV-1 infection to vaccine efficacy?* Retrovirology, 2018. **15**(1): p. 52.
183. Shibata, R., et al. , *Neutralizing antibody directed against the HIV–1 envelope glycoprotein can completely block HIV–1/SIV chimeric virus infections of macaque monkeys.* Nature Medicine, 1999. **5**(2): p. 204-210.
184. Mascola, J.R., et al. , *Protection of Macaques against Pathogenic Simian/Human Immunodeficiency Virus 89.6PD by Passive Transfer of Neutralizing Antibodies.* Journal of Virology, 1999. **73**(5): p. 4009.
185. Mascola, J.R., et al. , *Protection of macaques against vaginal transmission of a pathogenic HIV-1/SIV chimeric virus by passive infusion of neutralizing antibodies.* Nature Medicine, 2000. **6**(2): p. 207-210.
186. Barnett, S.W., et al. , *Protection of macaques against vaginal SHIV challenge by systemic or mucosal and systemic vaccinations with HIV-envelope.* AIDS, 2008. **22**(3).
187. Shingai, M., et al. , *Passive transfer of modest titers of potent and broadly neutralizing anti-HIV monoclonal antibodies block SHIV infection in macaques.* Journal of Experimental Medicine, 2014. **211**(10): p. 2061-2074.
188. Hessell, A.J., et al. , *Early short-term treatment with neutralizing human monoclonal antibodies halts SHIV infection in infant macaques.* Nature Medicine, 2016. **22**(4): p. 362-368.
189. Trkola, A., et al. , *Delay of HIV-1 rebound after cessation of antiretroviral therapy through passive transfer of human neutralizing antibodies.* Nature Medicine, 2005. **11**(6): p. 615-622.
190. Law, M., et al. , *Broadly neutralizing antibodies protect against hepatitis C virus quasispecies challenge.* Nature Medicine, 2008. **14**(1): p. 25-27.
191. de Jong, Y.P., et al. , *Broadly neutralizing antibodies abrogate established hepatitis C virus infection.* Science Translational Medicine, 2014. **6**(254): p. 254ra129.
192. Pinschewer, D.D., et al. , *Kinetics of protective antibodies are determined by the viral surface antigen.* The Journal of clinical investigation, 2004. **114**(7): p. 988-993.
193. Eschli, B., et al. , *Early antibodies specific for the neutralizing epitope on the receptor binding subunit of the lymphocytic choriomeningitis virus glycoprotein fail to neutralize the virus.* J Virol, 2007. **81**(21): p. 11650-7.
194. Gray, E.S., et al. , *The neutralization breadth of HIV-1 develops incrementally over four years and is associated with CD4+ T cell decline and high viral load during acute infection.* Journal of virology, 2011. **85**(10): p. 4828-4840.

195. Sommerstein, R., et al. , *Arenavirus Glycan Shield Promotes Neutralizing Antibody Evasion and Protracted Infection.* PLOS Pathogens, 2015. **11**(11): p. e1005276.
196. Kwong, P.D., et al. , *HIV-1 evades antibody-mediated neutralization through conformational masking of receptor-binding sites.* Nature, 2002. **420**(6916): p. 678-82.
197. Wei, X., et al. , *Antibody neutralization and escape by HIV-1.* Nature, 2003. **422**(6929): p. 307-12.
198. Pérez-Valero, I., et al. , *Cerebrospinal fluid viral escape in aviremic HIV-infected patients receiving antiretroviral therapy: prevalence, risk factors and neurocognitive effects.* Aids, 2019. **33**(3): p. 475-481.
199. Manesh, A., et al. , *Symptomatic HIV CNS viral escape among patients on effective cART.* International Journal of Infectious Diseases, 2019. **84**: p. 39-43.
200. Fallet, B., et al. , *Interferon-driven deletion of antiviral B cells at the onset of chronic infection.* Science Immunology, 2016. **1**(4): p. eaah6817.
201. Rusert, P., et al. , *Determinants of HIV-1 broadly neutralizing antibody induction.* Nat Med, 2016. **22**(11): p. 1260-1267.
202. Aasa-Chapman, M.M.I., et al. , *Development of the antibody response in acute HIV-1 infection.* AIDS, 2004. **18**(3).
203. Holl, V., et al. , *Nonneutralizing Antibodies Are Able To Inhibit Human Immunodeficiency Virus Type 1 Replication in Macrophages and Immature Dendritic Cells.* Journal of Virology, 2006. **80**(12): p. 6177.
204. Haynes, B.F., et al. , *Immune-Correlates Analysis of an HIV-1 Vaccine Efficacy Trial.* New England Journal of Medicine, 2012. **366**(14): p. 1275-1286.
205. Bonsignori, M., et al. , *Antibody-Dependent Cellular Cytotoxicity-Mediating Antibodies from an HIV-1 Vaccine Efficacy Trial Target Multiple Epitopes and Preferentially Use the VH1 Gene Family.* Journal of Virology, 2012. **86**(21): p. 11521.
206. Santra, S., et al. , *Human Non-neutralizing HIV-1 Envelope Monoclonal Antibodies Limit the Number of Founder Viruses during SHIV Mucosal Infection in Rhesus Macaques.* PLOS Pathogens, 2015. **11**(8): p. e1005042.
207. Moog, C., et al. , *Protective effect of vaginal application of neutralizing and nonneutralizing inhibitory antibodies against vaginal SHIV challenge in macaques.* Mucosal Immunology, 2014. **7**(1): p. 46-56.
208. Lewis, G.K., et al. , *Conformational Masking and Receptor-Dependent Unmasking of Highly Conserved Env Epitopes Recognized by Non-Neutralizing Antibodies That Mediate Potent ADCC against HIV-1.* Viruses, 2015. **7**(9).
209. Horwitz, J.A., et al. , *Non-neutralizing Antibodies Alter the Course of HIV-1 Infection In Vivo.* Cell, 2017. **170**(4): p. 637-648.e10.
210. Huang, D., et al. , *Vaccine elicitation of HIV broadly neutralizing antibodies from engineered B cells.* Nature communications, 2020. **11**(1): p. 5850-5850.
211. Revilla, I.D.R., et al. , *The B-cell identity factor Pax5 regulates distinct transcriptional programmes in early and late B lymphopoiesis.* Embo j, 2012. **31**(14): p. 3130-46.
212. Cattoretti, G., et al. , *BCL-6 protein is expressed in germinal-center B cells.* Blood, 1995. **86**(1): p. 45-53.
213. Ranuncolo, S.M., et al. , *Bcl-6 mediates the germinal center B cell phenotype and lymphomagenesis through transcriptional repression of the DNA-damage sensor ATR.* Nat Immunol, 2007. **8**(7): p. 705-14.

214. Teng, Y., et al. , *IRF4 negatively regulates proliferation of germinal center B cell-derived Burkitt's lymphoma cell lines and induces differentiation toward plasma cells.* Eur J Cell Biol, 2007. **86**(10): p. 581-9.
215. Patterson, D., C.D. Scharer, and J.M. Boss, *IRF4 regulates the rate of cell cycle during B cell differentiation.* The Journal of Immunology, 2018. **200**(1 Supplement): p. 48.16.
216. Willis, S.N., et al. , *Transcription Factor IRF4 Regulates Germinal Center Cell Formation through a B Cell–Intrinsic Mechanism.* The Journal of Immunology, 2014. **192**(7): p. 3200.
217. Kallies, A., et al. , *Plasma cell ontogeny defined by quantitative changes in blimp-1 expression.* The Journal of experimental medicine, 2004. **200**(8): p. 967-977.
218. Nutt, S.L., K.A. Fairfax, and A. Kallies, *BLIMP1 guides the fate of effector B and T cells.* Nature Reviews Immunology, 2007. **7**(12): p. 923-927.
219. Bönelt, P., et al. , *Precocious expression of Blimp1 in B cells causes autoimmune disease with increased self-reactive plasma cells.* The EMBO Journal, 2019. **38**(2): p. e100010.
220. Shaffer, A.L., et al. , *XBP1, Downstream of Blimp-1, Expands the Secretory Apparatus and Other Organelles, and Increases Protein Synthesis in Plasma Cell Differentiation.* Immunity, 2004. **21**(1): p. 81-93.
221. Todd, D.J., et al. , *XBP1 governs late events in plasma cell differentiation and is not required for antigen-specific memory B cell development.* Journal of Experimental Medicine, 2009. **206**(10): p. 2151-2159.
222. Miura, Y., et al. , *Bach2 Promotes B Cell Receptor-Induced Proliferation of B Lymphocytes and Represses Cyclin-Dependent Kinase Inhibitors.* J Immunol, 2018. **200**(8): p. 2882-2893.
223. Lin, K.-I., et al. , *Blimp-1-Dependent Repression of Pax-5 Is Required for Differentiation of B Cells to Immunoglobulin M-Secreting Plasma Cells.* Molecular and Cellular Biology, 2002. **22**(13): p. 4771.
224. Horcher, M., A. Souabni, and M. Busslinger, *Pax5/BSAP Maintains the Identity of B Cells in Late B Lymphopoiesis.* Immunity, 2001. **14**(6): p. 779-790.
225. Cobaleda, C., et al. , *Pax5: the guardian of B cell identity and function.* Nature Immunology, 2007. **8**(5): p. 463-470.
226. Muto, A., et al. , *Identification of Bach2 as a B-cell-specific partner for small Maf proteins that negatively regulate the immunoglobulin heavy chain gene 3' enhancer.* The EMBO Journal, 1998. **17**(19): p. 5734-5743.
227. Ye, B.H., et al. , *Alterations of a zinc finger-encoding gene, BCL-6, in diffuse large-cell lymphoma.* Science, 1993. **262**(5134): p. 747.
228. Chang, C.C., et al. , *BCL-6, a POZ/zinc-finger protein, is a sequence-specific transcriptional repressor.* Proceedings of the National Academy of Sciences, 1996. **93**(14): p. 6947.
229. Kitano, M., et al. , *Bcl6 Protein Expression Shapes Pre-Germinal Center B Cell Dynamics and Follicular Helper T Cell Heterogeneity.* Immunity, 2011. **34**(6): p. 961-972.
230. Keller, A.D. and T. Maniatis, *Identification and characterization of a novel repressor of beta-interferon gene expression.* Genes & Development, 1991. **5**(5): p. 868-879.
231. Shaffer, A.L., et al. , *Blimp-1 orchestrates plasma cell differentiation by extinguishing the mature B cell gene expression program.* Immunity, 2002. **17**(1): p. 51-62.
232. Ren, B., et al. , *PRDI-BF1/Blimp-1 repression is mediated by corepressors of the Groucho family of proteins.* Genes & Development, 1999. **13**(1): p. 125-137.

233. Yu, J., et al. , *Transcriptional Repression by Blimp-1 (PRDI-BF1) Involves Recruitment of Histone Deacetylase.* Molecular and Cellular Biology, 2000. **20**(7): p. 2592.
234. Győry, I., et al. , *PRDI-BF1 recruits the histone H3 methyltransferase G9a in transcriptional silencing.* Nature Immunology, 2004. **5**(3): p. 299-308.
235. Kuo, T.C. and K.L. Calame, *B Lymphocyte-Induced Maturation Protein (Blimp)-1, IFN Regulatory Factor (IRF)-1, and IRF-2 Can Bind to the Same Regulatory Sites.* The Journal of Immunology, 2004. **173**(9): p. 5556.
236. Shapiro-Shelef, M., et al. , *Blimp-1 is required for the formation of immunoglobulin secreting plasma cells and pre-plasma memory B cells.* Immunity, 2003. **19**(4): p. 607-20.
237. Shapiro-Shelef, M. and K. Calame, *Regulation of plasma-cell development.* Nature Reviews Immunology, 2005. **5**(3): p. 230-242.
238. Eisenbeis, C.F., H. Singh, and U. Storb, *Pip, a novel IRF family member, is a lymphoid-specific, PU.1-dependent transcriptional activator.* Genes & Development, 1995. **9**(11): p. 1377-1387.
239. Klein, U., et al. , *Transcription factor IRF4 controls plasma cell differentiation and class-switch recombination.* Nat Immunol, 2006. **7**(7): p. 773-82.
240. Pauken, K.E. and E.J. Wherry, *Overcoming T cell exhaustion in infection and cancer.* Trends in immunology, 2015. **36**(4): p. 265-276.
241. Titanji, K., et al. , *Primary HIV-1 infection sets the stage for important B lymphocyte dysfunctions.* Aids, 2005. **19**(17): p. 1947-55.
242. Kardava, L., et al. , *Abnormal B cell memory subsets dominate HIV-specific responses in infected individuals.* J Clin Invest, 2014. **124**(7): p. 3252-62.
243. Buckner, C.M., et al. , *Characterization of Plasmablasts in the Blood of HIV-Infected Viremic Individuals: Evidence for Nonspecific Immune Activation.* Journal of Virology, 2013. **87**(10): p. 5800.
244. Hart, M., et al. , *Loss of discrete memory B cell subsets is associated with impaired immunization responses in HIV-1 infection and may be a risk factor for invasive pneumococcal disease.* J Immunol, 2007. **178**(12): p. 8212-20.
245. Levesque, M.C., et al. , *Polyclonal B cell differentiation and loss of gastrointestinal tract germinal centers in the earliest stages of HIV-1 infection.* PLoS Med, 2009. **6**(7): p. e1000107.
246. Legendre, C., et al. , *CD80 expression is decreased in hyperplastic lymph nodes of HIV+ patients.* Int Immunol, 1998. **10**(12): p. 1847-51.
247. Muellenbeck, M.F., et al. , *Atypical and classical memory B cells produce Plasmodium falciparum neutralizing antibodies.* The Journal of experimental medicine, 2013. **210**(2): p. 389-399.
248. Malaspina, A., et al. , *Compromised B cell responses to influenza vaccination in HIV-infected individuals.* J Infect Dis, 2005. **191**(9): p. 1442-50.
249. Moir, S., et al. , *Decreased Survival of B Cells of HIV-viremic Patients Mediated by Altered Expression of Receptors of the TNF Superfamily.* Journal of Experimental Medicine, 2004. **200**(5): p. 587-600.
250. Moir, S., et al. , *Evidence for HIV-associated B cell exhaustion in a dysfunctional memory B cell compartment in HIV-infected viremic individuals.* The Journal of Experimental Medicine, 2008. **205**(8): p. 1797-1805.
251. Boliar, S., et al. , *B-Lymphocyte Dysfunction in Chronic HIV-1 Infection Does Not Prevent Cross-Clade Neutralization Breadth.* Journal of Virology, 2012. **86**(15): p. 8031.

252. Moir, S., et al. , *B cells in early and chronic HIV infection: evidence for preservation of immune function associated with early initiation of antiretroviral therapy.* Blood, 2010. **116**(25): p. 5571-5579.
253. Meffre, E., et al. , *Maturational characteristics of HIV-specific antibodies in viremic individuals.* JCI Insight, 2016. **1**(3).
254. Burton, A.R., et al. , *Circulating and intrahepatic antiviral B cells are defective in hepatitis B.* J Clin Invest, 2018. **128**(10): p. 4588-4603.
255. Salimzadeh, L., et al. , *PD-1 blockade partially recovers dysfunctional virus–specific B cells in chronic hepatitis B infection.* The Journal of Clinical Investigation, 2018. **128**(10): p. 4573-4587.
256. Charles, E.D., et al. , *Clonal B cells in patients with hepatitis C virus-associated mixed cryoglobulinemia contain an expanded anergic CD21low B-cell subset.* Blood, 2011. **117**(20): p. 5425-37.
257. Doi, H., S. Tanoue, and D.E. Kaplan, *Peripheral CD27-CD21- B-cells represent an exhausted lymphocyte population in hepatitis C cirrhosis.* Clinical immunology (Orlando, Fla.), 2014. **150**(2): p. 184-191.
258. Kardava, L., et al. , *Attenuation of HIV-associated human B cell exhaustion by siRNA downregulation of inhibitory receptors.* J Clin Invest, 2011. **121**(7): p. 2614-24.
259. Dai, B., et al. , *Hepatitis C virus upregulates B-cell receptor signaling: a novel mechanism for HCV-associated B-cell lymphoproliferative disorders.* Oncogene, 2016. **35**(23): p. 2979-2990.
260. Moorman, J., et al. , *Abnormal B-cell activation associated with TALL-1 over-expression and SOCS-1 suppression during chronic hepatitis C virus infection.* Immunology, 2009. **128**(2): p. 227-235.
261. Sullivan, R.T., et al. , *FCRL5 Delineates Functionally Impaired Memory B Cells Associated with Plasmodium falciparum Exposure.* PLOS Pathogens, 2015. **11**(5): p. e1004894.
262. Pérez-Mazliah, D., et al. , *Plasmodium-specific atypical memory B cells are short-lived activated B cells.* eLife, 2018. **7**: p. e39800.
263. Braddom, A.E., et al. , *Potential functions of atypical memory B cells in Plasmodium-exposed individuals.* International Journal for Parasitology, 2020. **50**(13): p. 1033-1042.
264. Anders, R.F., *Multiple cross-reactivities amongst antigens of Plasmodium falciparum impair the development of protective immunity against malaria.* Parasite Immunology, 1986. **8**(6): p. 529-539.
265. Labuda, L.A., et al. , *Alterations in Peripheral Blood B Cell Subsets and Dynamics of B Cell Responses during Human Schistosomiasis.* PLOS Neglected Tropical Diseases, 2013. **7**(3): p. e2094.
266. Xiao, J., et al. , *B cells induced by Schistosoma japonicum infection display diverse regulatory phenotypes and modulate CD4+ T cell response.* Parasites & Vectors, 2020. **13**(1): p. 147.
267. Joosten, S.A., et al. , *Patients with Tuberculosis Have a Dysfunctional Circulating B-Cell Compartment, Which Normalizes following Successful Treatment.* PLOS Pathogens, 2016. **12**(6): p. e1005687.
268. Dolasia, K., F. Nazar, and S. Mukhopadhyay, *Mycobacterium tuberculosis PPE18 protein inhibits MHC class II antigen presentation and B cell response in mice.* European Journal of Immunology, 2021. **51**(3): p. 603-619.

269. Abbott, R.K. and S. Crotty, *Factors in B cell competition and immunodominance.* Immunological Reviews, 2020. **296**(1): p. 120-131.
270. Zaheen, A., et al. , *AID constrains germinal center size by rendering B cells susceptible to apoptosis.* Blood, 2009. **114**(3): p. 547-554.
271. Shinnakasu, R., et al. , *Regulated selection of germinal-center cells into the memory B cell compartment.* Nature Immunology, 2016. **17**(7): p. 861-869.
272. Suan, D., et al. , *CCR6 Defines Memory B Cell Precursors in Mouse and Human Germinal Centers, Revealing Light-Zone Location and Predominant Low Antigen Affinity.* Immunity, 2017. **47**(6): p. 1142-1153.e4.
273. Wang, Y., et al. , *Germinal-center development of memory B cells driven by IL-9 from follicular helper T cells.* Nature Immunology, 2017. **18**(8): p. 921-930.
274. Takatsuka, S., et al. , *IL-9 receptor signaling in memory B cells regulates humoral recall responses.* Nature Immunology, 2018. **19**(9): p. 1025-1034.
275. Zhang, Y., et al. , *Plasma cell output from germinal centers is regulated by signals from Tfh and stromal cells.* Journal of Experimental Medicine, 2018. **215**(4): p. 1227-1243.
276. Mayer, C.T., et al. , *The microanatomic segregation of selection by apoptosis in the germinal center.* Science, 2017. **358**(6360): p. eaao2602.
277. Jacob, J., R. Kassir, and G. Kelsoe, *In situ studies of the primary immune response to (4-hydroxy-3-nitrophenyl)acetyl. I. The architecture and dynamics of responding cell populations.* Journal of Experimental Medicine, 1991. **173**(5): p. 1165-1175.
278. Jacob, J. and G. Kelsoe, *In situ studies of the primary immune response to (4-hydroxy-3-nitrophenyl)acetyl. II. A common clonal origin for periarteriolar lymphoid sheath-associated foci and germinal centers.* Journal of Experimental Medicine, 1992. **176**(3): p. 679-687.
279. Jacob, J., et al. , *In situ studies of the primary immune response to (4-hydroxy-3-nitrophenyl)acetyl. III. The kinetics of V region mutation and selection in germinal center B cells.* Journal of Experimental Medicine, 1993. **178**(4): p. 1293-1307.
280. Hu, J.K., et al. , *Murine Antibody Responses to Cleaved Soluble HIV-1 Envelope Trimers Are Highly Restricted in Specificity.* Journal of Virology, 2015. **89**(20): p. 10383.
281. Havenar-Daughton, C., et al. , *Direct Probing of Germinal Center Responses Reveals Immunological Features and Bottlenecks for Neutralizing Antibody Responses to HIV Env Trimer.* Cell Reports, 2016. **17**(9): p. 2195-2209.
282. Cirelli, K.M., et al. , *Slow Delivery Immunization Enhances HIV Neutralizing Antibody and Germinal Center Responses via Modulation of Immunodominance.* Cell, 2019. **177**(5): p. 1153-1171.e28.
283. Huang, J., et al. , *Identification of a CD4-Binding-Site Antibody to HIV that Evolved Near-Pan Neutralization Breadth.* Immunity, 2016. **45**(5): p. 1108-1121.
284. Huang, J., et al. , *Broad and potent neutralization of HIV-1 by a gp41-specific human antibody.* Nature, 2012. **491**(7424): p. 406-412.
285. Wu, X., et al. , *Rational Design of Envelope Identifies Broadly Neutralizing Human Monoclonal Antibodies to HIV-1.* Science, 2010. **329**(5993): p. 856.
286. Scheid, J.F., et al. , *Broad diversity of neutralizing antibodies isolated from memory B cells in HIV-infected individuals.* Nature, 2009. **458**(7238): p. 636-640.
287. Sok, D., et al. , *Priming HIV-1 broadly neutralizing antibody precursors in human Ig loci transgenic mice.* Science, 2016. **353**(6307): p. 1557.
288. Jardine, J.G., et al. , *HIV-1 broadly neutralizing antibody precursor B cells revealed by germline-targeting immunogen.* Science, 2016. **351**(6280): p. 1458.

289. Jardine, J., et al. , *Rational HIV Immunogen Design to Target Specific Germline B Cell Receptors.* Science, 2013. **340**(6133): p. 711.
290. Havenar-Daughton, C., et al. , *The human naive B cell repertoire contains distinct subclasses for a germline-targeting HIV-1 vaccine immunogen.* Science Translational Medicine, 2018. **10**(448): p. eaat0381.
291. Abbott, R.K., et al. , *Precursor Frequency and Affinity Determine B Cell Competitive Fitness in Germinal Centers, Tested with Germline-Targeting HIV Vaccine Immunogens.* Immunity, 2018. **48**(1): p. 133-146 e6.
292. Dosenovic, P., et al. , *Anti–HIV-1 B cell responses are dependent on B cell precursor frequency and antigen-binding affinity.* Proceedings of the National Academy of Sciences, 2018.
293. Sangesland, M., et al. , *Germline-Encoded Affinity for Cognate Antigen Enables Vaccine Amplification of a Human Broadly Neutralizing Response against Influenza Virus.* Immunity, 2019. **51**(4): p. 735-749.e8.
294. Liao, H.-X., et al. , *Co-evolution of a broadly neutralizing HIV-1 antibody and founder virus.* Nature, 2013. **496**(7446): p. 469-476.
295. Shih, T.-A.Y., M. Roederer, and M.C. Nussenzweig, *Role of antigen receptor affinity in T cell–independent antibody responses in vivo.* Nature Immunology, 2002. **3**(4): p. 399-406.
296. Kuraoka, M., et al. , *Complex Antigens Drive Permissive Clonal Selection in Germinal Centers.* Immunity, 2016. **44**(3): p. 542-552.
297. Tas, J.M.J., et al. , *Visualizing antibody affinity maturation in germinal centers.* Science, 2016. **351**(6277): p. 1048.
298. Silver, J., et al. , *Stochasticity enables BCR-independent germinal center initiation and antibody affinity maturation.* Journal of Experimental Medicine, 2017. **215**(1): p. 77-90.
299. Mesin, L., et al. , *Restricted Clonality and Limited Germinal Center Reentry Characterize Memory B Cell Reactivation by Boosting.* Cell, 2020. **180**(1): p. 92-106.e11.
300. Steichen, J.M., et al. , *A generalized HIV vaccine design strategy for priming of broadly neutralizing antibody responses.* Science, 2019. **366**(6470): p. eaax4380.
301. Huang, D., et al. , *B cells expressing authentic naive human VRC01-class BCRs can be primed and recruited to germinal centers in multiple independent mouse models.* bioRxiv, 2020: p. 2020.02.24.963629.
302. Pircher, H., et al. , *Viral escape by selection of cytotoxic T cell-resistant virus variants in vivo.* Nature, 1990. **346**(6285): p. 629-633.
303. Arcia, D., et al. , *Role of CD8(+) T Cells in the Selection of HIV-1 Immune Escape Mutations.* Viral Immunol, 2017. **30**(1): p. 3-12.
304. Warren, J.A., et al. , *Quantifying Virus Escape from T Cells in the Latent HIV Reservoir.* The Journal of Immunology, 2019. **202**(1 Supplement): p. 197.14.
305. Yang, O.O., et al. , *Determinants of HIV-1 Mutational Escape From Cytotoxic T Lymphocytes.* Journal of Experimental Medicine, 2003. **197**(10): p. 1365-1375.
306. Allen, T.M., et al. , *Selective Escape from CD8⁺ T-Cell Responses Represents a Major Driving Force of Human Immunodeficiency Virus Type 1 (HIV-1) Sequence Diversity and Reveals Constraints on HIV-1 Evolution.* Journal of Virology, 2005. **79**(21): p. 13239.
307. Sun, X., et al. , *Effects of a Single Escape Mutation on T Cell and HIV-1 Co-adaptation.* Cell Reports, 2016. **15**(10): p. 2279-2291.

308. Cao, J., et al. , *Evolution of CD8⁺ T Cell Immunity and Viral Escape Following Acute HIV-1 Infection.* The Journal of Immunology, 2003. **171**(7): p. 3837.
309. Moskophidis, D. and R.M. Zinkernagel, *Immunobiology of cytotoxic T-cell escape mutants of lymphocytic choriomeningitis virus.* Journal of Virology, 1995. **69**(4): p. 2187.
310. Dingens, A.S., et al. , *Comprehensive Mapping of HIV-1 Escape from a Broadly Neutralizing Antibody.* Cell host & microbe, 2017. **21**(6): p. 777-787.e4.
311. Schweighardt, B., et al. , *Immune escape mutations detected within HIV-1 epitopes associated with viral control during treatment interruption.* J Acquir Immune Defic Syndr, 2010. **53**(1): p. 36-46.
312. Kalia, V., et al. , *Antibody Neutralization Escape Mediated by Point Mutations in the Intracytoplasmic Tail of Human Immunodeficiency Virus Type 1 gp41.* Journal of Virology, 2005. **79**(4): p. 2097.
313. Gomes, S.T.M., et al. , *Immune escape mutations in HIV-1 controllers in the Brazilian Amazon region.* BMC Infectious Diseases, 2020. **20**(1): p. 546.
314. Wibmer, C.K., et al. , *Viral Escape from HIV-1 Neutralizing Antibodies Drives Increased Plasma Neutralization Breadth through Sequential Recognition of Multiple Epitopes and Immunotypes.* PLOS Pathogens, 2013. **9**(10): p. e1003738.
315. Dreja, H., et al. , *CD4 binding site broadly neutralizing antibody selection of HIV-1 escape mutants.* The Journal of general virology, 2015. **96**(Pt 7): p. 1899-1905.
316. Zhou, P., et al. , *Broadly resistant HIV-1 against CD4-binding site neutralizing antibodies.* PLOS Pathogens, 2019. **15**(6): p. e1007819.
317. Seiler, P., et al. , *In Vivo Selection of Neutralization-Resistant Virus Variants But No Evidence of B Cell Tolerance in Lymphocytic Choriomeningitis Virus Carrier Mice Expressing a Transgenic Virus-Neutralizing Antibody.* The Journal of Immunology, 1999. **162**(8): p. 4536.
318. Ciurea, A., et al. , *Impairment of CD4(+) T cell responses during chronic virus infection prevents neutralizing antibody responses against virus escape mutants.* The Journal of experimental medicine, 2001. **193**(3): p. 297-305.
319. Walker, L.M., et al. , *A Limited Number of Antibody Specificities Mediate Broad and Potent Serum Neutralization in Selected HIV-1 Infected Individuals.* PLOS Pathogens, 2010. **6**(8): p. e1001028.
320. Battegay, M., et al. , *Impairment and delay of neutralizing antiviral antibody responses by virus-specific cytotoxic T cells.* The Journal of Immunology, 1993. **151**(10): p. 5408-5415.
321. Hunziker, L., et al. , *Hypergammaglobulinemia and autoantibody induction mechanisms in viral infections.* Nature Immunology, 2003. **4**(4): p. 343-349.
322. Recher, M., et al. , *Deliberate removal of T cell help improves virus-neutralizing antibody production.* Nat Immunol, 2004. **5**(9): p. 934-42.
323. Schnittman, S.M., et al. , *Direct polyclonal activation of human B lymphocytes by the acquired immune deficiency syndrome virus.* Science, 1986. **233**(4768): p. 1084-6.
324. Zellweger, R.M., et al. , *Parameters governing exhaustion of rare T cell-independent neutralizing IgM-producing B cells after LCMV infection.* Eur J Immunol, 2006. **36**(12): p. 3175-85.
325. Mueller, S.N., et al. , *Regulation of homeostatic chemokine expression and cell trafficking during immune responses.* Science, 2007. **317**(5838): p. 670-4.

326. Leist, T.P., E. Rüedi, and R.M. Zinkernagel, *Virus-triggered immune suppression in mice caused by virus-specific cytotoxic T cells.* J Exp Med, 1988. **167**(5): p. 1749-54.
327. Mueller, S.N., et al. , *Viral targeting of fibroblastic reticular cells contributes to immunosuppression and persistence during chronic infection.* Proc Natl Acad Sci U S A, 2007. **104**(39): p. 15430-5.
328. Matter, M.S., et al. , *Destruction of Lymphoid Organ Architecture and Hepatitis Caused by CD4+ T Cells.* PLOS ONE, 2011. **6**(9): p. e24772.
329. Planz, O., et al. , *Specific cytotoxic T cells eliminate B cells producing virus-neutralizing antibodies [corrected].* Nature, 1996. **382**(6593): p. 726-9.
330. Planz, O., et al. , *Specific cytotoxic T cells eliminate cells producing neutralizing antibodies.* Nature, 2003. **426**(6965): p. 474.
331. Moseman, E.A., et al. , *Type I interferon suppresses virus-specific B cell responses by modulating CD8⁺ T cell differentiation.* Science Immunology, 2016. **1**(4).
332. Nagase, H., et al. , *Mechanism of hypergammaglobulinemia by HIV infection: circulating memory B-cell reduction with plasmacytosis.* Clin Immunol, 2001. **100**(2): p. 250-9.
333. De Milito, A., et al. , *Mechanisms of hypergammaglobulinemia and impaired antigen-specific humoral immunity in HIV-1 infection.* Blood, 2004. **103**(6): p. 2180-6.
334. Hunziker, L., et al. , *Hypergammaglobulinemia and autoantibody induction mechanisms in viral infections.* Nat Immunol, 2003. **4**(4): p. 343-9.
335. Gallimore, A., et al. , *Induction and exhaustion of lymphocytic choriomeningitis virus-specific cytotoxic T lymphocytes visualized using soluble tetrameric major histocompatibility complex class I-peptide complexes.* The Journal of experimental medicine, 1998. **187**(9): p. 1383-1393.
336. Bengsch, B., B. Martin, and R. Thimme, *Restoration of HBV-specific CD8+ T cell function by PD-1 blockade in inactive carrier patients is linked to T cell differentiation.* Journal of Hepatology, 2014. **61**(6): p. 1212-1219.
337. Boni, C., et al. , *Characterization of hepatitis B virus (HBV)-specific T-cell dysfunction in chronic HBV infection.* Journal of virology, 2007. **81**(8): p. 4215-4225.
338. Lechner, F., et al. , *Analysis of successful immune responses in persons infected with hepatitis C virus.* The Journal of experimental medicine, 2000. **191**(9): p. 1499-1512.
339. Barber, D.L., et al. , *Restoring function in exhausted CD8 T cells during chronic viral infection.* Nature, 2006. **439**(7077): p. 682-7.
340. Blattman, J.N., et al. , *Impact of epitope escape on PD-1 expression and CD8 T-cell exhaustion during chronic infection.* Journal of virology, 2009. **83**(9): p. 4386-4394.
341. McLane, L.M., M.S. Abdel-Hakeem, and E.J. Wherry, *CD8 T Cell Exhaustion During Chronic Viral Infection and Cancer.* Annu Rev Immunol, 2019. **37**: p. 457-495.
342. Mueller, S.N. and R. Ahmed, *High antigen levels are the cause of T cell exhaustion during chronic viral infection.* Proc Natl Acad Sci U S A, 2009. **106**(21): p. 8623-8.
343. Utzschneider, D.T., et al. , *T Cell Factor 1-Expressing Memory-like CD8+ T Cells Sustain the Immune Response to Chronic Viral Infections.* Immunity, 2016. **45**(2): p. 415-427.
344. Burton, A.R., et al. , *Circulating and intrahepatic antiviral B cells are defective in hepatitis B.* The Journal of clinical investigation, 2018. **128**(10): p. 4588-4603.
345. Moir, S. and A.S. Fauci, *B-cell exhaustion in HIV infection: the role of immune activation.* Current Opinion in HIV and AIDS, 2014. **9**(5): p. 472-477.

346. Moir, S. and A.S. Fauci, *Insights into B cells and HIV-specific B-cell responses in HIV-infected individuals.* Immunological Reviews, 2013. **254**(1): p. 207-224.
347. Moir, S. and A.S. Fauci, *B cell responses to HIV infection.* Immunological reviews, 2017. **275**(1): p. 33-48.
348. Salimzadeh, L., et al. , *PD-1 blockade partially recovers dysfunctional virus-specific B cells in chronic hepatitis B infection.* J Clin Invest, 2018. **128**(10): p. 4573-4587.
349. Malaspina, A., et al. , *Compromised B Cell Responses to Influenza Vaccination in HIV-Infected Individuals.* The Journal of Infectious Diseases, 2005. **191**(9): p. 1442-1450.
350. Wheatley, A.K., et al. , *HIV-dependent depletion of influenza-specific memory B cells impacts B cell responsiveness to seasonal influenza immunisation.* Sci Rep, 2016. **6**: p. 26478.
351. Moseman, E.A., et al. , *Type I interferon suppresses virus-specific B cell responses by modulating CD8(+) T cell differentiation.* Science immunology, 2016. **1**(4): p. eaah3565.
352. Sammicheli, S., et al. , *Inflammatory monocytes hinder antiviral B cell responses.* Science Immunology, 2016. **1**(4): p. eaah6789.
353. Di Niro, R., et al. , *Salmonella Infection Drives Promiscuous B Cell Activation Followed by Extrafollicular Affinity Maturation.* Immunity, 2015. **43**(1): p. 120-31.
354. Krishnamurty, A.T., et al. , *Somatically Hypermutated Plasmodium-Specific IgM(+) Memory B Cells Are Rapid, Plastic, Early Responders upon Malaria Rechallenge.* Immunity, 2016. **45**(2): p. 402-14.
355. Thouvenel, C.D., et al. , *Multimeric antibodies from antigen-specific human IgM+ memory B cells restrict Plasmodium parasites.* J Exp Med, 2021. **218**(4).
356. Bonilla, W.V., et al. , *Heterologous arenavirus vector prime-boost overrules self-tolerance for efficient tumor-specific CD8 T cell attack.* Cell reports. Medicine, 2021. **2**(3): p. 100209-100209.
357. Armstrong, C. and R.D. Lillie, *Experimental Lymphocytic Choriomeningitis of Monkeys and Mice Produced by a Virus Encountered in Studies of the 1933 St. Louis Encephalitis Epidemic.* Public Health Reports (1896-1970), 1934. **49**(35): p. 1019-1027.
358. Scott, T.F.M. and T.M. Rivers, *MENINGITIS IN MAN CAUSED BY A FILTERABLE VIRUS : I. TWO CASES AND THE METHOD OF OBTAINING A VIRUS FROM THEIR SPINAL FLUIDS.* Journal of Experimental Medicine, 1936. **63**(3): p. 397-414.
359. Pfau, C.J., et al. , *Lymphocytic choriomeningitis virus killer T cells are lethal only in weakly disseminated murine infections.* J Exp Med, 1982. **156**(1): p. 79-89.
360. Jacobson, S. and C.J. Pfau, *Viral pathogenesis and resistance to defective interfering particles.* Nature, 1980. **283**(5744): p. 311-313.
361. Trapido, H. and C. Sanmart?n, *Pichind? Virus: A New Virus of the Tacaribe Group from Colombia.* The American Journal of Tropical Medicine and Hygiene, 1971. **20**(4): p. 631-641.
362. Lan, S., et al. , *Development of Infectious Clones for Virulent and Avirulent Pichinde Viruses: a Model Virus To Study Arenavirus-Induced Hemorrhagic Fevers.* Journal of Virology, 2009. **83**(13): p. 6357.
363. Dhanwani, R., et al. , *A Novel Live Pichinde Virus-Based Vaccine Vector Induces Enhanced Humoral and Cellular Immunity after a Booster Dose.* Journal of virology, 2015. **90**(5): p. 2551-2560.

364. Maiztegui, J.I., et al. , *Protective Efficacy of a Live Attenuated Vaccine against Argentine Hemorrhagic Fever.* The Journal of Infectious Diseases, 1998. **177**(2): p. 277-283.
365. Penaloza-MacMaster, P., et al. , *Vaccine-elicited CD4 T cells induce immunopathology after chronic LCMV infection.* Science, 2015. **347**(6219): p. 278-282.
366. Chen, M., et al. , *Genomic and biological characterization of aggressive and docile strains of lymphocytic choriomeningitis virus rescued from a plasmid-based reverse-genetics system.* The Journal of general virology, 2008. **89**(Pt 6): p. 1421-1433.
367. Battegay, M., et al. , *Quantification of lymphocytic choriomeningitis virus with an immunological focus assay in 24- or 96-well plates.* J Virol Methods, 1991. **33**(1-2): p. 191-8.
368. Hangartner, L., et al. , *Antiviral immune responses in gene-targeted mice expressing the immunoglobulin heavy chain of virus-neutralizing antibodies.* Proceedings of the National Academy of Sciences of the United States of America, 2003. **100**(22): p. 12883-12888.
369. Hao, Z. and K. Rajewsky, *Homeostasis of peripheral B cells in the absence of B cell influx from the bone marrow.* The Journal of experimental medicine, 2001. **194**(8): p. 1151-1164.
370. Muller, U., et al. , *Functional role of type I and type II interferons in antiviral defense.* Science, 1994. **264**(5167): p. 1918.
371. Williams, N., N. Kraft, and K. Shortman, *The separation of different cell classes from lymphoid organs. VI. The effect of osmolarity of gradient media on the density distribution of cells.* Immunology, 1972. **22**(5): p. 885-899.
372. Costa-Silva, J., D. Domingues, and F.M. Lopes, *RNA-Seq differential expression analysis: An extended review and a software tool.* PloS one, 2017. **12**(12): p. e0190152-e0190152.
373. Law, C.W., et al. , *voom: precision weights unlock linear model analysis tools for RNA-seq read counts.* Genome Biology, 2014. **15**(2): p. R29.
374. Eschli, B., et al. , *Early Antibodies Specific for the Neutralizing Epitope on the Receptor Binding Subunit of the Lymphocytic Choriomeningitis Virus Glycoprotein Fail To Neutralize the Virus.* Journal of Virology, 2007. **81**(21): p. 11650-11657.
375. Traub, E., *A FILTERABLE VIRUS RECOVERED FROM WHITE MICE.* Science, 1935. **81**(2099): p. 298-299.
376. Crawford, A., et al. , *Molecular and Transcriptional Basis of CD4⁺ T Cell Dysfunction during Chronic Infection.* Immunity, 2014. **40**(2): p. 289-302.
377. Doering, T.A., et al. , *Network analysis reveals centrally connected genes and pathways involved in CD8+ T cell exhaustion versus memory.* Immunity, 2012. **37**(6): p. 1130-44.
378. Moskophidis, D., et al. , *Role of virus and host variables in virus persistence or immunopathological disease caused by a non-cytolytic virus.* J Gen Virol, 1995. **76 (Pt 2)**: p. 381-91.
379. Chen, M., et al. , *Genomic and biological characterization of aggressive and docile strains of lymphocytic choriomeningitis virus rescued from a plasmid-based reverse-genetics system.* J Gen Virol, 2008. **89**(Pt 6): p. 1421-1433.
380. Basters, A., K.-P. Knobeloch, and G. Fritz, *USP18 - a multifunctional component in the interferon response.* Bioscience reports, 2018. **38**(6): p. BSR20180250.
381. Randall, G., et al. , *Silencing of USP18 potentiates the antiviral activity of interferon against hepatitis C virus infection.* Gastroenterology, 2006. **131**(5): p. 1584-91.

382. Honke, N., et al. , *Multiple functions of USP18.* Cell Death & Disease, 2016. **7**(11): p. e2444-e2444.
383. Ketscher, L., et al. , *Selective inactivation of USP18 isopeptidase activity in vivo enhances ISG15 conjugation and viral resistance.* Proceedings of the National Academy of Sciences of the United States of America, 2015. **112**(5): p. 1577-1582.
384. Ritchie, K.J., et al. , *Role of ISG15 protease UBP43 (USP18) in innate immunity to viral infection.* Nat Med, 2004. **10**(12): p. 1374-8.
385. Papac-Milicevic, N., et al. , *The Interferon Stimulated Gene 12 Inactivates Vasculoprotective Functions of NR4A Nuclear Receptors.* Circulation Research, 2012. **110**(8): p. e50-e63.
386. Wilson, E.B., et al. , *Blockade of chronic type I interferon signaling to control persistent LCMV infection.* Science (New York, N.Y.), 2013. **340**(6129): p. 202-207.
387. Jamieson, B.D. and R. Ahmed, *T-cell tolerance: exposure to virus in utero does not cause a permanent deletion of specific T cells.* Proceedings of the National Academy of Sciences, 1988. **85**(7): p. 2265.
388. Rajewsky, K., *Clonal selection and learning in the antibody system.* Nature, 1996. **381**(6585): p. 751-758.
389. Burnet, F.M., *A modification of jerne's theory of antibody production using the concept of clonal selection.* CA: A Cancer Journal for Clinicians, 1976. **26**(2): p. 119-121.
390. Cohn, M., et al. , *Reflections on the clonal-selection theory.* Nature Reviews Immunology, 2007. **7**(10): p. 823-830.
391. Jordan, M.A. and A.G. Baxter, *Quantitative and qualitative approaches to GOD: the first 10 years of the clonal selection theory.* Immunology & Cell Biology, 2008. **86**(1): p. 72-79.
392. Hodgkin, P.D., W.R. Heath, and A.G. Baxter, *The clonal selection theory: 50 years since the revolution.* Nature Immunology, 2007. **8**(10): p. 1019-1026.
393. Buchmeier, M., E. Adam, and W.E. Rawls, *Serological Evidence of Infection by Pichinde Virus Among Laboratory Workers.* Infection and Immunity, 1974. **9**(5): p. 821-823.
394. Maiztegui, J.I., et al. , *Protective efficacy of a live attenuated vaccine against Argentine hemorrhagic fever. AHF Study Group.* J Infect Dis, 1998. **177**(2): p. 277-83.
395. Crotty, S., R.J. Johnston, and S.P. Schoenberger, *Effectors and memories: Bcl-6 and Blimp-1 in T and B lymphocyte differentiation.* Nat Immunol, 2010. **11**(2): p. 114-20.
396. Johnston, R.J., et al. , *Bcl6 and Blimp-1 are reciprocal and antagonistic regulators of T follicular helper cell differentiation.* Science, 2009. **325**(5943): p. 1006-10.
397. Zhang, Y., et al. , *Effect of TACI Signaling on Humoral Immunity and Autoimmune Diseases.* Journal of Immunology Research, 2015. **2015**: p. 247426.
398. Figgett, W.A., et al. , *The TACI receptor regulates T-cell-independent marginal zone B cell responses through innate activation-induced cell death.* Immunity, 2013. **39**(3): p. 573-83.
399. Zhang, T.-T., et al. , *Germinal center B cell development has distinctly regulated stages completed by disengagement from T cell help.* eLife, 2017. **6**: p. e19552.
400. Kato, Y., et al. , *Multifaceted Effects of Antigen Valency on B Cell Response Composition and Differentiation In Vivo.* Immunity, 2020. **53**(3): p. 548-563.e8.
401. Kardava, L., et al. , *Abnormal B cell memory subsets dominate HIV-specific responses in infected individuals.* The Journal of Clinical Investigation, 2014. **124**(7): p. 3252-3262.

402. Moir, S., et al. , *HIV-1 induces phenotypic and functional perturbations of B cells in chronically infected individuals.* Proceedings of the National Academy of Sciences of the United States of America, 2001. **98**(18): p. 10362-10367.
403. Cashman, S.B., B.D. Marsden, and L.B. Dustin, *The Humoral Immune Response to HCV: Understanding is Key to Vaccine Development.* Frontiers in immunology, 2014. **5**: p. 550-550.
404. Gray, E.S., et al. , *Neutralizing antibody responses in acute human immunodeficiency virus type 1 subtype C infection.* J Virol, 2007. **81**(12): p. 6187-96.
405. Logvinoff, C., et al. , *Neutralizing antibody response during acute and chronic hepatitis C virus infection.* Proc Natl Acad Sci U S A, 2004. **101**(27): p. 10149-54.
406. Oldstone, M.B.A. and F.J. Dixon, *PATHOGENESIS OF CHRONIC DISEASE ASSOCIATED WITH PERSISTENT LYMPHOCYTIC CHORIOMENINGITIS VIRAL INFECTION : I. RELATIONSHIP OF ANTIBODY PRODUCTION TO DISEASE IN NEONATALLY INFECTED MICE.* Journal of Experimental Medicine, 1969. **129**(3): p. 483-505.
407. Jardine, J.G., et al. , *HIV-1 broadly neutralizing antibody precursor B cells revealed by germline-targeting immunogen.* Science, 2016. **351**(6280): p. 1458-63.
408. Osmond, D.G., *The turnover of B-cell populations.* Immunol Today, 1993. **14**(1): p. 34-7.
409. Staupe, R.P., et al. , *Chronic viral infection promotes early germinal center exit of B cells and impaired antibody development.* bioRxiv, 2019: p. 849844.
410. Mueller, S.N. and R. Ahmed, *High antigen levels are the cause of T cell exhaustion during chronic viral infection.* Proceedings of the National Academy of Sciences, 2009. **106**(21): p. 8623-8628.
411. Zehn, D. and E.J. Wherry. *Immune Memory and Exhaustion: Clinically Relevant Lessons from the LCMV Model*. in *Crossroads Between Innate and Adaptive Immunity V*. 2015. Cham: Springer International Publishing.
412. Behring, E.v., Shibasaburo Kitasato, *Ueber Das Zustandekommen Der Diphtherie-Immunität Und Der Tetanus-Immunität Bei Thieren.* Deutsch. Med. Woch., 1890. **49**: p. 1113-1114.
413. Köhler, G. and C. Milstein, *Continuous cultures of fused cells secreting antibody of predefined specificity.* Nature, 1975. **256**(5517): p. 495-497.
414. Winter, G., *Harnessing Evolution to Make Medicines (Nobel Lecture).* Angewandte Chemie International Edition, 2019. **58**(41): p. 14438-14445.
415. Wu, X., et al. , *Rational Design of Envelope Identifies Broadly Neutralizing Human Monoclonal Antibodies to HIV-1.* Science, 2010. **329**(5993): p. 856-861.
416. Scheid, J.F., et al. , *Sequence and Structural Convergence of Broad and Potent HIV Antibodies That Mimic CD4 Binding.* Science, 2011. **333**(6049): p. 1633-1637.
417. Trono, D., et al. , *HIV Persistence and the Prospect of Long-Term Drug-Free Remissions for HIV-Infected Individuals.* Science, 2010. **329**(5988): p. 174-180.
418. Nishimura, Y., et al. , *Early antibody therapy can induce long-lasting immunity to SHIV.* Nature, 2017. **543**(7646): p. 559-563.
419. Nishimura, Y., et al. , *Immunotherapy during the acute SHIV infection of macaques confers long-term suppression of viremia.* Journal of Experimental Medicine, 2020. **218**(1).
420. Shingai, M., et al. , *Antibody-mediated immunotherapy of macaques chronically infected with SHIV suppresses viraemia.* Nature, 2013. **503**(7475): p. 277-280.

421. Barouch, D.H., et al. , *Therapeutic efficacy of potent neutralizing HIV-1-specific monoclonal antibodies in SHIV-infected rhesus monkeys.* Nature, 2013. **503**(7475): p. 224-228.
422. Mendoza, P., et al. , *Combination therapy with anti-HIV-1 antibodies maintains viral suppression.* Nature, 2018. **561**(7724): p. 479-484.
423. Lewis, A.D., et al. , *Generation of Neutralizing Activity against Human Immunodeficiency Virus Type 1 in Serum by Antibody Gene Transfer.* Journal of Virology, 2002. **76**(17): p. 8769-8775.
424. Priddy, F.H., et al. , *Adeno-associated virus vectored immunoprophylaxis to prevent HIV in healthy adults: a phase 1 randomised controlled trial.* The Lancet HIV, 2019. **6**(4): p. e230-e239.
425. Gardner, M.R., et al. , *AAV-delivered eCD4-Ig protects rhesus macaques from high-dose SIVmac239 challenges.* Science Translational Medicine, 2019. **11**(502): p. eaau5409.
426. Leborgne, C., et al. , *IgG-cleaving endopeptidase enables in vivo gene therapy in the presence of anti-AAV neutralizing antibodies.* Nature Medicine, 2020. **26**(7): p. 1096-1101.
427. Balazs, A.B., et al. , *Antibody-based protection against HIV infection by vectored immunoprophylaxis.* Nature, 2012. **481**(7379): p. 81-84.
428. Balazs, A.B., et al. , *Vectored immunoprophylaxis protects humanized mice from mucosal HIV transmission.* Nature Medicine, 2014. **20**(3): p. 296-300.
429. Fuchs, S.P., et al. , *AAV-Delivered Antibody Mediates Significant Protective Effects against SIVmac239 Challenge in the Absence of Neutralizing Activity.* PLOS Pathogens, 2015. **11**(8): p. e1005090.
430. de Jong, Y.P., et al. , *Broadly neutralizing antibodies abrogate established hepatitis C virus infection.* Science Translational Medicine, 2014. **6**(254): p. 254ra129-254ra129.
431. Robert, M.-A., et al. , *Gene Transfer of ZMapp Antibodies Mediated by Recombinant Adeno-Associated Virus Protects Against Ebola Infections.* Human Gene Therapy, 2017. **29**(4): p. 452-466.
432. van Lieshout, L.P., et al. , *Intramuscular Adeno-Associated Virus–Mediated Expression of Monoclonal Antibodies Provides 100% Protection Against Ebola Virus Infection in Mice.* The Journal of Infectious Diseases, 2018. **217**(6): p. 916-925.
433. Kisalu, N.K., et al. , *Enhancing durability of CIS43 monoclonal antibody by Fc mutation or AAV delivery for malaria prevention.* JCI Insight, 2021. **6**(3).
434. Horwitz, J.A., et al. , *HIV-1 suppression and durable control by combining single broadly neutralizing antibodies and antiretroviral drugs in humanized mice.* Proceedings of the National Academy of Sciences, 2013. **110**(41): p. 16538-16543.
435. Martinez-Navio, J.M., et al. , *Adeno-Associated Virus Delivery of Anti-HIV Monoclonal Antibodies Can Drive Long-Term Virologic Suppression.* Immunity, 2019. **50**(3): p. 567-575.e5.
436. Klein, F., et al. , *Enhanced HIV-1 immunotherapy by commonly arising antibodies that target virus escape variants.* The Journal of Experimental Medicine, 2014. **211**(12): p. 2361-2372.
437. Seiler, P., et al. , *In Vivo Selection of Neutralization-Resistant Virus Variants But No Evidence of B Cell Tolerance in Lymphocytic Choriomeningitis Virus Carrier Mice Expressing a Transgenic Virus-Neutralizing Antibody.* The Journal of Immunology, 1999. **162**(8): p. 4536-4541.

438. Iseda, S., et al. , *Biphasic CD8⁺ T-Cell Defense in Simian Immunodeficiency Virus Control by Acute-Phase Passive Neutralizing Antibody Immunization.* Journal of Virology, 2016. **90**(14): p. 6276-6290.
439. Schoofs, T., et al. , *HIV-1 therapy with monoclonal antibody 3BNC117 elicits host immune responses against HIV-1.* Science, 2016. **352**(6288): p. 997-1001.
440. Haigwood, N.L., et al. , *Passive Immunotherapy in Simian Immunodeficiency Virus-Infected Macaques Accelerates the Development of Neutralizing Antibodies.* Journal of Virology, 2004. **78**(11): p. 5983-5995.
441. Ng, C.T., et al. , *Passive neutralizing antibody controls SHIV viremia and enhances B cell responses in infant macaques.* Nature Medicine, 2010. **16**: p. 1117.
442. Gros, L., et al. , *Induction of Long-Term Protective Antiviral Endogenous Immune Response by Short Neutralizing Monoclonal Antibody Treatment.* Journal of Virology, 2005. **79**(10): p. 6272-6280.
443. Niessl, J., et al. , *Combination anti-HIV-1 antibody therapy is associated with increased virus-specific T cell immunity.* Nature Medicine, 2020. **26**(2): p. 222-227.
444. Yamamoto, T., et al. , *Polyfunctional CD4⁺ T-Cell Induction in Neutralizing Antibody-Triggered Control of Simian Immunodeficiency Virus Infection.* Journal of Virology, 2009. **83**(11): p. 5514-5524.
445. Fung-Leung, W.P., et al. , *Immune response against lymphocytic choriomeningitis virus infection in mice without CD8 expression.* Journal of Experimental Medicine, 1991. **174**(6): p. 1425-1429.
446. Mueller, S.N. and R. Ahmed, *High antigen levels are the cause of T cell exhaustion during chronic viral infection.* Proceedings of the National Academy of Sciences of the United States of America, 2009. **106**(21): p. 8623-8628.
447. Gallimore, A., et al. , *Induction and Exhaustion of Lymphocytic Choriomeningitis Virus–specific Cytotoxic T Lymphocytes Visualized Using Soluble Tetrameric Major Histocompatibility Complex Class I–Peptide Complexes.* The Journal of Experimental Medicine, 1998. **187**(9): p. 1383-1393.
448. Zajac, A.J., et al. , *Viral immune evasion due to persistence of activated T cells without effector function.* The Journal of experimental medicine, 1998. **188**(12): p. 2205-2213.
449. Barber, D.L., et al. , *Restoring function in exhausted CD8 T cells during chronic viral infection.* Nature, 2006. **439**(7077): p. 682-687.
450. Klein, M.A., et al. , *A crucial role for B cells in neuroinvasive scrapie.* Nature, 1997. **390**(6661): p. 687-690.
451. Pérarnau, B., et al. , *Single H2Kb, H2Db and double H2KbDb knockout mice: peripheral CD8+ T cell repertoire and antilymphocytic choriomeningitis virus cytolytic responses.* European Journal of Immunology, 1999. **29**(4): p. 1243-1252.
452. Goodnow, C.C., et al. , *Altered immunoglobulin expression and functional silencing of self-reactive B lymphocytes in transgenic mice.* Nature, 1988. **334**(6184): p. 676-682.
453. Pfau, C.J., et al. , *Lymphocytic choriomeningitis virus killer T cells are lethal only in weakly disseminated murine infections.* The Journal of Experimental Medicine, 1982. **156**(1): p. 79-89.
454. Lock, M., et al. , *Absolute Determination of Single-Stranded and Self-Complementary Adeno-Associated Viral Vector Genome Titers by Droplet Digital PCR.* Human Gene Therapy Methods, 2013. **25**(2): p. 115-125.

455. Schweier, O., et al. , *Residual LCMV antigen in transiently CD4+ T cell-depleted mice induces high levels of virus-specific antibodies but only limited B-cell memory.* European Journal of Immunology, 2019. **49**(4): p. 626-637.
456. Blackburn, S.D., et al. , *Coregulation of CD8+ T cell exhaustion by multiple inhibitory receptors during chronic viral infection.* Nature Immunology, 2009. **10**(1): p. 29-37.
457. Wherry, E.J., et al. , *Viral Persistence Alters CD8 T-Cell Immunodominance and Tissue Distribution and Results in Distinct Stages of Functional Impairment.* Journal of Virology, 2003. **77**(8): p. 4911-4927.
458. Moskophidis, D., et al. , *Role of virus and host variables in virus persistence or immunopathological disease caused by a non-cytolytic virus.* Journal of General Virology, 1995. **76**(2): p. 381-391.
459. Hunziker, L., et al. , *Public versus personal serotypes of a viral quasispecies.* Proceedings of the National Academy of Sciences, 2003. **100**(10): p. 6015-6020.
460. Coutelier, J.P., et al. , *IgG2a restriction of murine antibodies elicited by viral infections.* The Journal of Experimental Medicine, 1987. **165**(1): p. 64-69.
461. Hioe, C.E., et al. , *The use of immune complex vaccines to enhance antibody responses against neutralizing epitopes on HIV-1 envelope gp120.* Vaccine, 2009. **28**(2): p. 352-360.
462. Kumar, R., et al. , *Elicitation of broadly reactive antibodies against glycan-modulated neutralizing V3 epitopes of HIV-1 by immune complex vaccines.* Vaccine, 2013. **31**(46): p. 5413-5421.
463. Batista, F.D. and N.E. Harwood, *The who, how and where of antigen presentation to B cells.* Nature Reviews Immunology, 2009. **9**(1): p. 15-27.
464. Carroll, Michael C. and David E. Isenman, *Regulation of Humoral Immunity by Complement.* Immunity, 2012. **37**(2): p. 199-207.
465. Phan, T.G., et al. , *Immune complex relay by subcapsular sinus macrophages and noncognate B cells drives antibody affinity maturation.* Nature Immunology, 2009. **10**(7): p. 786-793.
466. Utzschneider, D.T., et al. , *T cells maintain an exhausted phenotype after antigen withdrawal and population reexpansion.* Nature Immunology, 2013. **14**: p. 603.
467. Harker, J.A., et al. , *Late Interleukin-6 Escalates T Follicular Helper Cell Responses and Controls a Chronic Viral Infection.* Science, 2011. **334**(6057): p. 825-829.
468. Xin, G., et al. , *Single-cell RNA sequencing unveils an IL-10-producing helper subset that sustains humoral immunity during persistent infection.* Nature Communications, 2018. **9**(1): p. 5037.
469. Fahey, L.M., et al. , *Viral persistence redirects CD4 T cell differentiation toward T follicular helper cells.* The Journal of experimental medicine, 2011. **208**(5): p. 987-999.
470. Crawford, A., et al. , *Molecular and Transcriptional Basis of CD4+ T Cell Dysfunction during Chronic Infection.* Immunity, 2014. **40**(2): p. 289-302.
471. Burton, A.R., et al. , *Circulating and intrahepatic antiviral B cells are defective in hepatitis B.* The Journal of Clinical Investigation, 2018. **128**(10): p. 4588-4603.
472. Doria-Rose, N.A., et al. , *Developmental pathway for potent V1V2-directed HIV-neutralizing antibodies.* Nature, 2014. **509**(7498): p. 55-62.
473. Liu, X., et al. , *USP18 inhibits NF-κB and NFAT activation during Th17 differentiation by deubiquitinating the TAK1-TAB1 complex.* J Exp Med, 2013. **210**(8): p. 1575-90.
474. Goldmann, T., et al. , *USP18 lack in microglia causes destructive interferonopathy of the mouse brain.* Embo j, 2015. **34**(12): p. 1612-29.

475. Zou, W., et al. , *Microarray analysis reveals that Type I interferon strongly increases the expression of immune-response related genes in Ubp43 (Usp18) deficient macrophages.* Biochem Biophys Res Commun, 2007. **356**(1): p. 193-9.
476. Fajgenbaum, D.C. and C.H. June, *Cytokine Storm.* New England Journal of Medicine, 2020. **383**(23): p. 2255-2273.
477. Kang, J.A. and Y.J. Jeon, *Emerging Roles of USP18: From Biology to Pathophysiology.* International journal of molecular sciences, 2020. **21**(18): p. 6825.
478. Cervantes-Badillo, M.G., et al. , *IFI27/ISG12 Downregulates Estrogen Receptor α Transactivation by Facilitating Its Interaction With CRM1/XPO1 in Breast Cancer Cells.* Front Endocrinol (Lausanne), 2020. **11**: p. 568375.
479. Wang, H., et al. , *Knockdown of IFI27 inhibits cell proliferation and invasion in oral squamous cell carcinoma.* World Journal of Surgical Oncology, 2018. **16**(1): p. 64.
480. Cho, H., et al. , *A Role for Ifit2 in Restricting West Nile Virus Infection in the Brain.* Journal of Virology, 2013. **87**(15): p. 8363-8371.
481. Uhrin, P., et al. , *ISG12 is a critical modulator of innate immune responses in murine models of sepsis.* Immunobiology, 2013. **218**(9): p. 1207-1216.
482. Kräutler, N.J., et al. , *Quantitative and Qualitative Analysis of Humoral Immunity Reveals Continued and Personalized Evolution in Chronic Viral Infection.* Cell Reports, 2020. **30**(4): p. 997-1012.e6.
483. Fallet, B., et al. , *Interferon-driven deletion of antiviral B cells at the onset of chronic infection.* Science Immunology, 2016. **1**(4).
484. Kallies, A. and S.L. Nutt, *Terminal differentiation of lymphocytes depends on Blimp-1.* Current Opinion in Immunology, 2007. **19**(2): p. 156-162.
485. Greczmiel, U., et al. , *Sustained T follicular helper cell response is essential for control of chronic viral infection.* Science Immunology, 2017. **2**(18): p. eaam8686.
486. Künzli, M., et al. , *Long-lived T follicular helper cells retain plasticity and help sustain humoral immunity.* Science Immunology, 2020. **5**(45): p. eaay5552.
487. Hill, D.L., et al. , *The adjuvant GLA-SE promotes human Tfh cell expansion and emergence of public TCRβ clonotypes.* Journal of Experimental Medicine, 2019. **216**(8): p. 1857-1873.

Acknowledgments

I would like to thank Daniel for the wonderful opportunity to work in his lab. Thank you, Daniel, for being a great mentor and always looking at data with a positive attitude. This gave me strength and confidence to keep exploring the field of immunology. Thank you for taking care that I was feeling comfortable and being ready to listen to any problem that I had, scientific or personal! I don't think I would have made it very far in this new for me field if you were not such a great support.

Prof. Urs Jenal and Prof. Doron Merkler were so kind to be part of my PhD committee. Both gave extensive feedback. Most importantly, they assured me that I am able to continue with my PhD after my first year and that I am supposed to be where I am.

Big thanks to all lab members, both former and present!
To Min and Karen for your kindness and readiness to help!
To Peter, Katrin, Weldy, Maggie for enthusiastic discussions and elaborate scientific ideas!
To "the gang" members (Yusuf, Mehmet, Anna, Lena, Marianna, Matias, Nicole and Tiago) for being so much fun. For being friends.
To Kerstin for helping me to start in the lab and always being ready to discuss anything.
To Lena for being extremely supportive friend and the best conference buddy ever!
To Sonia and Nicole for excellent administrative support!

A big thank you to my family and friends for always being there for me. My mother, Albena, my father, Dimitur, my aunt, Maria, my grandparents, Margichka, Maria, Atanas and Anton! Despite distance, I always felt loved and appreciated! I am just too lucky to be your kid!
My brother, Anton. Having you so close was one reason I made it! I am so grateful for your optimism and great humor!
Many, many thanks to my "extended" family: Uta, Diego, Ria. You have made me feel home in Switzerland and in Basel!
My auntie Mariana and uncle Toni back home and all of my cousins- thank you!

My friends, some of you still home, some living around the world! Thank you all for being the fantastic people you are! Thank you for your selfless friendship!

Finally, I would like to thank you, Nico. Living with a stressed-out PhD student was not always easy, I am sure! You are the most patient and loving person I know! Thank you for being who you are!

At this point I might have forgotten someone! Apologies if I did and thank you nevertheless!

Mirela